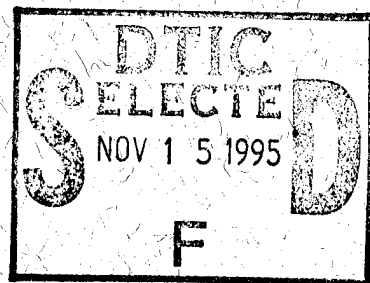


# A MASS REDUCTION EFFORT OF THE ELECTRIC AND HYBRID VEHICLE



## FINAL REPORT

TCR-0513

Richard B. Freeman  
and  
Herbert A. Jahnle

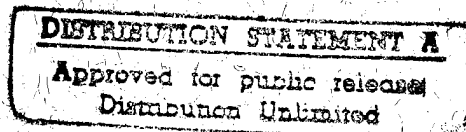
March 1980

19951114 101

DTIC QUALITY INSPECTED 5

Work performed under  
JPL Contract Number 955283  
by

The Budd Company  
Technical Center  
375 Commerce Drive  
Fort Washington, PA 19034



DEPARTMENT OF DEFENSE  
TECHNICAL EVALUATION CENTER  
ATTN: COM. DOVER, N. J. 07801

This work was performed for the Jet Propulsion Laboratory, California Institute of Technology, and was sponsored by the U. S. Department of Energy through an agreement with the National Aeronautics and Space Administration.

19951114 101

This report was prepared as an account of work sponsored by the United States Government. Neither the United States nor the United States Department of Energy, nor any of their employees, nor any of their contractors, subcontractors, or their employees, makes any warranty, express or implied, or assumes any legal liability or responsibility for the accuracy, completeness or usefulness of any information, apparatus, product or process disclosed, or represents that its use would not infringe privately owned rights.

-- 1 OF 1

\*\*\*DTIC DOES NOT HAVE THIS ITEM\*\*\*

-- 1 - AD NUMBER: D432153  
-- 5 - CORPORATE AUTHOR: BUDD CO FORT WASHINGTON PA TECHNICAL CENTER  
-- 6 - UNCLASSIFIED TITLE: A MASS REDUCTION EFFORT OF THE ELECTRIC AND  
-- HYBRID VEHICLE.  
-- 9 - DESCRIPTIVE NOTE: FINAL REPT.,  
--10 - PERSONAL AUTHORS: FREEMAN, R. B. ; JAHNLE, H. A. ;  
--11 - REPORT DATE: MAR , 1980  
--12 - PAGINATION: 164P  
--14 - REPORT NUMBER: TCR-0513, JPL-9950-374  
--15 - CONTRACT NUMBER: JPL-955283  
--18 - MONITOR ACRONYM: DOE/JPL  
--19 - MONITOR SERIES: 955283-1  
--20 - REPORT CLASSIFICATION: UNCLASSIFIED  
--22 - LIMITATIONS (ALPHA): APPROVED FOR PUBLIC RELEASE; DISTRIBUTION  
-- UNLIMITED. AVAILABILITY: NATIONAL TECHNICAL INFORMATION SERVICE;  
-- SPRINGFIELD, VA. 22161. DOE/JPL-955283-1.  
--33 - LIMITATION CODES: 1 24

-- END

Y FOR NEXT ACCESSION

END

Alt-Z FOR HELP3 ANSI 3 HDX 3 3 LOG CLOSED 3 PRINT OFF 3 PARITY

# A MASS REDUCTION EFFORT OF THE ELECTRIC AND HYBRID VEHICLE

## FINAL REPORT

TCR-0513

Richard B. Freeman  
and  
Herbert A. Jahnle

March 1980

Work performed under  
JPL Contract Number 955283  
by  
The Budd Company  
Technical Center  
375 Commerce Drive  
Fort Washington, PA 19034

Accession For	
NTIS CRA&I	<input checked="" type="checkbox"/>
DTIC TAB	<input type="checkbox"/>
Unannounced	<input type="checkbox"/>
Justification	
By <i>DTIC-AI ltr</i>	
Distribution / <i>11-2-95</i>	
Availability Codes	
Dist	Avail and/or Special
<i>A-1</i>	

This work was performed for the Jet Propulsion Laboratory, California Institute of Technology, and was sponsored by the U. S. Department of Energy through an agreement with the National Aeronautics and Space Administration.



## PREFACE

The assistance and contributions of Budd Company personnel; design - Laszlo Solymosi, estimating - Walter Klinger and secretarial - Antoinette Cirilli toward the completion of this program is acknowledged. Special thanks also go to Dr. Joseph N. Epel for his review and valuable comments.

The guidance and cooperation of the Contract Technical Manager, Jerome L. Bauer, Jr. of the Applied Mechanics Division, Jet Propulsion Laboratory, California Institute of Technology is also acknowledged.

## ABSTRACT

Weight reduction, cost competitiveness, and elimination of the intrusion beam resulted from the redesign and fabrication using composite materials of the door outer panel and intrusion beam from a 1977 Chevrolet Impala. The basis of the redesign involved replacing these two steel parts with a single compression molding using the unique approach of simultaneously curing a sheet molding compound outside panel with a continuous glass fiber intrusion strap. A weight reduction of nearly 11 pounds per door was achieved. Additional weight savings are possible by taking advantage of the elimination of the intrusion beam to design thinner door structures. The parts consolidation approach allows the composite structure to be cost competitive with the original steel design for both the lower production car models and for the near to mid-term production contemplated for electric and hybrid vehicles using current state-of-the-art composite production techniques.

In addition to the design, prototype fabrication, and costing phases of the report, two appendices containing material description, properties and compression molding production requirements are included.

## TABLE OF CONTENTS

ABSTRACT.....	ii
TABLE OF CONTENTS.....	iii
LIST OF FIGURES.....	iv
LIST OF TABLES.....	vi
1.0 SUMMARY.....	1
2.0 INTRODUCTION.....	2
3.0 TECHNICAL DISCUSSION.....	4
3.1 Baseline Steel Design.....	4
3.2 Composite Design.....	4
3.2.1 Material Considerations.....	16
3.2.2 Weight Summary.....	18
3.2.3 Structural Configuration.....	18
3.2.4 Simulated Intrusion Strap Tests.....	30
3.2.5 Prototype Mold Fabrication.....	41
3.2.6 Prototype Molding.....	41
3.3 Cost Evaluation.....	51
3.3.1 Material Cost.....	51
3.3.2 Labor and Overhead.....	52
3.3.3 Capital.....	53
3.3.4 Baseline Steel Design.....	54
3.3.5 Composite Design.....	65
3.3.6 Cost Comparison Between Steel and Composite Designs.....	75
3.4 Proposed Modification to the Composite Design.....	80
4.0 CONCLUSIONS.....	87
5.0 RECOMMENDATIONS.....	88
6.0 NEW TECHNOLOGY.....	89
7.0 REFERENCES.....	90
APPENDIX A - Material Selection Report.....	A-1
APPENDIX B - Process Selection Report.....	B-1

# LIST OF FIGURES

FIGURE		PAGE
3-1	1977 Chevrolet Impala Front Door.....	5
3-2	Impala Door After Removal of Outer Skin.....	6
3-3	Impala Door After Removal of Outer Skin and Intrusion Beam.....	7
3-4	Attachment of Intrusion Beam to Front of Door.....	8
3-5	Locations for Attachment of Hinges.....	9
3-6	Attachment of Intrusion Beam and Latch to Rear of Door.....	10
3-7	Outer Door Panel With Deadening Material.....	11
3-8	Existing Configuration for a Steel Impala Door at the Hinge.....	12
3-9	Existing Configuration for a Steel Impala Door at the Latch.....	13
3-10	1977 Chevrolet Impala Front Door With Composite Outer Panel and Intrusion Strap.....	15
3-11	Construction Details for Door Outer Panel Including Intrusion Protection.....	17
3-12	Results of Cocuring Unidirectional Strap With SMC Skin.....	19
3-13	Hinge Attachment Fitting to Intrusion Strap.....	21
3-14	Hinge Attachment to Composite Intrusion Strap.....	23
3-15	Effect of End Fixity on the Deformation Resistance of the Intrusion Strap.....	24
3-16	Steel Upper Hinge Bracket.....	25
3-17	Steel Lower Hinge Bracket.....	26
3-18	Steel Latch Bracket.....	27
3-19	Maximum Rotation Prior to a Mechanical Lockup in the Hinge.....	28
3-20	Volkswagen Type Fixity Hooks.....	29
3-21	Molded Rib Pocket Used in Intrusion Strap Tests.....	31
3-22	Evaluation of Shear/Peel Failure Mode and Load....	32
3-23	Simulated Intrusion Strap Test (Second Test).....	33
3-24	Distortion of Angle Iron End Attachment (First Test).....	34
3-25	Distortion of Gusseted Angle End Attachment (Second Test).....	35
3-26	Distortion of Steel Fitting (Second Test).....	36
3-27	Composite Damage Resulting from Steel Fitting Distortion (Second Test).....	38
3-28	Force/Deformation Response of Simulated Intrusion Strap Test.....	39
3-29	Tensile Strap Load from Simulated Intrusion Strap Test (Second Test).....	40
3-30	Intermediate Stage of Zinc Alloy Tool Construction.....	42

# LIST OF FIGURES (Cont.)

FIGURE		PAGE
3-31	Tooling Aids Used to Obtain Impala Door Dimensions.....	43
3-32	Detailed Drawing of Door Outer Panel Plus Intrusion Strap Compression Molding.....	44
3-33	Prototype Part as it Comes from the Zinc Alloy Mold and Prior to Trimming.....	46
3-34	Cross-Section of Molded Rib Showing Flow Pattern of SMC and Unidirectional Glass Material.....	47
3-35	Fabricated Checking Fixture used to Verify Dimensions and Shape of Molded Door Outer Panel.....	49
3-36	Location and Test Results of Intrusion Strap Tensile Specimens.....	50
3-37	Tooling Cost Comparison Between Steel Door and Composite Door with Composite Outer Panel Only.....	78
3-38	Cost Comparison Between Steel Door and Composite Door With Composite Outer Panel Only.....	79
3-39	Tooling Cost Comparison Between Steel Door and Composite Door With Composite Outer Panel which Includes Intrusion Protection.....	81
3-40	Cost Comparison Between Steel Door and Composite Door With Composite Outer Panel which Includes Intrusion Protection.....	82
3-41	Proposed Modification to the Composite Design which Eliminates Door-To-Hinge Adjustments.....	83

# LIST OF TABLES

TABLE		PAGE
3-1	Weight Breakdown of 1977 Impala Front Door.....	14
3-2	Weight Breakdown of Composite Outer Door Panel With Intrusion Strap.....	20
3-3	Baseline Impala Steel Door - Estimate For Door Outer Panel.....	55
3-4	Baseline Impala Steel Door - Estimate For Door Outer Panel Deadening Material.....	56
3-5	Baseline Impala Steel Door - Estimate For Intrusion Beam, Top (Component -1).....	57
3-6	Baseline Impala Steel Door - Estimate For Intrusion Beam, Bottom (Component -2).....	58
3-7	Baseline Impala Steel Door - Estimate For Intrusion Beam, Inner (Component -3).....	59
3-8	Baseline Impala Steel Door - Estimate For Intrusion Beam Assembly.....	60
3-9	Baseline Impala Steel Door - Estimate For Front Inner Reinforcement.....	61
3-10	Baseline Impala Steel Door - Estimate For Assembling Door Inner Panel and Front Inner Reinforcement.....	62
3-11	Baseline Impala Steel Door - Estimate For Assembling Door Inner Panel and Intrusion Beam.....	63
3-12	Baseline Impala Steel Door - Estimate For Assembling Door Inner and Outer Panels.....	64
3-13	Costing Scenarios For Composite Design.....	66
3-14	Impala Composite Door - Estimate For Upper Hinge Bracket (Component -4).....	67
3-15	Impala Composite Door - Estimate For Lower Hinge Bracket (Component -5).....	68
3-16	Impala Composite Door - Estimate For Latch Bracket (Component -6).....	69
3-17	Impala Composite Door - Estimate For Assembling Composite Door Outer Panel.....	70
3-18	Impala Composite Door - Estimate For Assembling Door Inner and Outer Panels.....	71
3-19	Baseline Impala Composite - Estimate For Door Outer Panel - Costing Scenario I.....	72
3-20	Impala Composite Door - Estimate For Door Outer Panel - Costing Scenario II.....	73
3-21	Impala Composite Door - Estimate For Door Outer Panel - Costing Scenario III.....	74
3-22	Impala Door With Composite Outer Panel - Estimate For Assembling Door Inner and Outer Panels.....	77
3-23	1978 U. S. Car Production Totals.....	85

## 1.0 SUMMARY

Low density composite materials have been touted to reduce automotive structural weight and thereby improve fuel economy for the combustion engine vehicle or improve range and performance for the electric vehicle. However, unless composite components can be fabricated at a cost, competitive with steel, they are unlikely to attain significant inroads. With the composite material costs ranging from a low of two times the cost of steel, a significant approach for composites to attain economic acceptance is by parts consolidation. Such a concept was used to evaluate the redesign of the steel door outer panel and intrusion beam of a 1977 Chevrolet Impala using glass/polyester composite materials. The redesign consisted of a single structure composed of a chopped glass/polyester outer skin co-molded with a continuous glass fiber/polyester intrusion protection in the form of a strap.

A full scale prototype was fabricated utilizing commercial composite materials and the compression molding fabrication approach which is found in an automotive mass production environment. While no complete door structure testing was performed, component tests indicated that the proposed composite design could satisfactorily meet the existing federal side door static intrusion test.

A significant weight reduction of nearly 11 pounds per door was established for the composite design compared to the baseline steel design based on replacement weight. In addition, thinner door structures would be possible due to the redesign of the intrusion protection. This could result in additional weight savings and lowered air resistance with a reduced frontal area.

A complete costing effort was performed to compare the composite design to the baseline steel design. The results indicate that for the current quantities of electric and hybrid vehicles considered, composite materials, used in a parts consolidation redesign effort of the door outer panel and intrusion beam or simply in a substitution mode for the outer panel would be cost competitive with steel. For automotive quantities, however, only the parts consolidation approach appears to be cost competitive using state-of-the-art production techniques. Only with the development of quicker cure resin systems or by using a multi-station curing arrangement does the substitution approach using composite material for steel appear to attain cost competitiveness. To fully understand the potential cost effective weight savings using composite materials, the total chosen vehicle would have to be reviewed and redesigned where possible.

It is recommended that the proposed composite door structure be tested, both to the existing federal static intrusion test and also to a more severe dynamic door impact test which has been proposed as a federal standard.

## 2.0 INTRODUCTION

With the objective of the program being to demonstrate production feasibility of cost competitive lightweight composite material components, a number of decisions need to be made - they involve which component is representative and also what composite material and manufacturing process will be chosen. Neither component of the problem, namely the part, material or manufacturing process, is independent from the other and hence cannot always be established separate from the others. One common concern, and that being low cost, allows, however, for the determination of general category answers.

Of all the families of structural composites, the one with glass fibers in a polyester resin has been shown to be the most economical for the majority of automotive applications and should find the widest acceptance. While specialty fabrication processes may be cheaper for a given part, the majority of automotive composite parts can be best made using compression molding. In light of the volume of parts required for an automotive application, compression molding is by far the most applicable process for the general automotive component. The most difficult decision then involves the choice of which component is structurally representative and can still utilize the glass/polyester system with compression molding.

In spite of the fact that raw composite materials costs range from a low of two times the per pound cost of steel, composites have found usage in such areas as grill opening panels. This application results from the fact that the single composite part is cheaper than the 10 to 16 metal parts that it replaces. In addition most composite applications result in a reduction in component weight which reduces the significance of the material cost differentiation. Parts consolidation, and its corresponding reduction of assembly steps, then becomes a significant approach to making composite structures cost competitive with the baseline metal design. Not all parts, however, are amenable to parts consolidation and must be therefore compared on a substitution basis.

The choice within these two distinct component categories, namely components which are associated with parts consolidation and ones which only involve direct substitution, was to attempt the more difficult consolidation effort. This approach resulted in a prototype component being built but both the consolidated concept and the substitution of the baseline metal design by composites were costed. Such an approach was used in the redesign of a driver's door outer panel from a 4-door 1977 Chevrolet Impala. The substitution costing phase came about through replacement of the outer panel with a chopped glass/polyester resin system. The parts consolidation effort involved the co-molding of the chopped glass/polyester resin system for the outer panel along with a continuous glass fiber/polyester resin system for the intrusion protection.



The title of the contract involves "A Mass Reduction Effort of the Electric and Hybrid Vehicle". The logical question then is why is a 1977 Chevrolet Impala door being used as the baseline? First of all the choice of a door structure is not unique to the type of vehicle. It has certain common functional and structural requirements independent of car type. The choice of this existing steel design as the baseline was based on a series of considerations starting with the fact that the Impala door represents an automotive industry accepted design. Also the baseline door weight is easily established and the door's costs can be reasonably estimated. Finally, if the redesigned door were to be tested to meet current federal Safety Standards, an actual vehicle structure would be required. It was therefore thought that it would be more realistic to obtain 1977 Chevrolet Impalas than electric vehicles for destructive testing purposes.

As far as the Impala door outer panel being a typical automotive component, it must satisfy a number of stringent design criteria. In the area of structural requirements, it must assist in satisfying the existing Federal Motor Vehicle Safety Standard (FMVSS) 214 which is a side door static intrusion test, as well as corporate standards. The corporate requirements would include such loading conditions as a vertical load applied to the latch when the door is opened; a vertical load applied to the rear edge of the opened door inner panel to create a torsional loading; and a transverse load on the door outer panel. Additional requirements would involve a deformation criteria on the window frame to insure that an acceptable wind and moisture seal is maintained. In addition to the stringent structural criteria, the door outer panel must also meet rigid finish and visual standards.

Prior to evaluating the existing and redesigned door outer panels, attention is brought to Appendix A, "Material Selection Report". This included report presents mechanical properties for the various types of glass/polyester systems considered in the study. A description of the materials and the fabrication processes for these materials are also included. In the remaining sections of this report it will be assumed that the reader is familiar with the various materials and the meanings of the standard nomenclature used. If questions arise along these lines, the answers will be found in Appendix A. In a similar manner, Appendix B, "Process Selection Report", describes the equipment and molding requirements for the compression molding process which was utilized to manufacture the prototype part.

### 3.0 TECHNICAL DISCUSSION

#### 3.1 Baseline Steel Design

The chosen baseline door, from a 1977 4-door Chevrolet Impala, is shown in Figure 3-1 where the major structural components of the door have been identified. Figures 3-2 and 3-3 show the baseline door after removal of the outer skin and then additionally the steel intrusion beam respectively. Figures 3-4 through 3-6 show the attachment of the built-up steel intrusion beam to both the front and rear of the door as well as the attachment of the hinges and the latch. Figure 3-7 shows the location of the deadening material which is applied to the exterior steel skin. The beam is welded to the door inner panel which is then mechanically attached to the hinges and latch as shown in Figures 3-8 and 3-9 respectively. All hardware except the exterior handle, lock, and side mirror are mechanically fastened to the door inner panel. The outer panel is a relatively simple shaped steel sheet which is attached to the inner panel with edge welds and a crimping of the outer panel over the inner panel's peripheral flange. The weight of the complete door is 68 pounds and the component breakdown is shown in Table 3-1. The weight of the items to be replaced is 25.5 pounds and includes the outer panel, intrusion beam, front inner reinforcement, and outer panel deadening material.

#### 3.2 Composite Design

The composite design concept is shown in Figure 3-10. It employs a sheet molding compound (SMC) outer panel co-molded with the continuous glass fiber intrusion protection to which is bonded the inner panel. As can be seen the inner panel, latch, and window frame remain identical to the baseline steel design. In this way, the mounting of the door hardware remains unchanged as well as the hardware itself, and a sturdy foundation for preventing excessive deformation of the window frame is insured. In addition, if the door would be subsequently tested per FMVSS 214, then a true assessment of a co-molded composite door outer panel with an intrusion resistant strap can be made since it is the only change made to the door structure.

The program as originally structured and funded was to redesign and fabricate a single representative component out of composite materials. Even if additional funding were provided, the concept chosen would not have benefited by designing an inner panel out of SMC material, even though it is technically feasible. Such a component probably would not be as cost effective as the baseline steel design because there is little chance for part consolidation. Attachment of door hardware could then become more expensive due to the possible need of metal inserts. Also it would be more difficult to provide acceptable deformation levels of the window frame to assure satisfactory sealing. To complete the picture for the structural aspects of door, the existing door design would not allow a low cost composite window frame due to the inability to duplicate the required stiffness with continuous glass fiber and still maintain the geometric constraints.

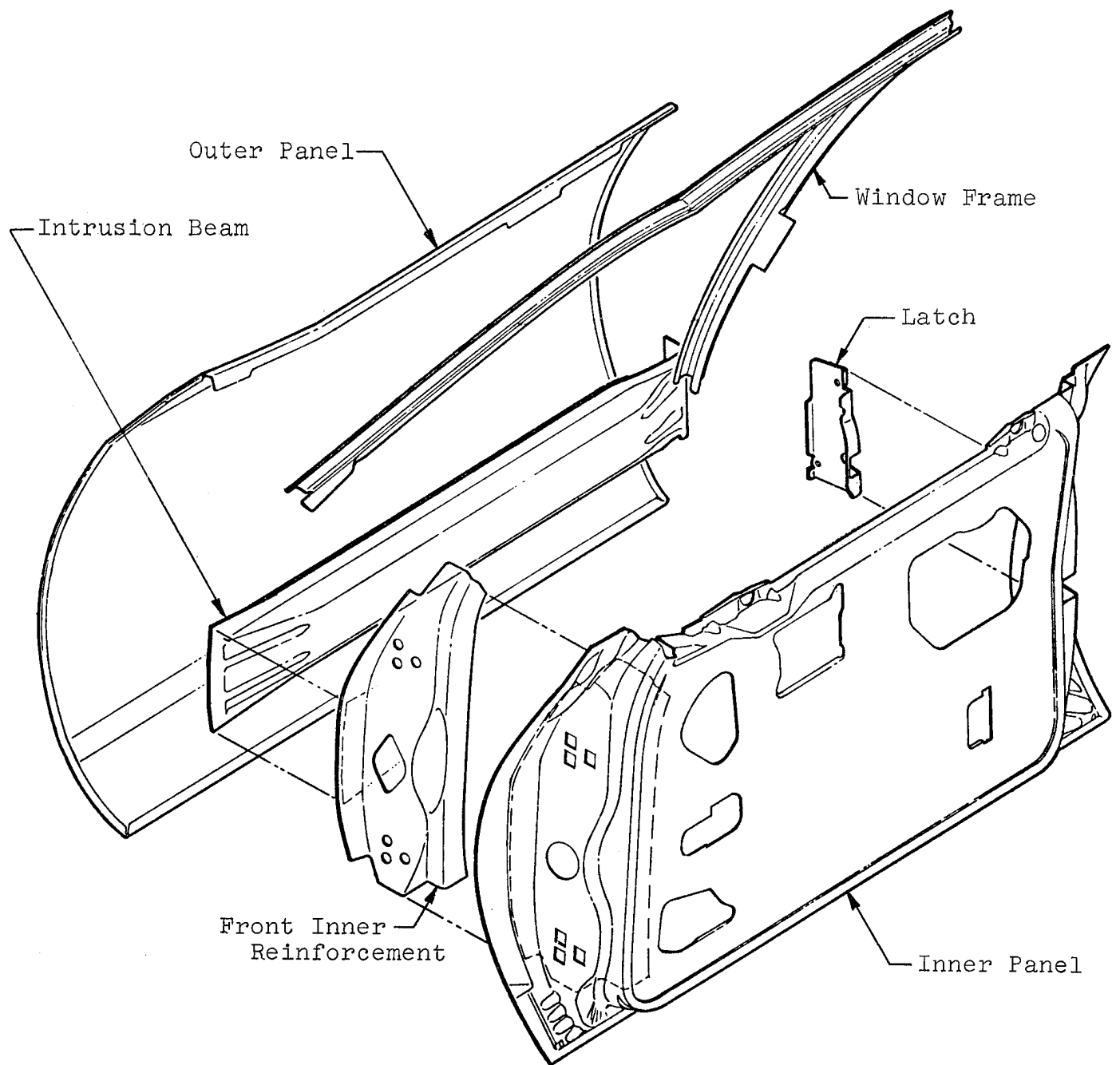


FIGURE 3-1 1977 CHEVROLET IMPALA FRONT DOOR

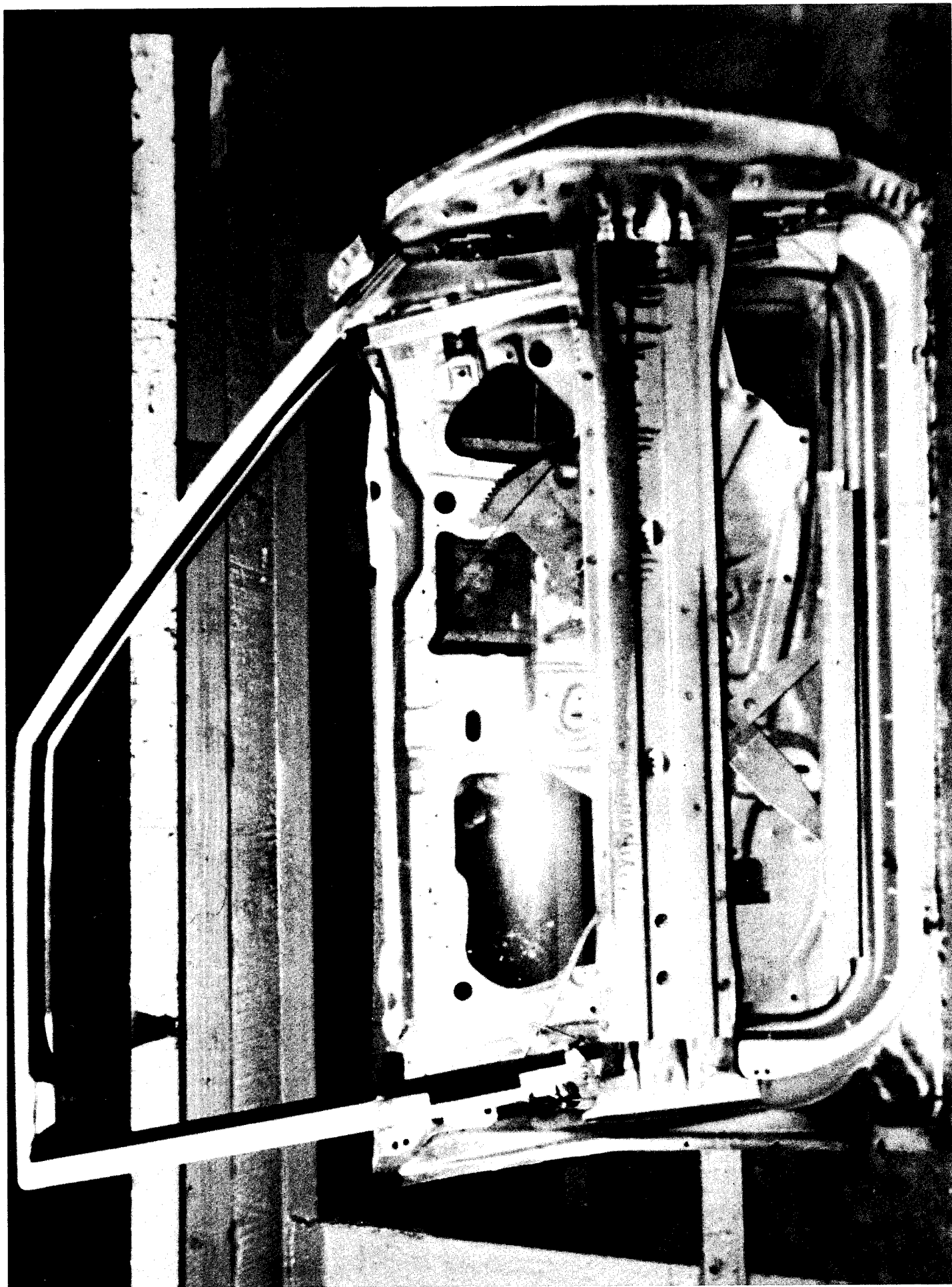


FIGURE 3-2 IMPALA DOOR AFTER REMOVAL OF OUTER SKIN

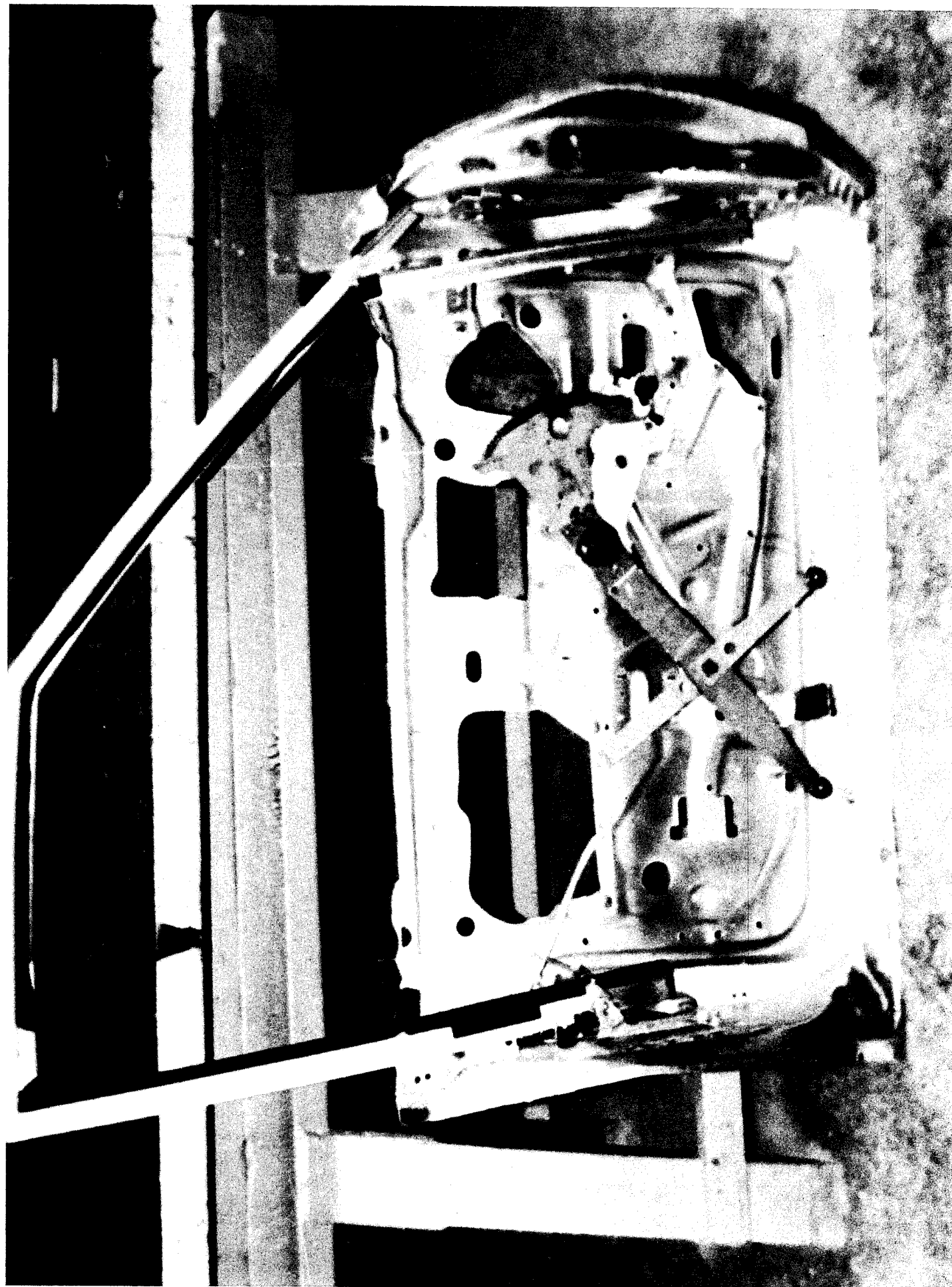


FIGURE 3-3 IMPALA DOOR AFTER REMOVAL OF OUTER SKIN AND INTRUSION BEAM



FIGURE 3-4 ATTACHMENT OF INTRUSION BEAM TO FRONT OF DOOR



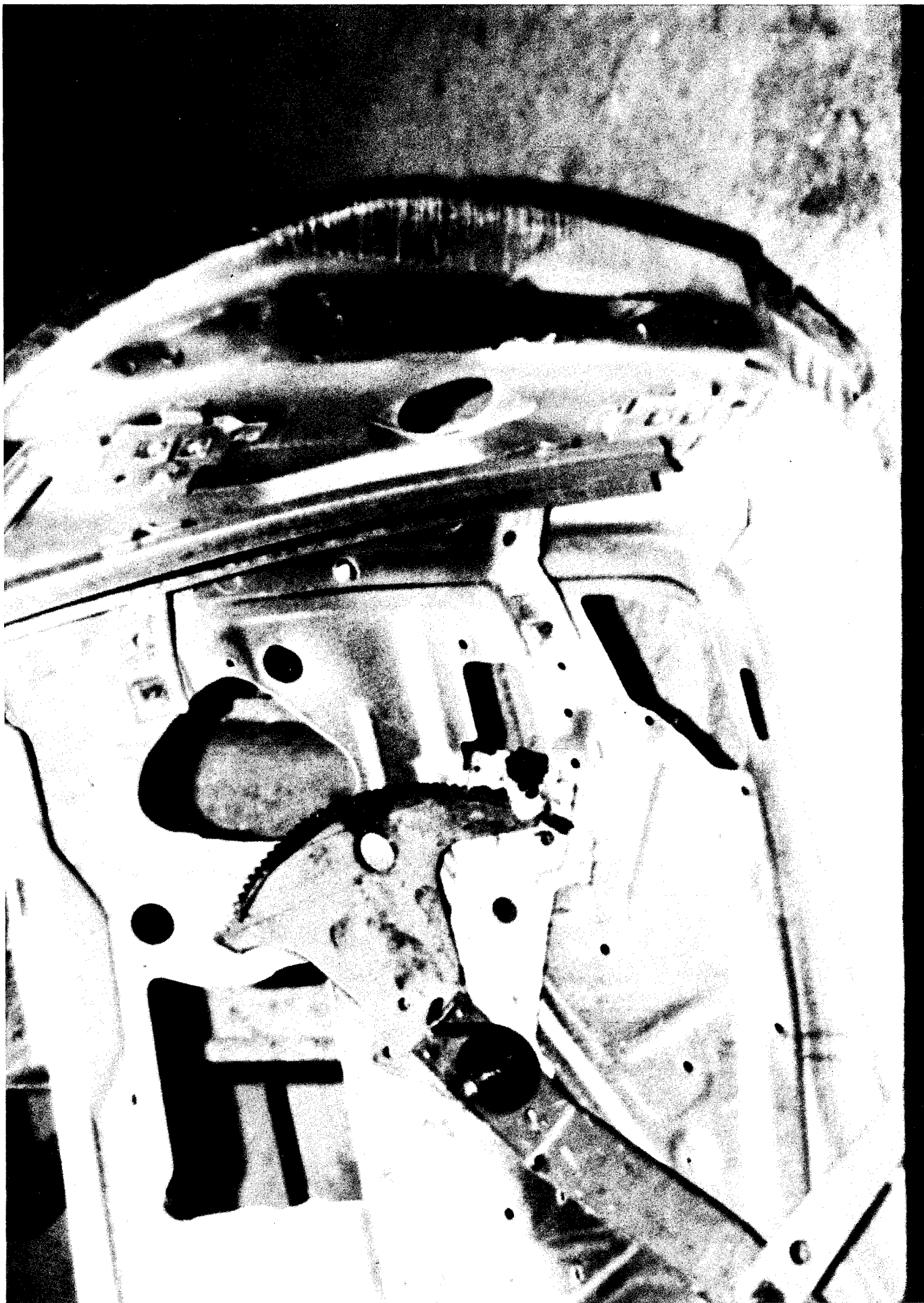


FIGURE 3-5 LOCATIONS FOR ATTACHMENT OF HINGES



FIGURE 3-6 ATTACHMENT OF INTRUSION BEAM AND LATCH TO REAR OF DOOR



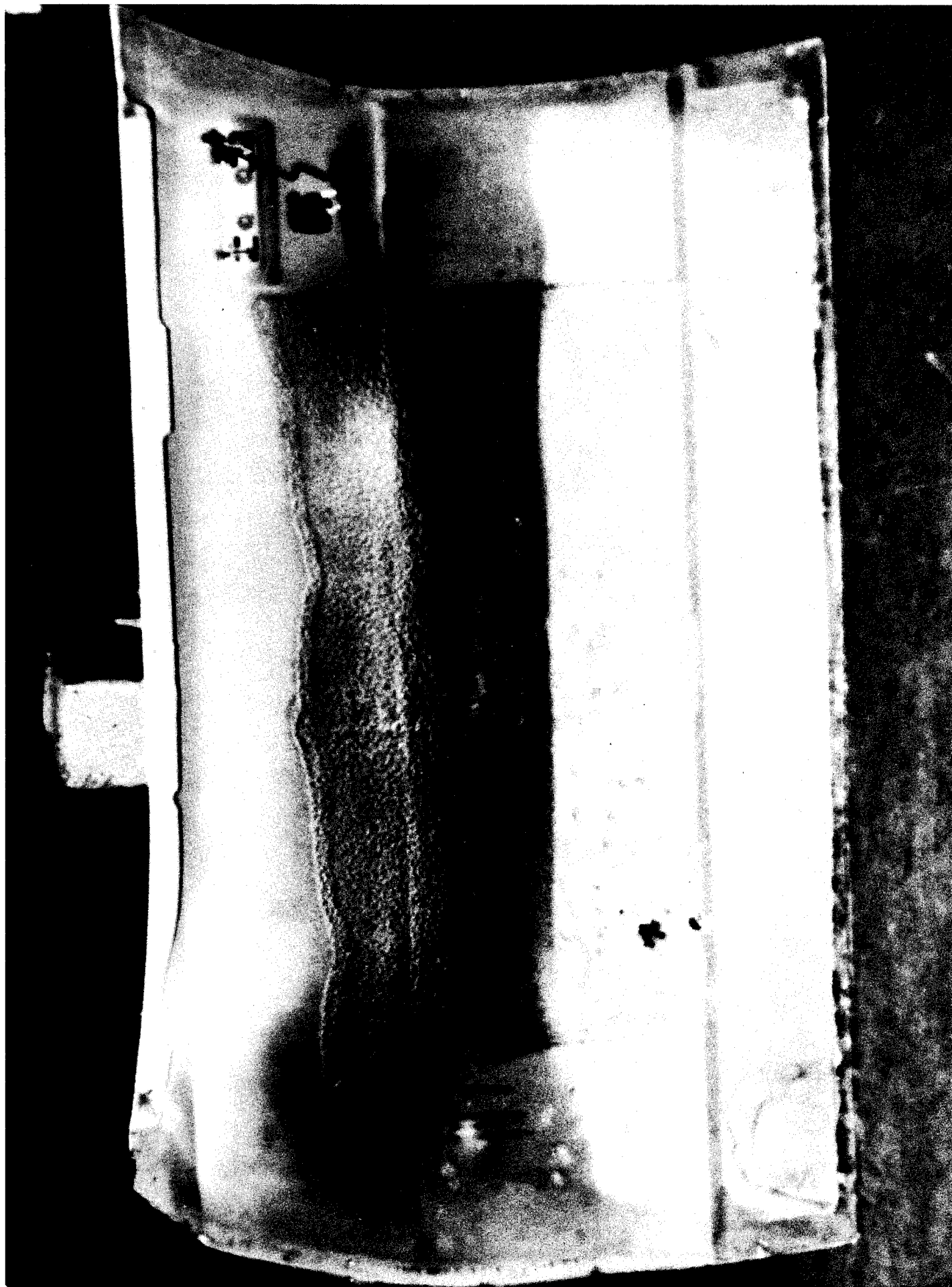


FIGURE 3-7 OUTER DOOR PANEL WITH DEADENING MATERIAL

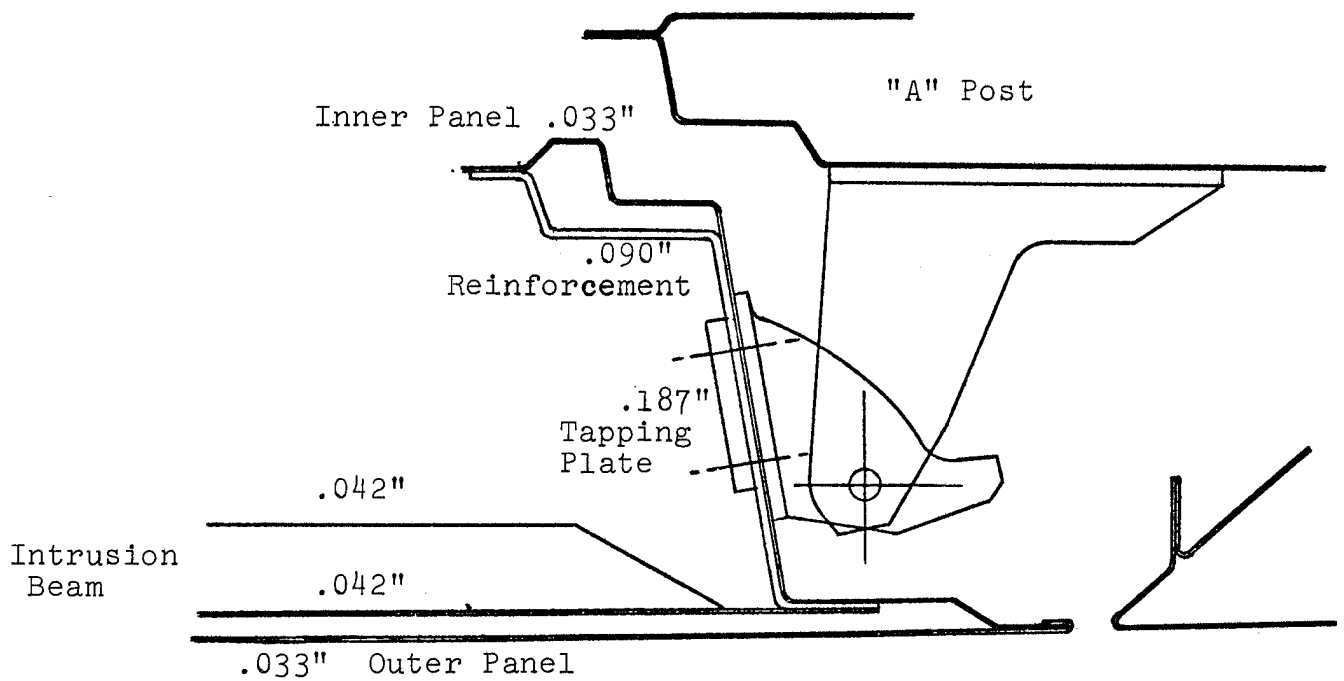


FIGURE 3-8 EXISTING CONFIGURATION FOR A STEEL IMPALA DOOR AT THE HINGE

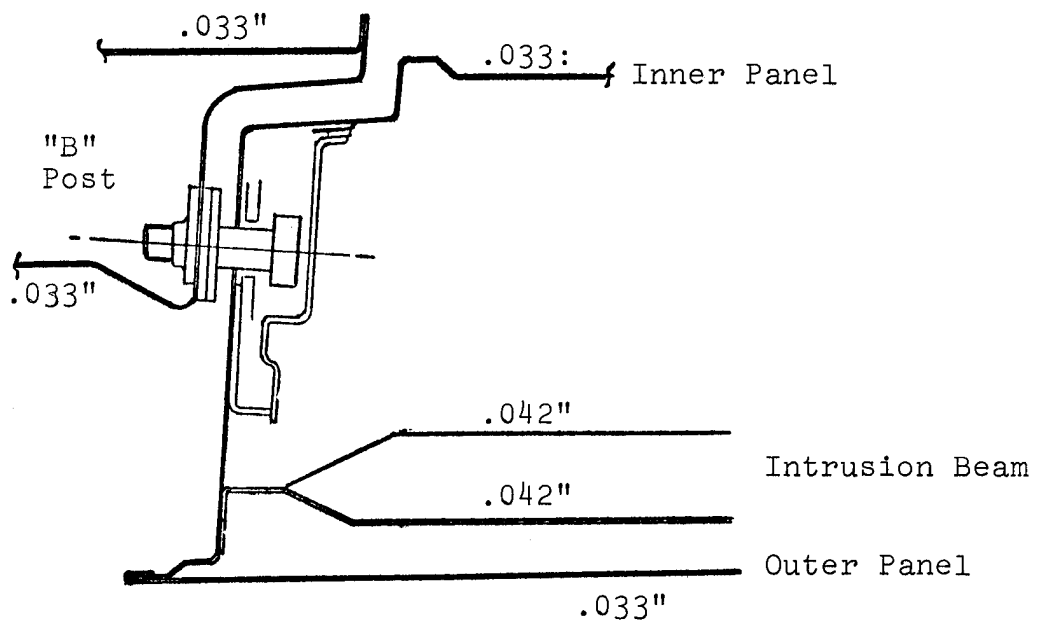


FIGURE 3-9 EXISTING CONFIGURATION FOR A STEEL IMPALA  
DOOR AT THE LATCH

TABLE 3-1 WEIGHT BREAKDOWN OF 1977 IMPALA FRONT DOOR

<u>PART</u>	<u>WEIGHT (LBS.)</u>
Inner Panel With Paint	11.5
Outer Panel With Paint	11.6
Outer Panel Deadening Material	1.3
Intrusion Beam	8.4
Upper Window Frame	5.0
Weather Stripping	2.0
Glass	9.0
Hinge Tapping Plates (2 Pieces)	0.6
Cage For Hinge Tapping Plates (2 Pieces)	0.2
Outside Handle Assembly	0.4
Outside Lock Cylinder	0.2
Window Channel Retainer	0.9
Front Inner Reinforcement	4.2
Front Window Channel Guide	0.8
Window Stop Bracket	0.3
Inside Latch Release Assembly	0.7
Latch Assembly	2.0
Window Regulator Assembly	4.0
Inner Trim Panel	3.3
Arm Rest	1.6
	<hr/>
TOTAL	68.0

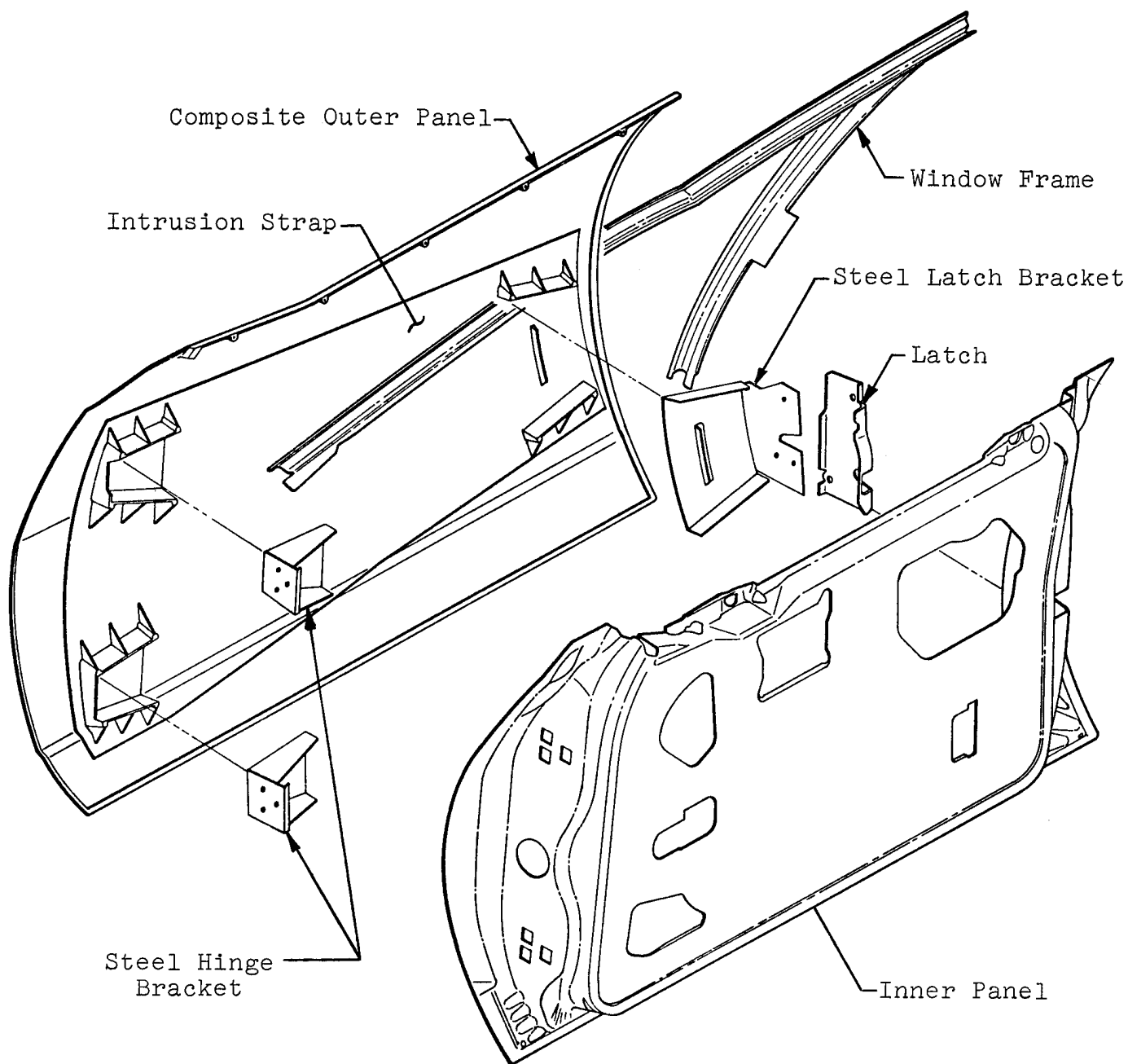


FIGURE 3-10 1977 CHEVROLET IMPALA FRONT DOOR WITH  
COMPOSITE OUTER PANEL AND INTRUSION STRAP

One further consideration regards the area of passenger safety. With a chopped glass SMC inner panel, intrusion into the door could cause its fracture thereby posing a threat to the occupant. This failure possibility could be minimized by including some amount of continuous fiber in the molding of the inner panel. Such a remedy would most assuredly cause the cost of the inner panel to not be competitive with the existing steel design. On the basis of strength and deformation requirements, safety considerations, and of course cost, the choice of a steel inner panel and window frame with a composite outer panel and intrusion protection provides an excellent first design for developing a lighter weight door structure.

Shown in Figure 3-10 are a series of ribs which form pockets and are co-molded with the outer panel. The attachment of the composite strap to the hinges is through steel brackets which are bonded to the intrusion strap and ribs and then bolted to the hinge. A similar steel bracket is used to attach the intrusion strap to the latch. The arrangement of the various material types used in the redesigned composite outer panel is shown in Figure 3-11. Mechanical properties and material descriptions for the various materials described in Figure 3-11 are presented in Appendix A.

### 3.2.1 Material Considerations

As seen in Figure 3-11, the door outer panel uses the common SMC material which can provide a class "A" automotive acceptable surface finish. The material is approximately 0.080 inches thick. The larger strength requirements of the ribs require that they utilize the higher fiber content HMC material. Additional weight savings could be obtained by replacing the SMC outer covering with an SMC material which contains microballoons. The price to be paid for this greater weight savings, however may be higher finishing costs.

The intrusion strap requires greater strength and impact resistance than what is afforded by the chopped glass SMC or HMC systems. Continuous glass fiber material was used, approximately 0.080 inches thick, to satisfy the required structural considerations. Two continuous fiberglass systems were tried with both being found acceptable. The two systems, neither of which can provide a class "A" finish by themselves, are PPG Industries' XMC-3 material and Owens Corning's C/R material. Both of these systems have combinations of continuous and chopped glass with the chosen system containing 50% continuous and 15% chopped glass.

The reason for including chopped glass in these predominantly continuous fiber materials is two-fold. First of all with a partial engagement of the strap, the chopped glass, which is interspersed between the continuous fiberglass, might assist in shearing the intrusion load to additional parts of the strap and to

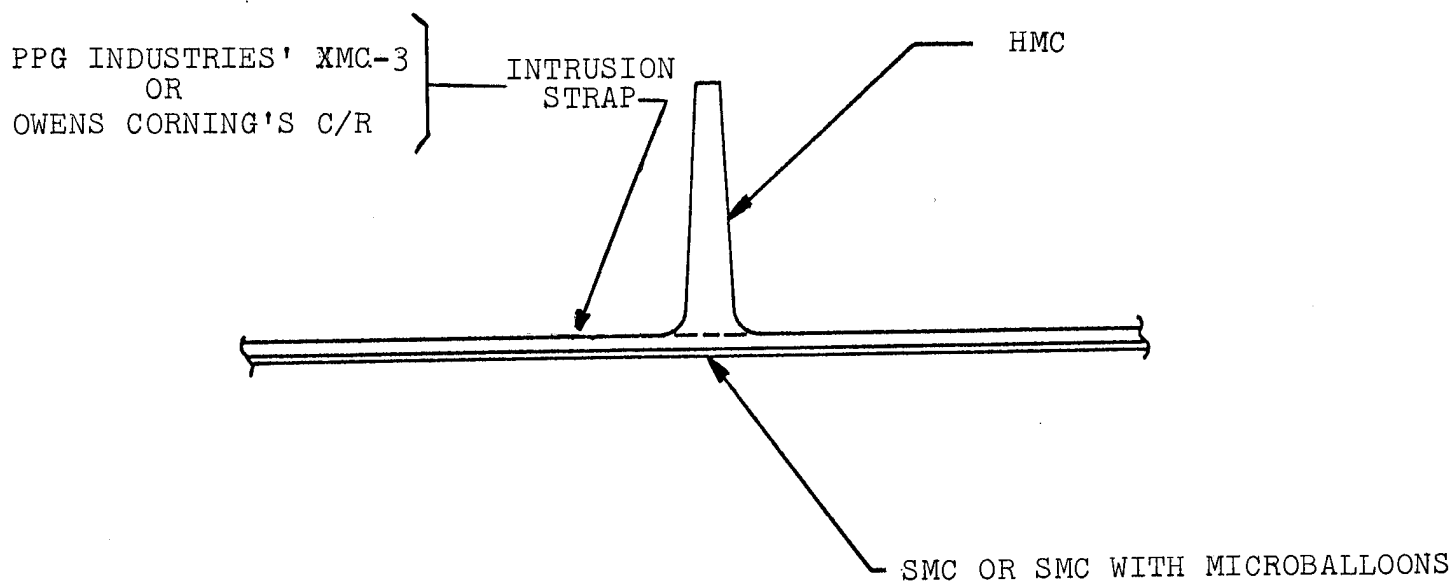


FIGURE 3-11 CONSTRUCTION DETAILS FOR DOOR OUTER  
PANEL INCLUDING INTRUSION PROTECTION

the other hinge reaction. Also the chopped glass provides a more thermally stable laminate which will minimize thermal distortion caused by cooling down from the cure temperature. The effect of the chopped fibers is seen dramatically in Figure 3-12. The use of a low shrink system by itself is not sufficient to eliminate the thermal distortion shown in Figure 3-12 without the use of chopped glass fibers.

Another important consideration was verified in Figure 3-12. When the continuous glass fiber system is placed in a mold and pressure applied, the system cannot flow parallel to the primary reinforcement direction. In the transverse direction, however, significant flow can occur unless the material was originally cut to fill the entire mold cavity. For the current design, minimum weight and cost efficiency could only be obtained by locating the continuous fiber material over a portion of the compression molded part. Figure 3-12 thereby verifies that this material can be restrained in the transverse direction with minimal fiber washing, if a well defined cavity is provided in the mold.

### 3.2.2 Weight Summary

The specific parts of Table 3-1 which are addressed in the redesign effort are tabulated in Table 3-2. The corresponding weights for the redesigned components are shown in the same table, with a weight savings of almost 11 pounds per door projected. The steel baseline outer panel is shown to have 1.3 pounds of dampening material applied to it. This material was not included on the composite panel because of its thicker construction. Support for not including this material comes from reviewing the Corvette door outer panel. It is made solely from SMC material, approximately 0.080 inches thick, and it also does not have the deadening material.

The weight savings presented in Table 3-2 is simply the substitution weight savings. No additional benefit was taken for interacting weight reduction which occurs by downsizing other components such as engine and drivetrain, suspension system, brakes, and so on. A major additional weight savings is possible because the intrusion beam has been eliminated. The result of this composite concept is that the door can be designed narrower. Following this thought one step further, the thinner doors would allow, for the same interior passenger room, narrower cars if the styling allows it. The weight savings with such an approach would be significant. In addition, additional fuel economy would occur as a result of reduced frontal air resistance.

### 3.2.3 Structural Configuration

The configuration of the steel hinge bracket bonded into the HMC rib pocket is shown in Figure 3-13 where the steel bracket is shown to be flaired open. The result of this configuration is a



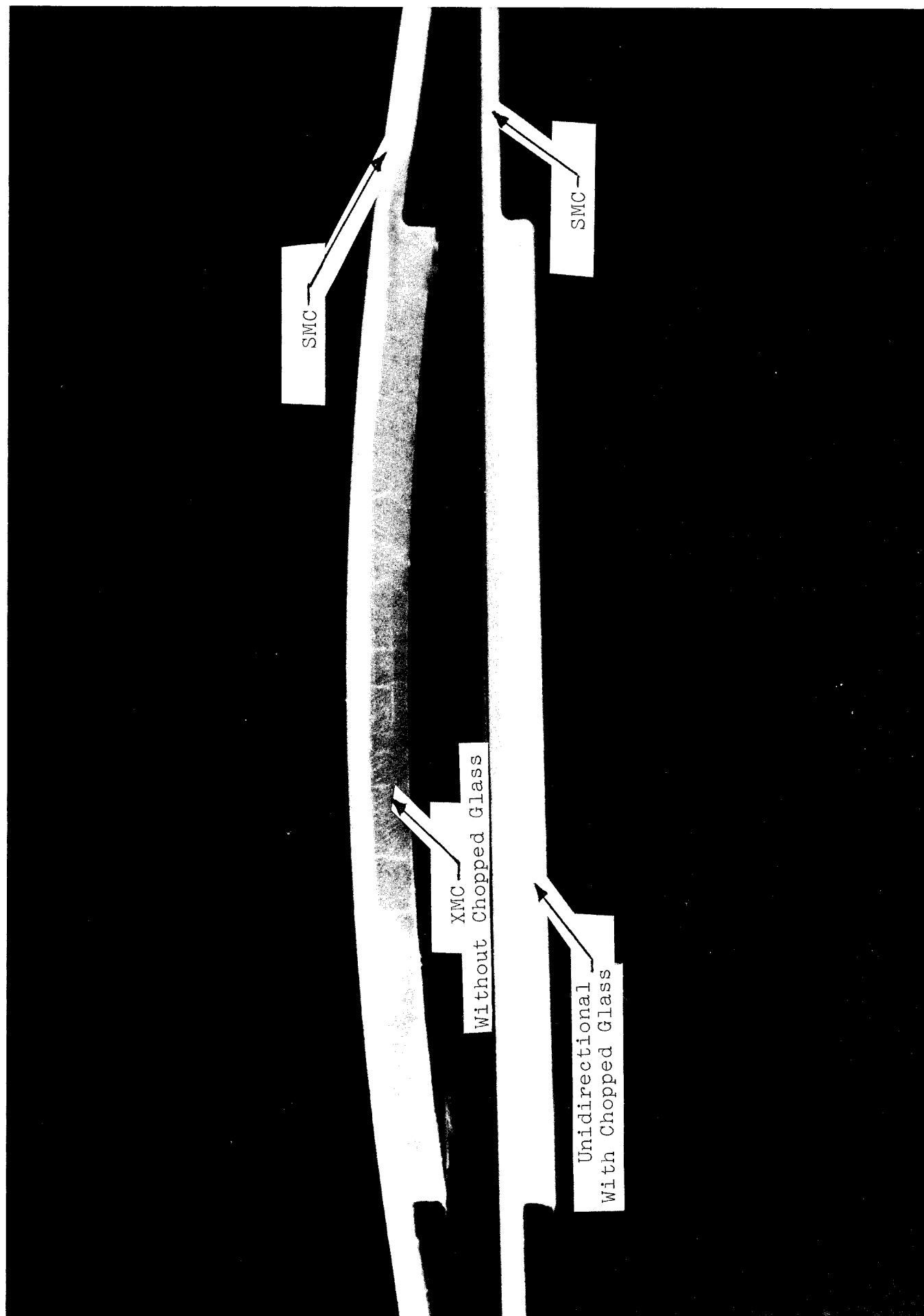


FIGURE 3-12 RESULTS OF COCURING UNIDIRECTIONAL STRAP WITH SMC SKIN

TABLE 3-2 WEIGHT BREAKDOWN OF COMPOSITE OUTER  
DOOR PANEL WITH INTRUSION STRAP

WEIGHT OF STEEL BASELINE:

Outer Panel With Paint	11.6 Lbs.
Outer Panel Deadening Material	1.3
Intrusion Beam	8.4
Front Inner Reinforcement	4.2
	<hr/>
	25.5 Lbs.

ESTIMATED WEIGHT OF COMPOSITE DESIGN:

Composite Material	11.0 Lbs.
Paint	0.3
Two Hinge Brackets	1.4
Latch Brackets	1.7
Adhesive	0.2
	<hr/>
	14.6 Lbs.

WEIGHT SAVINGS: 10.9 LBS. PER DOOR

43% WEIGHT SAVINGS

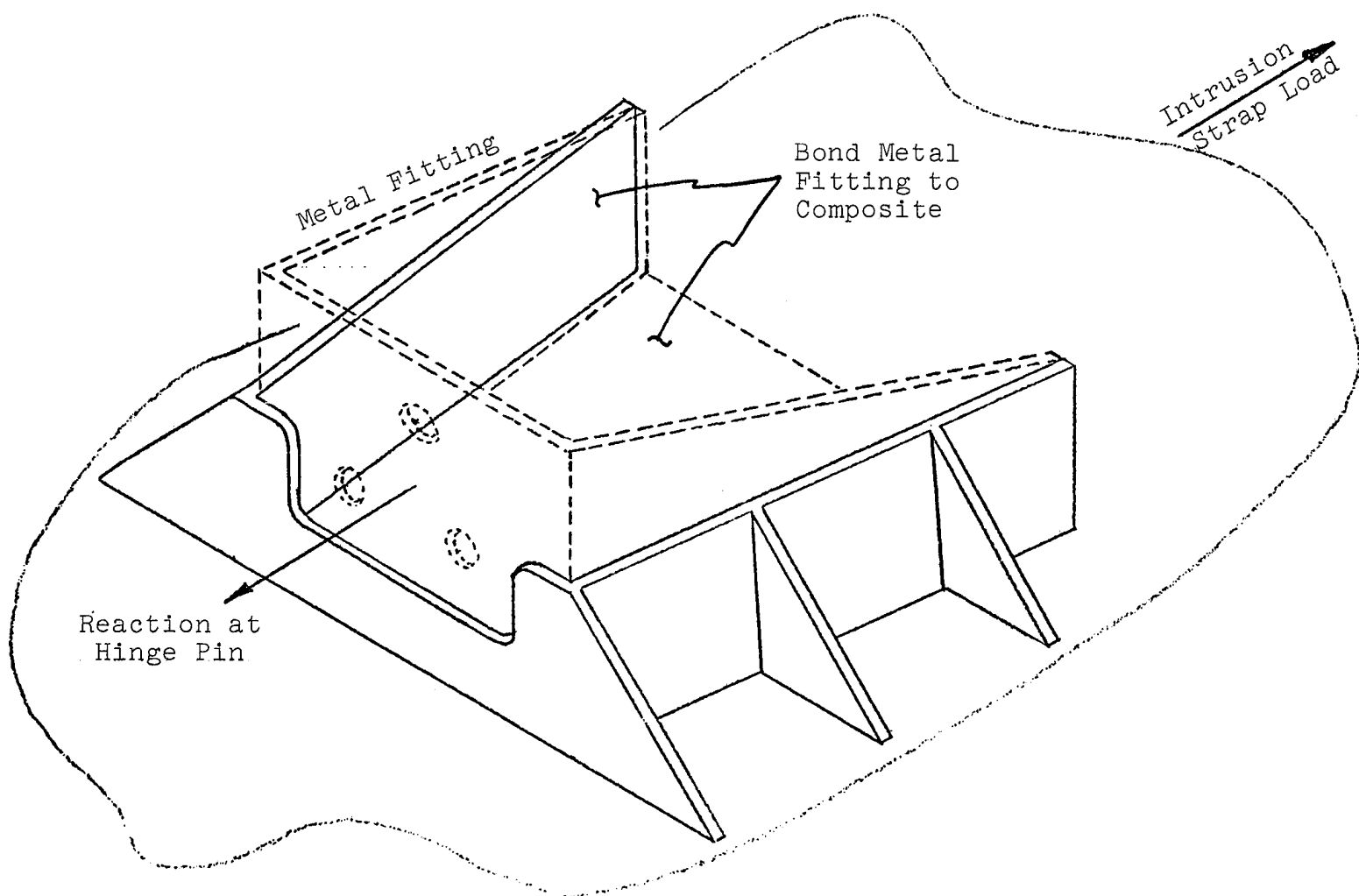


FIGURE 3-13 HINGE ATTACHMENT FITTING TO  
INTRUSION STRAP

mechanical lockup of the steel fitting into the ribbed pocket. While the steel fitting is bonded to the strap and ribs, it is hoped that the provision of the mechanical lockup will eliminate the need for excessive quality control checks using nondestructive testing. The small diagonal ribs shown in Figure 3-13 assist in reacting the loads developed by the mechanical locking. The subsequent attachment of the steel hinge bracket to the hinge using bolts is shown in Figure 3-14.

In providing a mechanical lock of the steel fitting in the rib pocket, the rib thickness was sized to provide adequate shear resistance to react the intrusion tensile load. As the tensile strap load is picked up by the steel bracket, a moment is generated which tends to rotate the bracket away from the strap. This peel loading is reacted by the ribs, with sufficient rib height required, through shear in the rib to bracket bond. In actuality there is a redundancy in the design in that these peel loads, caused by the overturning moment, can be taken out as a peel load through the larger bond attachment area of the inner panel to the outer panel.

With the existing steel intrusion beam, the side door intrusion is reacted initially by the bending resistance of the closed beam section as well as by the steel's plasticity. Subsequently, membrane tension occurs in the steel beam which draws the door posts into assisting with the energy dissipation. In going to an intrusion strap, the benefit of the initial bending resistance is lost. Hence it is important that the membrane tension loading in the strap occurs early in the door intrusion so other parts of the car structure assist to react the deformation. As can be seen in Figure 3-15 a, the structural configuration would allow excessive deformation with little resistance if the ends were allowed to rotate. If the fixity at the strap ends is increased, then the membrane tension occurs early with the intrusion as seen in Figure 3-15 b.

With the consideration of the end fixity, it was important to design the steel brackets with as little flexibility as possible. Figures 3-16 through 3-18 provide the detailed drawings of the upper and lower hinge brackets and latch bracket respectively. While these brackets would, in production, be formed out of single pieces of material using draw dies, they are shown as welded structures in the accompanying figures. They were drawn this way because that is how they would be fabricated for prototype parts. As can be seen, webs and flanges are provided where possible to create stiff brackets.

The hinge itself provides rigidity in that it locks up after approximately 11 degrees of inward rotation as shown in Figure 3-19. The latch remains a potential problem in that the present design does not provide significant fixity prior to the door contacting the car support pillar. If additional fixity is shown to be required, then the Volkswagen type of catch can be used as displayed in Figure 3-20.

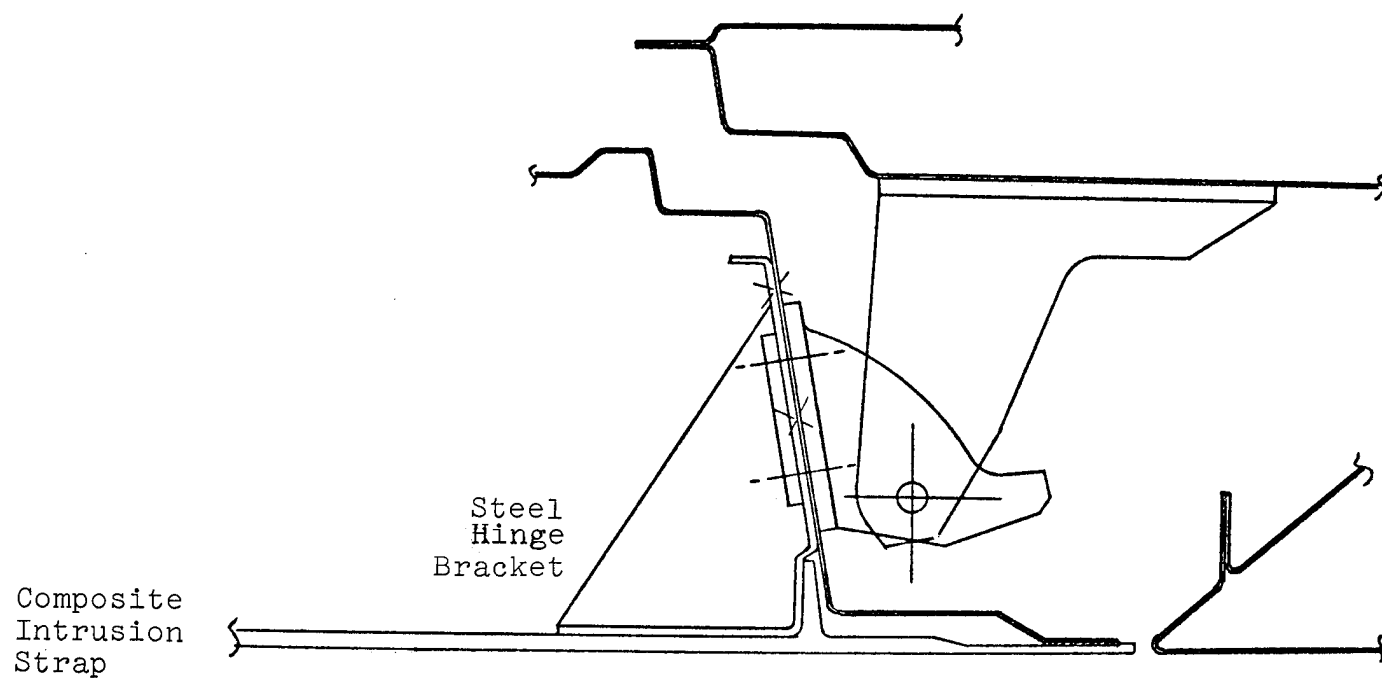
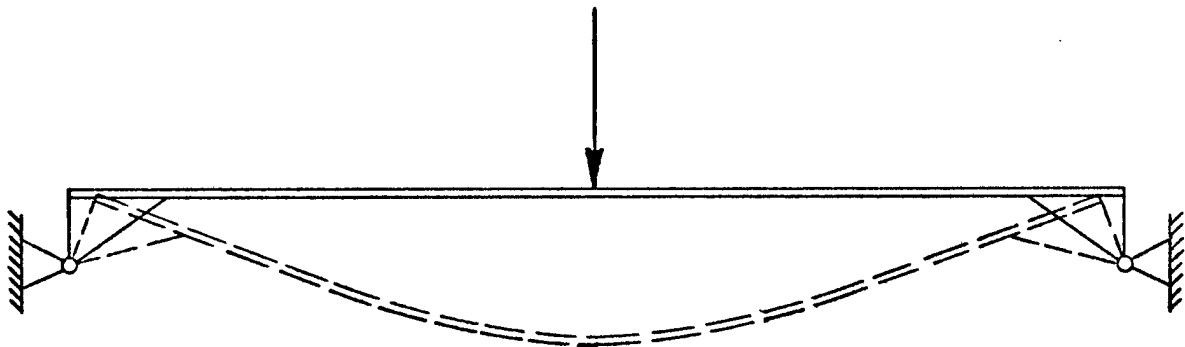
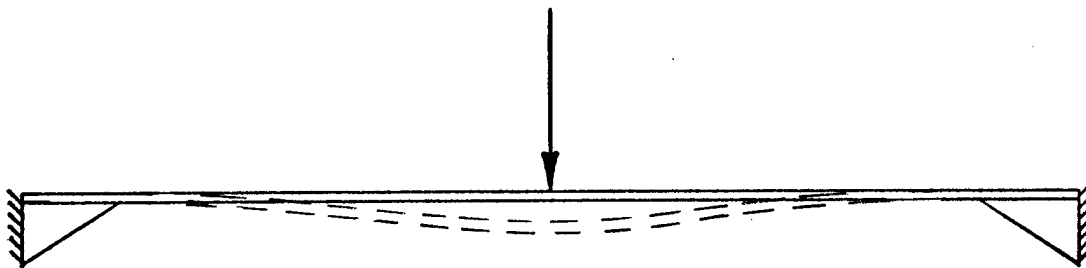


FIGURE 3-14 HINGE ATTACHMENT TO COMPOSITE  
INTRUSION STRAP



(a)



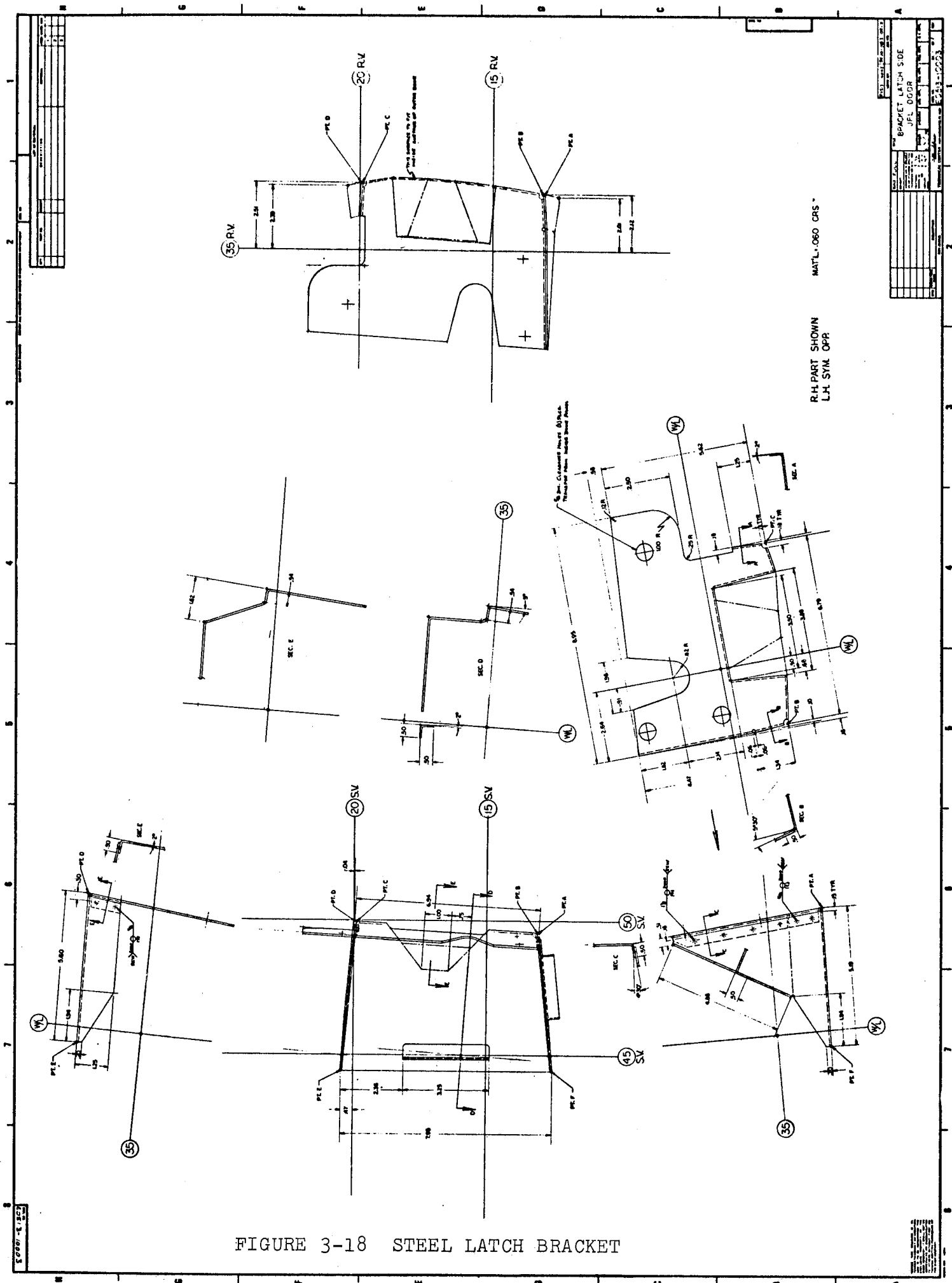
(b)

FIGURE 3-15 EFFECT OF END FIXITY ON THE DEFORMATION RESISTANCE OF THE INTRUSION STRAP



FIGURE 3-17 STEEL LOWER HINGE BRACKET





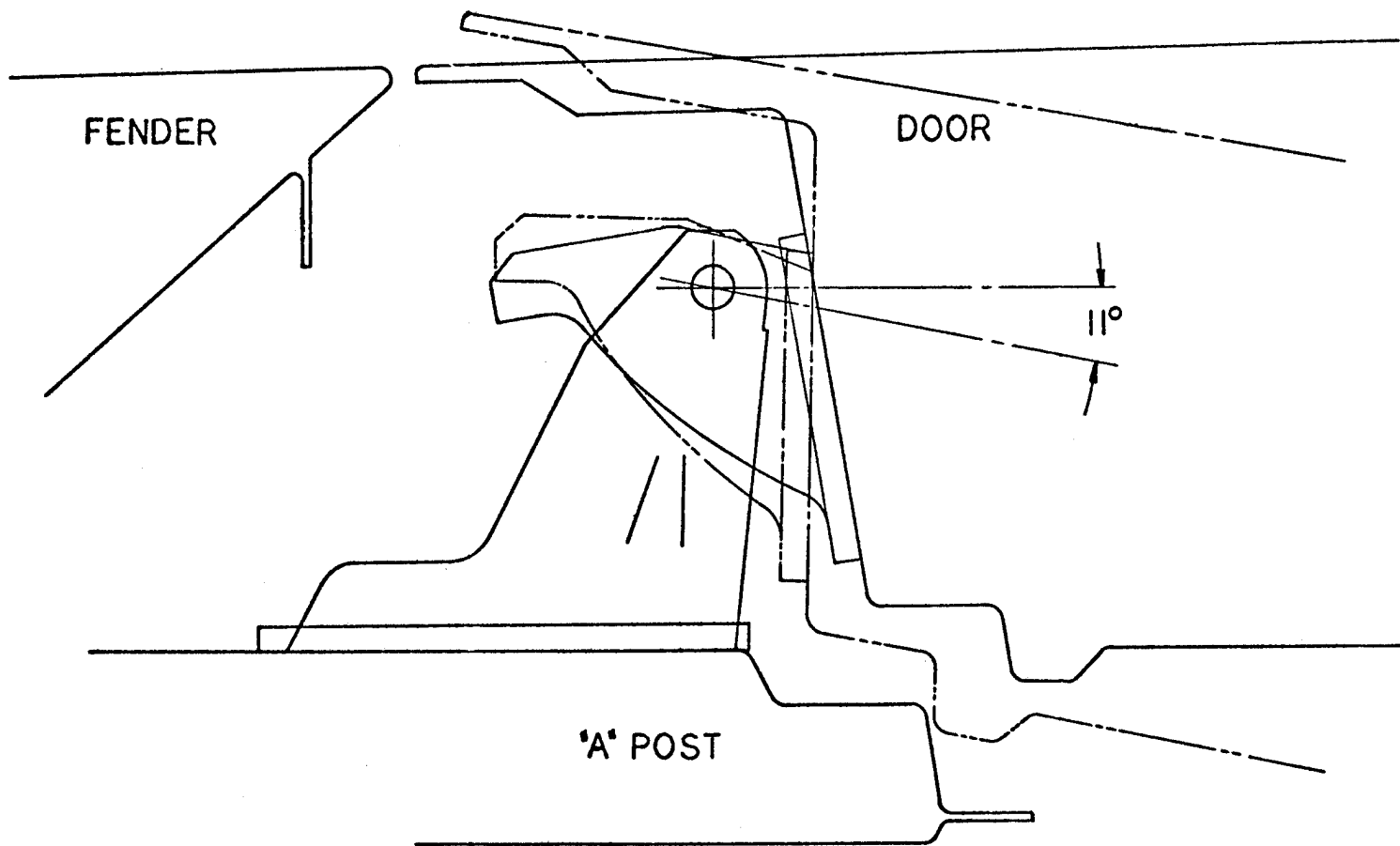


FIGURE 3-19 MAXIMUM ROTATION PRIOR TO A  
MECHANICAL LOCKUP IN THE HINGE

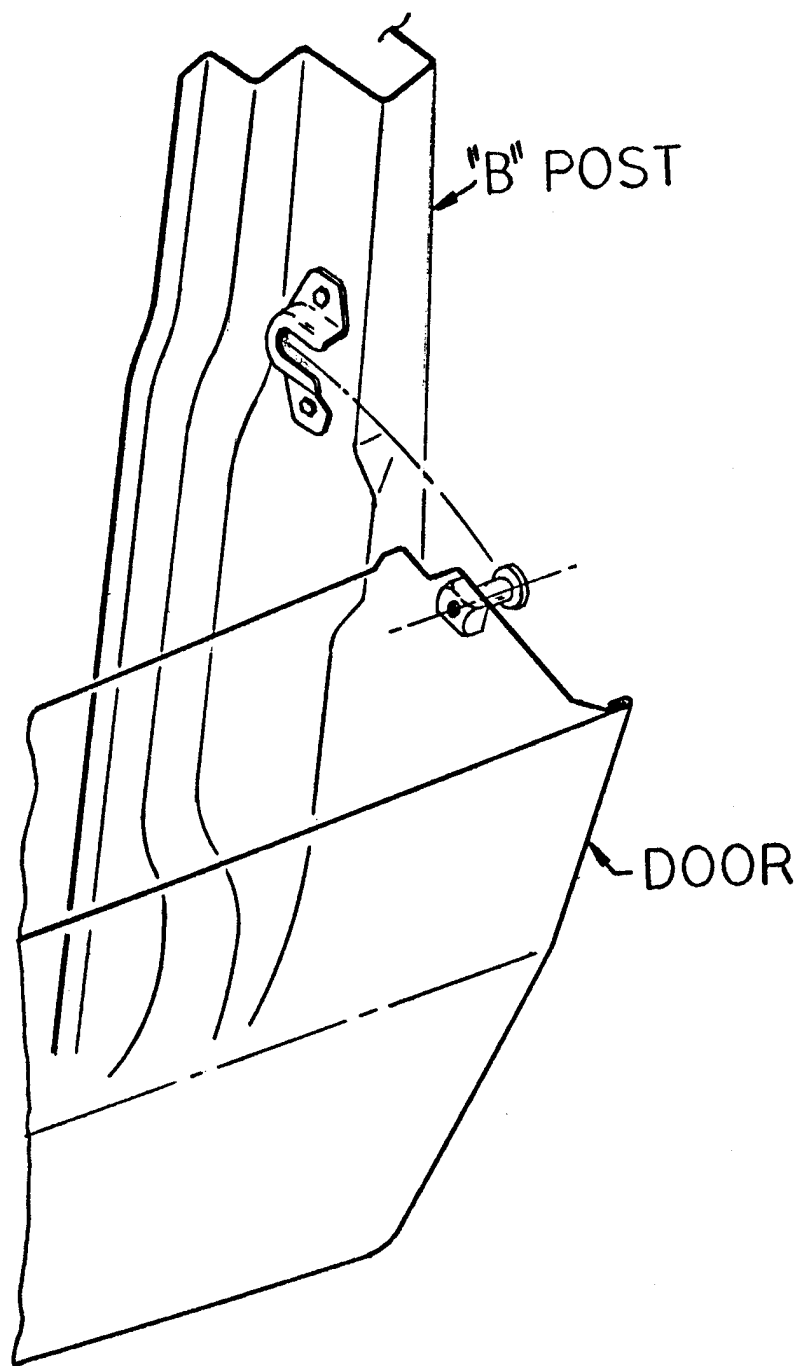


FIGURE 3-20 VOLKSWAGEN TYPE FIXITY HOOKS

In addition to the door structure seeing side intrusion loading, it must also react compressive loads coming from a frontal impact. The baseline steel design has a closed section which could react such loads efficiently. The end configurations of this steel beam are, however, flat plates as shown in Figures 3-8 and 3-9. The end configurations thus reduce the efficiency by which the existing steel intrusion beam can react these compressive loads. While the redesigned composite intrusion strap is just that, a strap, it does offer resistance to compressive end loads because of the curvature of the outer panel which the intrusion strap duplicates.

### 3.2.4 Simulated Intrusion Strap Tests

Prior to completion of the full size compression mold, an approximation of a portion of the intrusion strap and the ribbed pocket area of Figure 3-13 was molded. The simulated pocket was molded without a locking taper and without the short diagonal ribs (see Figure 3-21). The first test using the molding shown in Figure 3-21 involved putting a tensile load into the intrusion strap portion of the molding and reacting it at the location of the hinge pin as shown in Figure 3-22. This loading introduced both shear and peel loads into the joint configuration. The excessive peeling deformation caused premature failure. The resulting force/deformation response along with a photograph showing the failure mode are shown in Figure 3-22. While the test was not truly representative, it did confirm that a satisfactory shear tie existed between the intrusion strap and the ribs.

Two additional tests were performed using the molding shown in Figure 3-21. For both of these tests, two such moldings were joined with a steel strap and a central simulated intrusion load applied. Both tests were identical except for the end conditions. In the first test a 3/8" thick piece of angle iron connected the test frame to the steel brackets which were bonded into the ribbed pockets. In the second test the same angle iron attachments had steel gussets welded to the legs to prevent rotation. Figure 3-23 shows the post test photograph for the second test which was terminated due to yielding of the test frame. The gussets welded to the angle iron can be observed. Figure 3-24 presents the excessive distortion observed in the angle iron used in the first test which caused the test to be terminated after the intrusion strap bottomed out in the test fixture.

The gussets used in the second test eliminated the rotational distortion seen in Figure 3-24. As a result, higher force levels were developed which led to the distortion of the test fixture as shown in Figures 3-23 and 3-25. The only apparent damage to the composite molding and bond attachment resulted from the distortion of the steel fitting. Figure 3-26 shows the dishing of both the back face of the steel fitting and the nut plate as well

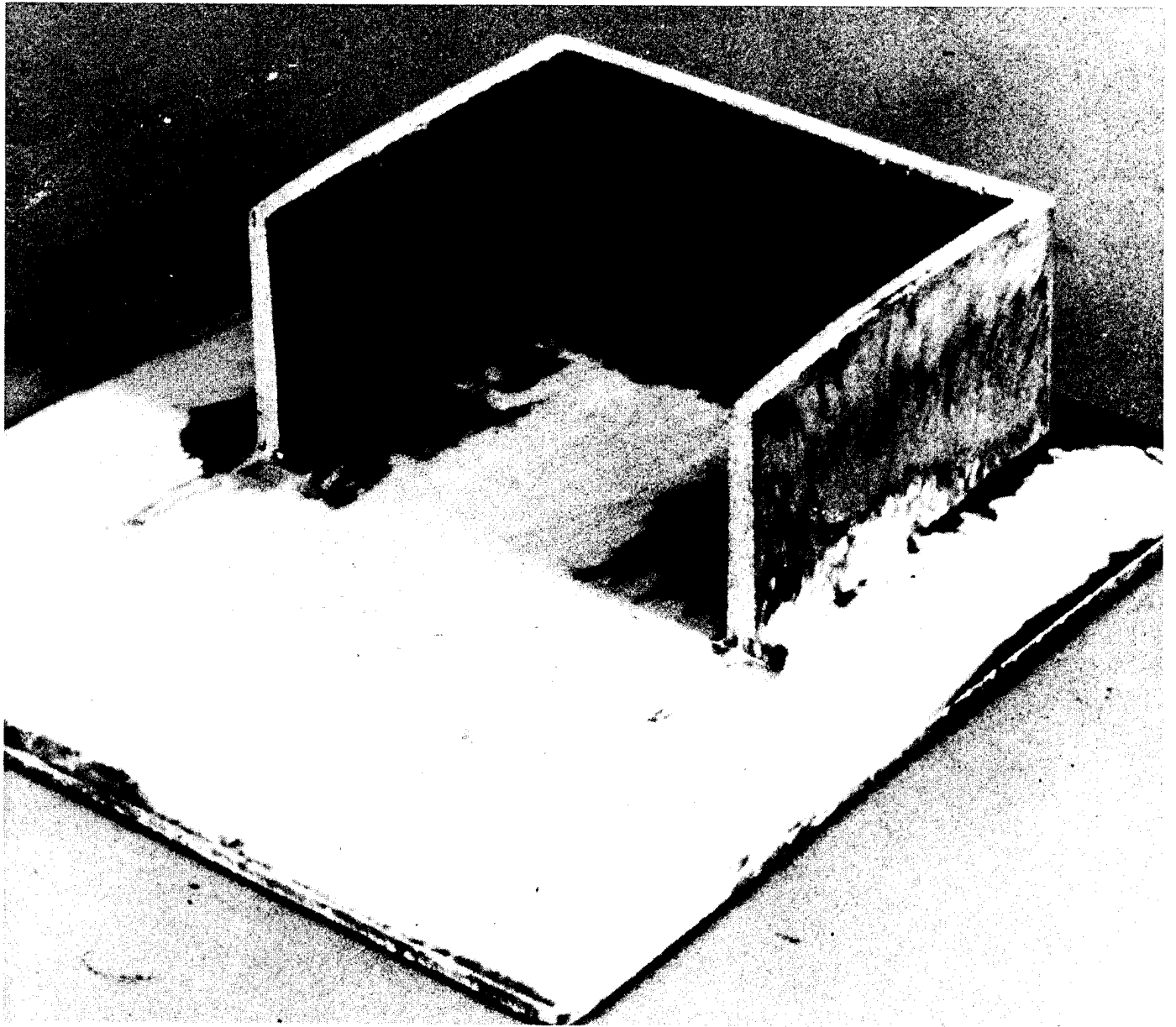


FIGURE 3-21 MOLDED RIB POCKET USED IN  
INTRUSION STRAP TESTS

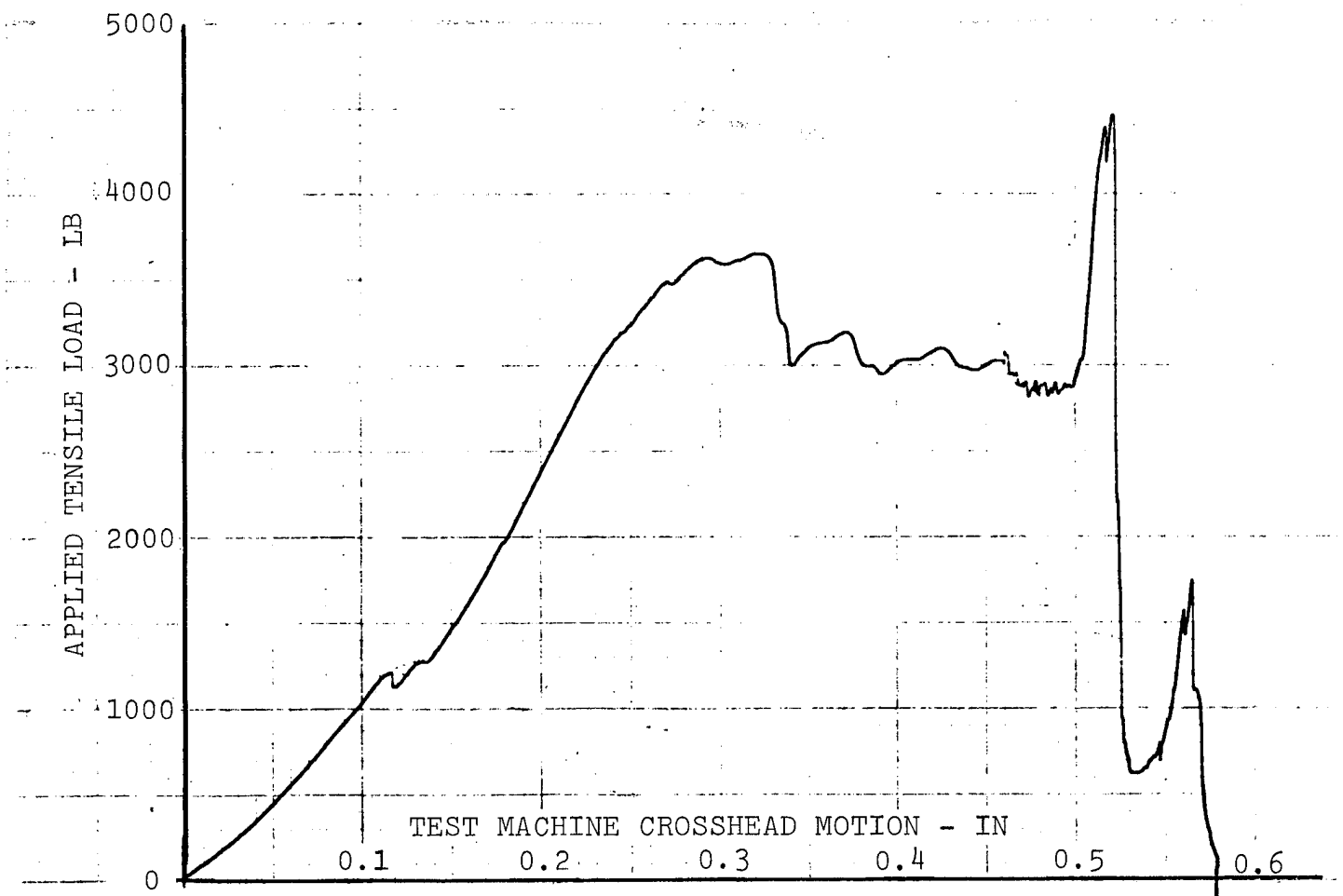
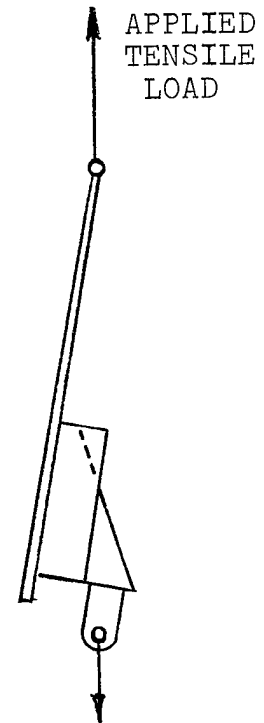
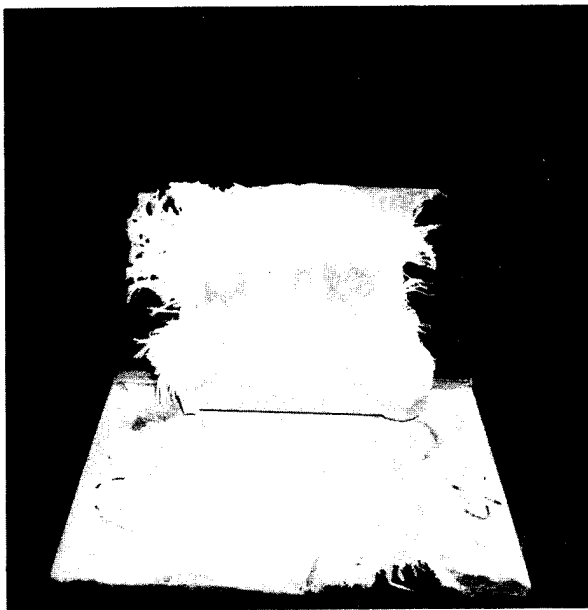


FIGURE 3-22 EVALUATION OF SHEAR/PEEL FAILURE MODE AND LOAD

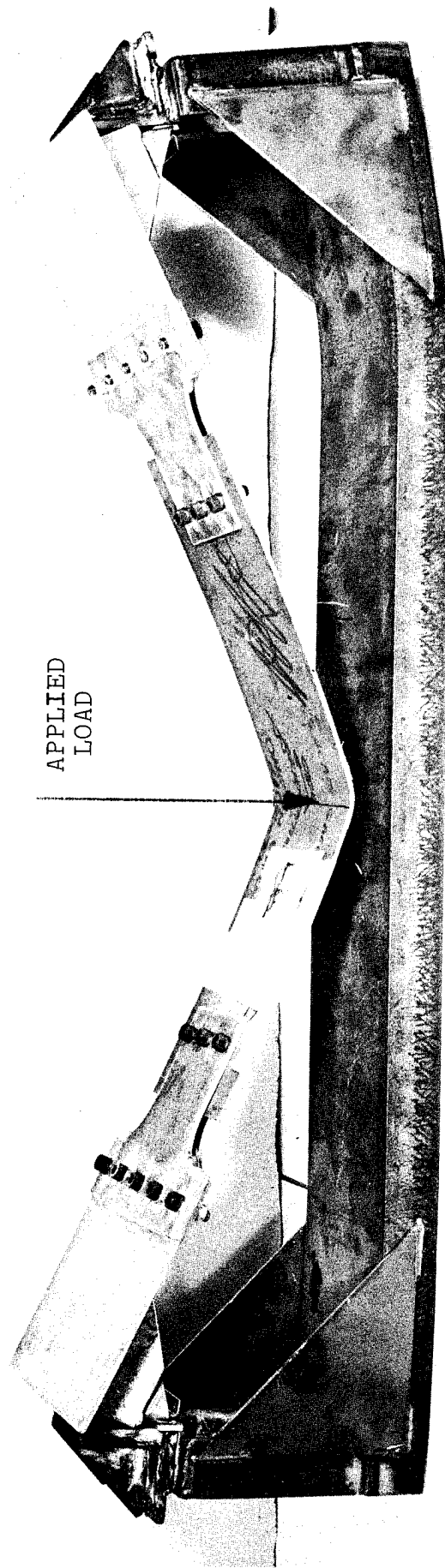


FIGURE 3-23 SIMULATED INTRUSION STRAP  
TEST (SECOND TEST)

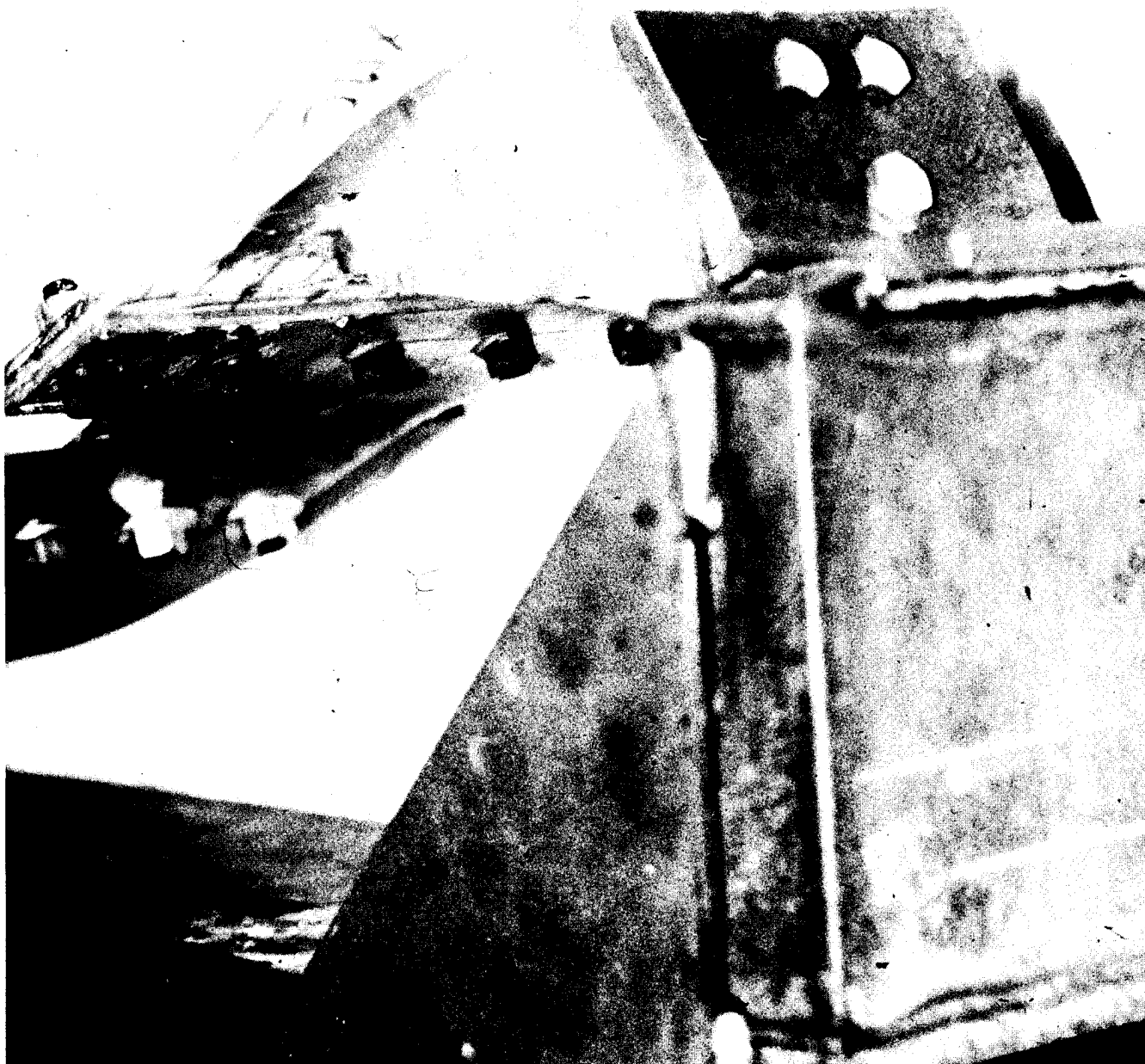


FIGURE 3-24 DISTORTION OF ANGLE IRON END ATTACHMENT  
(FIRST TEST)



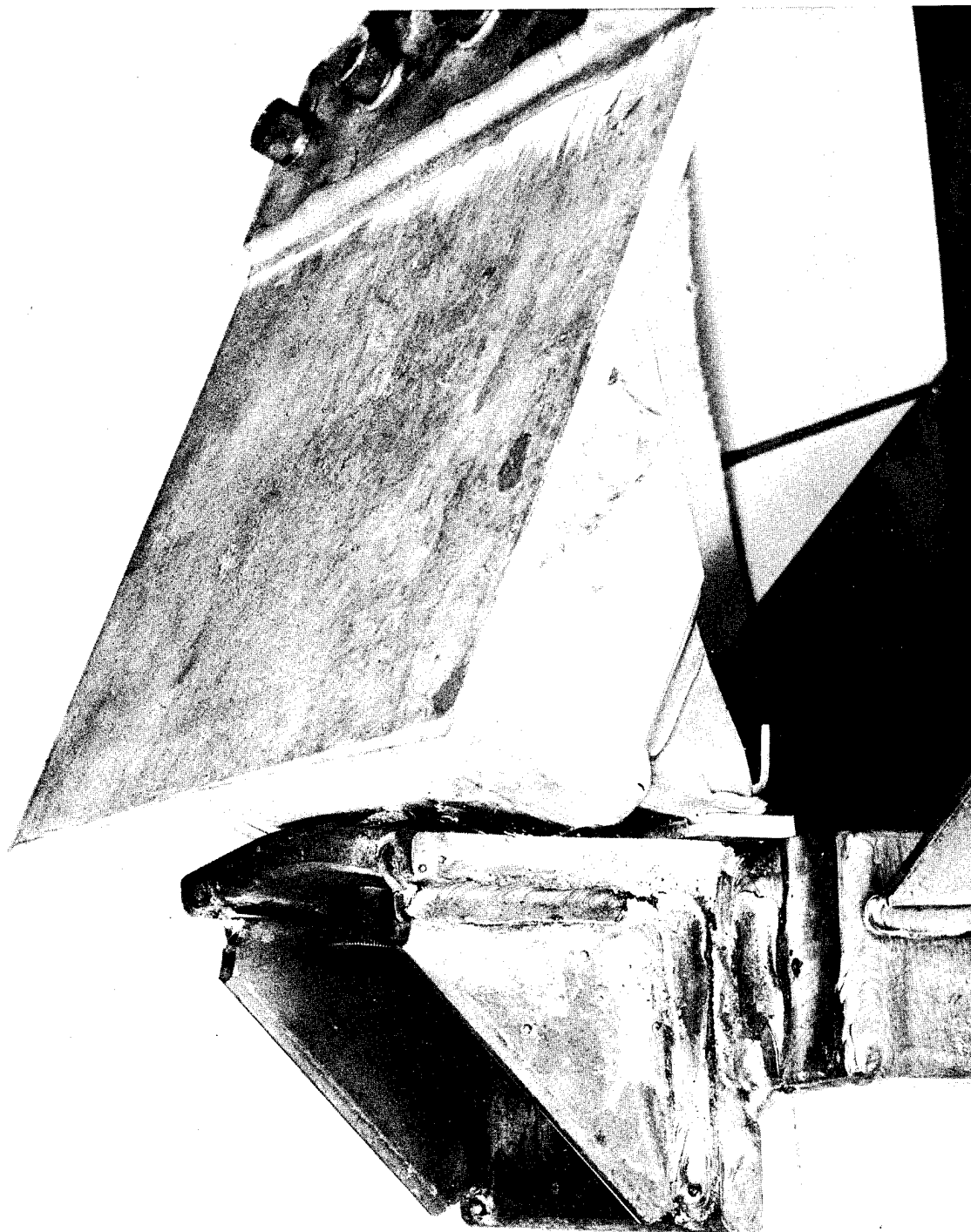


FIGURE 3-25 DISTORTION OF GUSSETED  
ANGLE END ATTACHMENT  
(SECOND TEST)

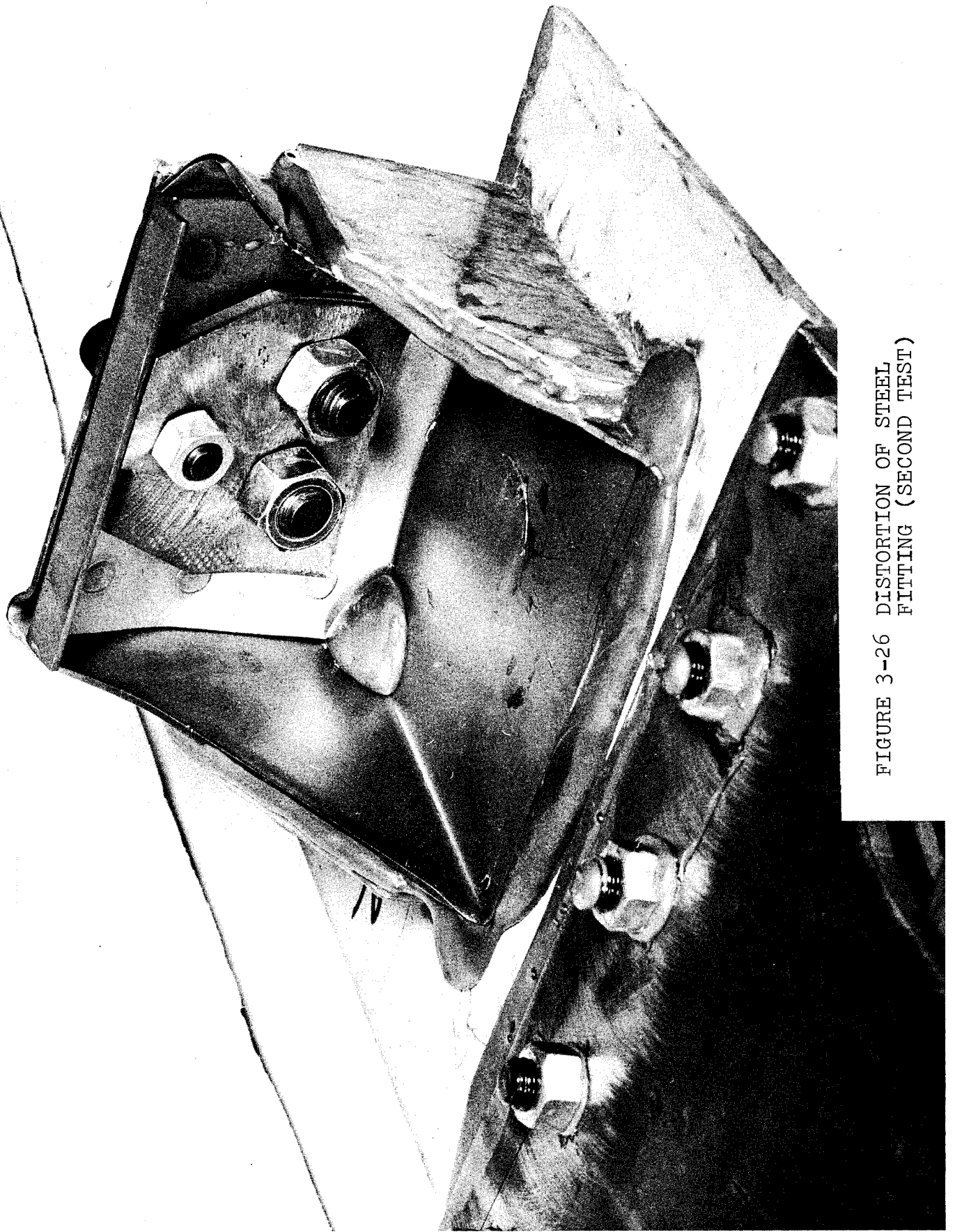


FIGURE 3-26 DISTORTION OF STEEL  
FITTING (SECOND TEST)

as the buckling of the side walls of the fitting. The distortion of the fitting caused the back rib to fail as shown in Figure 3-27.

The force/deformation response for these two tests are shown in Figure 3-28 where the requirements for the FMVSS 214, side door intrusion test, are noted. The results indicate that for a strap configuration with sufficiently fixed end conditions, it would be possible to satisfy the current federal side door intrusion test. This result highlights the previously noted concern regarding the need for providing rigid end attachments for the intrusion strap in order to meet current FMVSS standards.

The second test was strain gaged to allow for the determination of the intrusion strap load. With the gages located on either side of the steel center strap, it was possible to isolate the bending strain with the resulting tensile load shown in Figure 3-29 as a function of applied load. Also presented in Figure 3-29 is the predicted response using a formula from Reference 1 for beams under simultaneous axial and central transverse loading, where the axial loading was approximated by the strap load for small deflections. For the case of a fixed end beam with a central transverse load (W) and an axial load (P) the appropriate equation for the centerline deflection (y) is:

$$y = \frac{Wj}{2P} \left[ U/2 - \tanh U/2 - \frac{(1 - \cosh U/2)^2}{\sinh U/2 \cosh U/2} \right]$$

For the same configuration except with simply supported ends the equation becomes:

$$y = \frac{W}{P} \left[ L/4 - j/2 \tanh U/2 \right]$$

where

$$j = \sqrt{EI/P}$$

$$U = L/j$$

$$L = \text{length of beam}$$

The correlation appears reasonable considering the stiffness (EI) of the beam was not a constant and the axial load (P) is not quite the same as the strap load. In addition, attachment deformations quickly add to the centerline deflection thus preventing good correlation over the entire loading range.

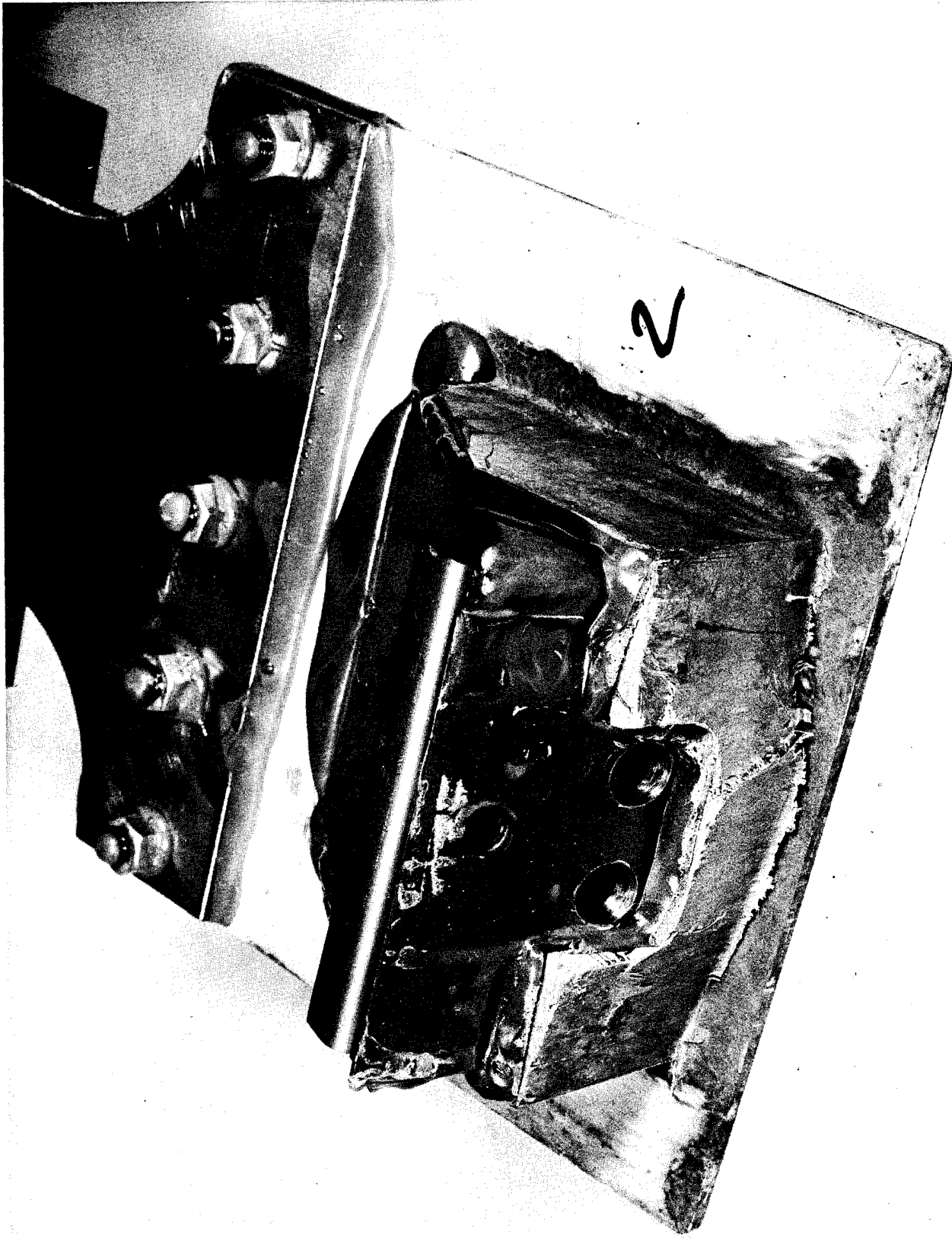


FIGURE 3-27 COMPOSITE DAMAGE  
RESULTING FROM STEEL  
FITTING DISTORTION  
(SECOND TEST)

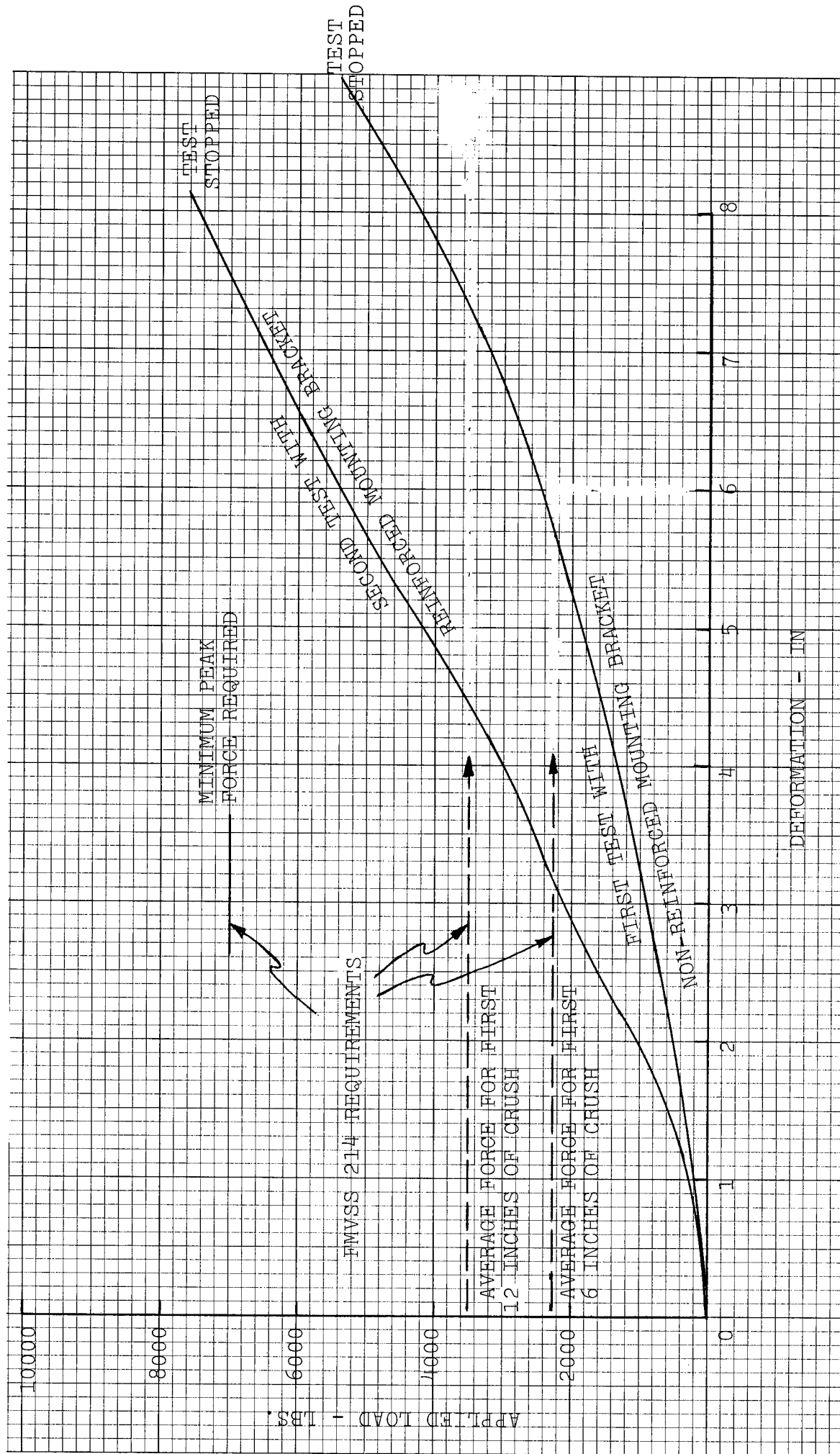


FIGURE 3-28 FORCE/DEFORMATION RESPONSE OF  
SIMULATED INTRUSION STRAP TEST

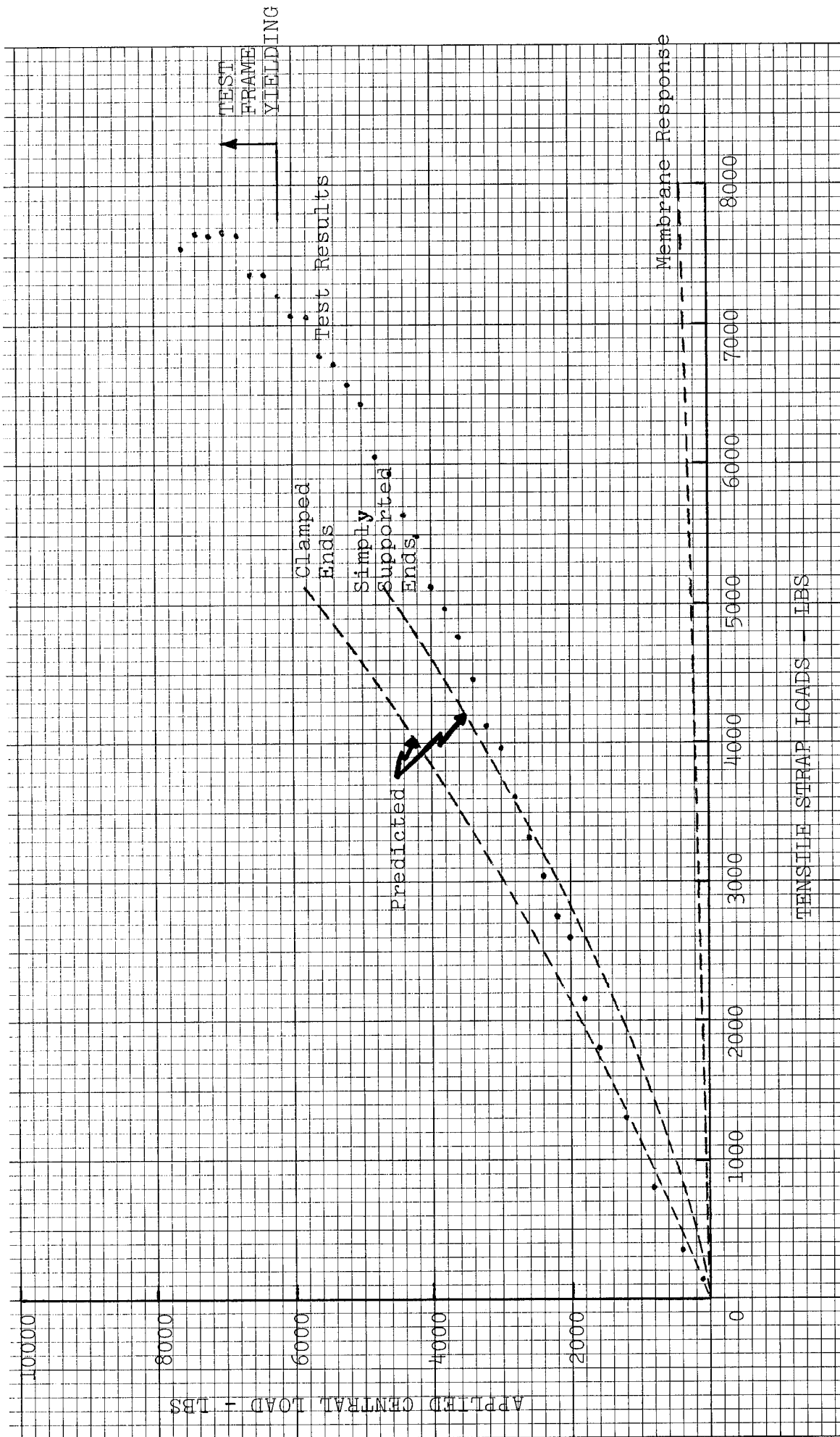


FIGURE 3-29 TENSILE STRAP LOAD FROM SIMULATED INTRUSION STRAP TEST (SECOND TEST)

An important result of the test was that the maximum tensile load measured in the steel intrusion strap was, from Figure 3-29, less than 8,000 pounds. Even if, as a conservative estimate, the load was to increase at the same rate which it saw prior to the test frame yielding, a maximum of approximately 11,000 pounds would be obtained from Figure 3-28 at a projected intrusion of 12 in. Such a load level is definitely within the load capability of the chosen intrusion strap configuration. Note that for the force/deformation response seen in Figure 3-28, a maximum test intrusion of 12 in. would have satisfied FMVSS 214 since the minimum peak force required had already been reached.

### 3.2.5 Prototype Mold Fabrication

A full size zinc alloy compression mold was fabricated for producing prototype parts. The various equipment requirements described in Appendix B, "Process Selection Report", were utilized with the zinc alloy prototype mold. The mold maker was W. K. Industries, Inc., of Sterling Heights, Michigan.

In the fabrication sequence of the mold a production steel baseline door structure was purchased from a local Chevrolet dealer. It was then mounted on an Impala car to insure that it would fit properly. Any imperfections in the door outer panel were corrected prior to shipping the door to W. K. Industries, Inc. for mold fabrication. This door was used to obtain the plaster patterns starting with an expansion plaster cast taken directly from the steel door outer panel which was restrained to the correct shape by the inner panel. Figure 3-30 shows the partially completed wooden and plaster construction for the appearance side of the mold. It was then used to form a sand cavity into which the zinc alloy material was cast.

The matching tool half corresponding to the inside surface of the outer panel was obtained by applying a wax and wood buildup to the molding surface of Figure 3-30 to account for part thickness and rib and boss configuration. Then another plaster cast was taken off the built-up structure for use in casting the other half of the zinc alloy tool. It was necessary to locate ribs, thickness variations, and bosses for the wax and wood buildup per detailed drawings. Figure 3-31 shows the setup used to obtain dimensions from the same door structure which was used to fabricate the compression mold. The final detailed drawing of the molded door outer panel including the intrusion strap is shown in Figure 3-32.

### 3.2.6 Prototype Molding

The molding parameters used to mold the prototype parts were identical to what would be expected in production except that the charge pattern was hand loaded and not performed by machine. The various molding requirements are specified in Appendix B, "Process Selection Report". The actual molding was performed at PPG In-

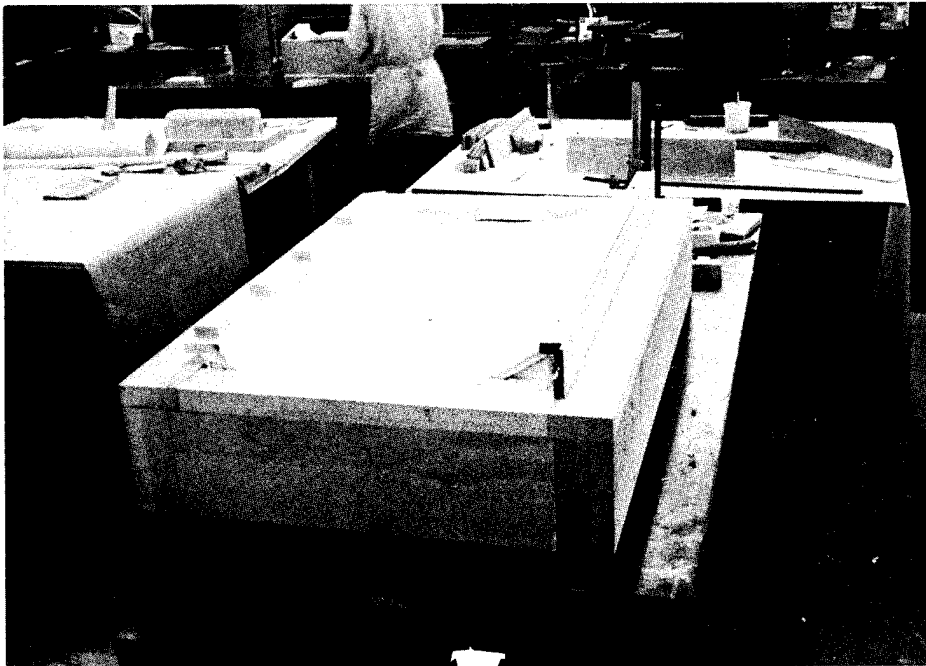


FIGURE 3-30 INTERMEDIATE STAGE OF ZINC  
ALLOY TOOL CONSTRUCTION



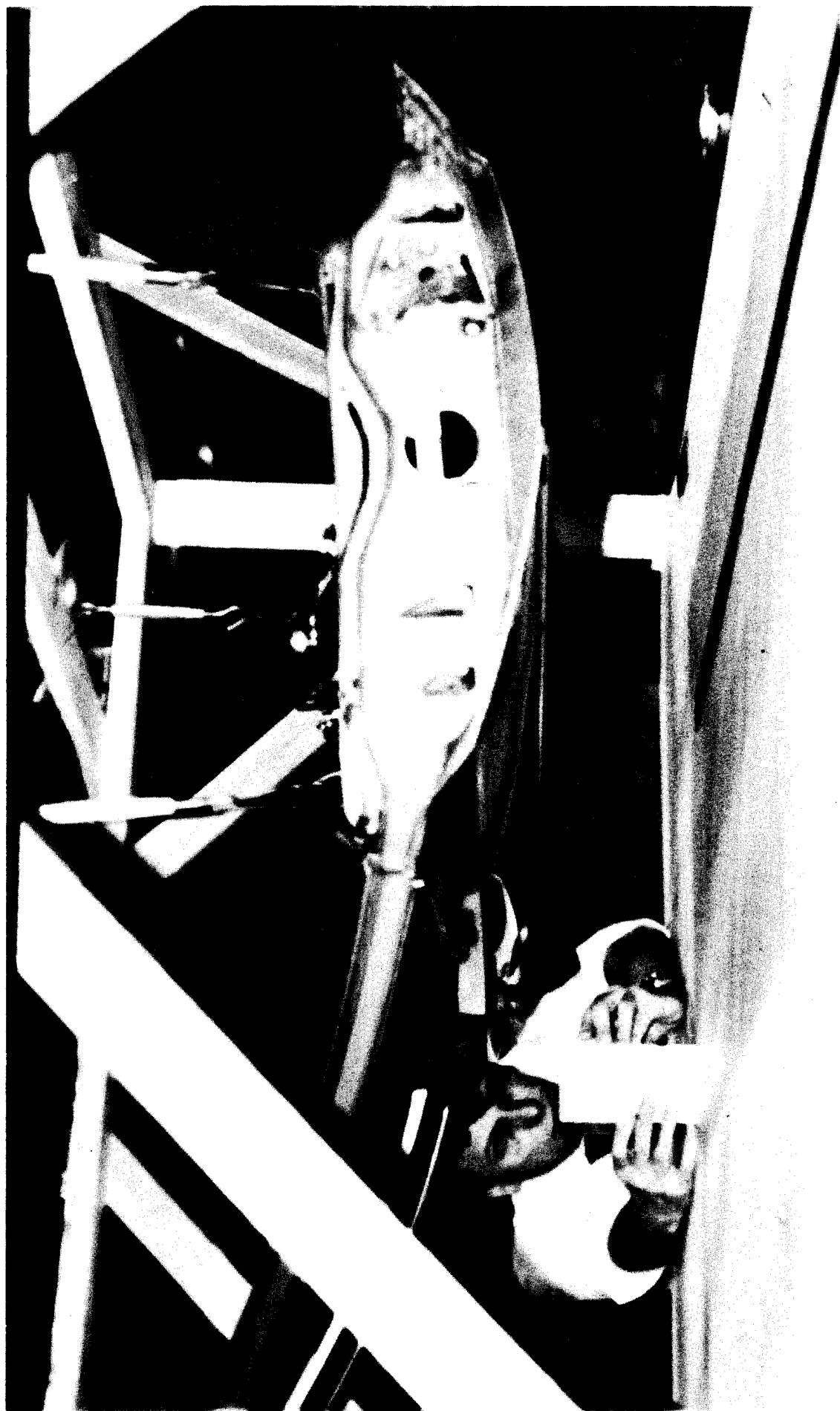


FIGURE 3-31 TOOLING AIDS USED TO OBTAIN IMPALA DOOR DIMENSIONS

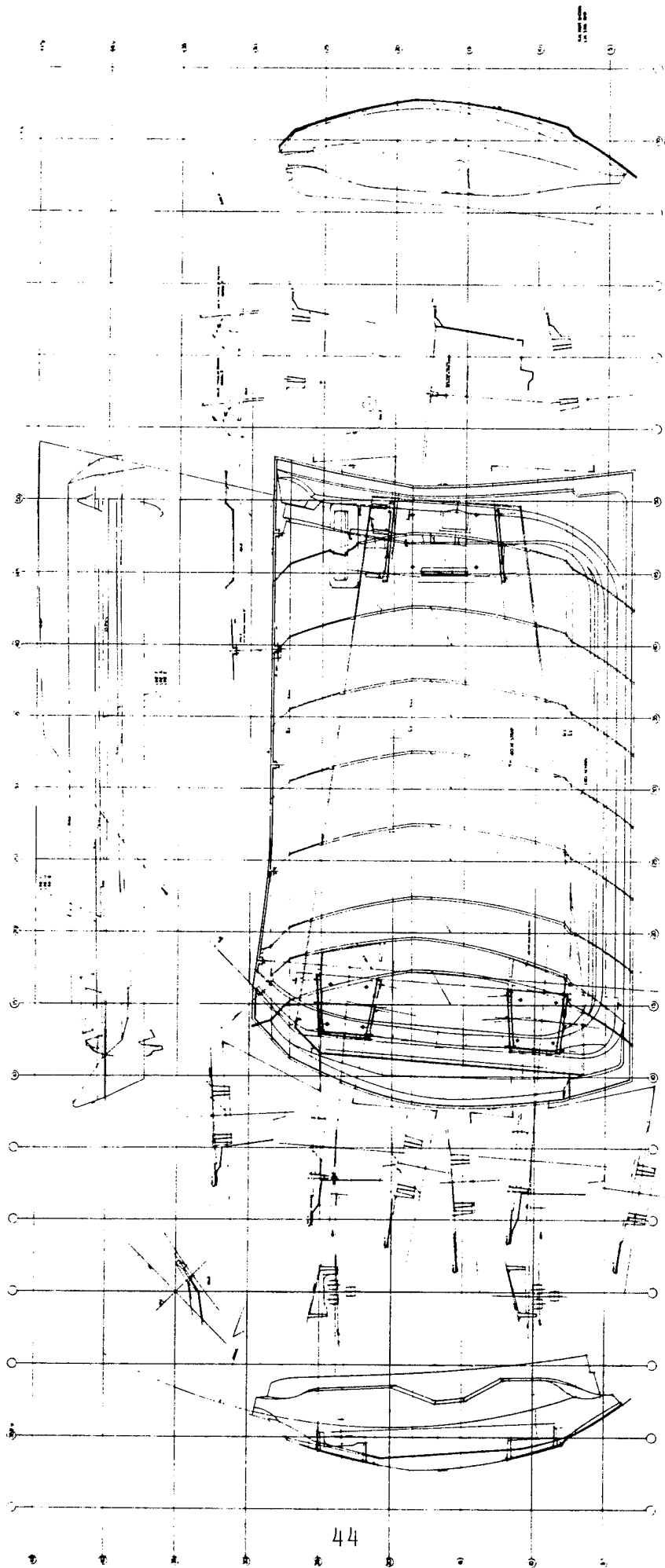


FIGURE 3-32 DETAILED DRAWING OF DOOR OUTER PANEL  
PLUS INTRUSION STRAP COMPRESSION MOLDING

dustries' Technical Center, in Pittsburgh, Pennsylvania using their 1000 ton hydraulic press.

The first molding effort involved the establishment of an acceptable charge pattern. The continuous fiber charge was cut approximately 0.5 inches narrower than the strap cavity to allow for expected variations in charge placement. It was determined that in order to get proper flow of the SMC material, its charge had to completely cover the continuous fiber material. In addition the ribs were slugged with HMC material pieces in order to obtain complete rib filling.

After completion of the three minute cure cycle (which was not necessarily the minimum required time), the part was removed from the mold (see Figure 3-33). Sectioning the ribs revealed the flow pattern shown in Figure 3-34. The partial filling of the rib by the continuous fiber material occurred for both systems evaluated and irrespective of whether the rib was oriented parallel or perpendicular to the continuous fibers. In addition, the partial flow of the continuous fiber into the rib apparently occurs without any distortion of the orientation of the continuous fiber immediately adjacent to or in the vicinity of the rib. What is significant is that the flow pattern should provide for an excellent shear transfer. Originally the ribs, including the short diagonal reinforcing ones, were sized to provide a sufficient shear area for transferring the axial strap load into the steel fitting. It is conceivable that as a result of the flow pattern observed, that the shear strength would be greater than that originally used. Hence the rib thickness might be reduced. With the apparent increase in shear strength of the joint the remaining prototype moldings were performed using the lower cost SMC material for the ribs in place of HMC.

Some sink marks were observed especially in the areas of the hinge brackets. This was partially caused by the fact that the pads under the hinge brackets was made thicker to allow for fabrication of a flat bottomed bracket instead of one which had a curved surface to follow the door contour. In production a curved lower surface of the bracket would be used. At the latch area, on the other hand, the panel thickness was kept constant, and the sink marks were less obvious. For either area, however, the possibility of a thinner rib would reduce further the sink marks observed. Another item which would reduce the sink marks is to reduce the height of the ribs. The rib height, however, cannot be reduced without sufficient testing since the rib serves to react the peel loading on the steel bracket to intrusion strap bond. As previously noted in Section 3.2.3, load path redundancy exists to react this peel loading by the support of the inner panel to which the steel brackets are attached, thus possibly providing a means for reducing the height of the ribs.

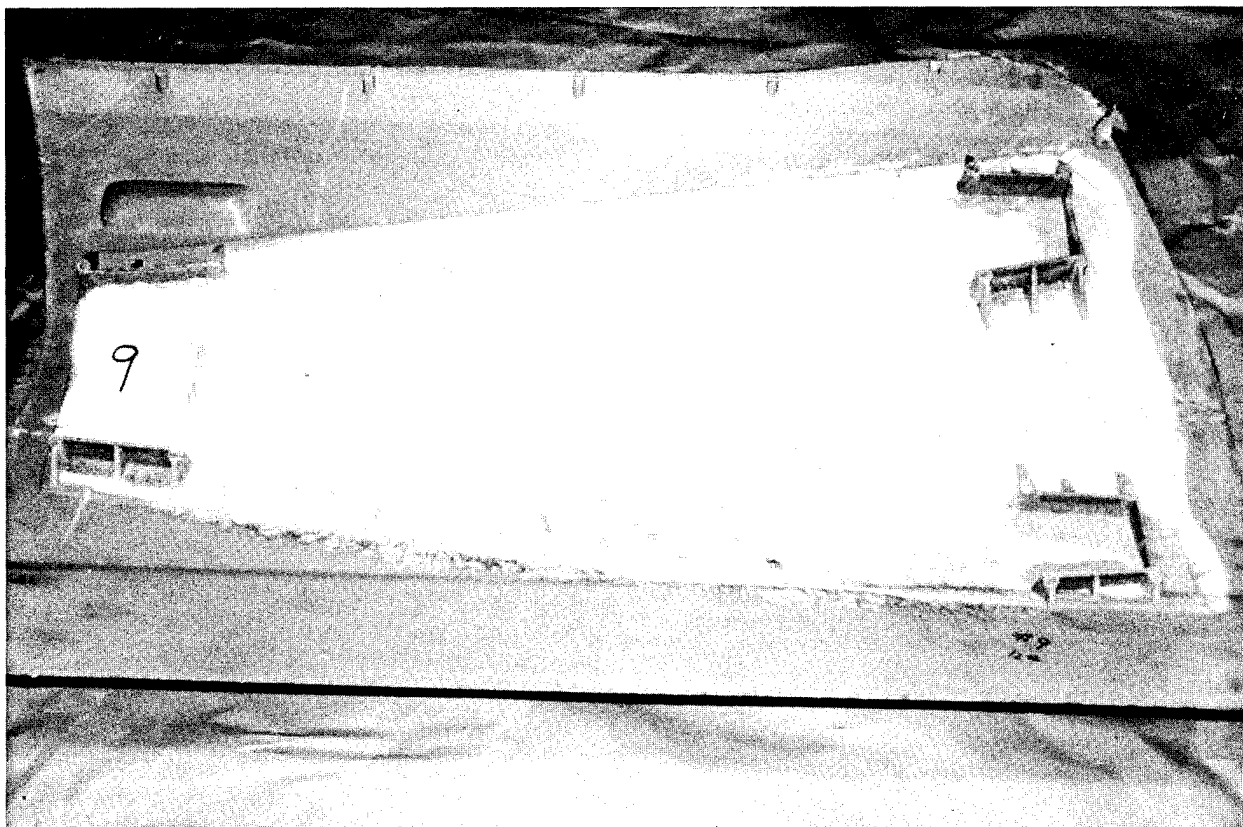


FIGURE 3-33 PROTOTYPE PART AS IT COMES FROM THE ZINC ALLOY MOLD AND PRIOR TO TRIMMING

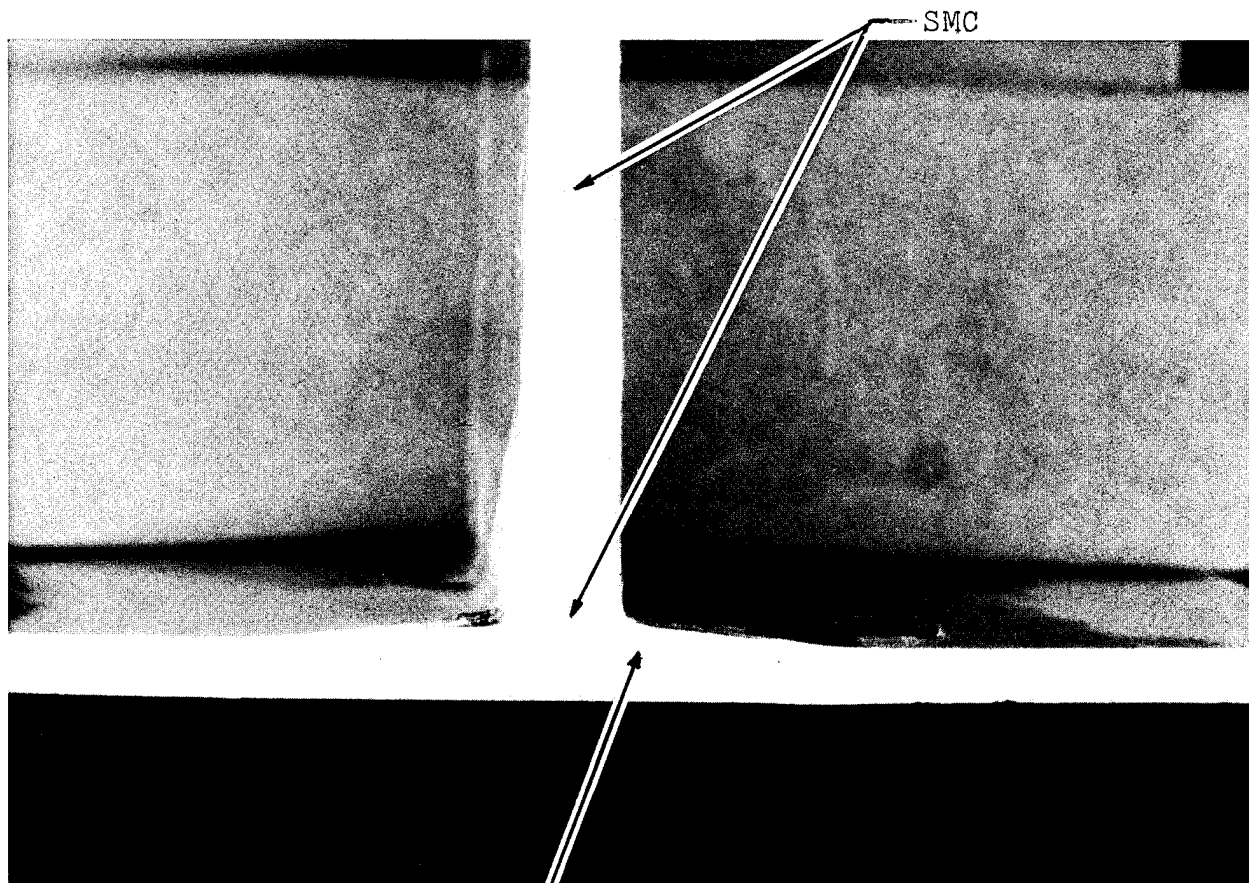


FIGURE 3-34 CROSS SECTION OF MOLDED RIB SHOWING FLOW  
PATTERN OF SMC AND UNIDIRECTIONAL GLASS MATERIAL

The projected weight of the molding from Table 3-2 was 11 pounds. After the best charge pattern was established, the actual prototype parts weighed out at approximately 11.4 pounds. Such a discrepancy is within normal tolerances for prototype moldings as the part thickness is not kept as accurate as in a production mold.

Prior to the prototype molding the steel baseline door which was used by W. K. Industries to fabricate the prototype mold was shipped back to The Budd Company. It was then utilized to fabricate a checking fixture as shown in Figure 3-35. The purpose of such a fixture was to check both the dimensions and the shape of the compression molded door outer panel. The molded parts were put in the checking fixture which verified that their dimensions were acceptable. Some thermal distortion was observed in the moldings about the car line horizontal axis. Only a slight force, however, was required to have the part conform to the checking fixture. When the molded part is bonded to the inner panel sufficient restraint exists to provide the correct shape. No thermal distortion was observed about the car line vertical axis partly because of the large moment of inertia created by the curvature of the door. In addition, no twisting of the molded part was observed.

One of the compression molded parts which utilized XMC material for the intrusion strap was cut into straight sided tensile specimens as shown in Figure 3-36. While the XMC covers a larger portion of the door panel than was actually cut-up into tensile specimens, it was assumed that the majority of the intrusion strap load would be taken by the two segments which were cut into specimens. The two hinge brackets are approximately 4 in. wide at the beginning of the ribbed pocket and the latch bracket is approximately 8 in. wide between the two longitudinal ribs. Hence two 4 in. wide strips were considered as the primary structural path connecting the latch and hinge brackets as shown in Figure 3-36.

With the chosen specimen width being 0.5 in. and with material losses due to saw cutting, a total of seven specimens were obtained from the 4 in. width. As shown in Figure 3-36, three sets of 9 in. long specimens were cut from each of the two strips. Aluminum doublers were then bonded to the specimens. Four of the seven specimens from each group were statically tested to failure. The four specimens chosen were every other one starting from one edge of the 4 in. wide band. The other three specimens would have been tested if a wide variation of test results existed for any one of the six groups of specimens. Such large variations, however, were not encountered.

The load values at failure for each of the four specimens were added together with the sum multiplied by two to arrive at an equivalent load capability for the 4 in. width strips. These

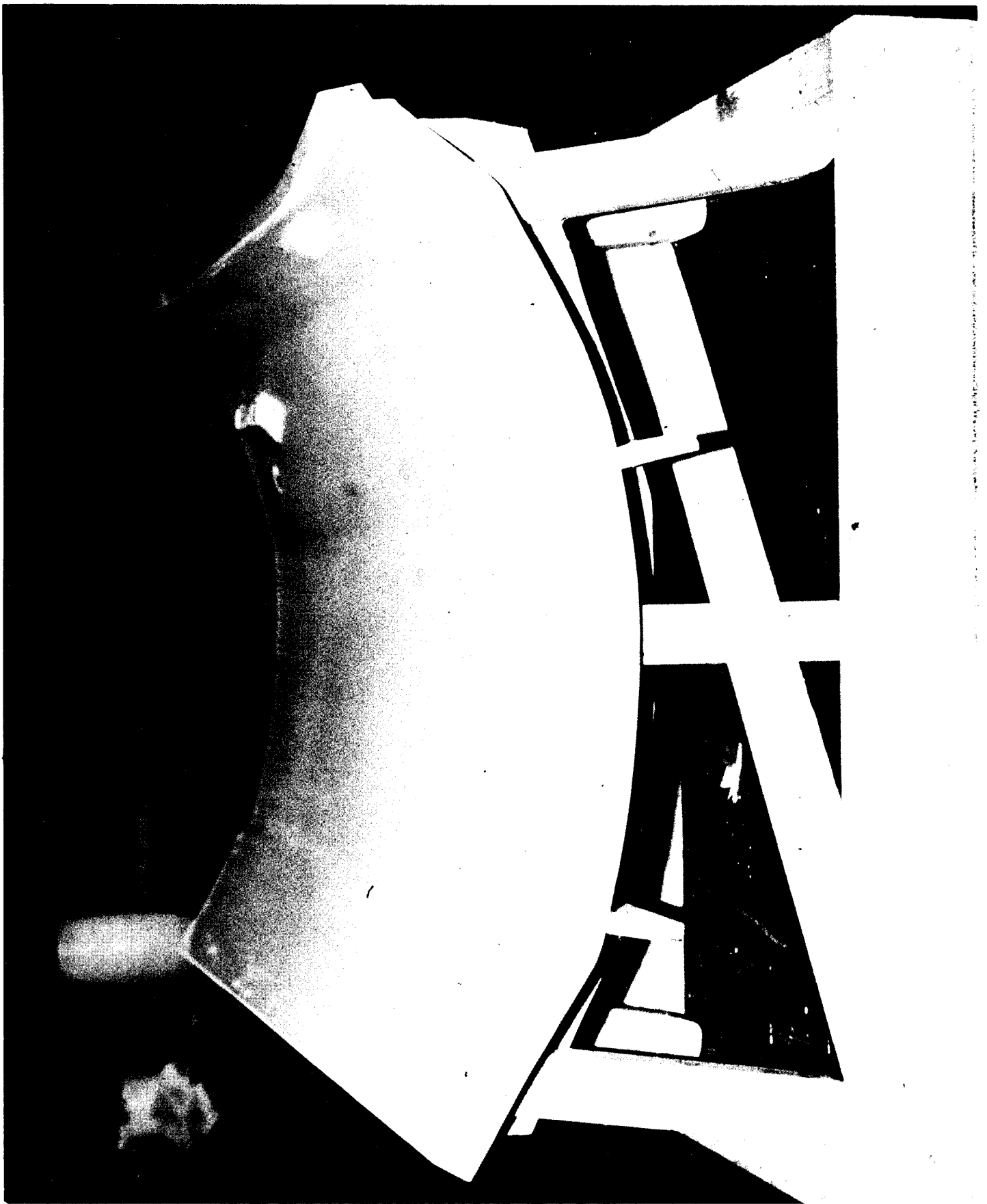
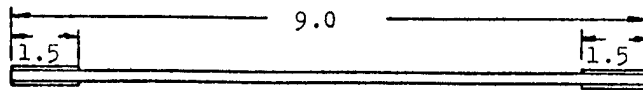


FIGURE 3-35 FABRICATED CHECKING FIXTURE USED TO  
VERIFY DIMENSIONS AND SHAPE OF MOLDED  
DOOR OUTER PANEL



ALUMINUM  
DOUBLERS

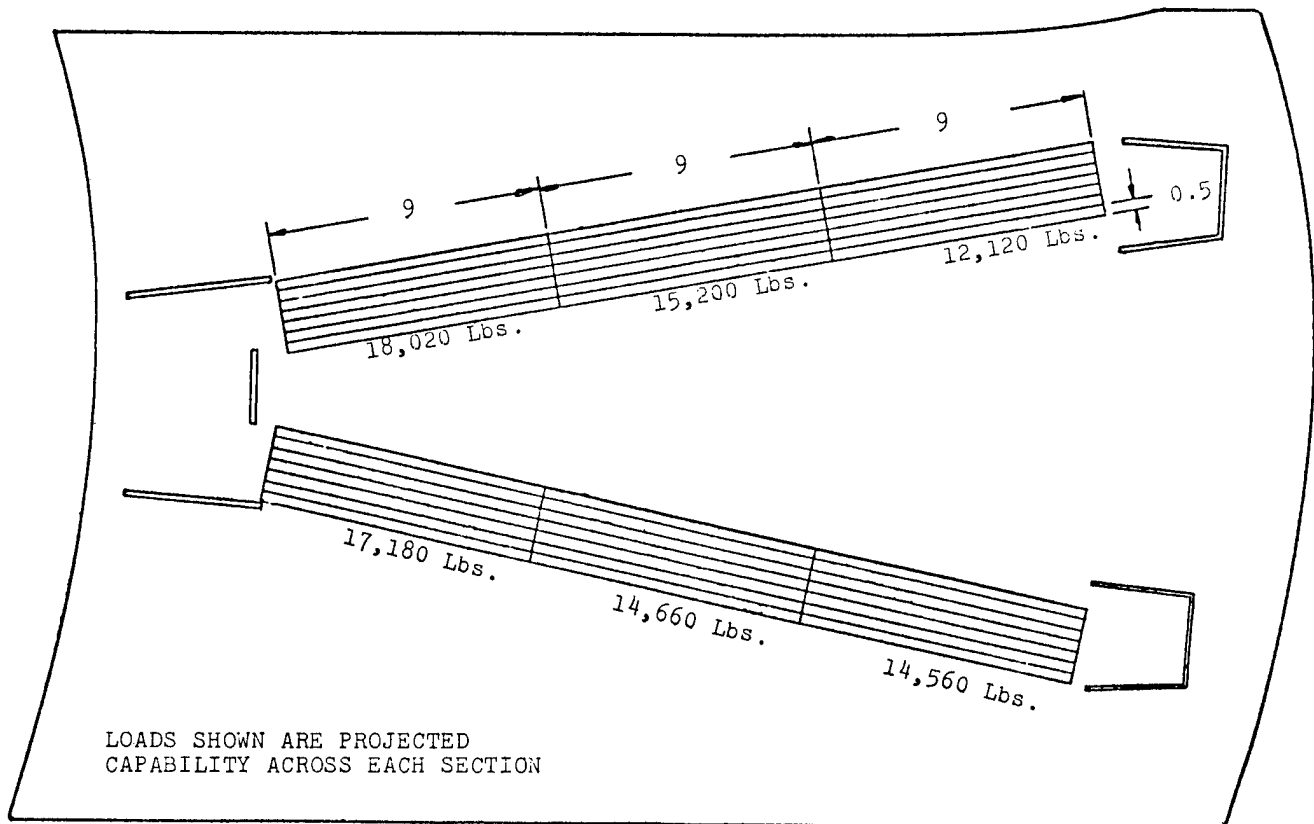


FIGURE 3-36 LOCATION AND TEST RESULTS OF  
INTRUSION STRAP TENSILE SPECIMENS



values are reported on Figure 3-36. From Figure 3-29, the maximum strap load reached in the simulated FMVSS 214 intrusion test was 8,000 lbs. This load corresponded to a failure of the test fixture. As far as the test was run, the simulated strap met the FMVSS 214 test requirements. If the results of the test are extended to the full 12 inches of intrusion (which is all that is required since the minimum required peak force had been reached) the peak test load would have been anywhere from 8,000 to 11,000 lbs. depending on what assumptions are used. With the FMVSS test, both 4 in. wide strips would be simultaneously loaded with the minimum load capability for both straps being 26,680 lbs. from Figure 3-36. This is approximately 2.4 to 3.3 times the maximum load expected in the actual test. If higher load requirements are needed then it is possible to obtain them by going to a two piece continuous/random material, each piece oriented specifically along the axis of one of the two 4 in. wide strips.

### 3.3 Cost Evaluation

The purpose of the costing evaluation phase of the program is to compare production costs of the baseline steel Impala door to those of the redesigned composite version. It is important to note that not all of the door has been evaluated because, in the redesign effort, an attempt was made to have as many common parts with the steel baseline as possible. Therefore in the costing effort only those actual parts which have been redesigned or replaced and the joining sequences which have been affected will be included. For instance, the clinching and welding of the inner to outer steel panels is included in the costing for the baseline steel design while the adhesive bonding of the inner steel panel to the outer composite panel was included for the costing of the redesign effort.

Two composite versions will actually be costed. The first represents the simple substitution of an 0.080 in. thick SMC outer panel to replace the existing steel. For this approach the remainder of the door, including the intrusion beam, will remain the same as for the all steel baseline. The significance of costing this approach is to evaluate direct composite material substitution which might be required for such automotive parts as fenders. The second composite version to be costed would be the complete redesign of the outer panel which includes the intrusion protection.

#### 3.3.1 Material Cost

Delivered price of cold rolled coil steel stock ranges from \$0.21 to \$0.23 per pound depending on the draw quality required. In order to form the steel stock in the die, additional clamping flanges are required to hold the material. This additional material, which is subsequently trimmed, is added to the cost of the steel part. While this steel scrap has value, the cost of collecting and returning it nearly offsets its scrap value.

Hence, it has been ignored in calculating the steel material costs.

The price for the composite material is not so clean. Estimates from two vendors indicated that purchased SMC material would range from \$0.60 to \$0.75 FOB the vendor's plant. In talking with a manufacturer of SMC equipment, a quantity of a few million pounds per year was the breakeven point, above which it would be cost competitive to manufacture the SMC in-house. With 7.5 lbs. of material per door, a yearly run of only 100,000 4 door vehicles would be required to reach 3,000,000 lbs. per year. Hence, for costing purposes, it will be assumed that the SMC material will be made in-house. Reference 2 calculated the raw material cost for SMC in the 1978 time frame at \$0.36 per pound not including the polyethylene film. To this would be added the labor (which was estimated by the equipment manufacturer at 1000 lbs. per man hour for a low level of automation), capitalization (\$100,000 to \$500,000 depending on the level of automation), negligible power consumption, and floor space. Even with adding inflation to the raw material costs a figure of \$0.50 per pound appears to be a reasonable cost if the SMC is made in-house. This also is consistent with the lower quote received from the vendors, if profit and G & A is subtracted.

The cost of the continuous fiber material should be increased over the SMC simply by the additional glass fiber cost. If the delta cost between the glass and the filler material which it replaces is taken as \$0.65 per pound, then in going from SMC with 27% glass content by weight to a continuous fiber system with 65% glass content, an increase of \$0.25 per pound results. The cost for the continuous glass system will then be \$0.75 per pound if it is made in-house. When a quicker curing resin system is considered in the costing effort, an arbitrary \$0.05 per pound is added to the base price for all of the composite systems used.

### 3.3.2 Labor and Overhead

According to Reference 3 the average hourly rate for General Motors for mid 1979 was \$9.07 an hour. To this figure is added fringe benefits which can average 40 - 50% above the hourly wage. An hourly rate was chosen which represented a somewhat higher value than the reported \$9.07 average because of the large number of higher paid press operators required. This rate was used for all fabrication steps for both the steel process and the composite version even though there is some indication that wages for plastics workers are not as high as those for steel workers.

Depending on the particular operation and equipment used in that operation a burdening rate is applied per part. This burdened rate includes capital amortization, interest, administrative, floor space, utilities, maintenance, as well as supportive personnel plus their equipment. For instance the burdening on a particular mechanical steel working press will include such things as material handler and oiler charges as well as a crane for die

setting and removal. While the presses used for composite fabrication are hydraulic and not mechanical, the burdening rate used was the same as for an equal capacity mechanical press. Here again some people have argued that the burdening rate should be less for the hydraulic presses because of reduced supportive personnel. On the other hand, maintenance requirements for compression molds are higher than for steel working molds. Therefore, without supporting data to the contrary, the burdening rates of the two types of presses were kept the same. Starting with this assumption, it then follows that there would not be a significant savings if two molds were used, side by side, in a single press. This results because, for mechanical presses, doubling the press capacity usually more than doubles the overhead rate thus offsetting any potential savings in labor and floor space. If, however, hydraulic presses were to show a less dramatic increase in overhead rate versus capacity, then there would be some advantage to using the larger press with two molds. This alternative was not investigated in this study.

No learning curve has been applied to establishing the part costs. This is because in establishing the three costing scenarios used for the composite version, very specific production rates were chosen. A learning curve was considered to have been required to achieve these chosen production rates. Also the degree of automation is somewhat limited by the slowest process which for the state-of-the-art composite fabrication would be the molding cycle. If a number of composite parts are being produced for various car models, then an integrated line could be established to handle such operations as preparation for bonding and painting, adhesive placement, deflashing, and assembly. For such integrated lines, greater use could be made of robotics and other automation techniques. There, however, may not be significant cost savings using these techniques since the reduced labor costs will be partially offset by higher overhead burdening rates. As will be seen, the quantity of state-of-the-art fabricated composite parts which prove to be cost effective, do not justify the large use of automation techniques except possibly with the previously mentioned integrated lines. For the composite costing, the automation techniques considered will be primarily concerned with the loading and unloading of the press with the remaining finishing, preparation, and assembly sequences primarily labor intensive with the use of fixtures where required.

### 3.3.3 Capital

If a particular mold or fixture is solely dedicated to the composite 1977 Chevrolet Impala door, then it will be included as tool cost which is amortized over the number of parts fabricated. If however, a piece of equipment is not dedicated to a particular component then it shows up in the overhead charged against the component using that equipment. Included in this overhead charge is the cost of the equipment amortized over a certain life. Hence, the actual capital requirements to set up a production line was

not established in the costing effort since the composite related equipment was assumed to exist with its cost showing up in the overhead charge. While this approach is acceptable for the costing effort, it is misleading with respect to understanding one of the serious obstacles facing the use of composites, namely the capital requirements.

As previously indicated, existing metal working presses are mechanical while hydraulic presses are used to perform the compression molding of composite parts. Attempts have been made to modify mechanical presses to be acceptable for compression molding, but with limited success due to current economics. In Reference 4, the equipment costs to make a complete state-of-the-art composite door were estimated to be \$35,000,000 in 1976. This estimate has been adjusted so the composite facility's door output equaled that of a steel facility which was estimated to be 1,232,000 doors per year. For the 1977 model year, there were 423,000 four door Impalas and Caprices built (Reference 5). These cars would have required 1,692,000 doors resulting in an equipment cost of \$48,000,000 (which was obtained by ratioing up the \$35,000,000 estimate from Reference 4 for 1,232,000 doors per year). This investment magnitude may slow down the inroads of composite materials into automotive structures. One further consideration is that even if the automotive industry were willing to make the investment required to fabricate composite structures, it would take years to produce all of the required presses.

### 3.3.4 Baseline Steel Design

The fabrication description for the baseline steel components and those joining sequences which are affected by the composite redesign are presented in Tables 3-3 through 3-12. Material costs, production rates, tool costs, and burdened labor costs have been established for the various fabrication sequences. The burdened labor cost includes, as discussed previously, the base rate plus fringes, and the burdened rate which depends on the particular equipment used. However, no profit or G & A is included in the burdened labor costs indicated, nor are such costs as sales, warranty, research and development or transportation. The total raw material cost from Table 3-3 through 3-12 is \$7.87 per door while the tooling costs are estimated at \$1,597,000 for both the left and right doors. The tooling for both front doors is included because in certain cases it was cheaper to form a single piece and then cut it to form both a left and a right part. Also this tooling cost is for a final typical steel assembly rate of 90 units per hour which could easily be increased with some additional clinching and welding fixtures. The total burdened labor cost for the baseline steel design is \$9.94 per door.

TABLE 3-3 BASELINE IMPALA STEEL DOOR - ESTIMATE FOR  
DOOR OUTER PANEL

PRODUCTION RATE/HOUR	FABRICATION DESCRIPTION	EQUIPMENT	TOOLS	TOOL COST (\$1,000's)
	Steel Blank Size:.033 in.x 37 in.x 52 in. Cold Rolled Deep Draw Quality Steel Costs \$0.23/lb. Cost of Coil Steel Stock is \$4.15/part			
			R&L* Engineer- ing Model	40
			R&L Form Frame	30
			R&L Keller Casts	20
600	Decoil & Flatten	Decoiler		
600	Rough Blank	Press	Blanking Die	80
400	Draw	Press	R&L Double Action Draw Dies	180
400	Trim Outside	Press	R&L Trim Dies	150
400	Pierce Door Latch and Side Mirror Slots	Press	R&L Piercing Dies	40
400	Flange Outside Flange and Window Flange	Press	R&L Flanging Dies	100
400	Final Form Window Flange Straight Down	Press	R&L Flanging Dies	60
	Forward to Spray Area	Conveyor		

\* Right and Left

TOTALS FOR TABLE:

MATERIAL COST	\$4.15
TOOL COST	\$700,000
BURDENED LABOR COST	\$1.95

DOOR OUTER PANEL DEADENING MATERIAL

[illegible]

TOTALS FOR TABLE:

MATERIAL COST	\$0.16
TOOL COST	<u>\$6,000</u>
BURDENED LABOR COST	\$0.27

TABLE 3-5 BASELINE IMPALA STEEL DOOR - ESTIMATE FOR  
INTRUSION BEAM, TOP (COMPONENT -1)

PRODUCTION RATE/HOUR	FABRICATION DESCRIPTION	EQUIPMENT	TOOLS	TOOL COST (\$1,000's)
	Steel Blank Size: .042 in. x 8 in. x 40 in. Cold Rolled Deep Draw Quality Steel Costs \$0.23/lb. Cost of Coil Steel Stock is \$0.88/part			
			R&L Engineer- ing Model	10
			R&L Form Frame	8
			R&L Keller Casts	6
1200	Decoil & Flatten	Decoiler		
1200	Cut 8 in. width	Shear		
400	Form Hat	Press	R&L Forming Dies	40
400	Form End Flange	Press	R&L Flanging Dies	10
400	Pierce 4 Holes & 1 Slot	Press	R&L Piercing Dies	14
	Forward to Assembly Area	Conveyor		

TOTALS FOR TABLE:

MATERIAL COST	<u>\$0.88</u>
TOOL COST	<u>\$88,000</u>
BURDENED LABOR COST	<u>\$0.85</u>

TABLE 3-6 BASELINE IMPALA STEEL DOOR - ESTIMATE FOR  
INTRUSION BEAM, BOTTOM (COMPONENT -2)

PRODUCTION RATE/HOUR	FABRICATION DESCRIPTION	EQUIPMENT	TOOLS	TOOL COST (\$1,000's)
	Steel Blank Size: .042 in. x 5.5 in. x 33 in. Cold Rolled Steel Costs \$0.21/lb. Cost of Coil Steel Stock is \$0.45/part			
			Model & Aids	7
1200	Decoil & Flatten	Decoiler		
1200	Cut Off	Shear		
600	Form 2 Beads	Press	Forming Die	10
	Forward to Assembly Area	Conveyor		

TOTALS FOR TABLE:

MATERIAL COST	\$0.45
TOOL COST	<u>\$17,000</u>
BURDENED LABOR COST	<u>\$0.27</u>



TABLE 3-7 BASELINE IMPALA STEEL DOOR - ESTIMATE FOR  
INTRUSION BEAM, INNER (COMPONENT -3)

PRODUCTION RATE/HOUR	FABRICATION DESCRIPTION	EQUIPMENT	TOOLS	TOOL COST (\$1,000's)
	Steel Blank Size: .042 in. x 7.75 in. x 17 in. Cold Rolled Steel Costs \$0.21/lb. Cost of Coil Steel Stock is \$0.33/part			
1200	Decoil & Flatten	Decoiler		
1200	Cut Off	Shear		
600	Form Hat	Press	Forming Die	15
600	Form Return Flange	Press	Flanging Die	10
600	Pierce 1 Hole	Press	Piercing Die	2
	Forward to Assembly Area	Conveyor		

TOTALS FOR TABLE:

MATERIAL COST	<u>\$0.33</u>
TOOL COST	<u>\$27,000</u>
BURDENED LABOR COST	<u>\$0.49</u>

TABLE 3-8 BASELINE IMPALA STEEL DOOR - ESTIMATE FOR  
INTRUSION BEAM ASSEMBLY

PRODUCTION RATE/HOUR	FABRICATION DESCRIPTION	EQUIPMENT	TOOLS	TOOL COST (\$1,000's)
Total Assembly 90	Consists of components -1, -2 & -3			
	Set up & weld -3 to -2, 4 Welds Each Flange (8 total)	Pedestal Welder	R&L Welding Fixture	8
	Set up above assembly with -1 & weld 15 places each flange (30 total)	Pedestal Welder	R&L Welding Fixture	4
	Forward to Next Station	Conveyor		

TOTALS FOR TABLE:

MATERIAL COST	<u>\$0.00</u>
TOOL COST	<u>\$12,000</u>
BURDENED LABOR COST	<u>\$0.90</u>

TABLE 3-9 BASELINE IMPALA STEEL DOOR - ESTIMATE FOR  
FRONT INNER REINFORCEMENT

PRODUCTION RATE/HOUR	FABRICATION DESCRIPTION	EQUIPMENT	TOOLS	TOOL COST (\$1,000's)
	Steel Blank Size: .090 in. x 12 in. x 27 in. Cold Rolled Deep Draw Quality Steel Costs \$0.23/lb. Cost of Coil Steel Stock is \$1.90/part			
			R&L Engineer- ing Model	7
			R&L Form Frame	6
			R&L Keller Casts	4
1200	Decoil & Flatten	Decoiler		
1200	Cut Off	Shear		
400	Draw Double (i.e. 2 at a time)	Press	Double Draw Die	75
400	Trim Except Middle	Press	Double Trim Die	70
400	Pierce 12 Rectangular Holes, 2 Holes, 2 Slots & 2 Cutouts	Press	Double Piercing Die	35
400	Part 2 Pieces	Press	Parting Die	40
400	Flange (Parted Flange)	Press	R&L Flanging Dies	28
400	Restrike	Press	R&L Restrike Dies	42
400	Pierce 2 Holes	Press	R&L Piercing Dies	10
400	Pierce 4 Holes	Press	R&L Piercing Dies	14
	Forward to Assembly Area	Conveyor		

TOTALS FOR TABLE:

MATERIAL COST	\$1.90
TOOL COST	\$331,000
BURDENED LABOR COST	\$1.29

TABLE 3-10 BASELINE IMPALA STEEL DOOR - ESTIMATE FOR  
ASSEMBLING DOOR INNER PANEL AND FRONT INNER REINFORCEMENT

PRODUCTION RATE/HOUR	FABRICATION DESCRIPTION	EQUIPMENT	TOOLS	TOOL COST (\$1,000's)
	Locate and Clamp Front Inner Reinforcement to Door Inner Panel		R&L Welding Fixture	50
	Spot Weld 8 Welds at Side Flange to Door Inner Panel (One at a Time)	Overhead Spot Welder	Special Weld Tips	1
	Spot Weld 3 Welds at Side End to Door Inner Panel (One at a Time)	Overhead Spot Welder	Special Weld Tips	2
	Spot Weld 8 Welds at Top Flange to Door Inner Panel (One at a Time)	Overhead Spot Welder	Special Weld Tips	1
	Spot Weld 8 Welds at Bottom Flange to Door Inner Panel (One at a Time)	Overhead Spot Welder	Special Weld Tips	2
Total Assembly  90	Forward to Next Station	Roller Table		

TOTALS FOR TABLE:

MATERIAL COST	\$0.00
TOOL COST	\$56,000
BURDENED LABOR COST	\$0.76

TABLE 3-11 BASELINE IMPALA STEEL DOOR - ESTIMATE FOR  
ASSEMBLING DOOR INNER PANEL AND INTRUSION BEAM

PRODUCTION RATE/HOUR	FABRICATION DESCRIPTION	EQUIPMENT	TOOLS	TOOL COST (\$1,000's)
Total Assembly  90	Locate & Clamp Intrusion Beam To Door Inner Panel		Use R&L Welding Fixture from Table 4-8	
	Spot Weld 6 Welds at Hinge Side of Door (One at a Time)	Overhead Spot Welder	Standard Weld Tips	
	Spot Weld 6 Welds at Lock Side of Door (One at a Time)	Overhead Spot Welder	Standard Weld Tips	
	Forward to Next Station	Roller Table		

TOTALS FOR TABLE:

MATERIAL COST	\$0.00
TOOL COST	0
BURDENED LABOR COST	\$0.60

TABLE 3-12 BASELINE IMPALA STEEL DOOR - ESTIMATE FOR  
ASSEMBLING DOOR INNER AND OUTER PANELS

PRODUCTION RATE/HOUR	FABRICATION DESCRIPTION	EQUIPMENT	TOOLS	TOOL COST (\$1,000's)
90	Position Door Outer and Inner Panels in Fixture and 45° Clinch Door Outer Panel Flange  Forward to Next Station	Roller Table	R&L Clinching Fixture	150
90	Final Form Clinch Flange  Forward to Next Station	Press  Roller Table	R&L Clinching Dies	120
90	Indirect Weld Clinch Flange (20 Total)  Forward to Next Station	Overhead Spot Welder  Roller Table	R&L Welding Fixture	90

TOTALS FOR TABLE:

MATERIAL COST	<u>\$0.00</u>
TOOL COST	<u>\$360,000</u>
BURDENED LABOR COST	<u>\$2.56</u>

### 3.3.5 Composite Design

Three scenarios were being evaluated in the costing effort to mold the composite door outer panel. The highlight features of the three scenarios are presented in Table 3-13. The first approach consists of using state-of-the-art techniques to arrive at a production rate of 20 pieces per hour using one mold and one press. An automatic loading and unloading arrangement which is described in Appendix B is utilized but hand placement of the material in the loader is used.

The second approach would assume that a maximum rate of 50 pieces per hour is possible for one mold and one press if much quicker curing resins were available. The same automatic loader and unloader as before will be used but in addition the loader will be automatically charged. Preheating costs of the material are included on the assumption that this may be one way of reducing the curing time during the molding cycle as discussed in Appendix B. While resin companies are working to obtain much quicker curing systems none have yet been commercialized.

The third approach uses the standard resin system currently available and consists of the fully automatic loading and unloading sequence of the second approach. However, several dies are used which are moved from station to station within the curing sequence. They start at the loading station, move to the pressure application, the in-mold coating (if needed), and then to the automatic unloaded stations. The projected rate of such an approach is 200 parts per hour. While such a system has been discussed in the literature and is presented in Appendix B, it has yet to become a viable approach.

Within the three composite costing scenarios, the three steel brackets which attach the intrusion strap to the hinges and latch remain the same. Also the bonding of three brackets to the composite door outer panel remains the same for all three scenarios. The only difference here might be an increase in the fixture costs to accomodate a higher assembly rate. In addition the assembly of the inner to the outer panel is the same for all three scenarios with again the same comment regarding fixture costs and assembly rates appropriate. These common elements of the three scenarios are presented in Tables 3-14 through 3-18.

The actual molding of the outer panel including the intrusion protection for the three scenarios are presented in Tables 3-19 through 3-21. For the 20 units per hour scenario the total raw material cost, including composite material offal, is \$8.77 per door while the tooling costs are estimated at \$762,000 for both the right and left doors. The corresponding burdened labor costs are \$14.97 per door.

TABLE 3-13 COSTING SCENARIOS FOR COMPOSITE DESIGN

- I. STATE OF THE ART (20 UNITS/HR)
  - STANDARD RESINS
  - HAND PLACEMENT OF CHARGE
  - AUTOMATIC LOADER AND UNLOADER
  - ONE MOLD AND ONE PRESS
- II. MODIFIED STATE OF THE ART (50 UNITS/HR)
  - QUICKER CURE RESIN SYSTEMS
  - PREHEATING COMPOSITE MATERIAL
  - AUTOMATIC PLACEMENT OF CHARGE
  - AUTOMATIC LOADER AND UNLOADER
  - ONE MOLD AND ONE PRESS
- III. MULTI-STATION MOLD TRANSFER (200 UNITS/HR)
  - STANDARD RESINS
  - PREHEATING COMPOSITE MATERIAL
  - AUTOMATIC PLACEMENT OF CHARGE
  - AUTOMATIC LOADER AND UNLOADER
  - 8 MOLDS AND 4 STATIONS



TABLE 3-14 IMPALA COMPOSITE ~~DOOR~~ - ESTIMATE FOR  
UPPER HINGE BRACKET (COMPONENT -4)

PRODUCTION RATE/HOUR	FABRICATION DESCRIPTION	EQUIPMENT	TOOLS	TOOL COST (\$1,000's)
	Steel Blank Size: .060 in. x 10 in. x 11 in. Cold Rolled Deep Draw Quality Steel Costs \$0.23/lb. Cost of Coil Steel Stock is \$0.43/part			
1200	Decoil and Flatten	Decoiler	R&L Engineering Models	3.5
			R&L Form Frames	2.5
			R&L Keller Casts	2
600	Rough Blank	Press	Blanking Die	8
600	Draw (Pull Over Plug)	Press	R&L Forming Dies	22
600	Trim	Press	R&L Trim Dies	18
600	Pierce 3 Square Holes	Press	R&L Piercing Dies	12
600	Form Return Flange	Press	R&L Flanging Dies	12
	Forward to Cleaning and Priming Area	Containers		

TOTALS FOR TABLE:

MATERIAL COST	\$0.43
TOOL COST	<u>\$80,000</u>
BURDENED LABOR COST	<u>\$0.59</u>

TABLE 3-15 IMPALA COMPOSITE DOOR - ESTIMATE FOR  
LOWER HINGE BRACKET (COMPONENT -5)

PRODUCTION RATE/HOUR	FABRICATION DESCRIPTION	EQUIPMENT	TOOLS	TOOL COST (\$1,000's)
	Steel Blank Size:.060 in. x 11 in. x 12 in. Cold Rolled Deep Draw Quality Steel Costs \$0.23/lb. Cost of Coil Steel Stock is \$0.52/part			
			R&L Engineering Models	3.5
			R&L Form Frames	2.5
			R&L Keller Casts	2
1200	Decoil and Flatten	Decoiler		
600	Rough Blank	Press	Blanking Die	8
600	Draw (Pull Over Plug)	Press	R&L Forming Dies	22
600	Trim	Press	R&L Trim Dies	18
600	Pierce 3 Square Holes	Press	R&L Piercing Dies	12
600	Form Return Flange	Press	R&L Flanging Dies	12
	Forward to Cleaning and Priming Area	Containers		

TOTALS FOR TABLE :

MATERIAL COST	<u>\$0.52</u>
TOOL COST	<u>\$80.000</u>
BURDENED LABOR COST	<u>\$0.59</u>

TABLE 3-16 IMPALA COMPOSITE DOOR - ESTIMATE FOR  
LATCH BRACKET (COMPONENT -6)

PRODUCTION RATE/HOUR	FABRICATION DESCRIPTION	EQUIPMENT	TOOLS	TOOL COST (\$1,000's)
	Steel Blank Size: .060 in. x 13 in. x 17 in. Cold Rolled Deep Draw Quality Steel Costs \$0.23/lb. Cost of Coil Steel Stock is \$0.87/part			
			R&L Engineering Models	4
			R&L Form Frames	3
			R&L Keller Casts	2
1200	Decoil and Flatten	Decoiler		
600	Rough Blank	Press	Blanking Die	9
600	Draw	Press	R&L Forming Dies	26
600	Trim 2 Sides	Press	R&L Double Trim Dies	16
600	Trim 1 End	Press	R&L Trim Dies	8
600	Trim & Flange Other End	Press	R&L Trim Dies	12
600	Form Return Flange	Press	R&L Flanging Dies	12
600	Pierce 3 Holes	Press	R&L Piercing Dies	12
	Forward to Cleaning and Priming Area	Containers		

TOTALS FOR TABLE :

MATERIAL COST	\$0.87
TOOL COST	<u>\$104.000</u>
BURDENED LABOR COST	<u>\$0.79</u>

TABLE 3-17

IMPALA COMPOSITE DOOR - ESTIMATE FOR.

ASSEMBLING COMPOSITE DOOR OUTER PANEL

PRODUCTION RATE/HOUR	FABRICATION DESCRIPTION	EQUIPMENT	TOOLS	TOOL COST (\$1,000's)
	Consists of Components -4, -5, -6, and Composite Outer Panel			
	Adhesive Required is \$.08/part			
	Degrease, Spray Prime (Air Dry) Composite Panel	Conveyor, Clean & Spray Equipment		
	Degrease, Dip Prime (Force Dry) 3 Steel Brackets	Conveyor, Clean & Dip Equipment		
	Position Door Panel in Fixture & Apply Adhesive to 3 Bracket Areas	Dispensing Equipment	R&L Bonding Fixture	30
	Position 3 Brackets to Composite Panel and Clamp			
	Move Clamped Assembly to Curing Station (8 Minute Cure Cycle)			
	Remove Clamps from Brackets			
Total Assembly  90	Forward to Next Station	Conveyor		

TOTALS FOR TABLE :

MATERIAL COST	<u>\$0.08</u>
TOOL COST	<u>\$30.000</u>
BURDENED LABOR COST	<u>\$1.74</u>

TABLE 3-18 IMPALA COMPOSITE DOOR - ESTIMATE FOR  
ASSEMBLING DOOR INNER AND OUTER PANELS

PRODUCTION RATE/HOUR	FABRICATION DESCRIPTION	EQUIPMENT	TOOLS	TOOL COST (\$1,000's)
Total Assembly  50	Adhesive Required is \$0.09/part			70
	Degrease, Spray Prime (Air Dry) Steel Inner Panel	Conveyor, Clean & Spray Equipment		
	Position Composite Assembly in Fixture & Apply Adhesive to Bonding Flange	Dispensing Equipment	R&L Bonding Fixture	
	Position Inner Panel on Composite Assembly & Clamp			
	Spot Weld Inner Panel to 3 Steel Brackets (6 Welds Total)	Overhead Spot Welder		
	Remove Assembly from Fixture and Forward to Next Station	Conveyor		

TOTALS FOR TABLE :

MATERIAL COST	\$0.09
TOOL COST	<u>\$70,000</u>
BURDENED LABOR COST	<u>\$2.56</u>

TABLE 3-19

BASELINE IMPALA COMPOSITE - ESTIMATE FOR

DOOR OUTER PANEL - COSTING SCENARIO I

PRODUCTION RATE/HOUR	FABRICATION DESCRIPTION	EQUIPMENT	TOOLS	TOOL COST (\$1,000's)
	SMC Ribs 1.0 lb. x \$0.50/lb. = \$0.50			
	Continuous Fiber 3.84 lb. x \$0.75/lb. = 2.88			
	Strap			
	SMC Outer Skin 6.8 lb. x \$0.50/lb. = 3.40			
			R&L Engineering Models	40
			R&L Form Frames	30
			R&L Keller Casts	20
600	Blank 9 Pieces SMC for Ribs	Press	Blanking Die	8
600	Blank 1 Piece Continuous Fiber Strap	Press	Blanking Die	30
600	Blank 1 Piece SMC for Outer Skin	Press	Blanking Die	30
20	Manually Strip Plastic Backing from Each Blanked Piece & Manually Place in Loading Tray		R&L Loading Trays	20
20	Cure Composite Part (90 Second Cure)	Press with Automatic Loader & Unloader	R&L Molds	180
60	Position Panel in Fixture & Pierce Door Latch & Window Mirror Slots. Trim Excess Flash from Composite Panel	Portable Grinder	R&L Trim & Piercing Fixtures	40
	Remove from Fixture & Forward to Next Station	Conveyor		

TOTALS FOR TABLE :

MATERIAL COST	\$6.78
TOOL COST	\$398,000
BURDENED LABOR COST	\$8.70

TABLE 3-20

IMPALA COMPOSITE DOOR - ESTIMATE FOR

DOOR OUTER PANEL - COSTING SCENARIO II

PRODUCTION RATE/HOUR	FABRICATION DESCRIPTION	EQUIPMENT	TOOLS	TOOL COST (\$1,000's)
	SMC Ribs 1.0 lb. x \$0.55/lb. = \$0.55 Continuous Fiber Strap 3.84 lb. x \$0.80/lb. = \$3.07 SMC Outer Skin 6.8 lb. x \$0.55/lb. = \$3.74		R&L Engineering Models R&L Form Frames R&L Keller Casts	40 30 20
600	Blank 9 Pieces SMC for Ribs	Press	Blanking Die	8
600	Blank 1 Piece Continuous Fiber Strap	Press	Blanking Die	30
600	Blank 1 Piece SMC for Outer Skin	Press	Blanking Die	30
50	Automatically Strip Plastic Backing from Each Blanked Piece & Automatically Place in Loading Tray Loaded Tray is Placed in Preheated Oven and Held for 35 Seconds	Automatic Stripper & Loader Oven	R&L Loading Trays	25
50	Cure Composite Part (40 Second Cure)	Press with Automatic Loader & Unloader	R&L Molds	180
60	Position Panel in Fixture & Pierce Door Latch & Window Mirror Slots. Trim Excess Flash from Composite Panel Remove from Fixture & Forward to Next Station	Portable Grinder Conveyor	R&L Trim & Piercing Fixtures	40

TOTALS FOR TABLE :

MATERIAL COST	\$7.36
TOOL COST	\$403,000
BURDENED LABOR COST	\$4.29

TABLE 3-21 IMPALA COMPOSITE DOOR - ESTIMATE FOR  
DOOR OUTER PANEL - COSTING SCENARIO III

PRODUCTION RATE/HOUR	FABRICATION DESCRIPTION	EQUIPMENT	TOOLS	TOOL COST (\$1,000's)
	SMC Ribs 1.0 lb. x \$0.50/lb. = \$0.50 Continuous Fiber Strap 3.84 lb. x \$0.75/lb. = 2.88 SMC Outer Skin 6.8 lb. x \$0.50/lb. = \$3.40		R&L Engineering Models	40
			R&L Form Frames	30
			R&L Keller Casts	20
600	Blank 9 Pieces SMC for Ribs	Press	Blanking Die	8
600	Blank 1 Piece Continuous Fiber Strap	Press	Blanking Die	30
600	Blank 1 Piece SMC for Outer Skin	Press	Blanking Die	30
200	Automatically Strip Plastic Backing from Each Blanked Piece & Automatically Place in Loading Tray	Automatic Stripper & Loader, Carrousel Conveyor Oven	12 R&L Loading Trays	130
	Loaded Tray Passes Through a Preheat Oven			
200	Cure Composite Part (90 Second Cure)	Press with Automatic Loader & Unloader	8 R&L Molds	1,060
200	Position Panel in Fixture & Pierce Door Latch & Window Mirror Slots. Trim Excess Flash from Composite Panel	Portable Grinder	R&L Trim & Piercing Fixture	145
	Remove from Fixture & Forward to Next Station	Conveyor		

TOTALS FOR TABLE :

MATERIAL COST	\$6.78
TOOL COST	<u>\$1,493,000</u>
BURDENED LABOR COST	<u>\$2.35</u>



For the 50 units per hour approach, the total raw material cost is \$9.35, with burdened labor costing \$10.56, and tooling for both the right and left doors estimated at \$767,000. For the 200 units per hour scenario the total raw material cost is \$8.77, with burdened labor costing \$8.62, and tooling for both the right and left doors estimated at \$1,917,000. As with the baseline steel design the tooling costs for this last scenario were based on a final assembly rate of 90 units per hour. This rate could be increased with some additional bonding fixture costs.

### 3.5.6 Cost Comparison Between Steel and Composite Designs

Direct cost comparisons between the baseline steel design and the composite version are difficult because of a number of variables. In order to make the comparison, the number of years the particular design will be used and the total number of parts of that design to be manufactured over the model life need to be established. Once these facts are known then an hourly rate can be determined so that the total number of parts required can be fabricated in the required time frame.

Steel parts are commonly manufactured on 8 hour shifts of which typically 6.5 hours are considered productive. Two such shifts per day are used in the costing exercise to arrive at a total number of units which can be produced. For the composite design, two 10 hour shifts per day are assumed to be usually run in order to conserve the energy required to heat the molds. Of each 10 hour shift, 8 hours are assumed to be productive. Hence in comparing steel to composite production, two different hourly rates are required to arrive at the same total production within a given time frame. This difference will be reflected in some of the graphs presented.

For the current cost study the added cost for part rejection and rework will be considered to be the same for both the steel and composite designs and therefore will be ignored. In addition it was assumed that the finishing costs for the composite version will be eventually comparable to that for steel and it therefore was not included in the study.

Selecting the appropriate numbers from Tables 3-3 through 3-12 and 3-14 through 3-21 allows for the comparison of just replacing the steel outer skin by the composite skin, without any intrusion protection. For the steel design, the outer panel would only involve the information on Tables 3-3, 3-4 and 3-12. For the composite design the outer panel would involve the information in one of the three Tables 3-19 through 3-21, depending on which costing scenario is being used. The material cost of the composite material would be reduced for Tables 3-19 through 3-21 since no ribs or continuous fiber material is required. In addition, Table 3-18 would have to be modified to reflect the elimination of weld-

ing the inner steel panel to the three brackets which are bonded to the strap. Table 3-22 presents the costing of this modified assembly.

The results are presented in Figures 3-37 and 3-38. In Figure 3-37, the number of units required for the life of a model car are related to the required hourly production rate through the life of the particular model. This rate then establishes the total tooling costs required to manufacture the required quantity. Some general comments are necessary to understand Figure 3-37. First of all the tooling costs start with the amounts shown in the previous tables describing the processes. Additional tooling costs have been added where required to obtain the proper manufacturing rate. The actual costs would follow a step-like response with increasing production rate since additional tooling requirements will be step additions. For the data presentation, however, straight line results have been shown. Note that the actual tooling costs used represent one half the values previously shown in the tables describing the process. Such costs should more correctly reflect the actual tooling costs per right or left hand door.

Also as seen in Figure 3-37 is the fact that a minimum amount of tooling costs exist for each costing scenario. If the required production rate is less than the costing scenario was tailored for, the tooling cost would not be reduced. In fact none of the manufacturing processes would be reduced in production rate below their targeted value. Instead they would be run at their design production speed until all the required parts were made, at which time the overhead equipment would be used for other jobs.

This concept of a minimum tooling charge becomes important in comparing the steel to the composite design. Figure 3-38 starts the same way as Figure 3-37 by comparing a total model run versus production requirements, except this time a four year model life is chosen for the example. This production rate is next presented as a function of the tooling cost per unit which is obtained from the total tooling cost of Figure 3-37 divided by the total model run. When the model production run falls too low then the tool cost per part can become significant because as indicated previously, there is a minimum tooling charge for each of the costing scenarios.

Once the tooling cost per part is established in Figure 3-38, then the part cost can be established by adding in the appropriate labor and material costs. The last item to be determined is the breakeven point which is defined as the number of model units above which it is cheaper to manufacture the part out of steel and below which the composite version is cheaper. These breakeven points which are a function of the costing scenario are also shown in Figure 3-38.

TABLE 3-22 IMPALA DOOR WITH COMPOSITE OUTER PANEL -

ESTIMATE FOR ASSEMBLING DOOR INNER &amp; OUTER PANELS

PRODUCTION RATE/HOUR	FABRICATION DESCRIPTION	EQUIPMENT	TOOLS	TOOL COST (\$1,000's)
Total Assembly  30	Adhesive Required is \$0.09/part Degrease, Spray Prime (Air Dry) Steel Inner Panel	Conveyor, Clean & Spray Equipment		70
	Position Composite Assembly in Fixture & Apply Adhesive to Bonding Flange	Dispensing Equipment	R&L Bonding Fixture	
	Position Inner Panel on Composite Outer Panel & Clamp			
	Hand Clamp 3 Flange Sides, 2 Clamps Each Side		Hand Clamps	
	Remove from Fixture to Complete the Cure Cycle	Conveyor		
	Remove the 6 Hand Clamps			
	Forward to Next Station	Conveyor		

TOTALS FOR TABLE :

MATERIAL COST	\$0.09
TOOL COST	<u>\$70,000</u>
BURDENED LABOR COST	<u>\$2.47</u>

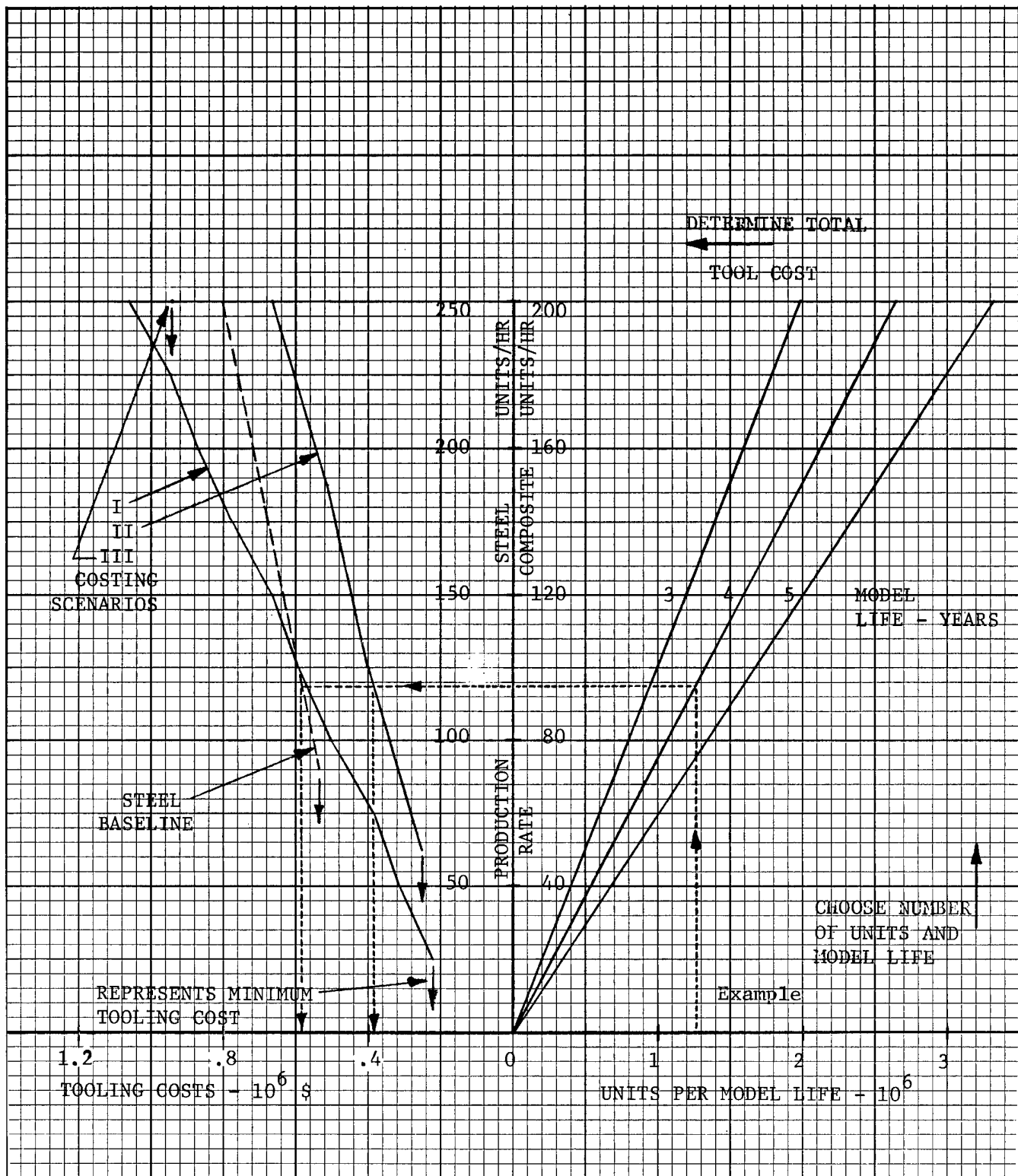


FIGURE 3-37 TOOLING COST COMPARISON BETWEEN STEEL DOOR AND COMPOSITE DOOR WITH COMPOSITE OUTER PANEL ONLY

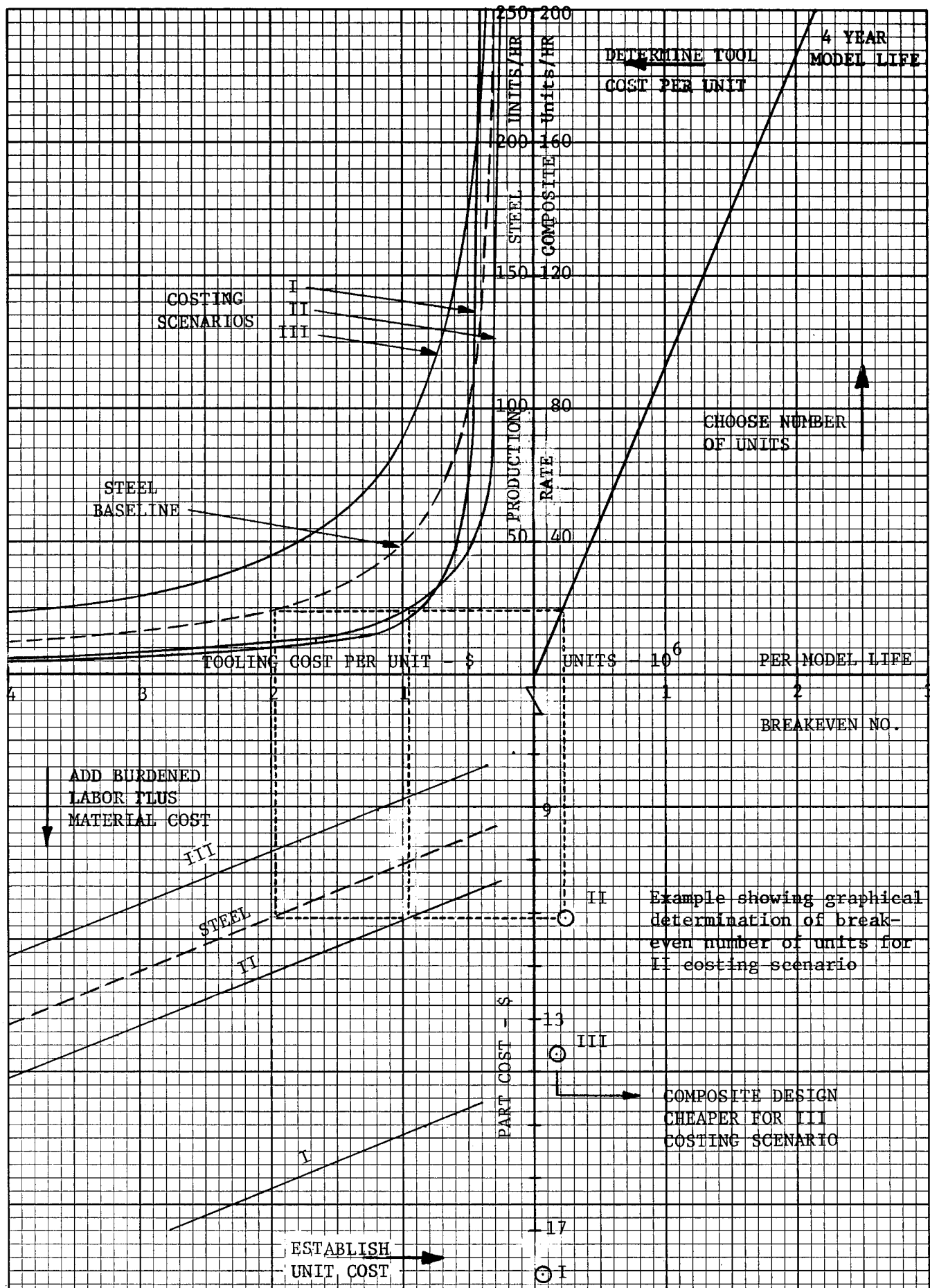


FIGURE 3-38 COST COMPARISON BETWEEN STEEL DOOR AND COMPOSITE DOOR WITH COMPOSITE OUTER PANEL ONLY

In a comparable fashion to Figures 3-37 and 3-38, Figures 3-39 and 3-40 present the same type of information for the complete composite redesign of the outer panel which includes the intrusion protection.

The costs that have been compared are the estimated manufacturing costs between a baseline steel design and a composite redesign. In Reference 6, however, a pound of weight saved for an electric or hybrid vehicle would save in the neighborhood of 0.6 pounds of additional weight as a result of downsizing other components such as the engine and drivetrain, suspension system, brakes, and so on. The resultant cost savings associated with this interacting weight reduction has not been included in this study. In addition the cost of the energy saved as a result of lighter vehicle weight has also not been included.

#### 3.4 Proposed Modification to the Composite Design

The premise under which the Impala door outer panel was redesigned using composites was that the redesign effort could not change the original form or function requirements. In comparing the results between just the composite outer panel replacement and the complete redesign of the outer panel including intrusion resistance, there was not a significant improvement in their relative cost competitiveness compared to the baseline steel version. Originally it was anticipated that a consolidation of parts would be more cost competitive than mere substitution. In the redesign effort which included the intrusion protection, the baseline steel outer panel, intrusion beam (three pieces) and the inner reinforcement were replaced by a single compression molding. Part consolidation was lost, however, when three steel brackets had to be bonded to the strap for attachment to the hinges and latch.

The existing door configuration has adjustments for the hinge, in the form of enlarged mounting holes and floating nut plates, at both the post attachment and the door attachment. The composite design also has this provision. If, however, both adjustments per hinge were not required than a design which insures parts consolidation exists. Some justification exists for looking at this alternative since the Volkswagen Rabbit has its hinges permanently welded to the door with the only adjustment occurring at the hinge to post attachment. If this approach would be acceptable for the Impala design, then the elimination of the two steel hinge brackets of Figure 3-14 can be accomplished with a possible configuration being shown in Figure 3-41. The concept shown in Figure 3-41 has that portion of the hinge, which was bolted to the steel hinge bracket of Figure 3-10, now directly bonded to the intrusion strap and the ribbed pocket. In addition to eliminating the two steel brackets, six bolts with lockwashers, two tapping plates, and two tapping plate retainers are also eliminated. Even with allowing for some increase in size of the hinge bracket which is bonded to the intrusion strap, the concept shown in Figure 3-41 could save up to an additional 1.5 pounds over what is shown in Table 3-2.

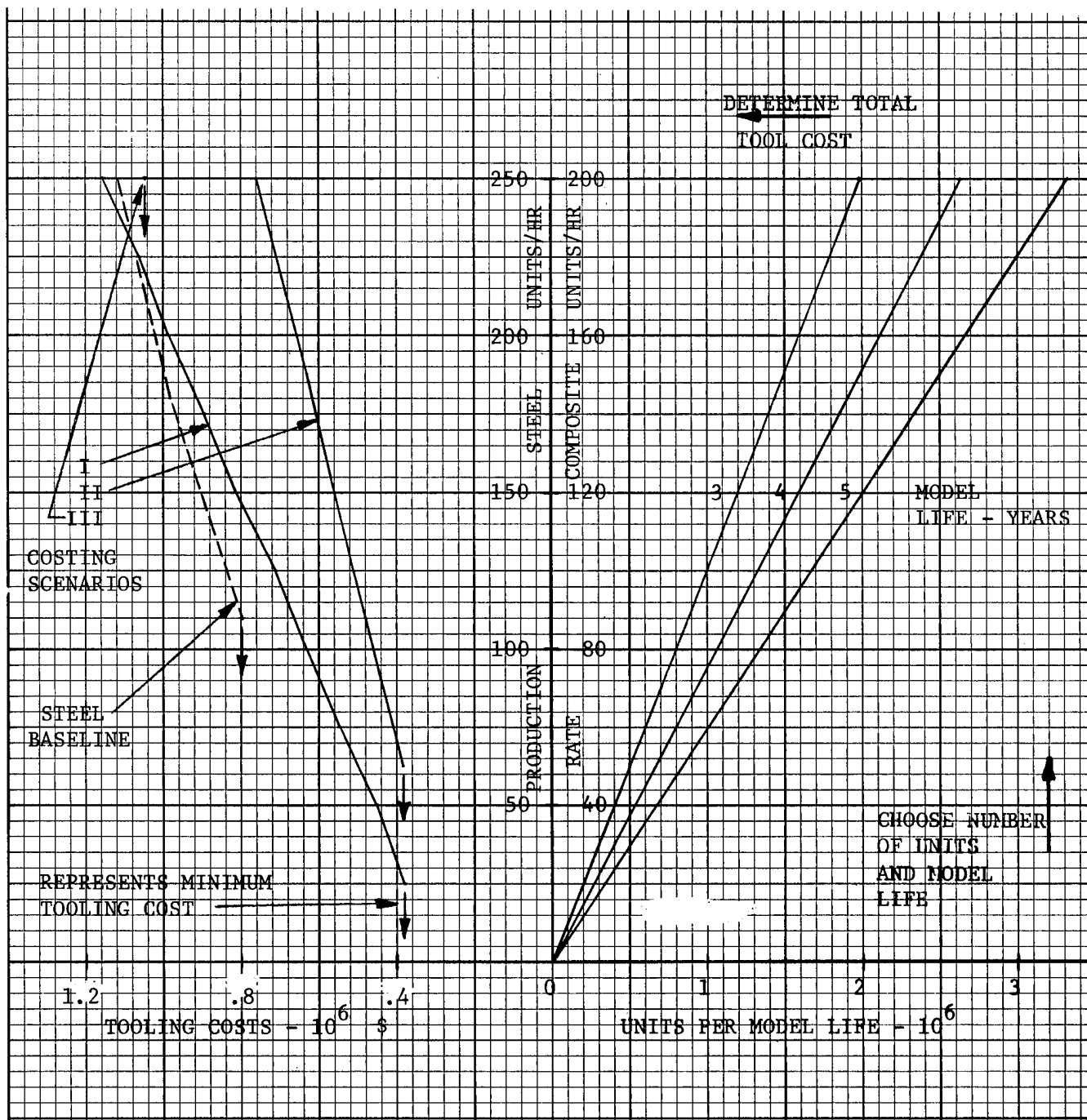


FIGURE 3-39 TOOLING COST COMPARISON BETWEEN STEEL DOOR AND COMPOSITE DOOR WITH COMPOSITE OUTER PANEL WHICH INCLUDES INTRUSION PROTECTION

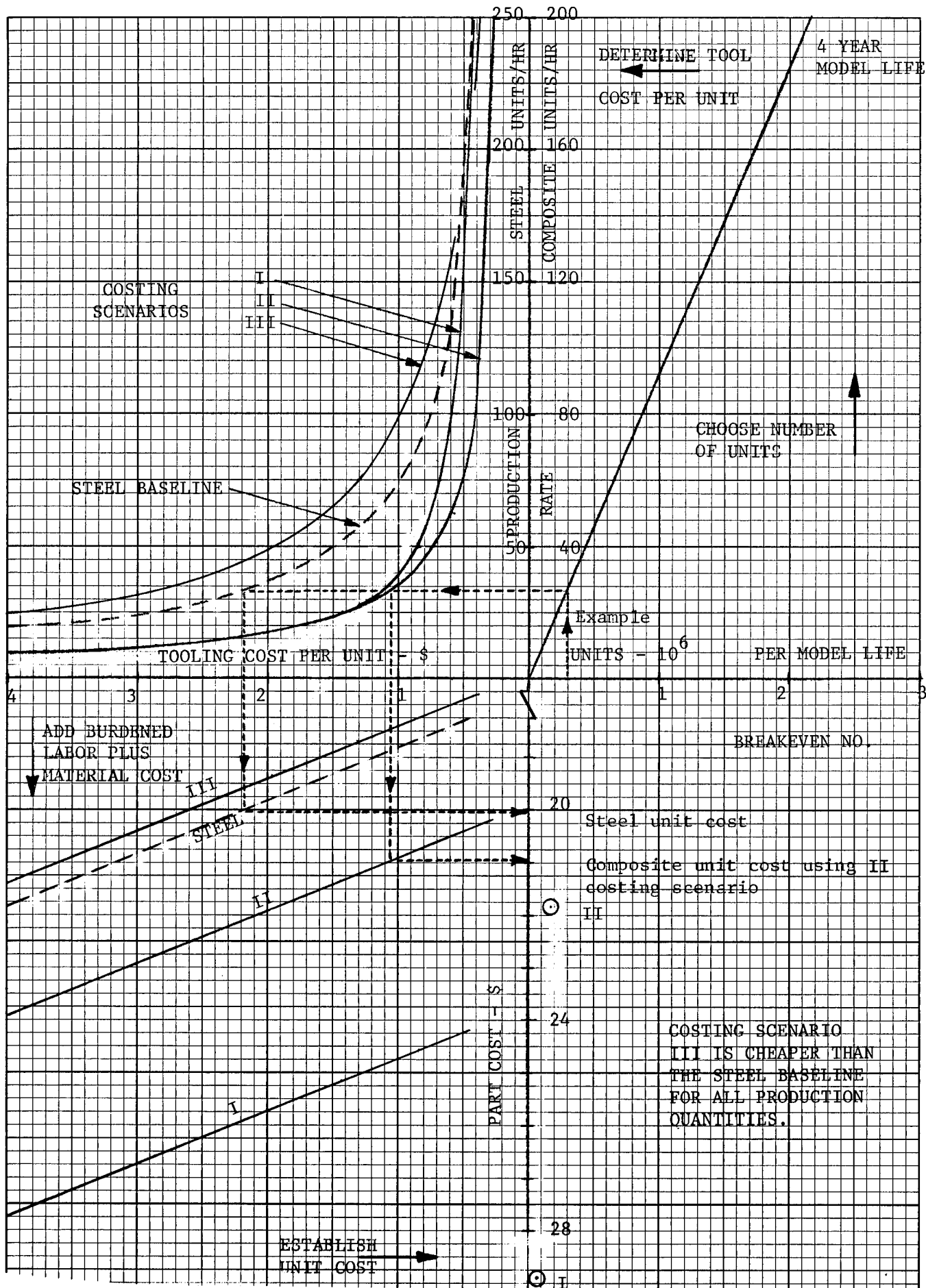


FIGURE 3-40 COST COMPARISON BETWEEN STEEL DOOR AND COMPOSITE DOOR WITH COMPOSITE OUTER PANEL WHICH INCLUDES INTRUSION PROTECTION



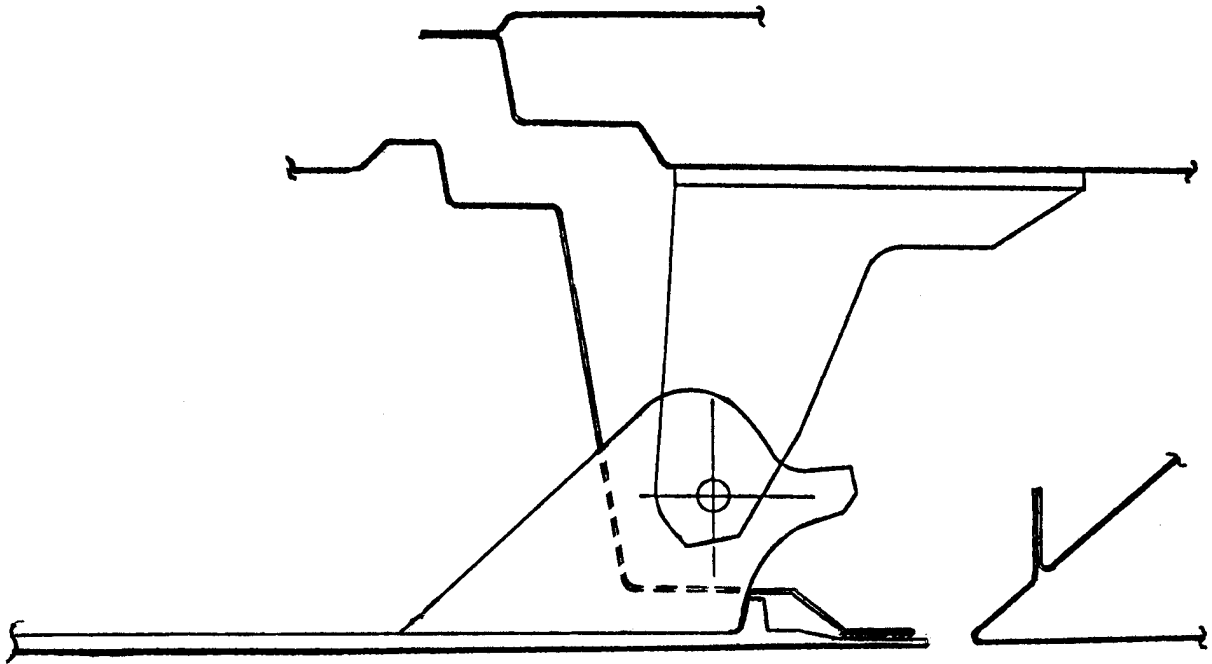


FIGURE 3-41 PROPOSED MODIFICATION TO THE COMPOSITE DESIGN WHICH ELIMINATES DOOR-TO-HINGE ADJUSTMENTS.

Some additional redesign effort would be required for the inner panel to accommodate the concept shown in Figure 3-41. Also some modifications to the assembly sequence previously presented may be required. Taking a conservative estimate of the cost savings for the proposed modification, a total of \$4.50 possibly could be saved per door. With the state-of-the-art costing effort (scenario I) of Section 3.3, the calculated breakeven point would go from approximately 70,000 units presented in Figure 3-40 to approximately 292,000 units. Remembering that these numbers represent the number of units per model life, then an assumed four year model life would yield a yearly run of 73,000 units for a breakeven number, below which composites are cheaper using the scenario I costing approach. Using the assumed \$4.50 per door savings the other two costing scenarios would show that the composite version would be cheaper than the baseline steel design for all production quantities.

Returning to the 73,000 units per year for scenario I, which corresponds to state-of-the-art technology, it is interesting to note a significant number of car models fall within this yearly production. From Reference 7, the total 1978 model run is presented in Table 3-23 for all cars manufactured in the United States. The number of models for which the composite design would be cost competitive is even greater than that presented in Table 3-23 since many models are available in either a two or four door version, each usually requiring a different door design.

In reviewing these statements for the proposed modification to the composite design of Section 3.2, it must be remembered that no detailed evaluation of effect on weight, cost, or design have been attempted other than a very cursory look. Within the framework of such an effort, however, the proposed modification appears to be a viable one.

TABLE 3-23 1978 U. S. CAR PRODUCTION TOTALS

<u>CORPORATION</u>	<u>DIVISION</u>	<u>MODEL</u>	<u>NO. OF CARS</u>
American Motors		Gremlin	7,644
		Concord	106,697
		AMX	2,720
		Pacer	15,385
		Matador	4,803
Chrysler	Plymouth	Spirit	27,102
		Horizon	162,011
		Voyager	10,673
		Volare	221,761
		Fury	49,176
		Caravelle	4,493
		Chrysler	85,596
	Chrysler	LeBaron	150,908
		Omni	126,225
	Dodge	St. Regis	15,453
		Diplomat	75,755
		Sportsman	33,220
		Aspen	162,661
		Monaco	28,246
		Pinto	185,091
		Mustang	240,162
Ford Motor	Ford	Fairmont	286,046
		Club Wagon	45,309
		Granada	246,407
		LTD II/Torino	134,608
		Thunderbird/ Elite	326,873
		Ford	278,949
	Mercury	Bobcat	38,601
		Capri	37,143
		Zephyr	88,254
		Monarch	89,974
		Cougar	218,108
		Mercury	152,149
	Lincoln	Lincoln	98,119
		Versailles	15,559
		Mark V	75,845
General Motors	Buick	Skyhawk	24,980
		Skylark	107,302
		Century	77,205
		'78/'79 Regal	275,007
		Buick	300,677
	Cadillac	Riviera	25,179
		Seville	59,794
		Cadillac	244,355
		Eldorado	46,612
	Chevrolet	Chevette	301,615
		Monza	166,948
		Camaro	281,754
		Nova	279,789
		Sportvan	30,150

TABLE 3-23 1978 U. S. CAR PRODUCTION TOTALS (CONT.)

<u>CORPORATION</u>	<u>DIVISION</u>	<u>MODEL</u>	<u>NO. OF CARS</u>
		Malibu/Chevelle	435,753
		Monte Carlo	325,786
		Chevrolet	524,074
		Corvette	48,966
	Oldsmobile	Starfire	15,274
		Omega	40,896
		Cutlass	377,251
		Oldsmobile	363,061
		Toronado	28,142
	Pontiac	Sunbird	88,714
		Phoenix/ Ventura	67,951
		Firebird	195,377
		LeMans	124,035
		Grand Prix	206,605
		Pontiac	184,327
Volkswagen			40,194
Checker			4,225

#### 4.0 CONCLUSIONS

A significant new design/fabrication concept was investigated in the redesign effort of a standard automotive door using composite materials. The approach which resulted in significant part replacement weight savings demonstrated the ability to selectively and locally reinforce a general chopped glass composite structure with continuous fiber material. The concept, if carried to its fullest potential, could account for thinner door structures and hence narrower car bodies, keeping the same interior space, which would result in major weight savings and reduced air resistance. Even without these added secondary weight and hence cost savings, parts consolidation resulting from the simultaneous molding of different materials is shown to have the potential of being cost competitive with the existing steel baseline even with today's current composite manufacturing technology and practices.

For automotive parts which are not amenable to parts consolidation, the development of shorter cure times, either through development of faster curing resins or by changing the curing arrangement, will be required before such parts would start to become cost competitive with steel.

For electric and hybrid vehicles, however, the number of units per year are low enough, at least for the current quantities considered, so that composite structural parts are cost competitive with steel for both the material substitution or part consolidation approaches.

## 5.0 RECOMMENDATIONS

The door structure is an especially critical one in that it must resist very severe impact conditions. Presently the federal regulation regarding door intrusion, FMVSS 214, is a static test. Efforts are underway, however, to update the federal regulations to include a dynamic intrusion test of the door structure. Hence from a structural consideration, it would be beneficial to statically and dynamically test the composite intrusion strap and compare it to results for the baseline steel design.

To fully develop the composite intrusion strap concept along the lines of the proposed modification of Section 3.4, where the hinge adjustment at the door was eliminated, a detailed review should be performed. Finally along the lines of acceptance by the automotive industry, tests should be performed to determine the minimum size ribs which are required to provide adequate structural integrity. Any reduction from the present size would further reduce the sink marks observed and hence the door would be more readily accepted by the industry.

The previous recommendations pertain specifically to the chosen component studied. To fully understand the potential weight savings available through the use of composites, the total chosen electric or hybrid vehicle should be reviewed or redesigned to take advantage of parts consolidation where possible.

## 6.0 NEW TECHNOLOGY

Under the terms and conditions of the contract a listing of new technology is required. For this study, no new technology which has not already been previously proposed in part in literature and patent applications, has been identified or reported under this contract.

## 7.0 REFERENCES

1. Roark, Raymond J., "Formulas for Stress and Strain", Fourth Edition, McGraw-Hill Book Company, 1965.
2. "Structural SMC - Material Process and Performance Review", by Jutte, Ralph B., SAE Paper No. 780355, February 1978.
3. "UAW Scored 3 Big Goals - but at Cost", Page 21A or the Detroit Free Press, September 17, 1979.
4. "Fiberglas/Plastic Door Study", Publication No. 5-ETR-7616, Owens-Corning Fiberglas Corporation, October 1976.
5. Personal correspondence with Dr. Joseph Epel, The Budd Company, November 6, 1979.
6. "Electric and Hybrid Vehicle System Research and Development Project", presented by Bauer, J. L., at the DOE Third Electric and Hybrid Vehicle Program Contractors Meeting, June 1979.
7. Automotive News, 1979, Market Data Book Issue, April 25, 1979.



APPENDIX A  
MATERIAL SELECTION REPORT

## ABSTRACT

A mechanical properties report was developed for the three types of fiberglass/polyester composite materials used in the fabrication of the door outer panel which incorporates an intrusion strap. The data presented was obtained primarily from published literature and as such the number of variables encountered in polyester resin formulation, and fabrication and testing techniques prohibited the generation of design allowables. The data thus presented provides the basis for preliminary designs using these materials.

Both static and fatigue data and the effect of temperature are included. In addition some environmental data is presented. An example of how laboratory flat plaque test specimens correlate with tests made from specimens cut from actual components is also discussed.

The processes for fabrication of the three types of material are included as well as a brief description of the individual material components.

## TABLE OF CONTENTS

1.0	MATERIAL PRODUCTION PROCESS.....	A 1
2.0	MATERIAL PROPERTIES.....	A 9
2.1	SMC Data.....	A10
2.2	HMC Data.....	A12
2.3	XMC and C/R Data.....	A12
2.4	Supplemental Test Results.....	A14
2.5	Mechanical Properties from Actual Production Moldings.....	A15
3.0	REFERENCES.....	A17

## LIST OF FIGURES

FIGURE	PAGE
1-1 Construction Details for Door Outer Panel Including Intrusion Protection.....	A2
1-2 SMC Production Process.....	A3
1-3 Effects of Chopped Strand Length on Strength Properties for HMC Material.....	A4
1-4 Addition of Continuous Roving to the SMC Production Set-up.....	A6
1-5 XMC Composite Manufacturing Equipment.....	A8
2-1 Tensile Strength Versus Temperature for SMC (R25 and R35).....	A20
2-2 Compressive Strength Versus Temperature for SMC (R35).....	A21
2-3 Flexural Strength Versus Temperature for SMC (R35).....	A22
2-4 Tensile Modulus Versus Temperature for SMC (R25 and R35).....	A23
2-5 Compressive Modulus Versus Temperature for SMC (R35).....	A24
2-6 Flexural Modulus Versus Temperature for SMC (R35).....	A25
2-7 Tensile Strain to Fracture Versus Temperature for SMC (R25 and R35).....	A26
2-8 Room Temperature S-N Curves for SMC and MAT R25 and R35) Loaded in Tension-Tension Fatigue...	A27
2-9 S-N Curves for SMC (R25) Loaded in Tension-Tension Fatigue for Various Temperatures.....	A28
2-10 Room Temperature S-N Curve for Notched SMC (R25) Loaded in Tension-Tension Fatigue.....	A29
2-11 Room Temperature S-N Curve for SMC (R25) Loaded in Tension-Compression Fatigue.....	A30

# LIST OF FIGURES (Cont.)

FIGURE		PAGE
2-12	Room Temperature E-N Curves for SMC (R25) Loaded in Tension-Tension Fatigue.....	A31
2-13	Room Temperature S-N Curve for SMC (R25) Loaded in Flexural Fatigue.....	A32
2-14	Tensile Strength Versus Temperature for HMC (R65).....	A33
2-15	Flexural Strength Versus Temperature for HMC (R65).....	A34
2-16	Tensile Modulus Versus Temperature for HMC (R65).....	A35
2-17	Flexural Modulus Versus Temperature for HMC (R65).....	A36
2-18	Tensile Strain to Fracture Versus Temperature for HMC (R65).....	A37
2-19	Room Temperature S-N Curve for HMC (R65 and R50) Loaded in Tension-Tension Fatigue.....	A38
2-20	S-N Curves for HMC (R65 and R50) Loaded in Tension-Tension Fatigue for Various Temperatures.....	A39
2-21	Room Temperature S-N Curve for Notched HMC (R65) Loaded in Tension-Tension Fatigue.....	A40
2-22	Room Temperature E-N Curve for HMC (R65) Loaded in Tension-Tension Fatigue.....	A41
2-23	Room Temperature S-N Curve for HMC (R65) Loaded in Flexural Fatigue.....	A42
2-24	Room Temperature Tensile Strength Versus Percentage of Chopped Glass for XMC and C/R.....	A43
2-25	Room Temperature Flexural Strength Versus Percentage of Chopped Glass for XMC and C/R.....	A44
2-26	Room Temperature Tensile Modulus Versus Percentage of Chopped Glass for C/R.....	A45
2-27	Room Temperature Flexural Modulus Versus Percentage of Chopped Glass for XMC and C/R.....	A46

# LIST OF FIGURES (Cont.)

FIGURE		PAGE
2-28	Room Temperature Interlaminar Shear Strength Versus Percentage of Chopped Glass for SMC.....	A47
2-29	Tensile Strength Versus Temperature for XMC and C/R.....	A48
2-30	Flexural Strength Versus Temperature for C/R.....	A49
2-31	Tensile Modulus Versus Temperature for XMC and C/R.....	A50
2-32	Flexural Modulus Versus Temperature for C/R.....	A51
2-33	Tensile Strain to Fracture Versus Temperature for C/R.....	A52
2-34	Room Temperature S-N Curves for XMC Loaded in Tension-Tension Fatigue.....	A53
2-35	Fatigue Strength at 10° Versus Wind Angle for XMC.....	A54
2-36	Room Temperature E-N Curves for XMC Loaded in Tension-Tension Fatigue.....	A55
2-37	Room Temperature S-N Curve for SMC Loaded in Flexural Fatigue.....	A56
2-38	Static Tensile Creep Versus Temperature for SMC (R25).....	A57
2-39	Room Temperature Water Absorption Versus Time for SMC (R30).....	A58
2-40	Environmental Stress Rupture Data for SMC (R25)..	A59
2-41	Environmental Stress Rupture Data for HMC (R65)..	A60
2-42	Room Temperature Environmental Influence on Tensile Strength for SMC (R25).....	A61
2-43	Room Temperature Environmental Influence on Tensile Modulus for SMC (R25).....	A62
2-44	Room Temperature Environmental Influence on Flexural Strength for SMC.....	A63
2-45	Room Temperature Environmental Influence on Flexural Modulus for SMC.....	A64

# LIST OF FIGURES (Cont.)

FIGURE		PAGE
2-46	Room Temperature Environmental Influence on Tensile Strength for Prestrained SMC (R25).....	A65
2-47	Room Temperature Environmental Influence on Tensile Modulus for Prestrained SMC (R25).....	A65
2-48	Room Temperature S-N Curve for MAT (R21) Loaded in Tensile Impact Fatigue.....	A66
2-49	Room Temperature Fatigue Crack Growth Rate for SMC.....	A67
2-50	Bond Shear Strength Versus Temperature for SMC, HMC, and XMC Bonded to Cold Rolled Steel.....	A68
2-51	Prototype Plastic Seat.....	A69

## LIST OF TABLES

Table 2-1	Room Temperature Mechanical Properties for SMC (R25).....	A11
Table 2-2	Room Temperature Mechanical Properties for HMC (R65).....	A13
Table 2-3	Typical Coefficient of Variations for SMC and HMC.....	A16



## 1.0 MATERIAL PRODUCTION PROCESS

Figure 1-1 identifies the materials considered for use in the actual molding of the door outer panel. Sheet molding compound (SMC) consists of chopped reinforcing fiber and a thermosetting resin which includes thickeners and other fillers. These materials are deposited on a carrier film to form a continuous sheet of material as depicted in Figure 1-2. A number of manufacturing variables can be evaluated using this production set-up, including fiber type, length of chopped reinforcement, speed of the machine, and viscosity and type of the resin.

With a continuous fiber composite, the resulting mechanical strengths and stiffnesses are dependent on fiber type and fiber orientation. When these same fibers are chopped and then randomly oriented in a resin matrix, the range and magnitude of material properties are significantly reduced compared to the possible properties of a continuous fiber composite. The fiber selection process then becomes one of economics which has dictated that the reinforcement should be glass. Within the glass family "E" glass was chosen primarily on the basis of economics although other factors such as being able to be chopped, having good impregnation characteristics, providing good flow and leaving good surface characteristics during molding had to be considered. The glass roving used has been chemically treated, or "sized", primarily to provide good adhesion to the resin system used.

The glass fiber in an SMC material can be of any length with Figure 1-3 showing the effect of fiber length for an HMC material (Reference 2). For good laydown after chopping, uniformity of glass content and random orientation in the material, lengths of less than 2 in. are used. Lengths less than one-half inch are difficult to wet-out and are therefore not usually considered. For the automotive industry, however, a length of 1 in. has become standard. Typical glass loading for SMC material is 20 to 35% by weight. With the replacement of only a few percent by weight of the fillers with glass microballoons a savings of up to 25% of the weight of the SMC material is possible with essentially no cost per pound change (Reference 3). The high-strength molding compound (HMC) is produced on the same production set-up shown in Figure 1-2 except that the fiber content is 50 to 65% by weight.

An SMC production line can be presently run at weights up to 28 oz./ft<sup>2</sup>. (Reference 4) and at speeds up to 30 ft./min (Reference 5). Working at 100% efficiency and operating continuously, a single 4 ft. wide machine can produce approximately 25 million pounds of molding compound per year (Reference 6).

Along with fiberglass being the prime fiber reinforcement of SMC, thermosetting unsaturated polyester is the universally used resin.

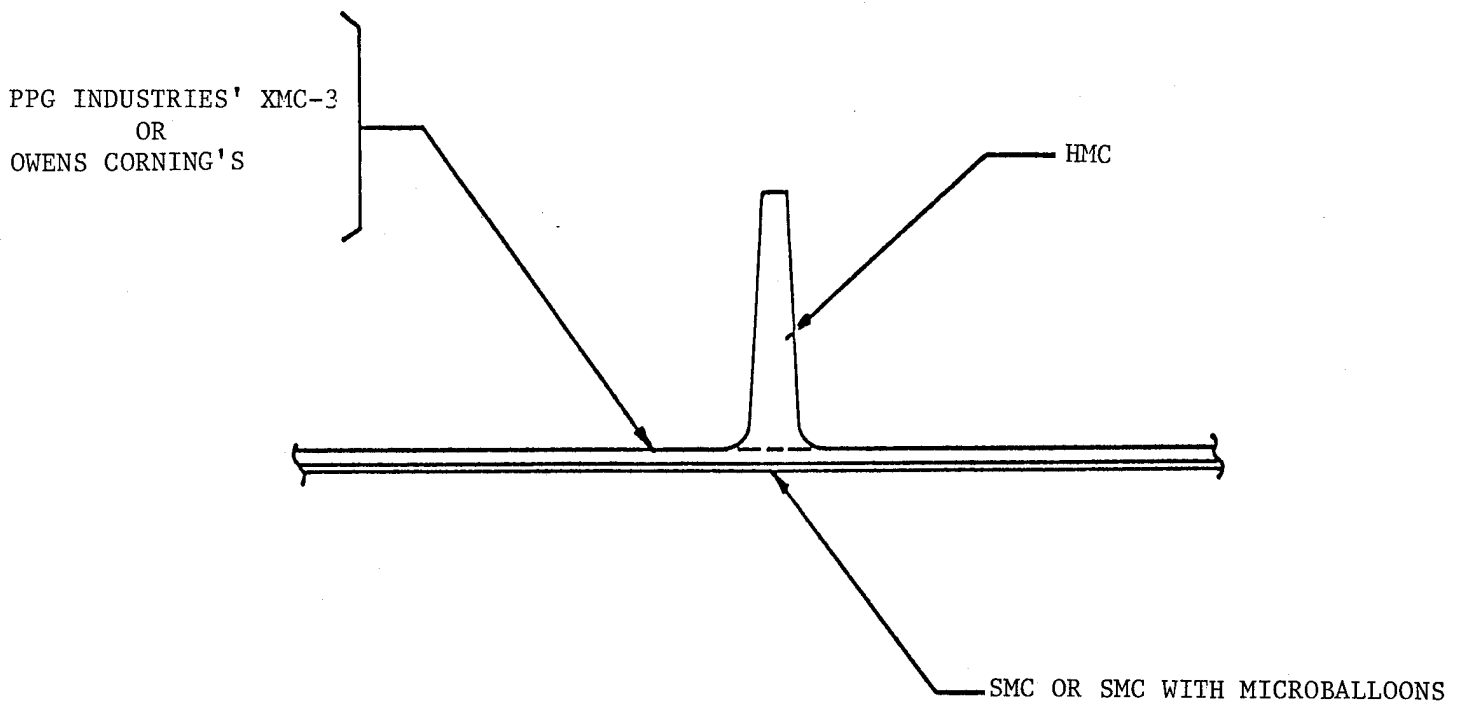


FIGURE 1-1 CONSTRUCTION DETAILS FOR DOOR OUTER  
PANEL INCLUDING INTRUSION PROTECTION

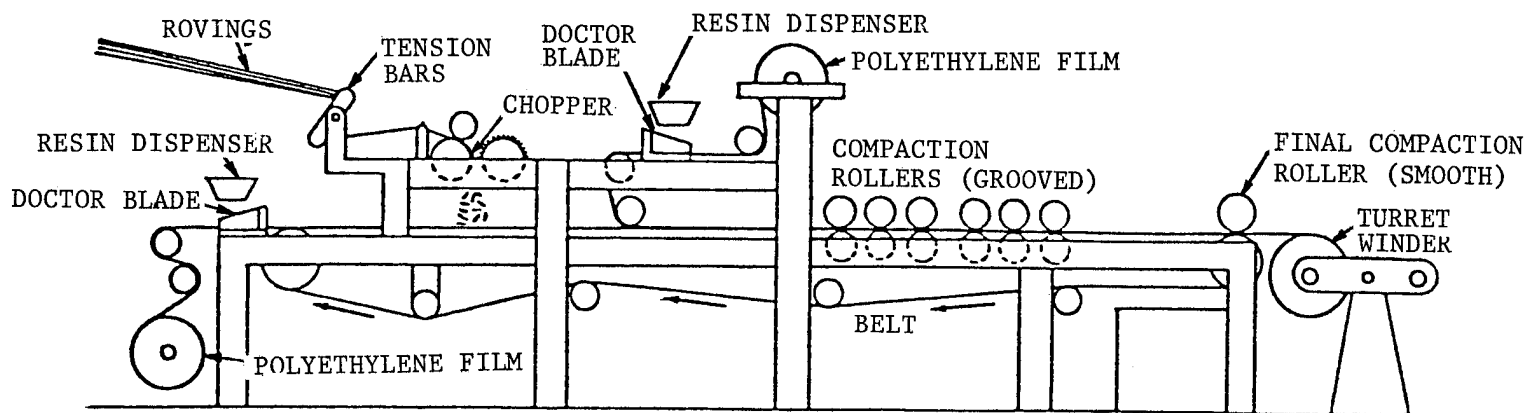


FIGURE 1-2 SMC PRODUCTION PROCESS (Reference 1)

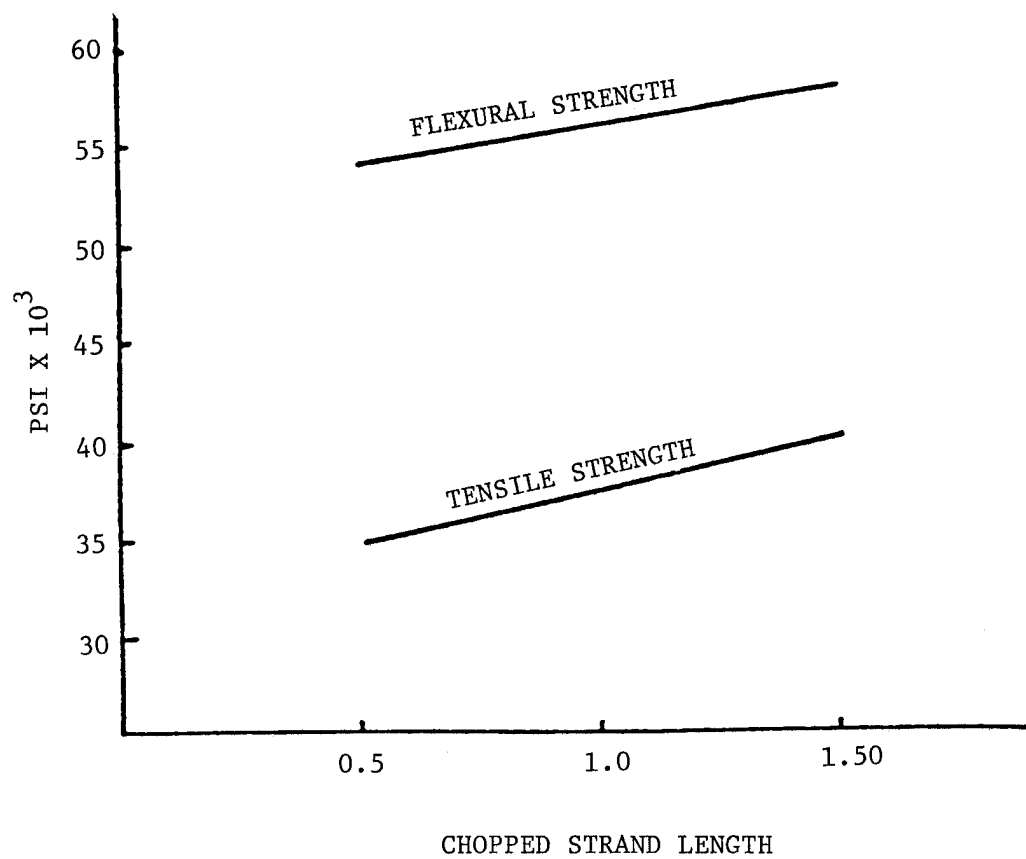


FIGURE 1-3 EFFECTS OF CHOPPED STRAND LENGTH  
ON STRENGTH PROPERTIES FOR HMC MATERIAL  
(Reference 2)

Its appeal results from good mechanical, chemical, and electrical properties, allowing easy and quick processing, and it is available at low cost. An alternative to the polyesters are vinyl ester resins. This system provides excellent chemical resistance to a large number of chemicals as well as providing excellent mechanical properties which are superior for higher temperature environments to those obtained with polyesters (Reference 7). The polyesters are, however, still lower cost than the vinyl esters and are being used predominantly in the automotive industry.

In addition to the catalyst, which is chosen primarily for a quick cure time, a number of additives (Reference 6 and 8) are combined with the polyester resin. Fillers are added to reduce cost, reduce shrinkage, improve surface appearance and to enhance moldability by promoting the flow of the glass reinforcement during curing. The fillers are usually inorganic, inert materials such as calcium carbonate, clay, talc, and hydrated alumina. For the HMC material the higher glass content replaces most if not all of the filler.

The most common thickening agents added are calcium and magnesium oxides and hydroxides. The primary purposes of the thickeners are to provide a proper molding viscosity and to prevent separation of the resin from the glass reinforcement during the flow of SMC and HMC in the mold.

A number of thermoplastic polymers are available to add to the polyester resin to achieve low polymerization shrinkage. The three general categories of polyester resins according to Owens Corning (Reference 6) are general purpose, low shrink and low profile. The most prominent distinction between the 3 types is the amount of thermoplastic material present. The general purpose polyester resin has no additives especially added to provide low-shrink or low-profile results (although the filler material may have low shrink characteristics), while the low-shrink systems have up to 10% by weight of thermoplastic polymers and low-profile systems have up to 15%. This distinction as to categories of polyester resins is not necessarily a universal one and it may vary from company to company.

Other additives include metallic stearates for mold release, pigments, flame retardants, tougheners, and ultraviolet absorbers.

After the composite material has been compounded using the arrangement shown in Figure 1-2, the SMC or HMC sheet is then matured in a temperature controlled environment to provide a uniform, reproducible viscosity for molding. The maturation process can take from one to seven days depending on resin formulation with three days being required for most systems.

Returning to Figure 1-1, one of the candidate materials for the intrusion strap is Owens-Corning's continuous/random system. Basically it starts with the same SMC production process depicted in Figure 1-2, but an additional continuous roving is fed onto the chopped glass prior to the resin impregnation as shown in Figure 1-4. Many combinations of

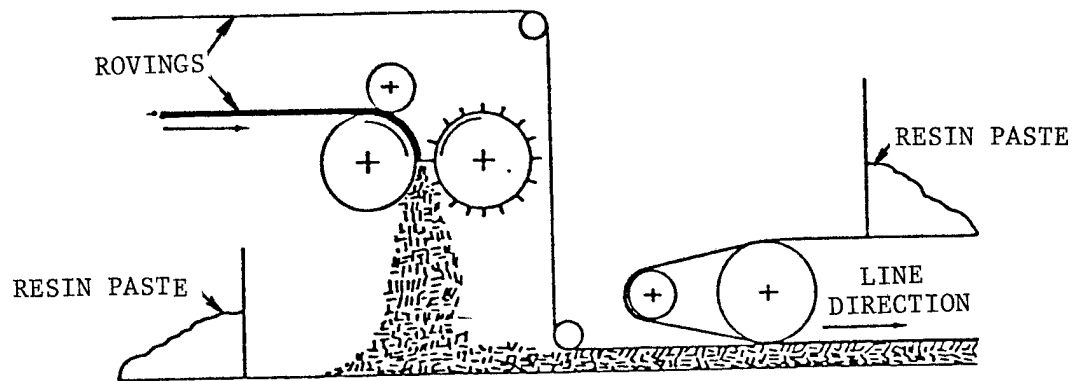


FIGURE 1-4 ADDITION OF CONTINUOUS ROVING  
TO THE SMC PRODUCTION SET-UP  
(Reference 1)

continuous and chopped glass can be constructed using this production process. The continuous roving glass placed onto the chopped glass, however, is a fixed quantity. The polyethylene film speed is varied, keeping a constant chopper speed, to vary the percentage of continuous to chopped glass content. For a high percentage of continuous glass this would result in a fairly thin material. A thicker material is possible only if more continuous glass could be fed into the system. This would be possible if more creels were used or if a prepared highly unidirectional mat was available. For many automotive applications, however, a thick section of continuous fiber is not required.

The problem with this production process in a thick section, if required, is that the continuous fiber appears on just one side of the composite and may cause thermal distortion upon curing. If a thinner compounded sheet material is used, then a thicker section could be obtained by stacking several plies, with care taken to insure a balanced layup. For mass produced automotive parts, this stacking arrangement might prove to be a source of problems.

The last material considered in Figure 1-1 is PPG Industries' XMC-3 material. Continuous glass roving is filament wound onto a large diameter mandrel to form the basic XMC-2 material. If chopped glass is added during the filament winding, then the XMC-3 material is obtained as shown in Figure 1-5. Resin is applied by first passing the roving through a resin bath prior to winding it onto the mandrel. The winding angle is relatively small, usually  $\pm 7.5^\circ$ , so the fiber reinforcement is essentially unidirectional. A number of traverses back and forth along the length of the mandrel is required to completely cover the surface of the mandrel, thus forming a single ply. With continual addition of chopped glass during the required three traverses per ply, a good distribution of chopped fiber is obtained. The chopped glass has been designed to be predominantly oriented at  $90^\circ$  to the primary composite strength direction and a wide range of continuous to chopped glass combinations are possible.

A number of plies can be added to the mandrel to form the desired thickness. A maximum thickness, however, is dictated by the size of the drum because excessive fiber distortion will occur if too thick of a material is cut from the mandrel and then laid flat.

If a dual mandrel set-up is used whereby one mandrel is being filament wound while the other one is having the composite removed and prepared for the next winding, a capacity of 300 pounds per hour is presently possible (Reference 9).

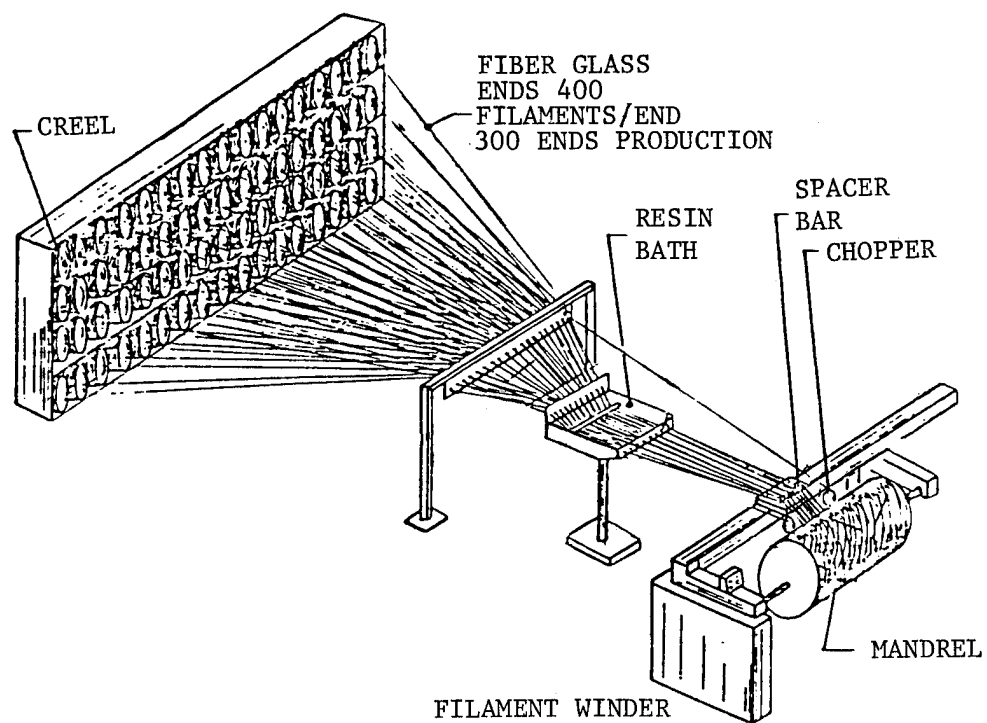


FIGURE 1-5 XMC COMPOSITE MANUFACTURING EQUIPMENT (Reference 10)



## 2.0 MATERIAL PROPERTIES

Material property data has been collected for the three classes of composite material which are used in the compression molding of the door outer panel including the intrusion strap. These material types are shown in Figure 1-1.

In presenting material data it must be kept in mind that the information is obtained from numerous sources and no guarantee exists with respect to the consistency between test techniques and accuracy. While the only resin system evaluated was polyesters, there are still differences in the various polyester formulations to cause additional variations from one data source to another. In some instances chopped glass mat data was reported to supplement data obtained from compression molded specimens. The correlation of chopped mat and compression molded specimens has not been documented and so including such data can be questioned.

Only fatigue data reported in the literature is included where the individual data points were presented. Even here the data includes inaccuracies because it had to be estimated from fatigue curves which in most cases were found in reports in a much reduced format. Individual static data were not reported in the references but instead usually just the average. In presenting the data here, when more than one source of data was found, any mean of static data curves therefore represent the mean of average data points. With the lack of individual data points and with variations of resin and fabrication and test techniques, it makes it impossible to establish design allowables. Therefore the data presented provides general information and could be used for preliminary design to evaluate the cost and weight effectiveness of utilizing the composite material presented in this report. For any critical areas, actual testing would be needed using the chosen material while maintaining all of the relevant testing considerations such as environment and stress concentrations.

One further comment is required when performing actual representative tests which were just mentioned. Such testing generally utilizes controlled laboratory specimens which are not usually made in the same way that the part will be fabricated in production. The controlled laboratory testing generally shows a lower scatter in the test data than specimens taken from a production or simulated production hardware component. A typical example will be presented, after the data presentation, in Section 2.5. This concern is primarily directed toward the chopped fiber systems because variations in flow pattern between the laboratory specimen and the specimens cut from the production part lead to the differences in data scatter observed. Such discrepancies for continuous fiber composites should not be as noticeable unless the curvature or processing of the actual part introduces fiber wrinkling which would result in a reduction of properties.

In reviewing the data presented, a number of items must be considered. For both the static and fatigue data, when a curve is marked "Mean of test points" the data has been statistically reduced. If the curve is unmarked or is labeled "estimated", it is just that, an estimated trend. For the fatigue data, the "Mean of test points" curve assumes a straight line relationship between stress and cycles on a log-log plot and the curve represents a least square, linear regression fit. Fatigue runout data points, which are indicated by an arrow attached to the data point, are not included in the statistical analysis. Also static data points are not included in the fatigue data.

The only static data which have "Mean of test points" curves are the temperature dependent properties. Here the same statistical approach was taken but a straight line was assumed, something which may not be completely justified.

In reviewing the data note that all glass percentages will be presented as a percentage of the total composite by weight. Furthermore a designation of SMC (R25) will refer to a sheet molding compound which contains 25% by weight of random chopped glass fibers. Similarly a designation of HMC (R65) refers to a high-strength molding compound containing 65% by weight of random chopped glass fibers. The glass fiber description for the continuous fiber systems will be specified on the individual data pages. If chopped glass mat data is reported it is reported in the format of MAT (R25).

## 2.1 SMC Data

Table 2-1 presents the range of room temperature mechanical properties and physical constants for SMC (R25 unless otherwise noted). Figures 2-1 through 2-6 present tensile, compressive, and flexural strength and modulus versus temperature respectively for SMC (R25 and/or R35). Some "Mean of test points" curves have been put through both R25 and R35 data points because there is an unexplained lack of distinction between them. Figure 2-7 presents the tensile strain to fracture versus temperature for these same materials.

Fatigue data for SMC is presented in Figures 2-8 through 2-13. Data with different load rates are lumped together to form a common "Mean of test points" curve for a number of these figures. Studies on the effect of cyclic rates for SMC materials appear to show the same type of scatter as is evident for a single load rate testing. Consequently distinctions will not be made for data of different load rates. In addition, no Goodman corrections have been made in the data to arrive at a common stress ratio even though slight variations between referenced data sets exist (Stress ratio is the minimum stress divided by the maximum stress for a given fatigue cycle).

TABLE 2-1 ROOM TEMPERATURE MECHANICAL PROPERTIES FOR SMC (R25)

TYPICAL PROPERTIES		UNITS	ROOM TEMPERA- TURE VALUE	REFERENCES
Strengths	Tensile Ultimate	MPa	69 - 82	11, 12, 15
	Flexural Ultimate	MPa	187	15
	Compressive Ultimate	MPa	143	12
	In-plane Shear Ultimate	MPa	---	---
	Interlaminar Shear Ultimate	MPa	14.7* - 22.1	15, 23
	Ultimate Tensile Strain	%	1.34	12
	Notched Izod Impact	kJ/m	0.72	15
Elastic	Tensile Modulus	GPa	13.2 - 13.7	12, 15
	Flexural Modulus	GPa	11.5	15
	Compressive Modulus	GPa	13.7	12
	In-plane Shear Modulus	GPa	5.3 - 5.5**	---
	Poisson's Ratio		0.25	12
Physical Constants	Density	kg/m <sup>3</sup>	1800 - 1910	12, 15
	Coefficient of Thermal Expansion	mm/mm/°C	14.4 - 23.2 x 10 <sup>-6</sup>	12, 15

\* For R30 Data

\*\* Calculated from  $G = E/2 (1 + \nu)$

Room temperature tensile fatigue is presented in Figure 2-8 where the curve for SMC (R35) is composed of the three sets of data with chopped glass ranging from 32 to 38% by weight. Within this group are two sets of chopped glass mat data with the third set containing 2 in. long chopped fiber instead of the standard 1 in. The room temperature "Mean of test points" curve for SMC (R25) taken from Figure 2-8 is compared to various temperature extremes in Figure 2-9, to notched fatigue data in Figure 2-10, and to tension-compression fatigue in Figure 2-11. Tensile modulus degradation with fatigue cycles is presented in Figure 2-12 while Figure 2-13 presents flexural fatigue data.

## 2.2 HMC Data

Table 2-2 presents the range of room temperature mechanical properties and physical constants for HMC (R65 unless otherwise noted). Figures 2-14 through 2-17 present tensile and flexural strength and modulus respectively versus temperature for HMC (R65). Figure 2-18 presents the tensile strain to fracture versus temperature for the same material.

Fatigue data for HMC (R65 and R50) is presented in Figures 2-19 through 2-23. Room temperature tensile fatigue is presented in Figure 2-19 where the data for both R50 and R65 are lumped together to form a single curve. While a different fatigue response between R50 and R65 data would be expected the two sets of data points fell so close together that a single curve was established. The room temperature "Mean of test points" curve for HMC (R65 and R50) taken from Figure 2-19 is compared to various temperature extremes in Figure 2-20, and to notched fatigue data in Figure 2-21. Tensile modulus degradation with fatigue cycles is presented in Figure 2-22 while Figure 2-23 presents flexural fatigue data.

## 2.3 XMC and C/R Data

A summary chart for the XMC and C/R material would be difficult because of the number of variables involved; the total amount of glass, the ratio of continuous to chopped glass and for the XMC material, the wind angle. The individual data values, where they are available, will have to be read from the presented data plots.

Figures 2-24 through 2-28 present the room temperature tensile and flexural strength and modulus and interlaminar shear strength respectively for XMC and/or C/R material as a function of the ratio of chopped glass to total glass content. Figures 2-29 through 2-32 present tensile and flexural strength and modulus versus temperature respectively for a single composition of the XMC and/or, C/R families. Figure 2-33 presents the tensile strain to fracture versus temperature for this same member of the C/R family. Where available, the static data presents strengths and modulus for both the primary load direction and for the transverse direction.

TABLE 2-2 ROOM TEMPERATURE MECHANICAL PROPERTIES FOR HMC (R65)

TYPICAL PROPERTIES		UNITS	ROOM TEMPERA- TURE VALUE	REFERENCES
Strengths	Tensile Ultimate	MPa	191 - 245	11, 12, 14, 15
	Flexural Ultimate	MPa	319 - 405	14, 15
	Compressive Ultimate	MPa	225*	17
	In-plane Shear Ultimate	MPa	62*	17
	Interlaminar Shear Ultimate	MPa	35.9	15
	Ultimate Tensile Strain	%	1.67	12, 14
	Notched Izod Impact	kJ/m	1.09 - 2.03	15, 18
Elastic	Tensile Modulus	GPa	14.2 - 17.0	11, 12, 14, 15
	Flexural Modulus	GPa	15.3 - 15.4	14, 15
	Compressive Modulus	GPa	16.0*	17
	In-plane Shear Modulus	GPa	5.6 - 6.7**	----
	Poisson's Ratio		0.26	12
Physical Constants	Density	kg/m <sup>3</sup>	1800 - 1820	12, 15
	Coefficient of Thermal Expansion	mm/mm/°C	7.2 - 13.7 x 10 <sup>-6</sup>	12, 15

\* For R50 Data

\*\* Calculated from  $G = E/2 (1 + \nu)$

Fatigue data for XMC is presented in Figures 2-34 through 2-37. Room temperature tensile fatigue is presented in Figure 2-34 as a function of wind angle. This data for  $10^6$  cycles is replotted in Figure 2-35 to provide an indication of wind angle effect on fatigue strength. Tensile modulus degradation with fatigue cycles is presented in Figure 2-36 while Figure 2-37 presents flexural fatigue data.

## 2.4 Supplemental Test Results

In addition to displaying a loss in stiffness with fatigue loading as shown in Figures 2-12 and 2-22, the chopped systems also creep under static loading. Figure 2-38 gives the magnitude of creep for SMC (R25) material versus temperature for a single loading. While the amount of creep for the continuous fiber systems is considerably less, they also do exhibit a stiffness reduction with fatigue loading.

Water absorption by the composite systems considered is possible with Figure 2-39 providing data for an uncoated SMC (R30) system. The detrimental effect of the moisture absorption can be seen in Figures 2-40 and 2-41 where environmental stress rupture data is presented for SMC (R25) and HMC (R65) respectively. At each temperature the higher humidity data showed a lower time to failure.

Effects of exposure of SMC (R25) to various automotive type fluids and environments are presented in Figures 2-42 and 2-43 for tensile strength and modulus respectively. Additional environmental exposure influence on SMC flexural strength and modulus are presented in Figures 2-44 and 2-45 respectively. The previous four figures presented data on exposure while the specimen was in an unloaded state. It is believed, although supporting data could not be found, that for similar data where the specimen was exposed while loaded would prove to be more damaging. In Figures 2-46 and 2-47 the SMC (R25) specimens were first prestrained (to an unreported level) and then subjected to environmental exposure resulting in the tensile strength and modulus data presented.

Very little impact data was available in the literature. Reference 28 made the comment that for continuous glass fiber/polyester composites that "stone impact, as simulated by subjecting samples to repeated cycles on the Ford gravelometer, results in no detectable deterioration of fatigue properties." In Figure 2-48 a MAT (R21) specimen was subjected to repeated tensile impact loads. The results are compared to the mean curve of SMC (R25) tensile fatigue data of Figure 2-8.

Fatigue crack growth for SMC is presented in Figure 2-49 with the usual metals format. While a well defined crack, propagating in the material, is not observed with the chopped fiber systems, the zone of damage growth has been likened to crack propagation in metals.

The continuous fiber systems do not display this same type of damage growth. For instance, for the C/R systems loaded in tensile fatigue, crack growth from a notch runs parallel to the continuous fibers starting at the edge of the notch.

The metal fittings which attach to the car's door hinges and latch are first bonded to the composite door outer panel. Figure 2-50 provides bond shear strength versus temperature for steel bonded to SMC, HMC, and XMC. The test results are for a single overlap test specimen which fails prematurely due to induced peel loads. The ribs which are molded with the door outer panel will react the peel loads and as a result the bond shear strength will be significantly increased.

## 2.5 Mechanical Properties from Actual Production Moldings

The problem of variations in test results between controlled laboratory specimens and specimens cut from actual production components was previously mentioned. The following discussion will review this problem for a specific example where both the laboratory specimens and the production component were fabricated using the same material and both sets of specimens were tested at The Budd Company Technical Center.

Flexural and tensile test results were obtained using specimens cut from compression molded flat plaques of SMC (R27) or HMC (R60) material. The coefficient of variation (COV), which is defined as the standard deviation of a number of samples divided by the mean of the samples, is used as the measure of scatter in the data. The COV for the specimens tested from the flat plaques are presented in Table 2-3.

For comparison flexural properties of a prototype plastic seat, Figure 2-51, were measured. The four components of the seat, the cushion (1), the cushion reinforcement (2), the back (3), and the back reinforcement (4), were cut into flexural specimens and tested for strength and modulus. Results indicate that the average strengths and moduli are within 8% of the values measured from the flat test plaques. The coefficient of variations, however, were much larger than those observed in Table 2-3. For the SMC (R27) material the COV was 37 and 17% for flexural strength and stiffness respectively. Similarly the COV was 43 and 28% for flexural strength and stiffness respectively for HMC (R60). The conclusion is that although the flexural strength and modulus are approximately the same for the two sets of specimens, the design level based on tests using actual hardware will be much lower.

TABLE 2-3

TYPICAL COEFFICIENT OF VARIATIONS FOR SMC AND HMC

Composite Material	Flexural Strength	Flexural Modulus	Tensile Strength	Tensile Modulus
SMC (R27)	19%	7%	17%	12%
HMC (R60)	17%	13%	17%	12%



### 3.0 REFERENCES

1. "The Molding-Compound Alphabet Soups...A Cookbook of Basic Recipes", by Stedfeld, Robert, Materials Engineering, September 1978.
2. "HMC, High Strength Molding Composites - New Formulations, Processing and Molding", Technical Service Bulletin TS-201A, PPG Industries, June 1977.
3. "Glass Microspheres: Bubbles and Beads as Plastic Additives", by Muck, Darrel L. and Ritter, James R., Plastics Compounding, January/February 1979.
4. "What to Look for in SMC Production Machines", by Miller, Everett R., Plastics Technology, December 1970.
5. "Upping Manufacturing Productivity: Detroit's Plans for the Eighties", by von Hassell, Agostino, Plastics Technology, November 1978.
6. "Sheet Molding Compound", Owens-Corning Fiberglas Publication No. 5-TM-6991-A, June 1976.
7. "Unsaturated Polyester", Plastics Design Forum, May/June 1979.
8. "Reinforced Thermosets", by Rehm, M. A., Modern Plastics Encyclopedia, 1978-1979.
9. "XMC Moldable High Strength Fiber Glass/Resin Sheets - A General Guideline to Processing and Molding", Technical Service Bulletin TS-202B, PPG Industries, May 1978.
10. "XMC-3 Composite Material - Structural Molding Compound", by Ackley, Richard H., and Carley, Earl P., presented at The 34th Annual Technical Conference, Reinforced Plastics/Composites Institute, SPI, 1979.
11. "Engineering Properties of Automotive Fiber Reinforced Plastics", by Sanders, Barbara A., and Heimbuch, Roger A., presented at The Conference on Environmental Degradation of Engineering Materials, October 1977.
12. "Mechanical Properties of Automotive Chopped Fiber Reinforced Plastics", by Heimbuch, Roger A., and Sanders, Barbara A., presented at The ASME Winter Annual Meeting, December, 1978.

13. "HMC - A High Performance Sheet Molding Compound", by Maaghul, J., and Potkanowicz, E. J., presented at The 31st Annual Technical Conference, Reinforced Plastics/Composites Institute, SPI, 1976.
14. "Structural SMC: Material, Process and Performance Review", by Jutte, Ralph B., presented at The 33rd Annual Technical Conference, Reinforced Plastics/Composites Institute, SPI, 1978.
15. "A Comparison of Typical Properties of High Pressure, Fiber Glass Reinforced Composites for Transportation Applications", Technical Service Bulletin TS-206, PPG Industries.
16. "Role of Matrix Resins in High Modulus Composites of Fiber Glass", by Das, B., and Tucker, B. D., presented at The 34th Annual Technical Conference, Reinforced Plastics/Composites Institute, SPI, 1979.
17. "Mechanical Properties Characterization of an SMC-R50 Composite", by Denton, Douglas L., presented at The 34th Annual Technical Conference, Reinforced Plastics/Composites Institute, SPI, 1979.
18. "Technical Data: SMC-R50 & SMC-R65", Owens/Corning Fiberglas Publication No. 5-TM-8363-A, May 1978.
19. "Engineering Design Handbook - Short Fiber Plastic Base Composites", U. S. Army Material Command Pamphlet No. 706-313, July 1975.
20. "Fiber Glass Reinforced Plastics...by Design", PPG Industries' brochure.
21. "Polyester Flexibility Versus Fatigue Behavior of RP", by Owen, M. J., and Rose, R. G., Modern Plastics, November 1970.
22. "Fatigue Crack Growth in Fiber Reinforced Plastics", by Mandell, J. F., presented at The 34th Annual Technical Conference, Reinforced Plastics/Composites Institute, SPI, 1979.
23. "Unique Electrical and Mechanical Properties of ITP SMC", by Magrans, Juan J., and Ferrarini, James, presented at The 34th Annual Technical Conference, Reinforced Plastics/Composites Institute, SPI, 1979.
24. "Fatigue and Failure Mechanisms in GRP with Special Reference to Random Reinforcements", by Owen, M. J., Dukes, R., and Smith, T. R., presented at The 23rd Annual Technical Conference, Reinforced Plastics/Composites Institute, SPI, 1968.

25. "The Effect of Various Chemical Environments on the Flexural Properties of Molded SMC", by McCabe, Michael V., presented at The 34th Annual Technical Conference, Reinforced Plastics/Composites Institute, SPI, 1979.
26. "Effect of Thermal Cycling on FRP Materials", by Docks, E. L., and Buck, D. E., presented at The 34th Annual Technical Conference, Reinforced Plastics/Composites Institute, SPI, 1979.
27. "Impact Fatigue Strength and Fracture of Glass Fiber Composites", by Fujii, Taichi, and Miki, Mitsunori, Presented at The 31st Annual Technical Conference, Reinforced Plastics/Composites Institute, SPI, 1976.
28. "Flexural Fatigue of Unidirectional Fiberglass-Reinforced Polyester", by Fesko, Donald G., Polymer Engineering and Science, April 1977.
29. "XMC and HMC - Structural Molding Compounds", by Ackley, Richard H., Society of Automotive Engineering Paper No. 760053, February 1976.
30. "Wheel Wells of Structural SMC - For Transportation Industry", by Stanley, Art, presented at The 34th Annual Technical Conference, Reinforced Plastics/Composites Institute, SPI, 1979.
31. "Processing and Mechanical Properties of Carbon Fiber/Glass Reinforced XMC Composite", Technical Service Bulletin TS-705-1, PPG Industries, March 1978.
32. Personal correspondence between J. C. Palermo of Owens-Corning Fiberglas Corporation and H. A. Jahnle of The Budd Company Technical Center, October 1977.
33. "The Bonding of High Strength Plastics", by Carapellotti, Lawrence R., and Rabito, Thomas G., from a handout at the paper's presentation at The 32nd Annual Technical Conference, Reinforced Plastics/Composites Institute, SPI, 1977.

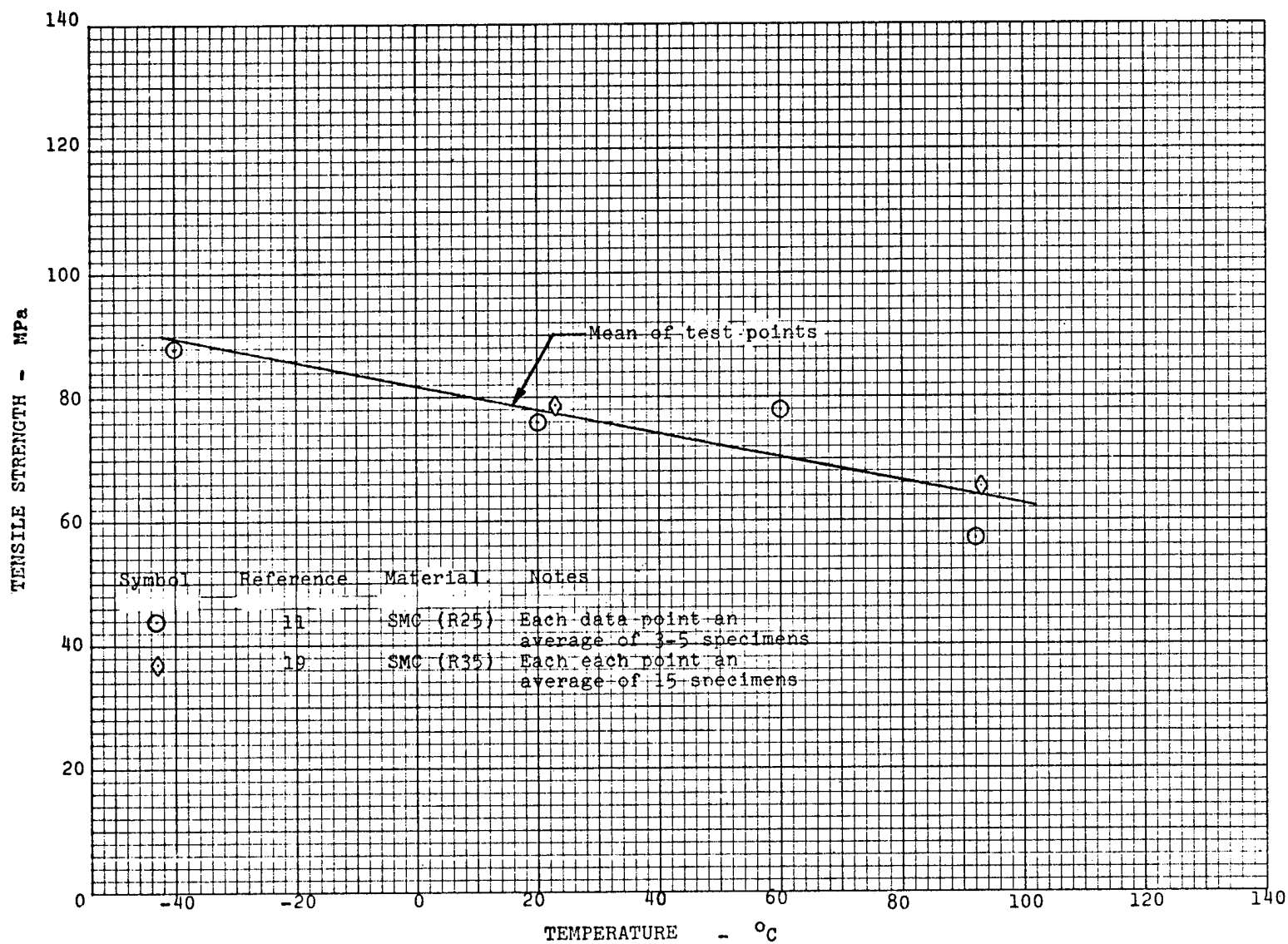


FIGURE 2-1 TENSILE STRENGTH VERSUS TEMPERATURE FOR SMC (R25 and R35)

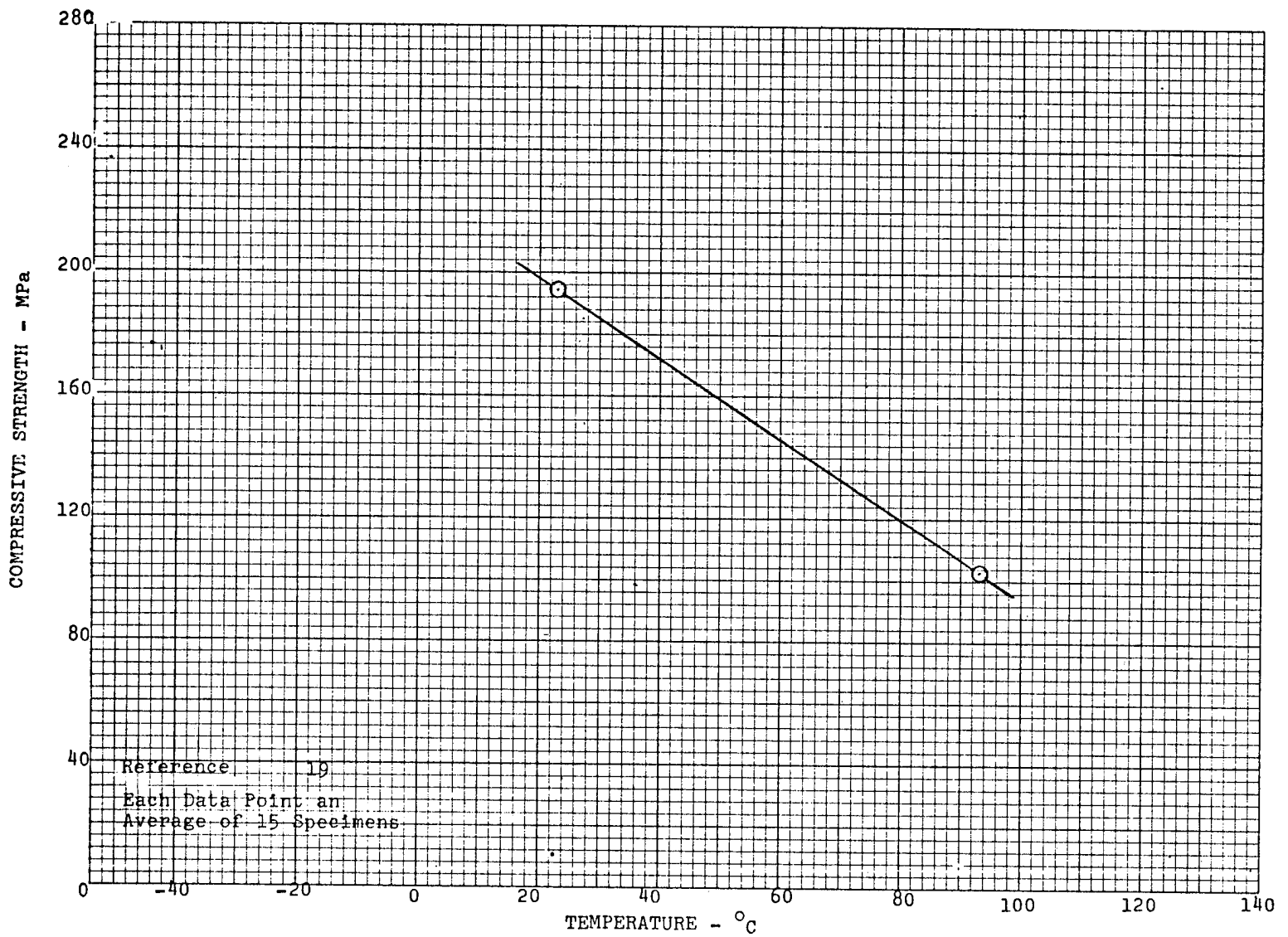


FIGURE 2-2 COMPRESSIVE STRENGTH VERSUS TEMPERATURE FOR SMC (R35)

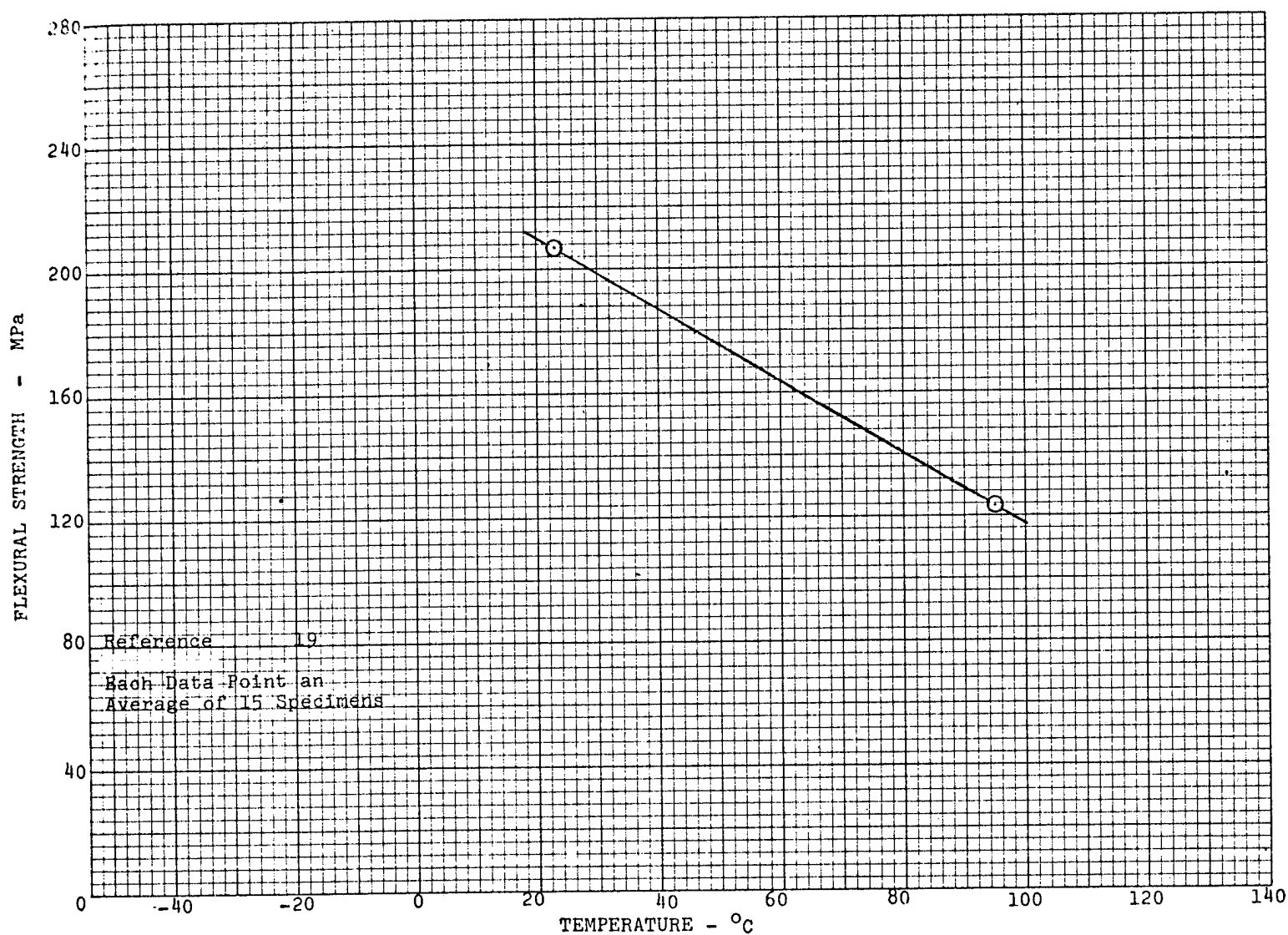


FIGURE 2-3 FLEXURAL STRENGTH VERSUS TEMPERATURE FOR SMC (R35)

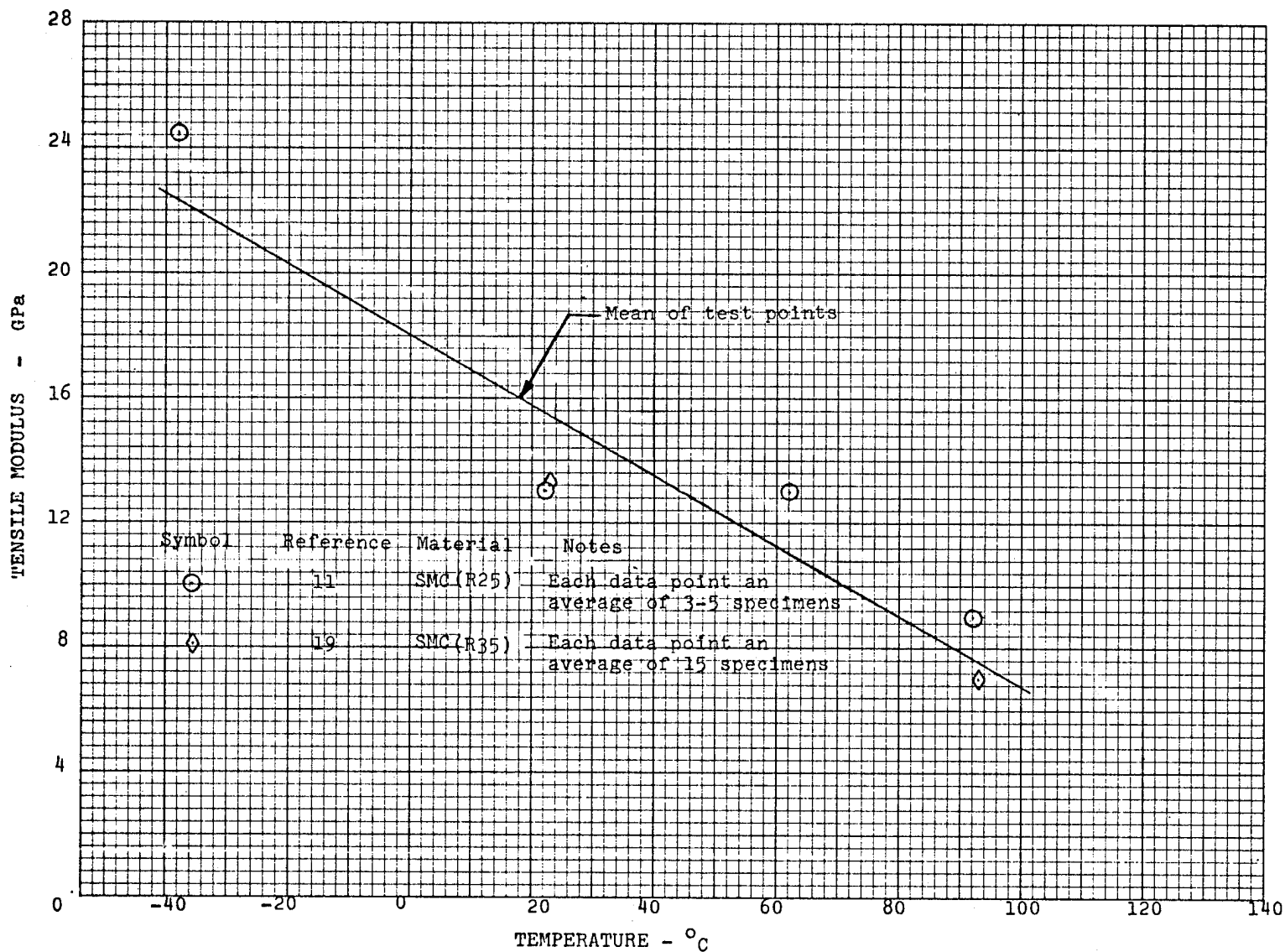


FIGURE 2-4 TENSILE MODULUS VERSUS TEMPERATURE, FOR SMC (R25 and R35)

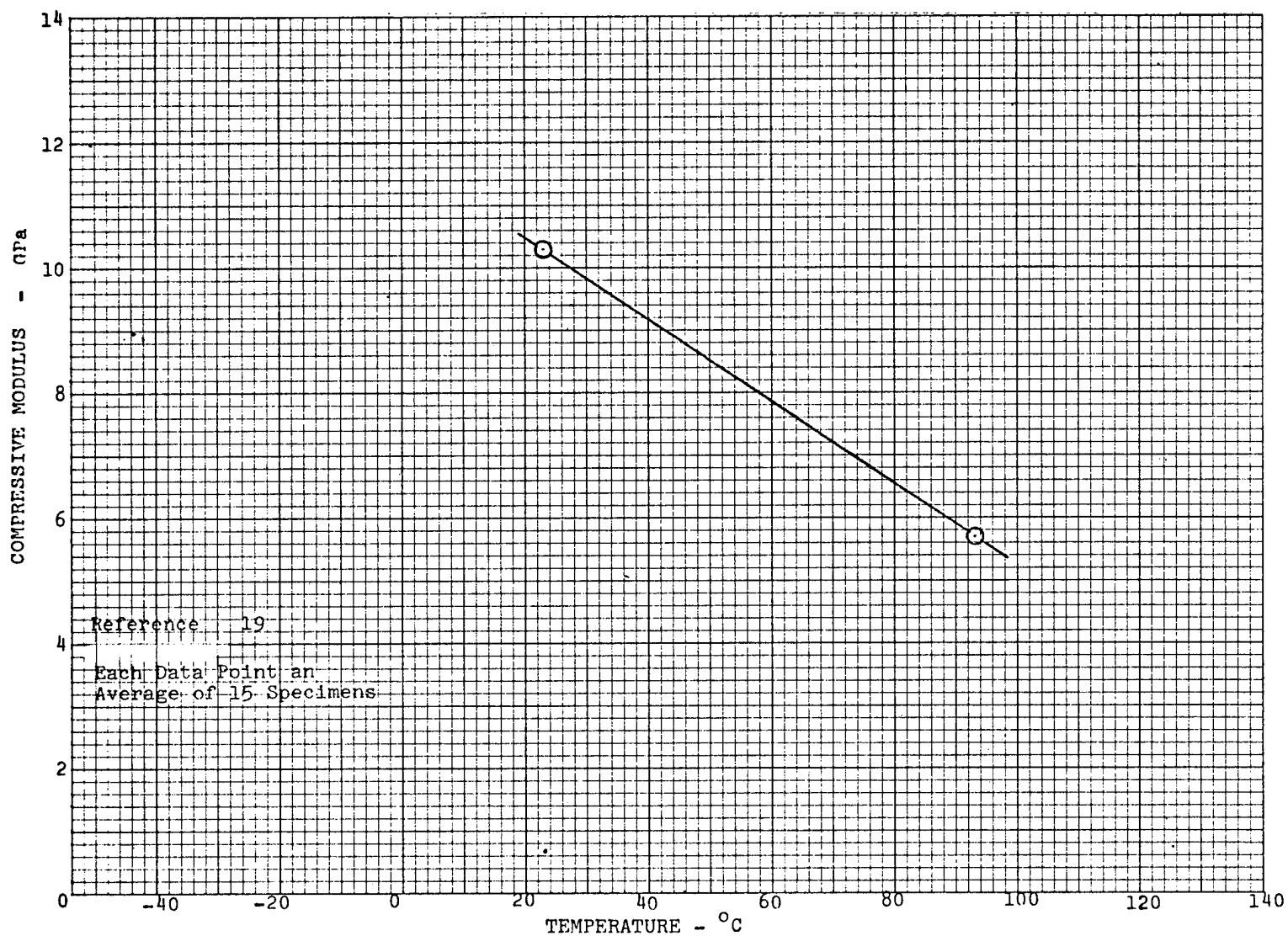


FIGURE 2-5 COMPRESSIVE MODULUS VERSUS TEMPERATURE FOR SMC (R35)



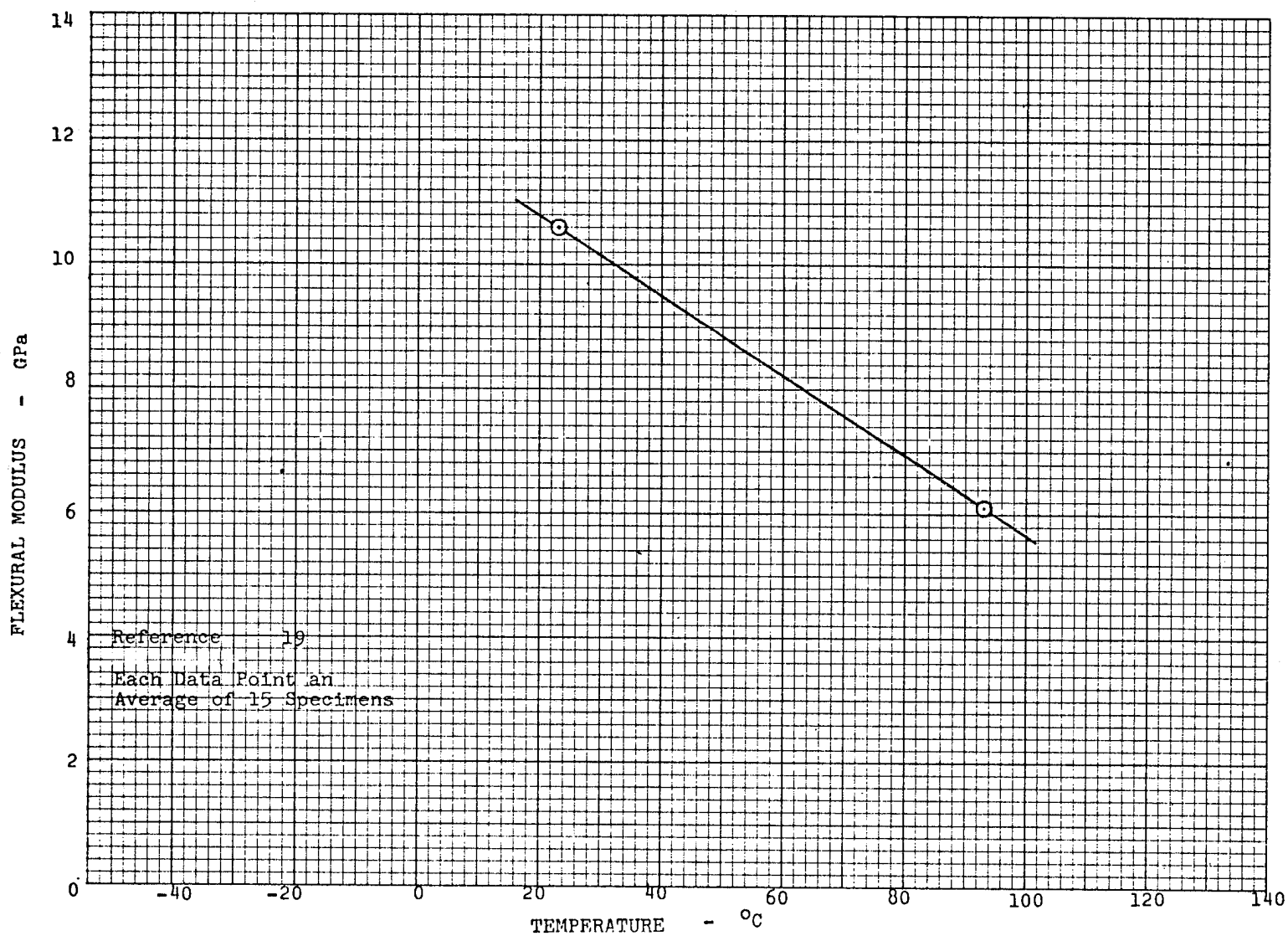


FIGURE 2-6 FLEXURAL MODULUS VERSUS TEMPERATURE FOR SMC (R35)

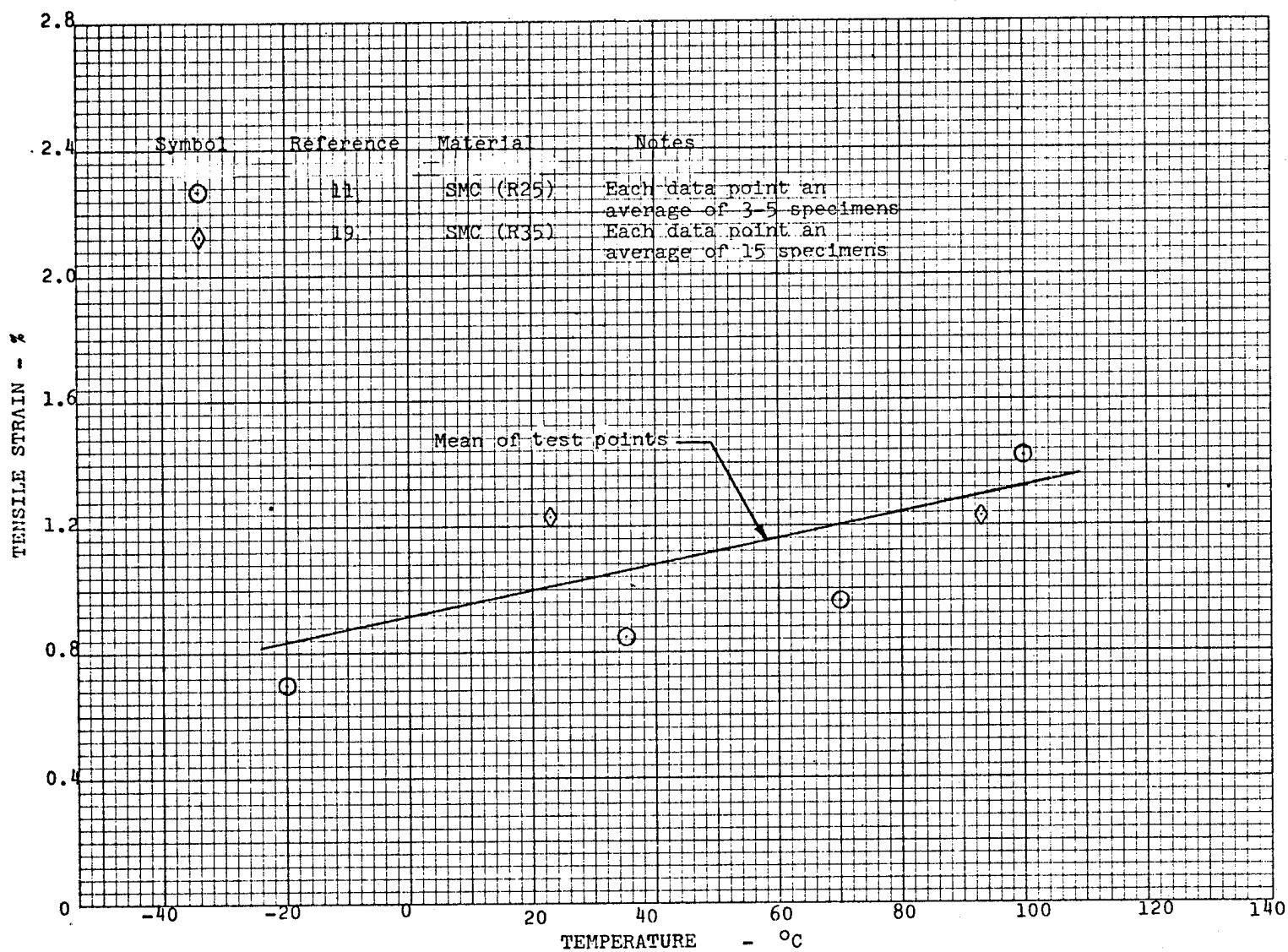


FIGURE 2-7 TENSILE STRAIN TO FRACTURE VERSUS TEMPERATURE FOR SMC (R25 and R35)

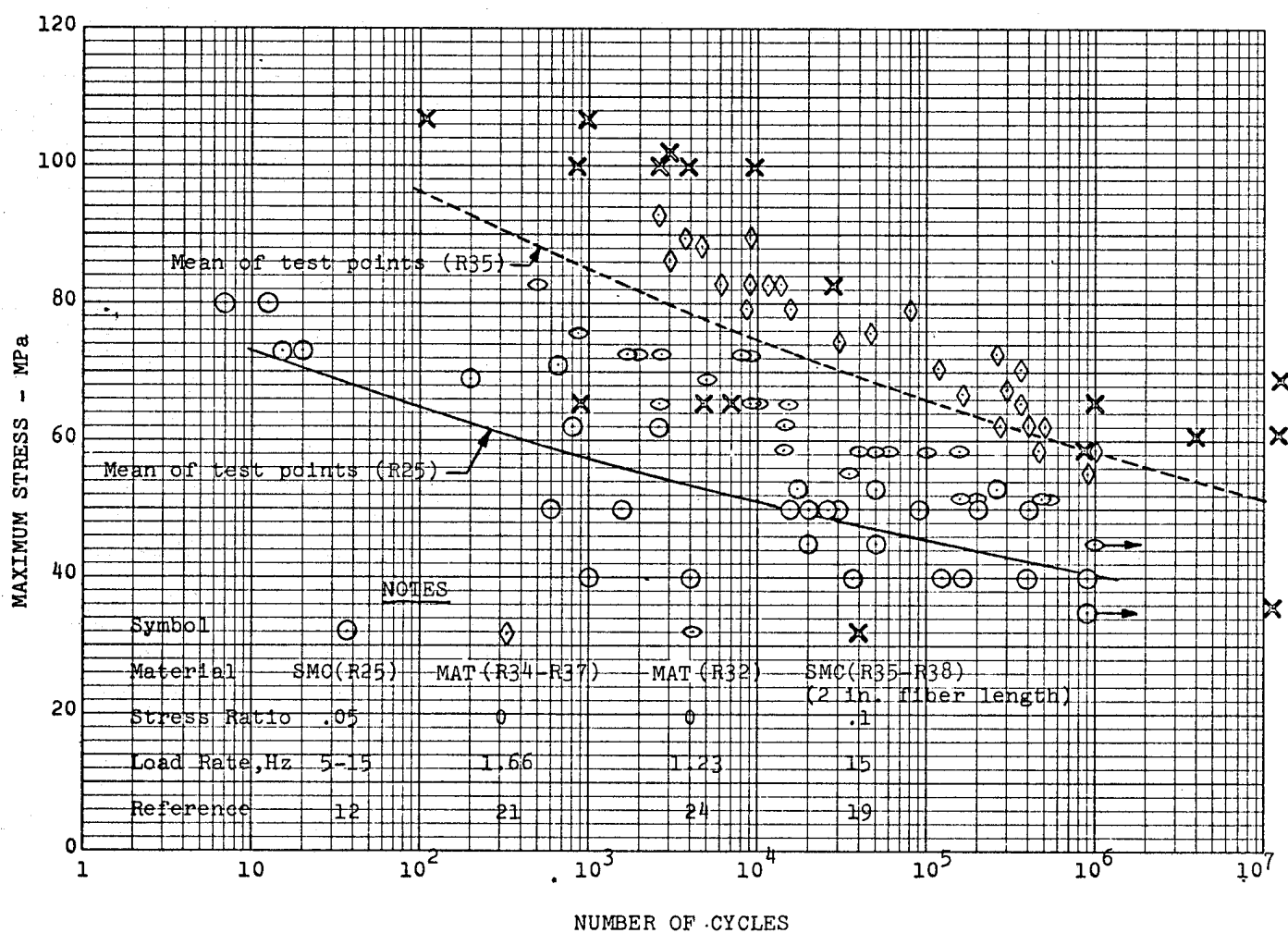


FIGURE 2-8 ROOM TEMPERATURE S-N CURVES FOR SMC AND MAT (R25 AND R35) LOADED IN TENSION-TENSION FATIGUE

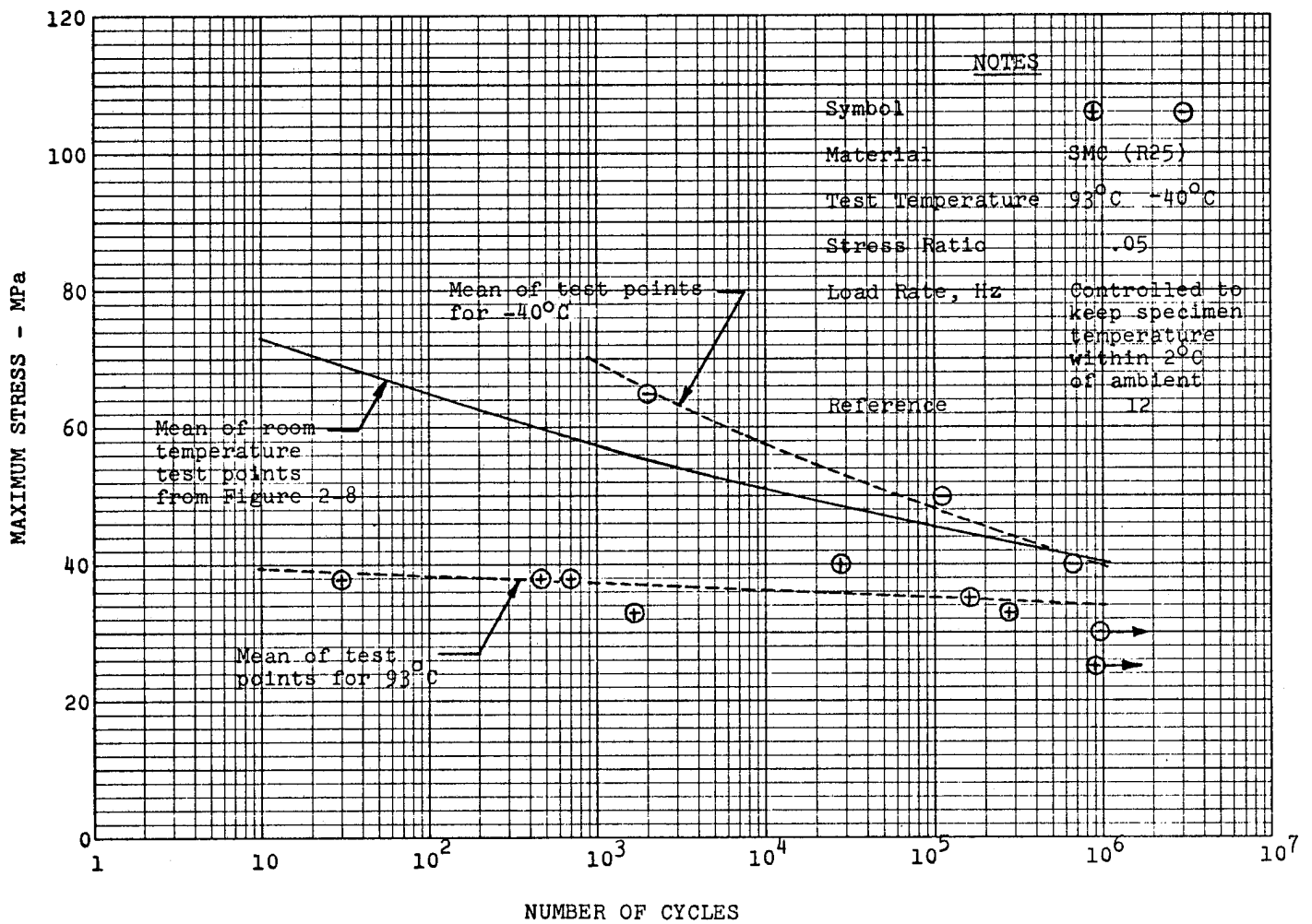


FIGURE 2-9 S-N CURVES FOR SMC (R25) LOADED IN TENSION-TENSION FATIGUE FOR VARIOUS TEMPERATURES

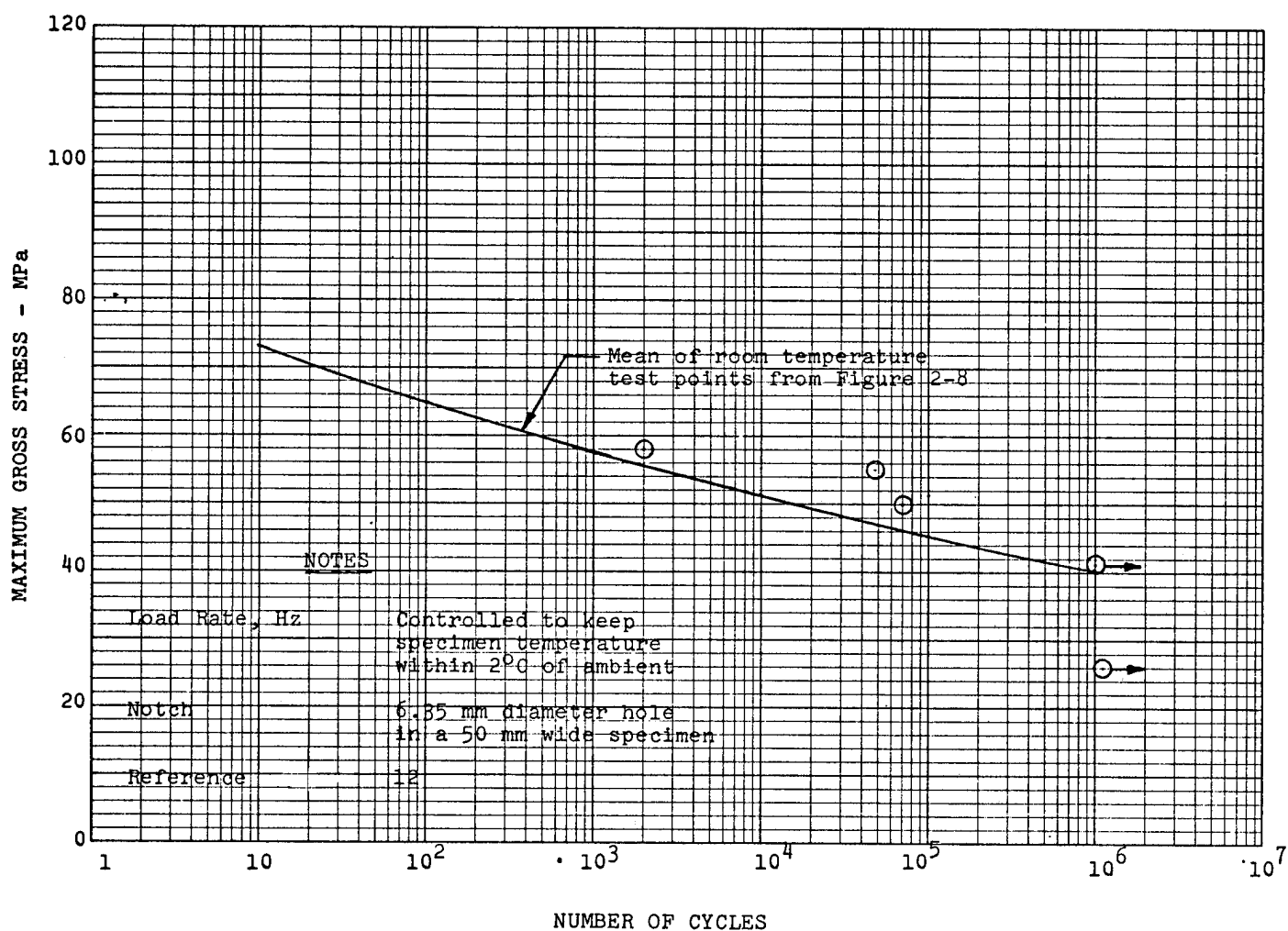


FIGURE 2-10 ROOM TEMPERATURE S-N CURVE FOR NOTCHED SMC (R25) LOADED IN TENSION-TENSION FATIGUE

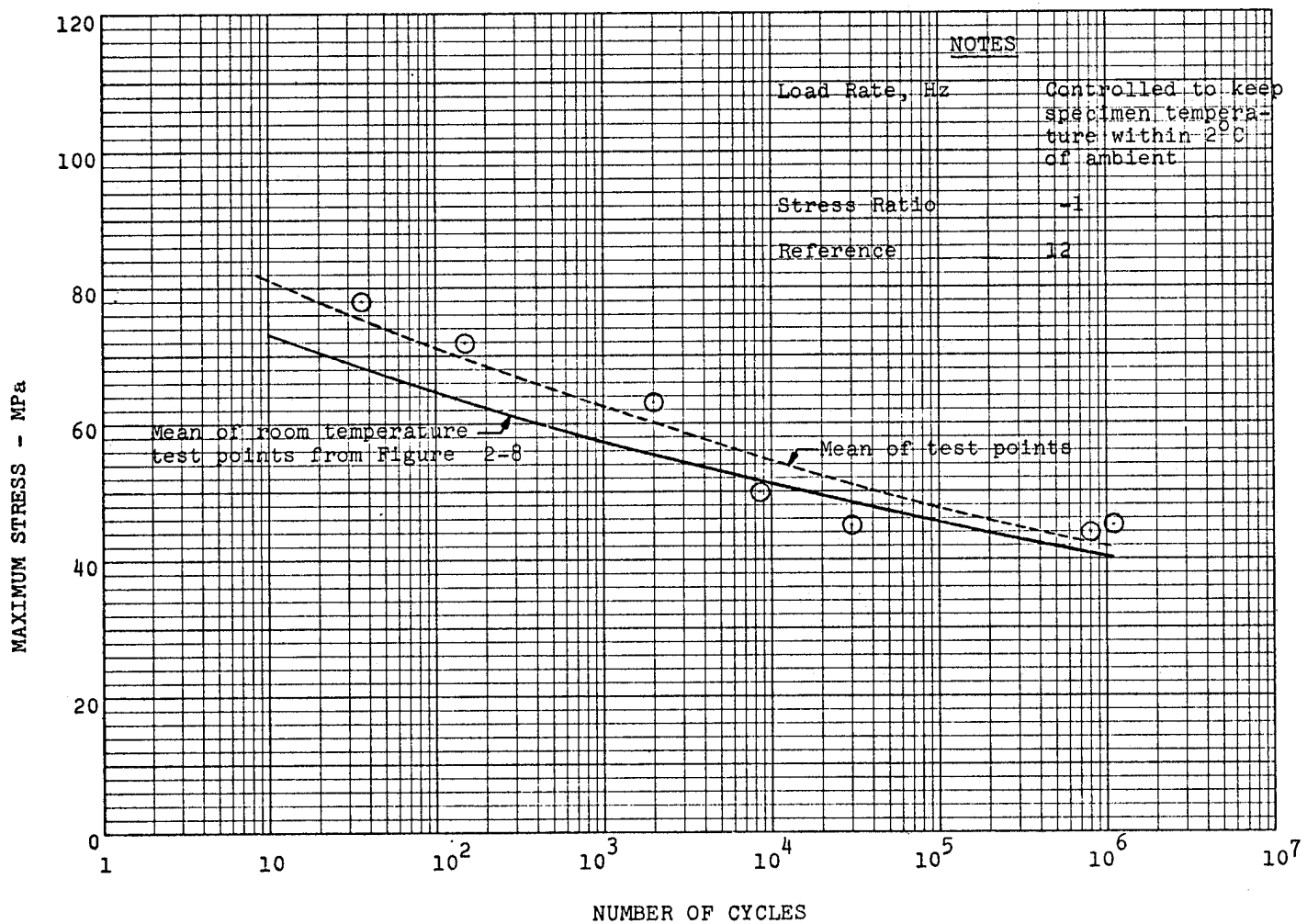


FIGURE 2-11 ROOM TEMPERATURE S-N CURVE FOR SMC (R25)  
LOADED IN TENSION-COMPRESSION FATIGUE

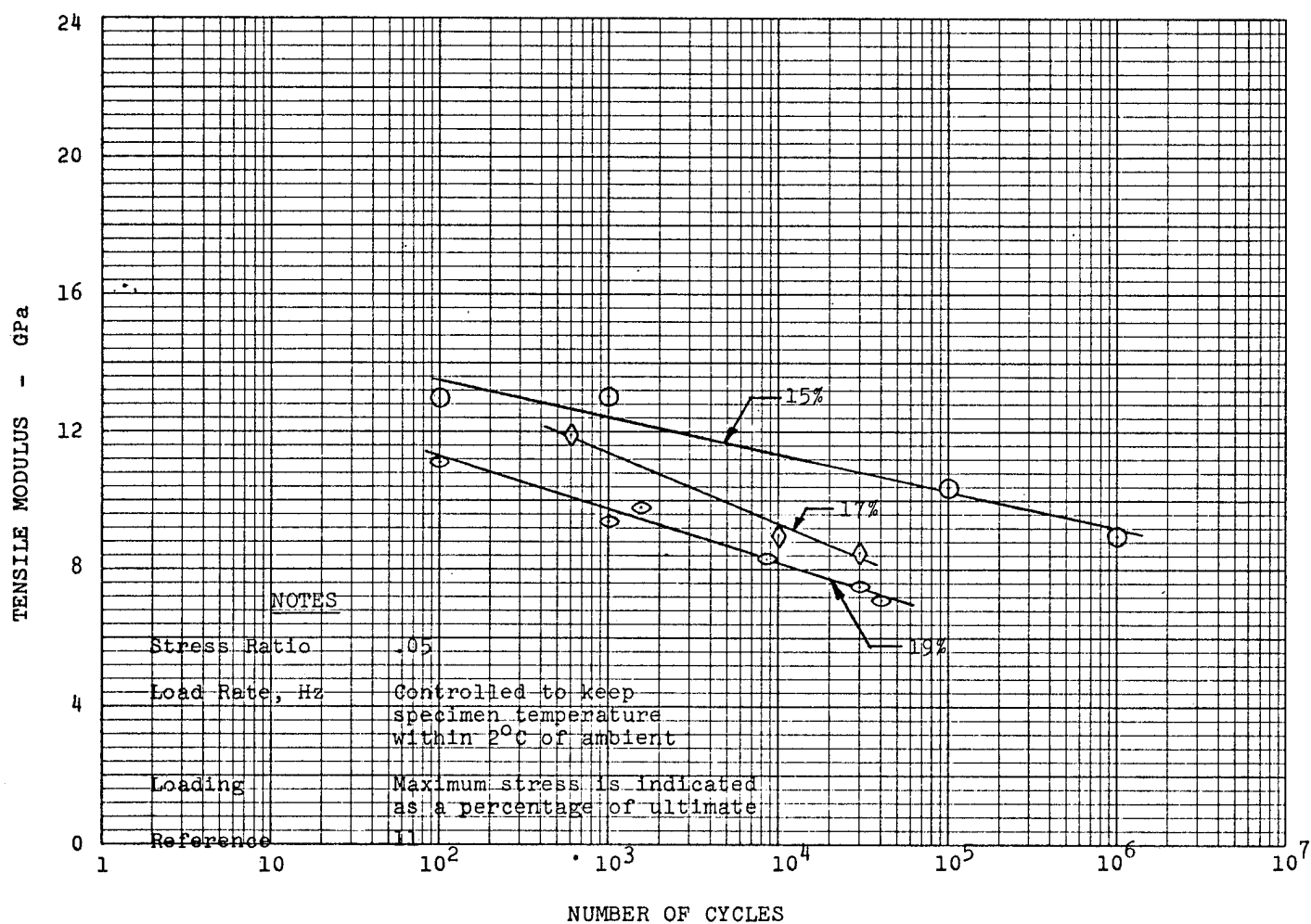


FIGURE 2-12 ROOM TEMPERATURE E-N CURVES FOR SMC (R25)  
LOADED IN TENSION-TENSION FATIGUE

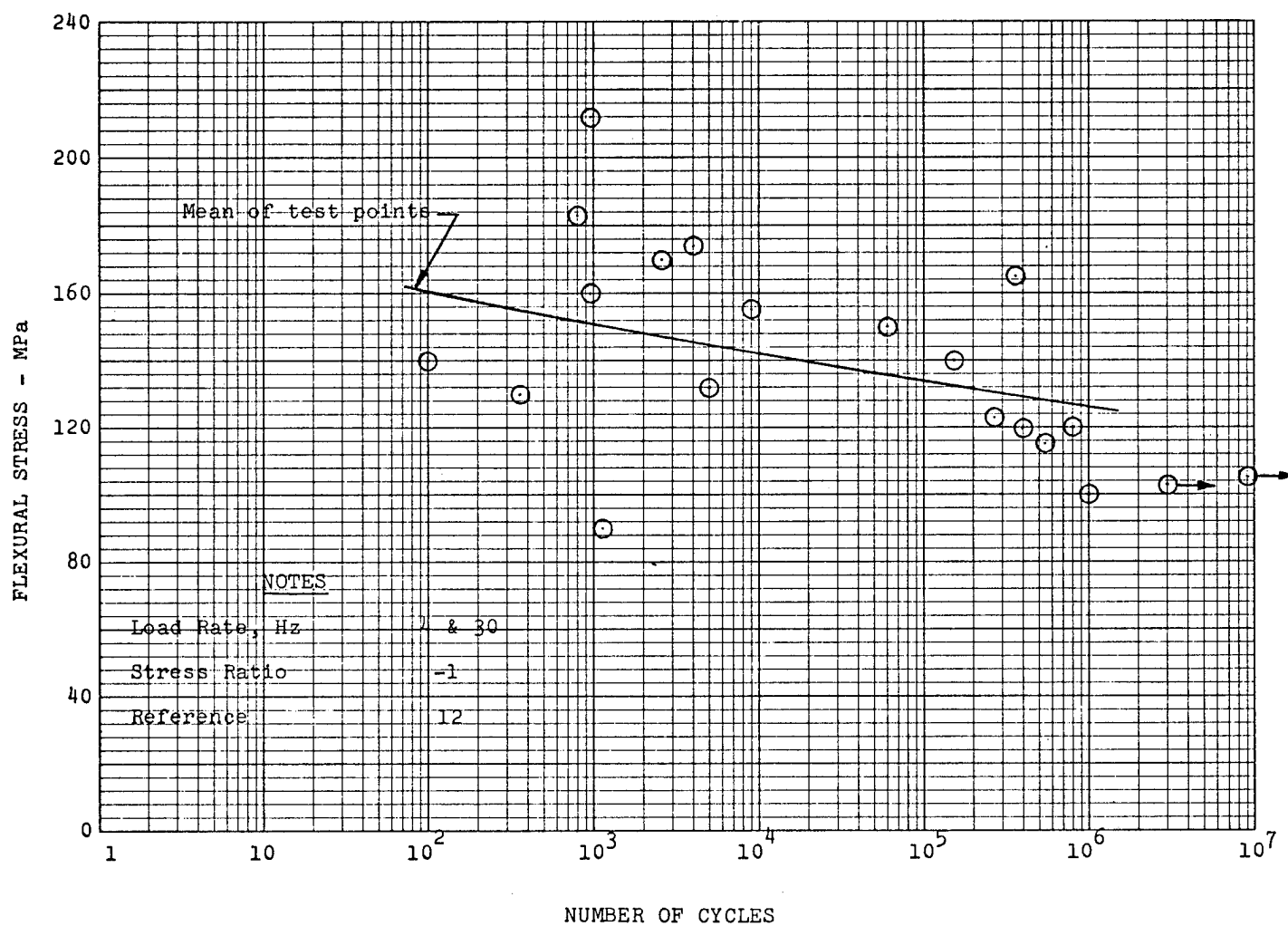


FIGURE 2-13 ROOM TEMPERATURE S-N CURVE FOR SMC (R25)  
LOADED IN FLEXURAL FATIGUE



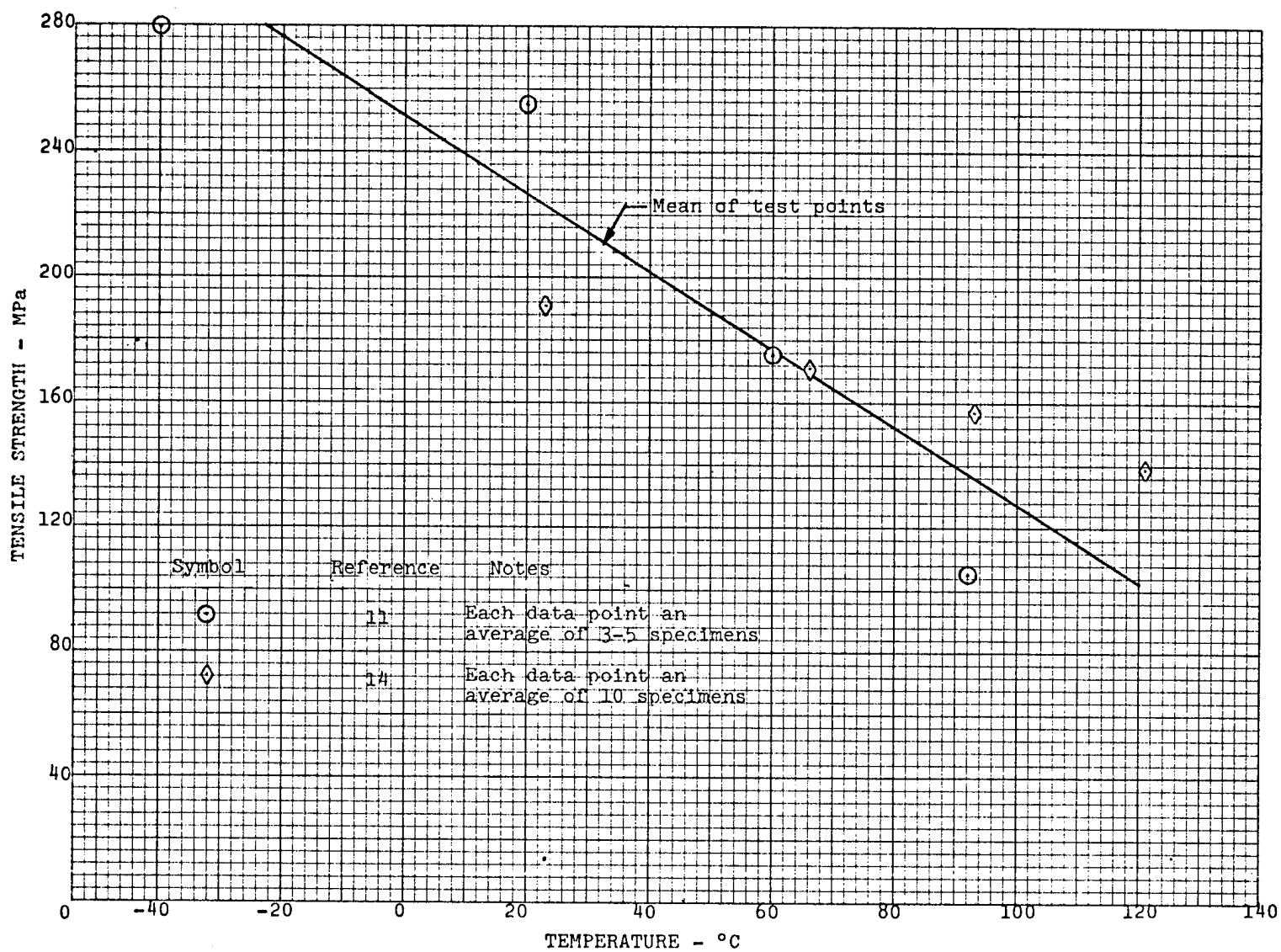


FIGURE 2-14 TENSILE STRENGTH VERSUS TEMPERATURE FOR HMC (R65)

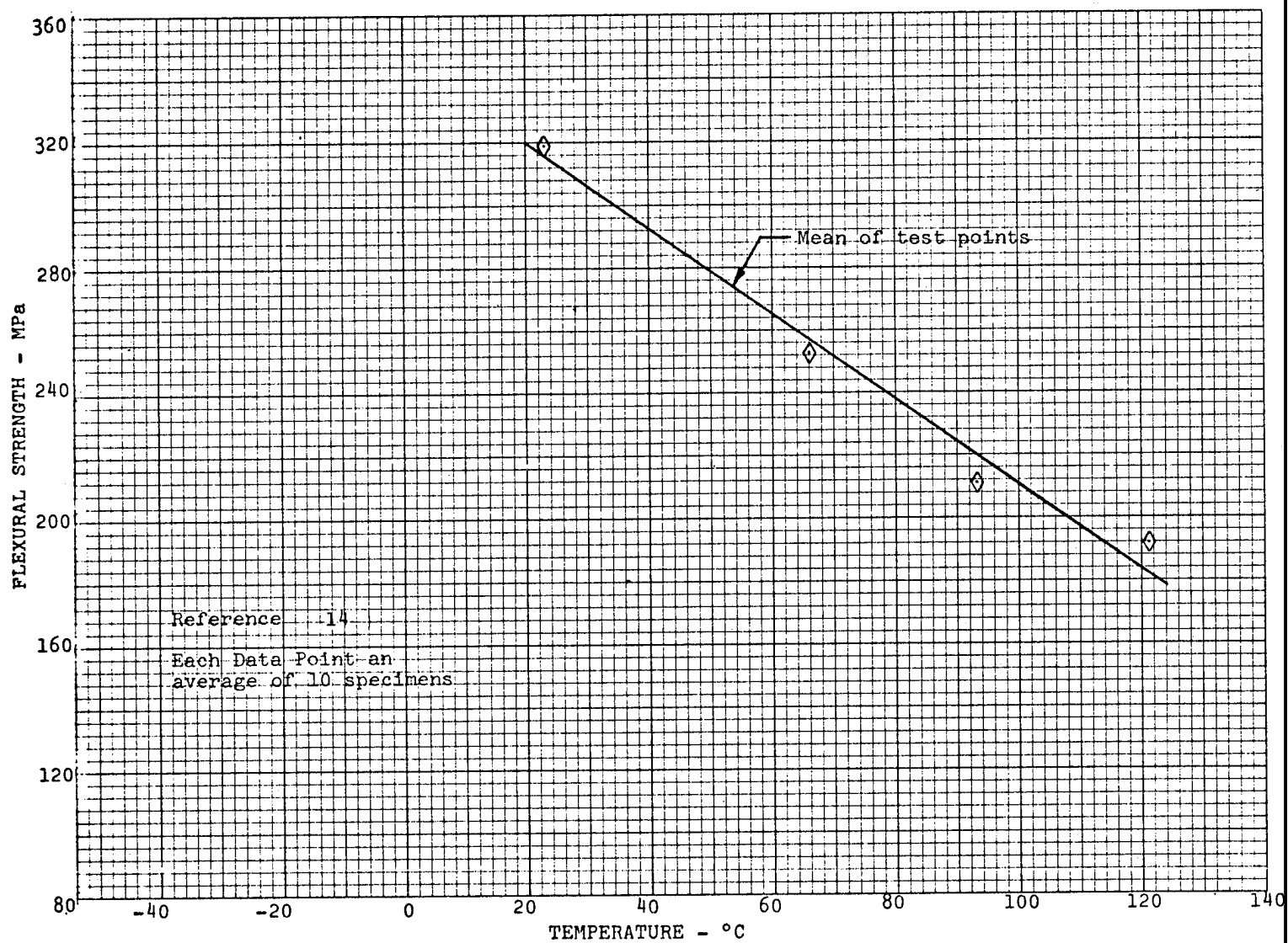


FIGURE 2-15 FLEXURAL STRENGTH VERSUS TEMPERATURE FOR HMC (R65)

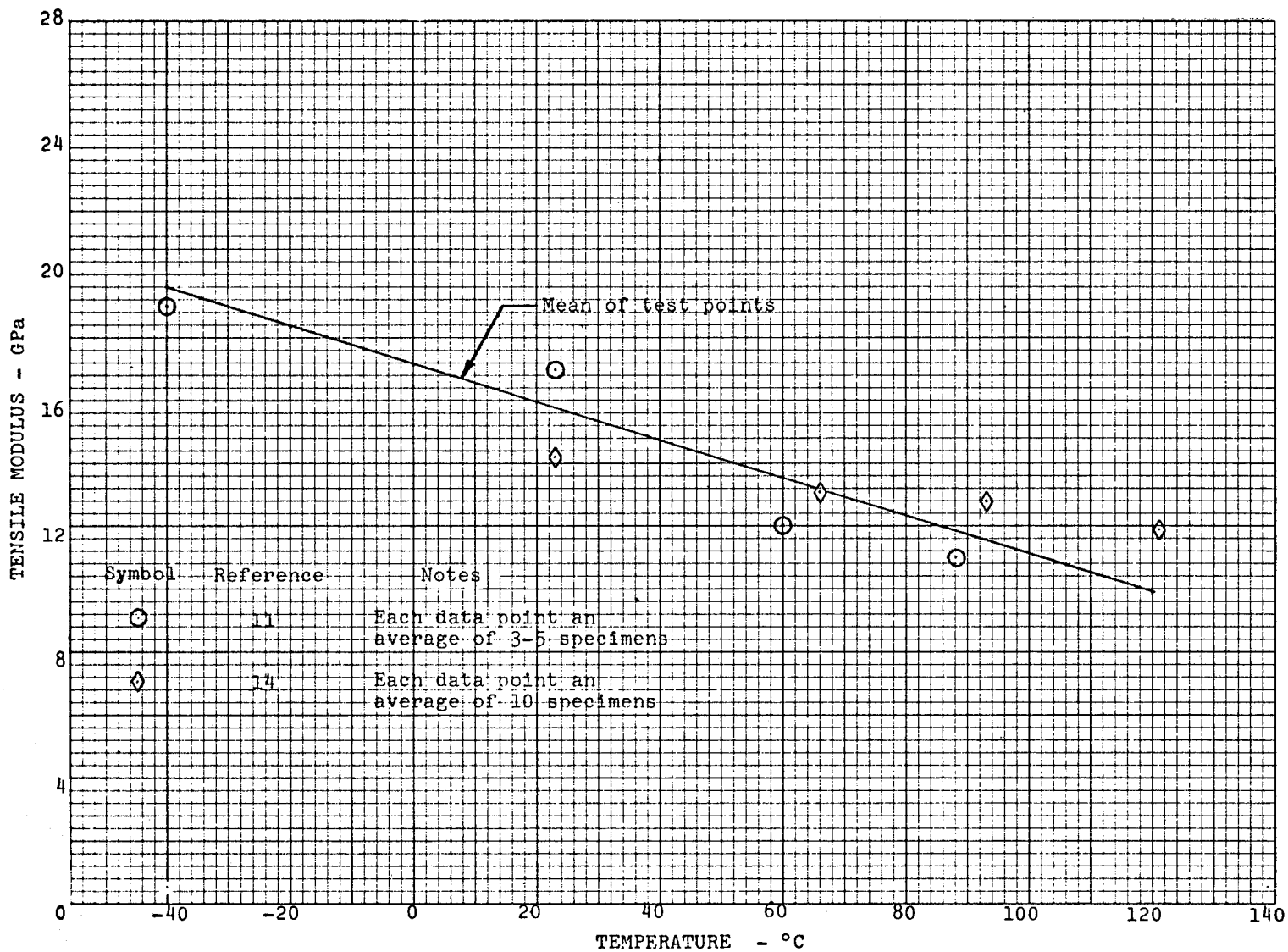


FIGURE 2-16 TENSILE MODULUS VERSUS TEMPERATURE FOR HMC (R65)

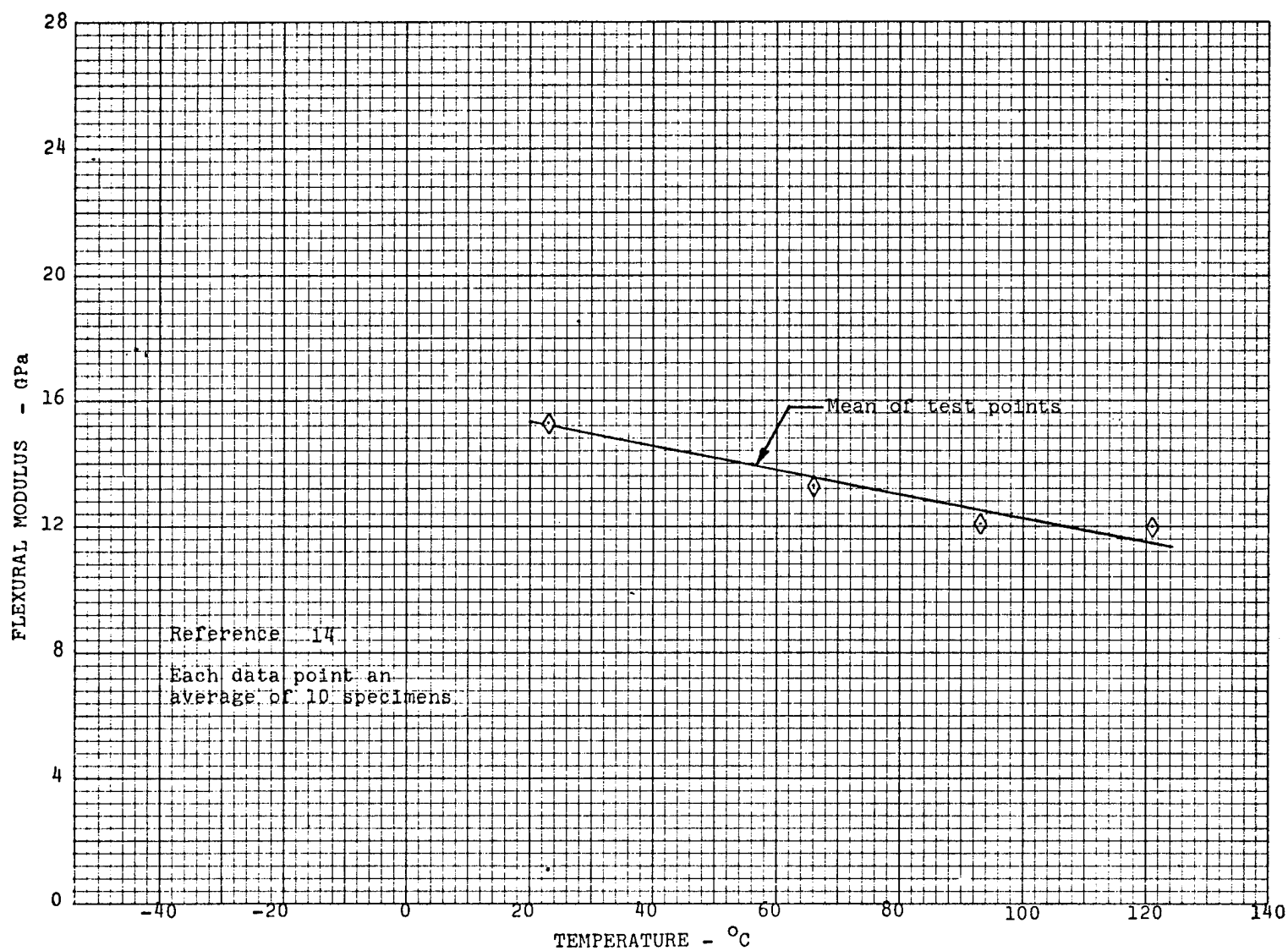


FIGURE 2-17 FLEXURAL MODULUS VERSUS TEMPERATURE FOR HMC (R65)

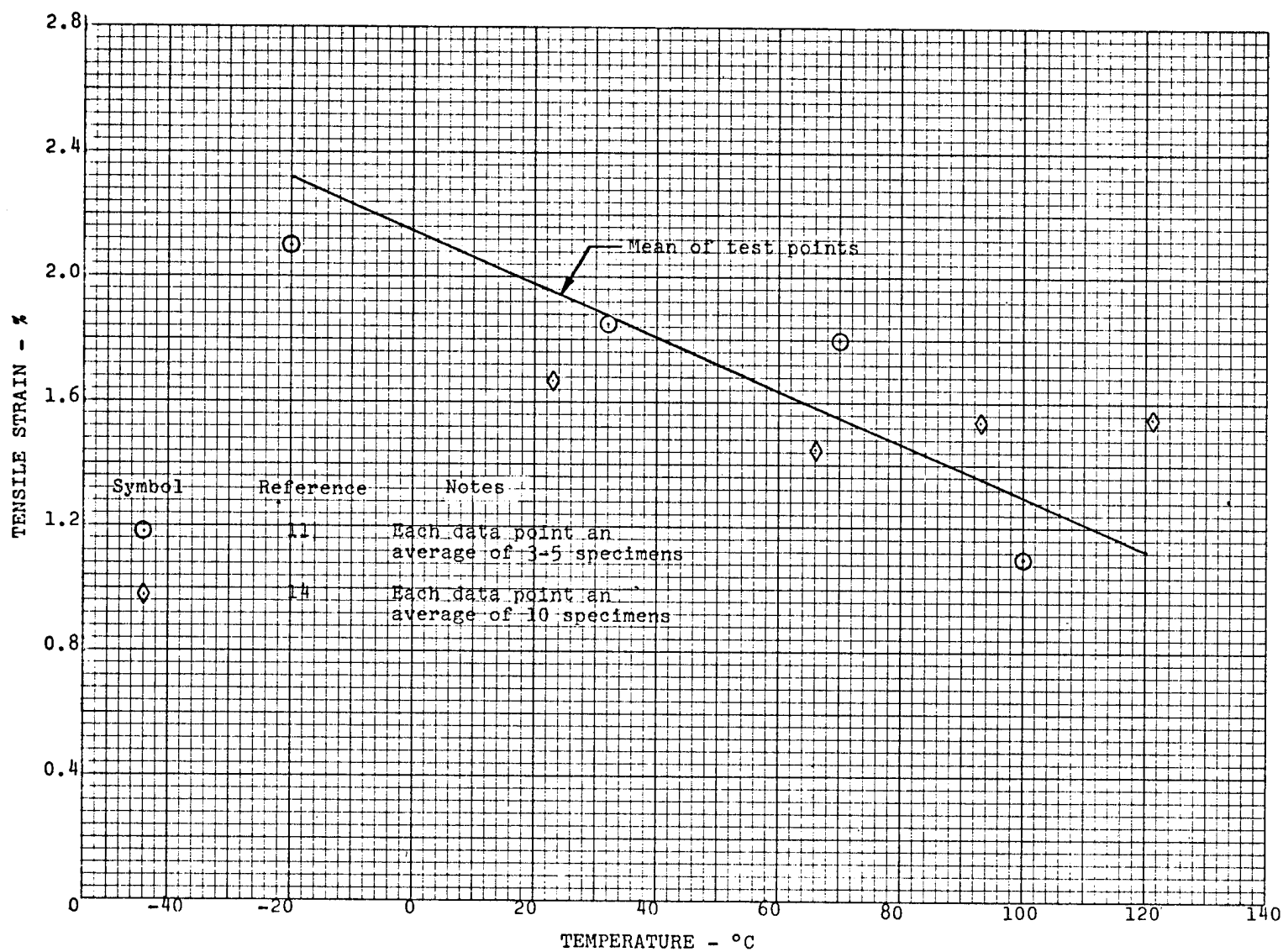


FIGURE 2-18 TENSILE STRAIN TO FRACTURE VERSUS TEMPERATURE FOR HMC (R65)

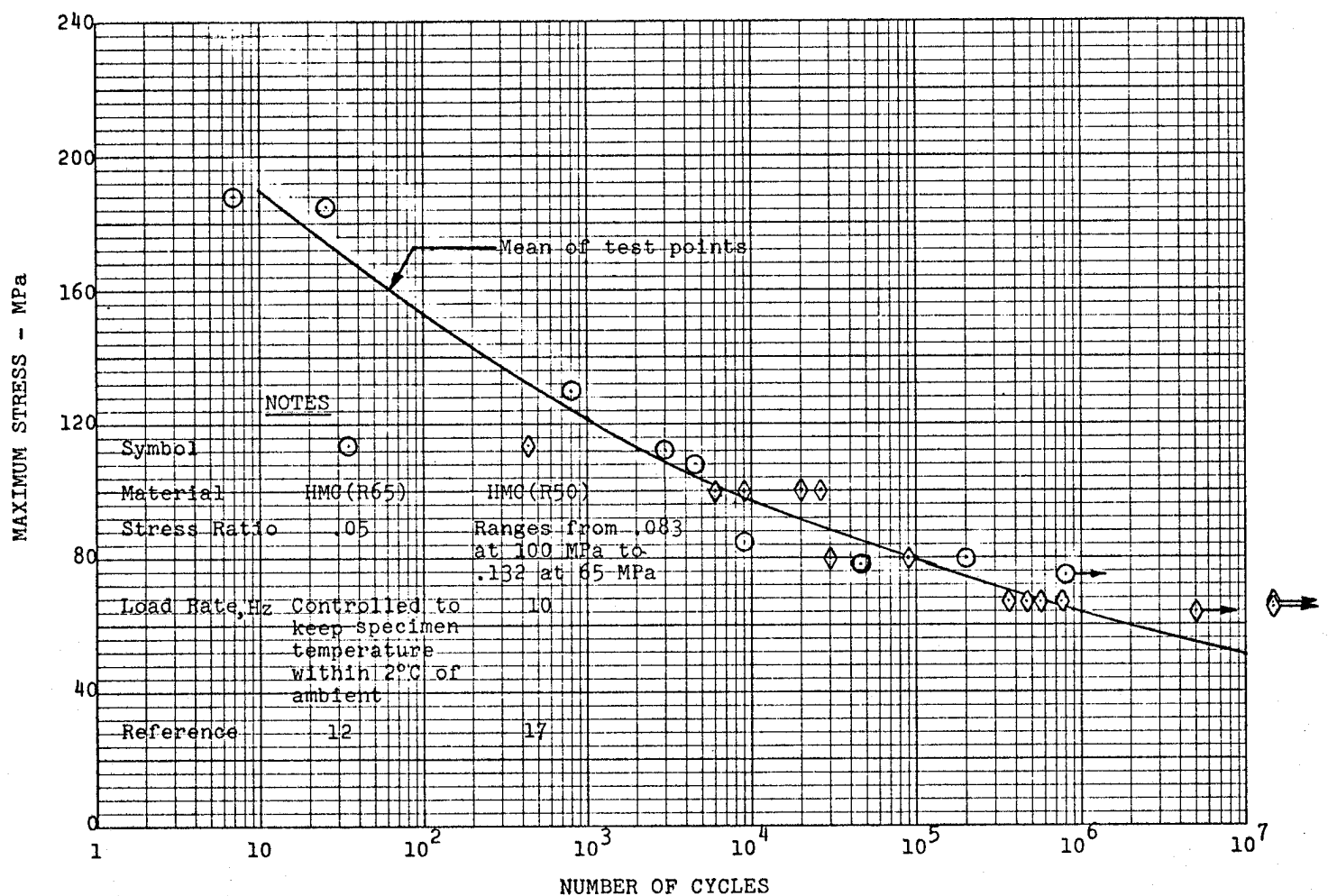


FIGURE 2-19 ROOM TEMPERATURE S-N CURVE FOR HMC (R65 AND R50) LOADED IN TENSION-TENSION FATIGUE

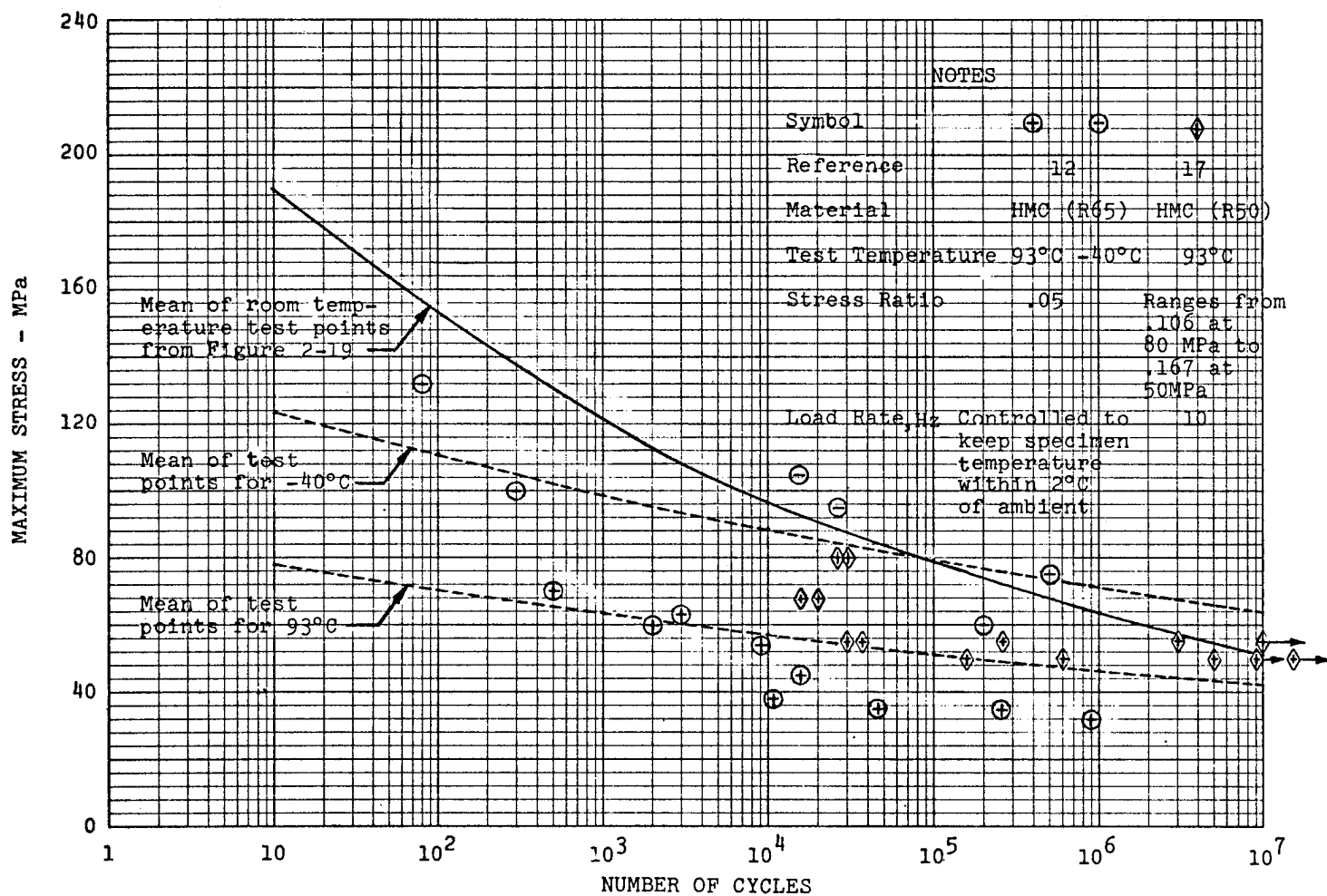


FIGURE 2-20 S-N CURVES FOR HMC (R65 and R50) LOADED IN TENSION-TENSION FATIGUE FOR VARIOUS TEMPERATURES

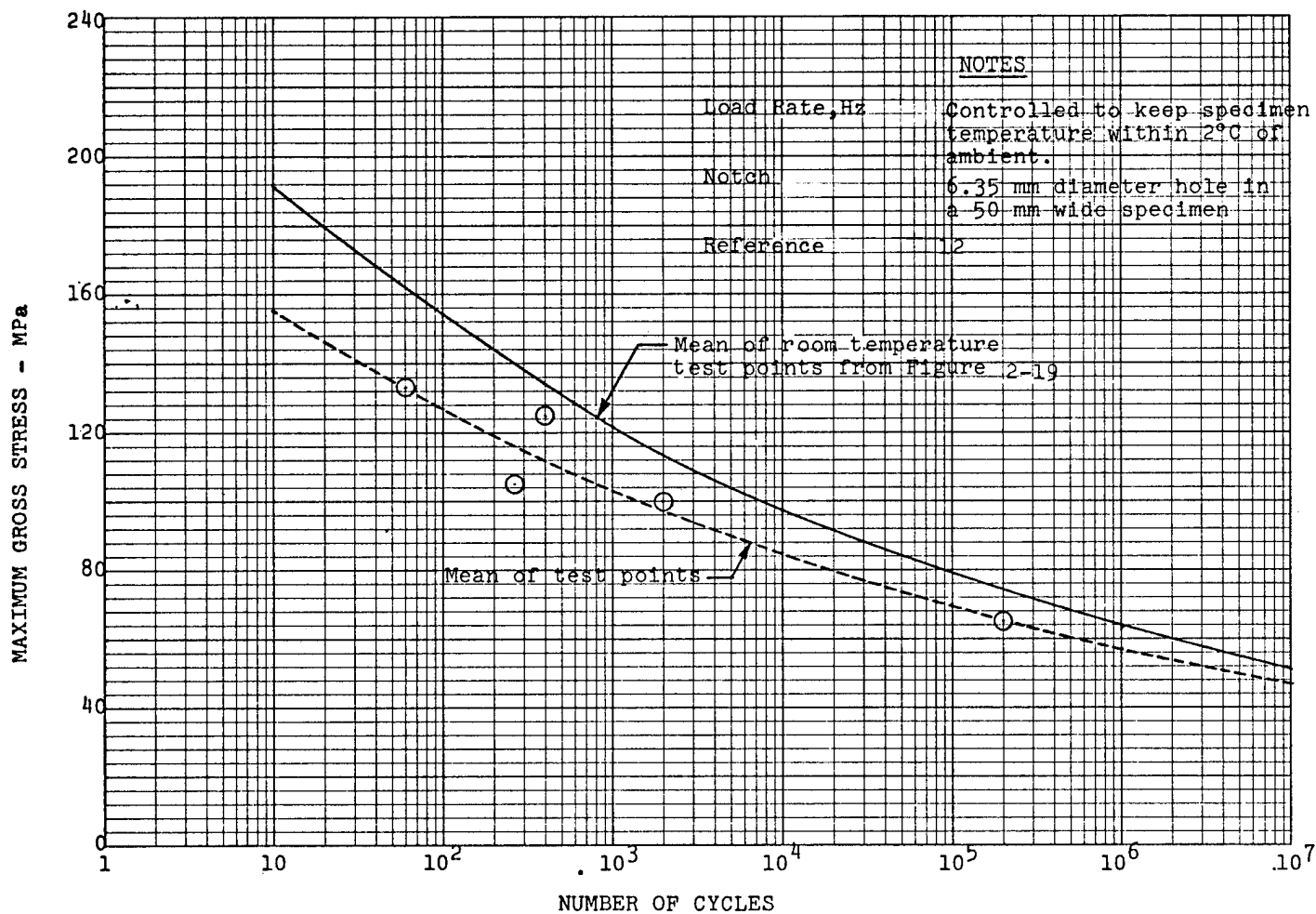


FIGURE 2-21 ROOM TEMPERATURE S-N CURVE FOR NOTCHED HMC (R65) LOADED IN TENSION-TENSION FATIGUE



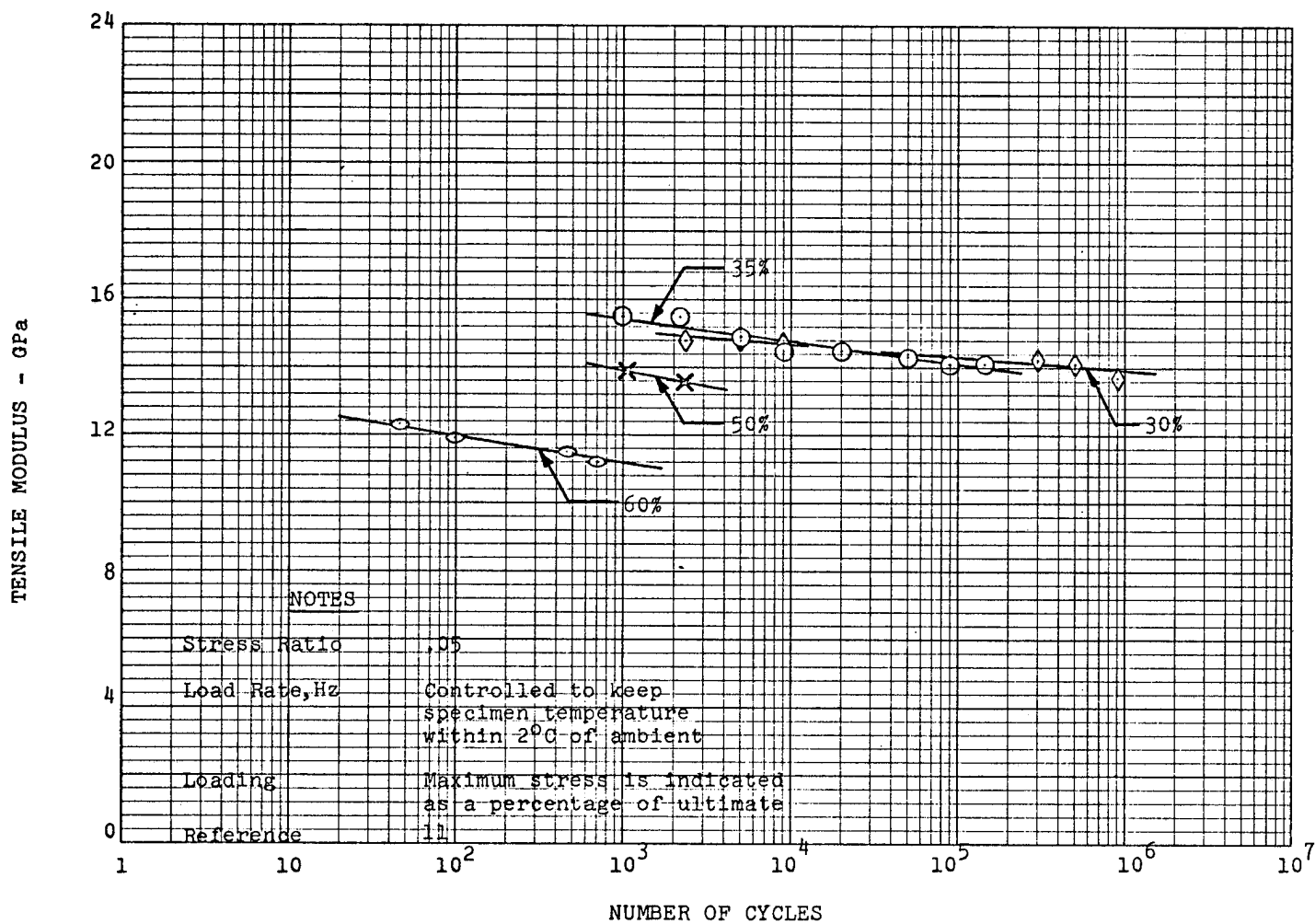


FIGURE 2-22 ROOM TEMPERATURE E-N CURVE FOR HMC (R65)  
LOADED IN TENSION-TENSION FATIGUE

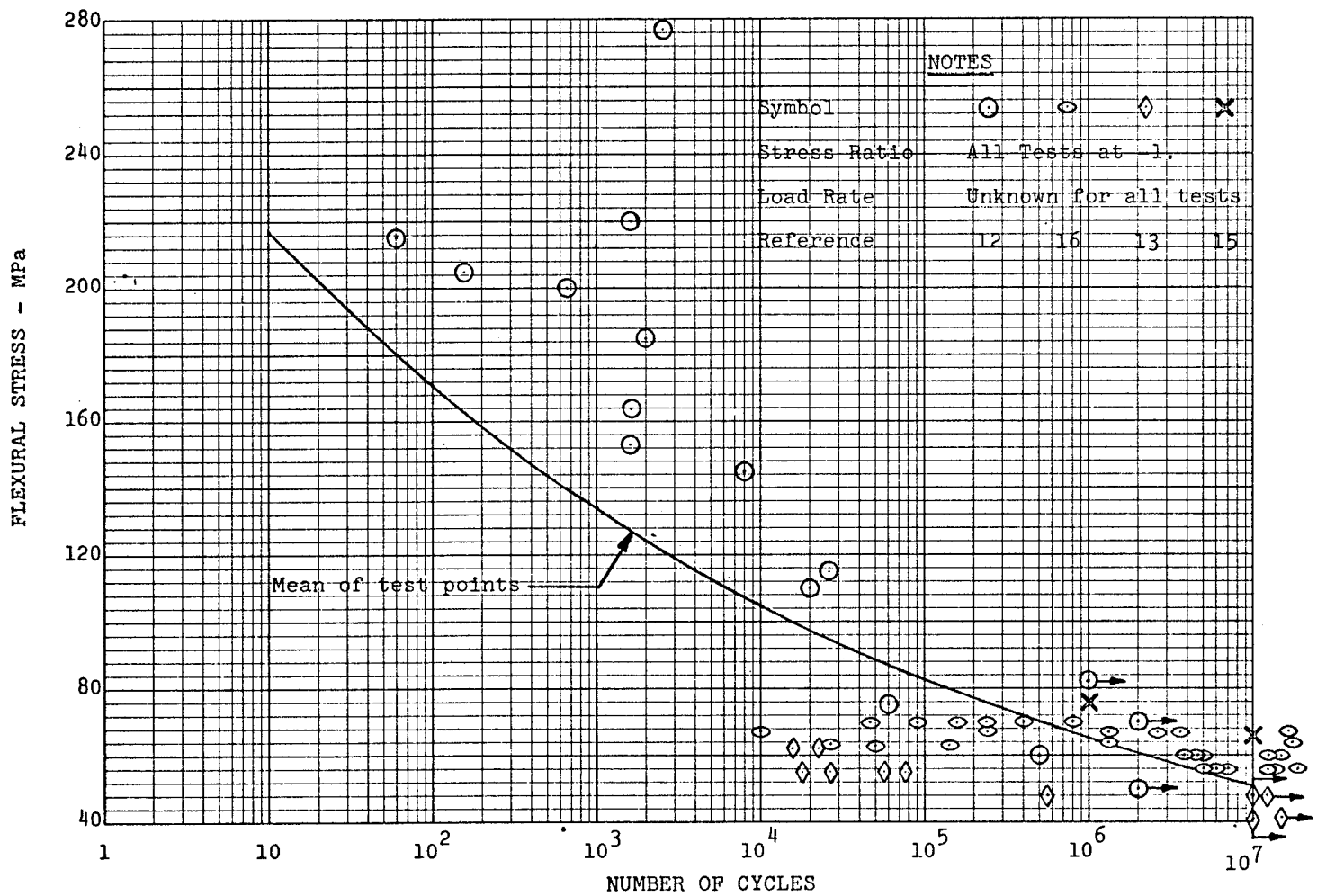


FIGURE 2-23 ROOM TEMPERATURE S-N CURVE FOR HMC (R65) LOADED IN FLEXURAL FATIGUE

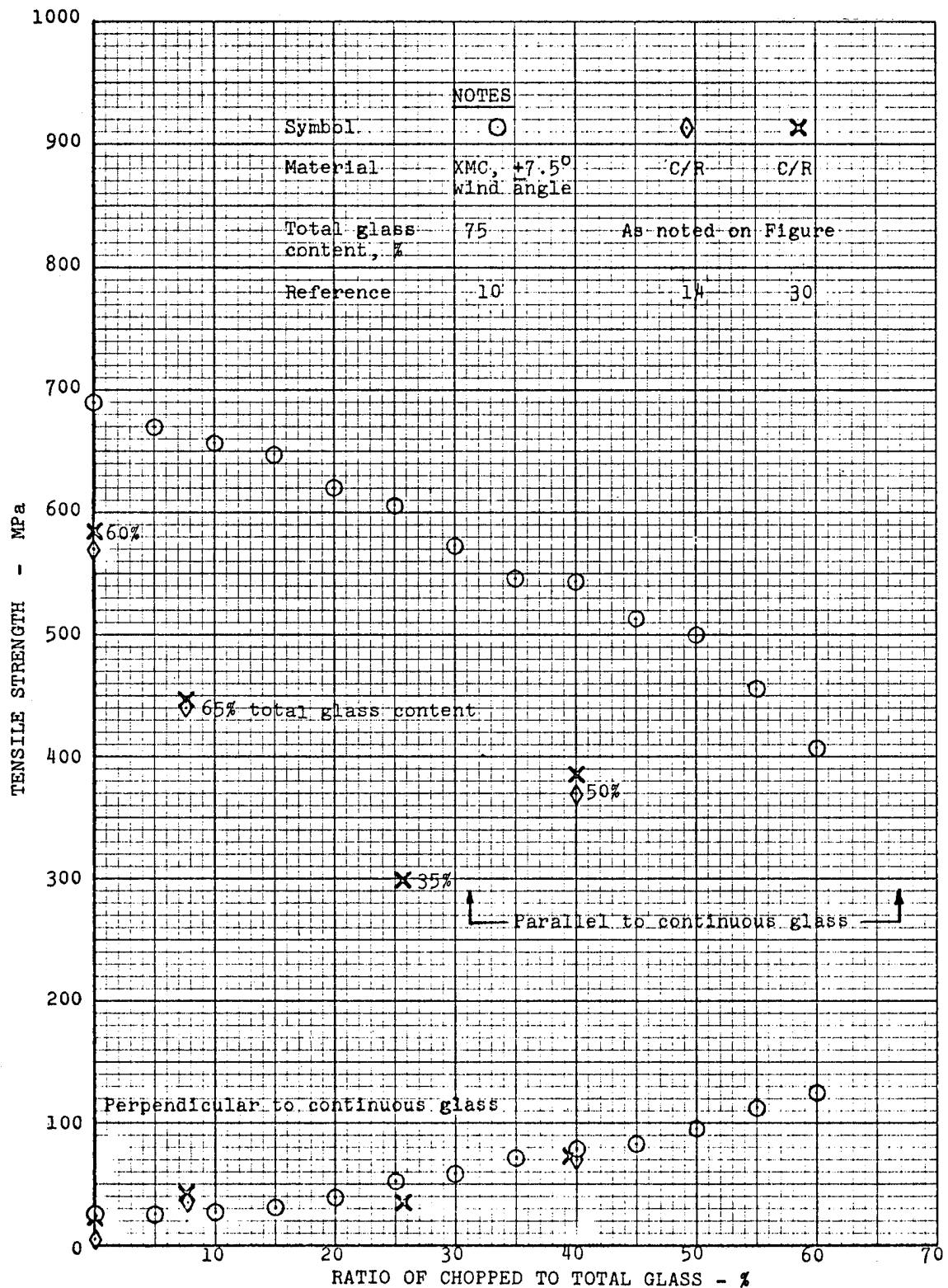


FIGURE 2-24 ROOM TEMPERATURE TENSILE STRENGTH VERSUS PERCENTAGE OF CHOPPED GLASS FOR XMC AND C/R

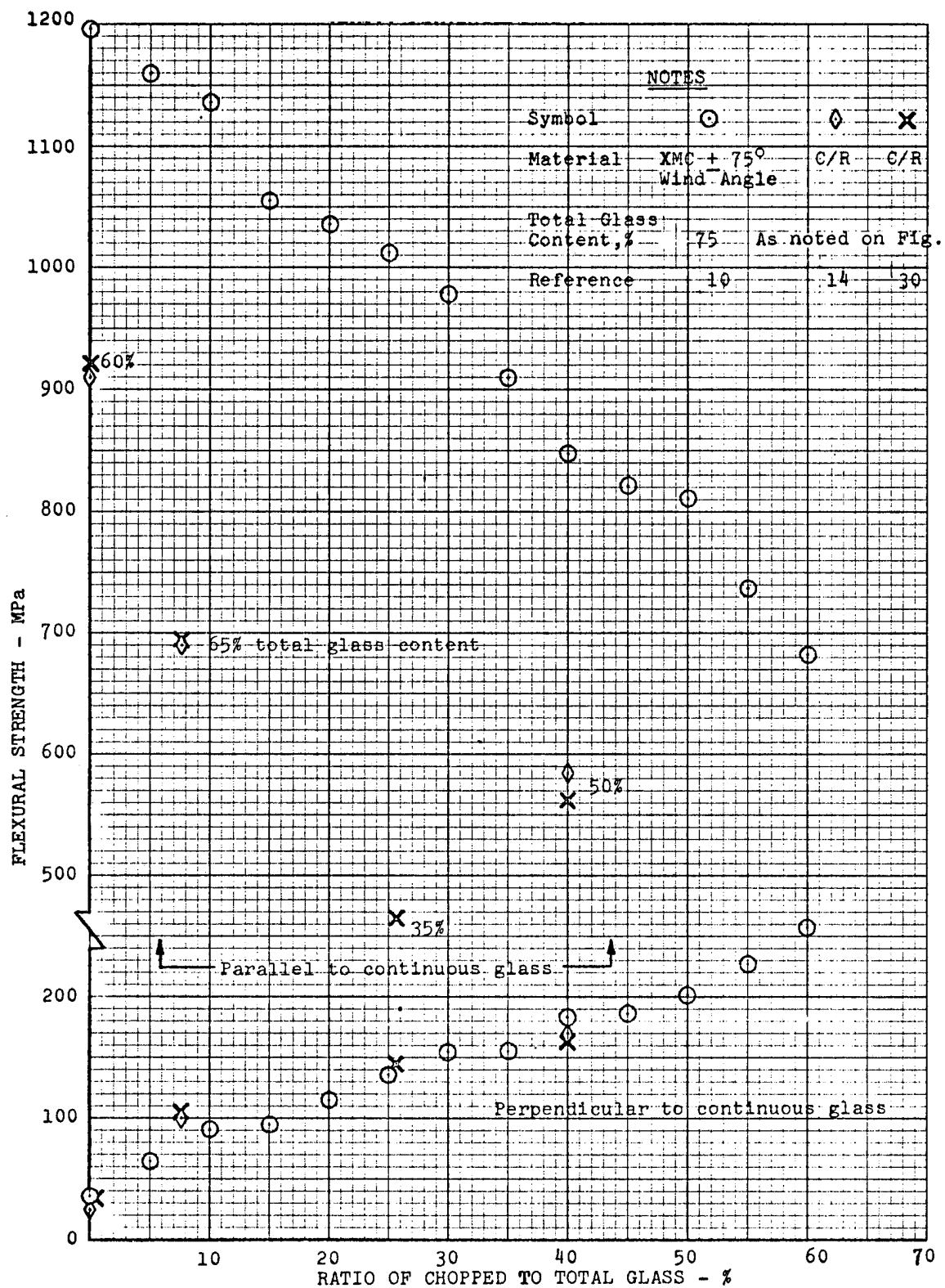


FIGURE 2-25 ROOM TEMPERATURE FLEXURAL STRENGTH VERSUS PERCENTAGE OF CHOPPED GLASS FOR XMC AND C/R

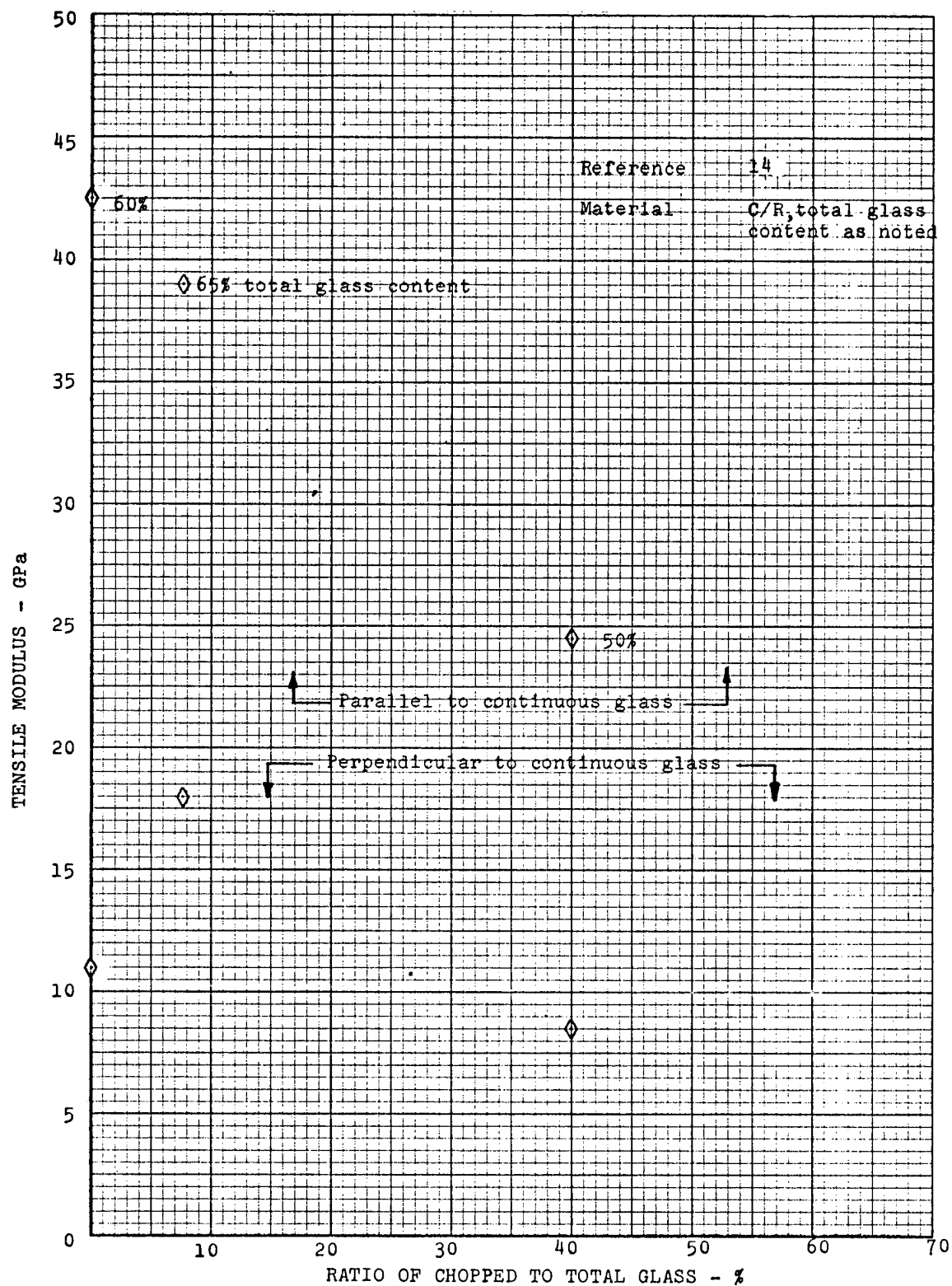


FIGURE 2-26 ROOM TEMPERATURE TENSILE MODULUS VERSUS PERCENTAGE OF CHOPPED GLASS FOR C/R

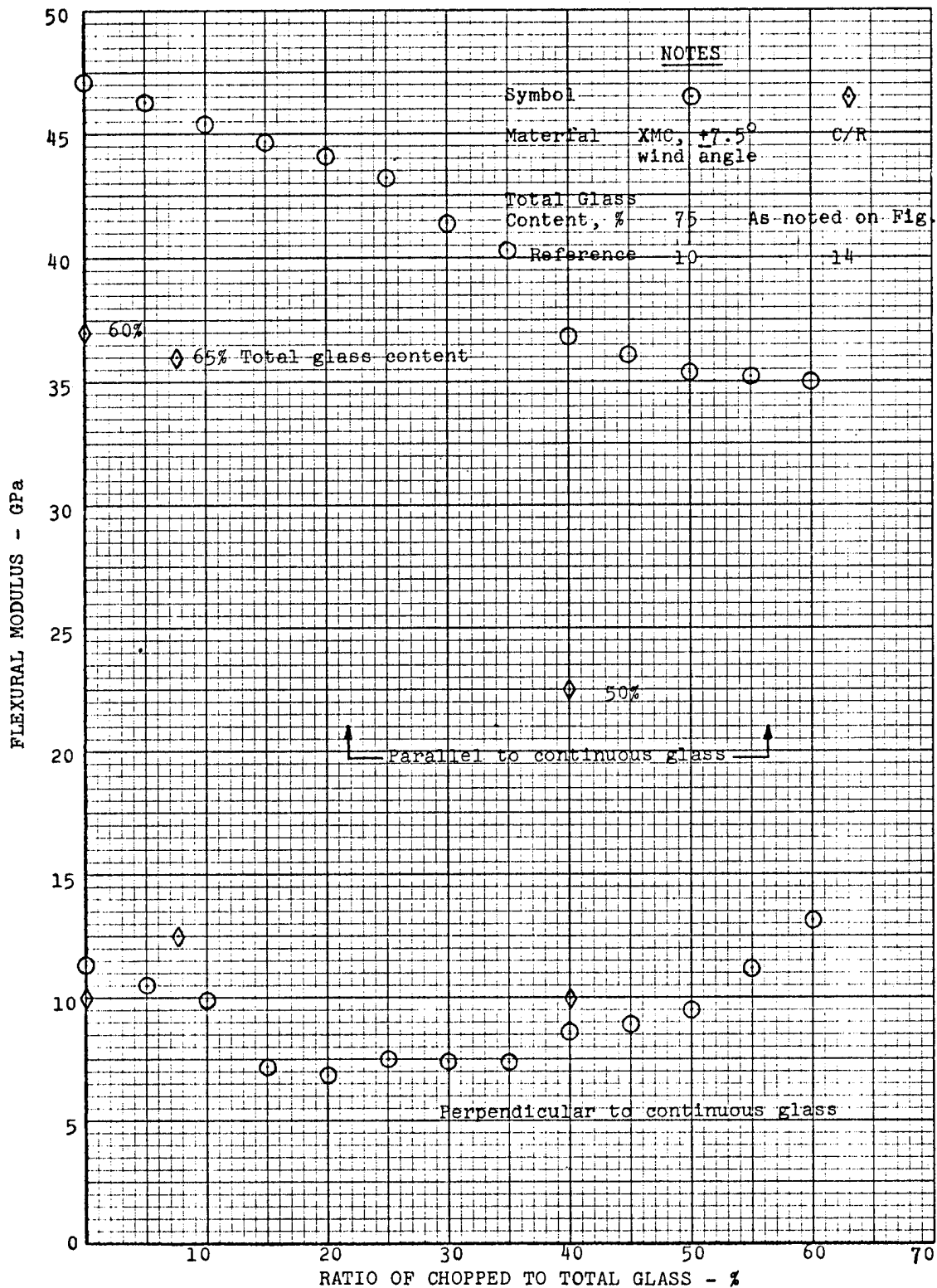


FIGURE 2-27 ROOM TEMPERATURE FLEXURAL MODULUS VERSUS PERCENTAGE OF CHOPPED GLASS FOR XMC AND C/R

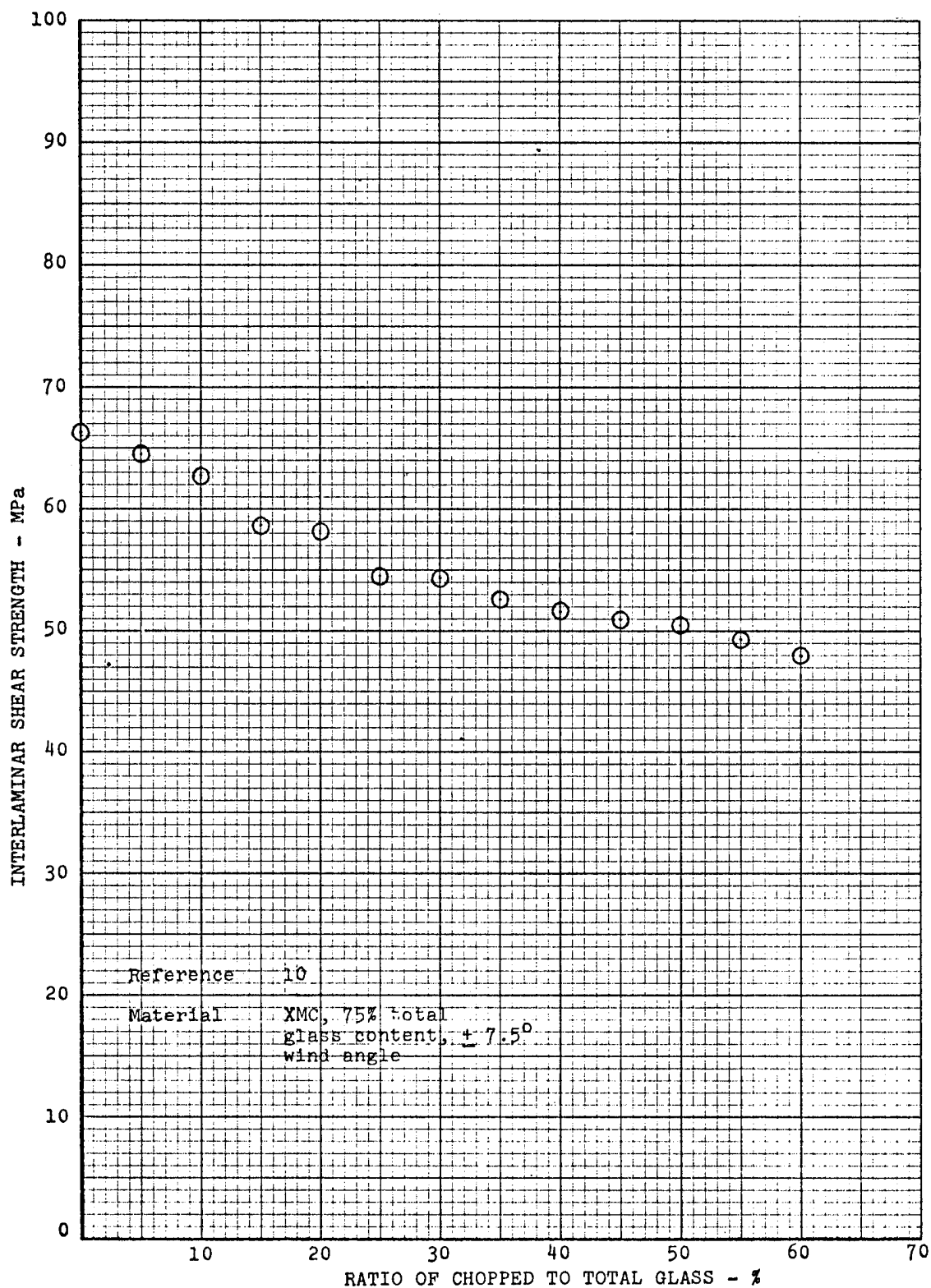


FIGURE 2-28 ROOM TEMPERATURE INTERLAMINAR SHEAR STRENGTH VERSUS PERCENTAGE OF CHOPPED GLASS FOR XMC

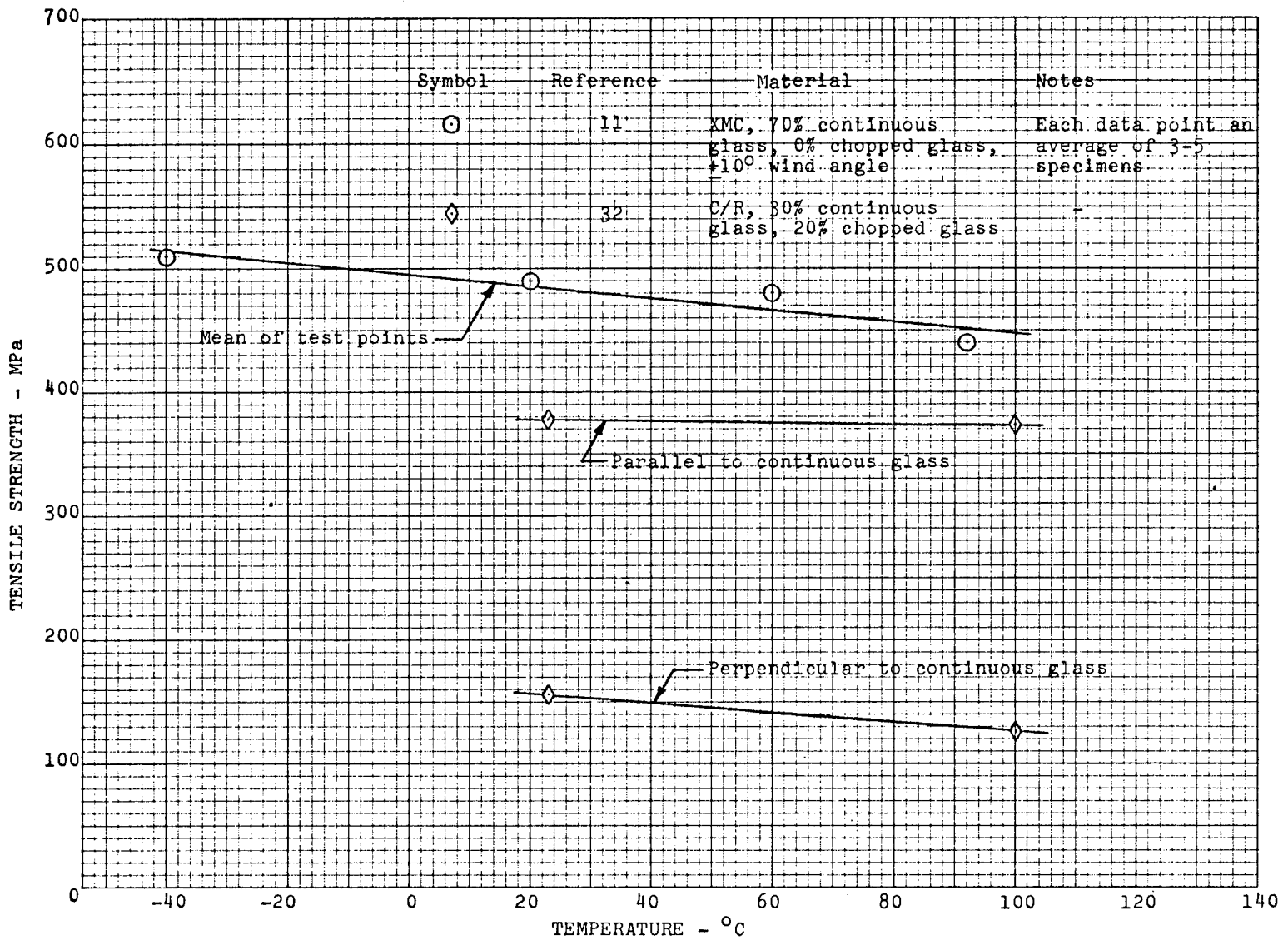


FIGURE 2-29 TENSILE STRENGTH VERSUS TEMPERATURE FOR XMC AND C/R



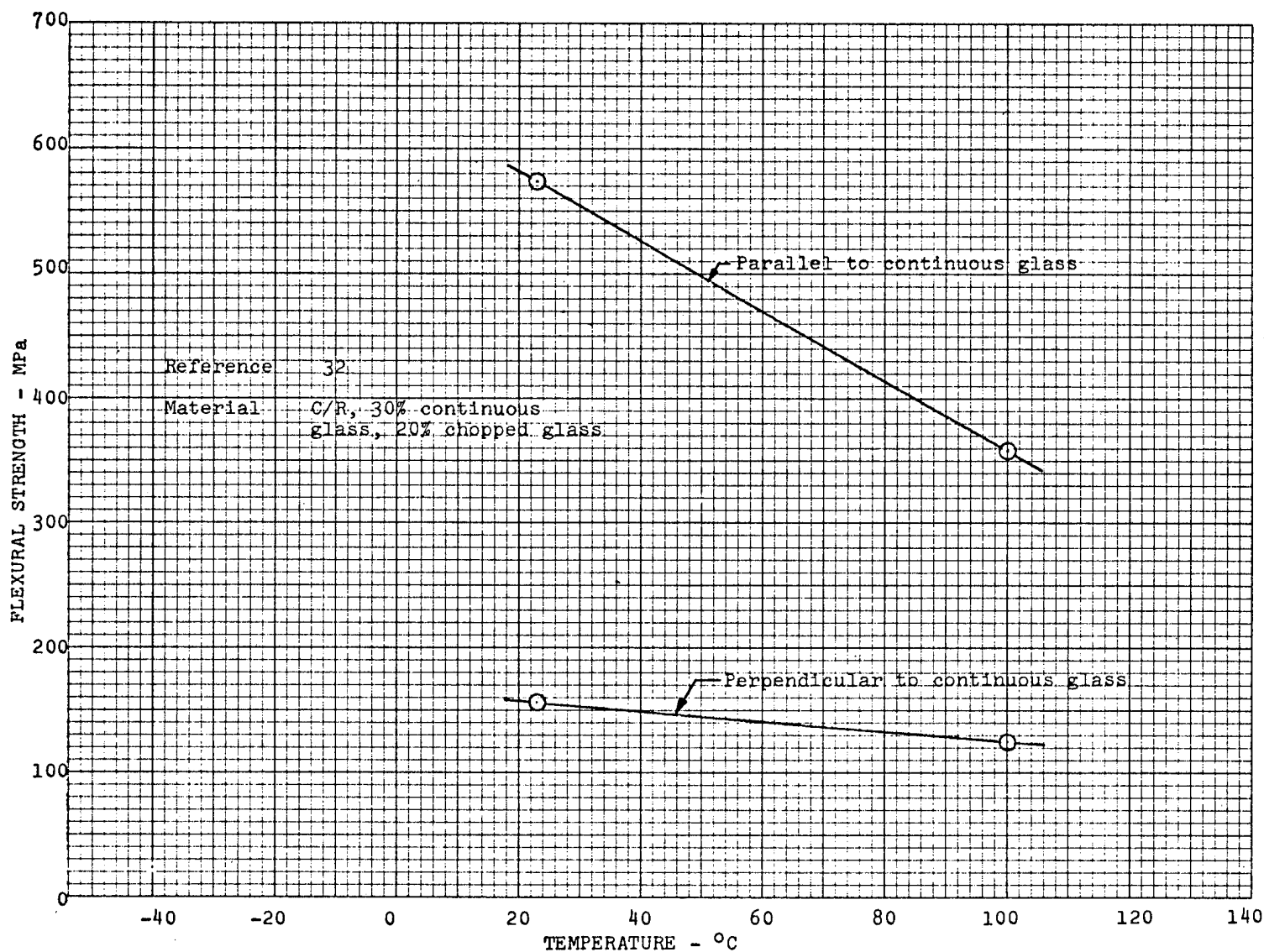


FIGURE 2-30 FLEXURAL STRENGTH VERSUS TEMPERATURE FOR C/R

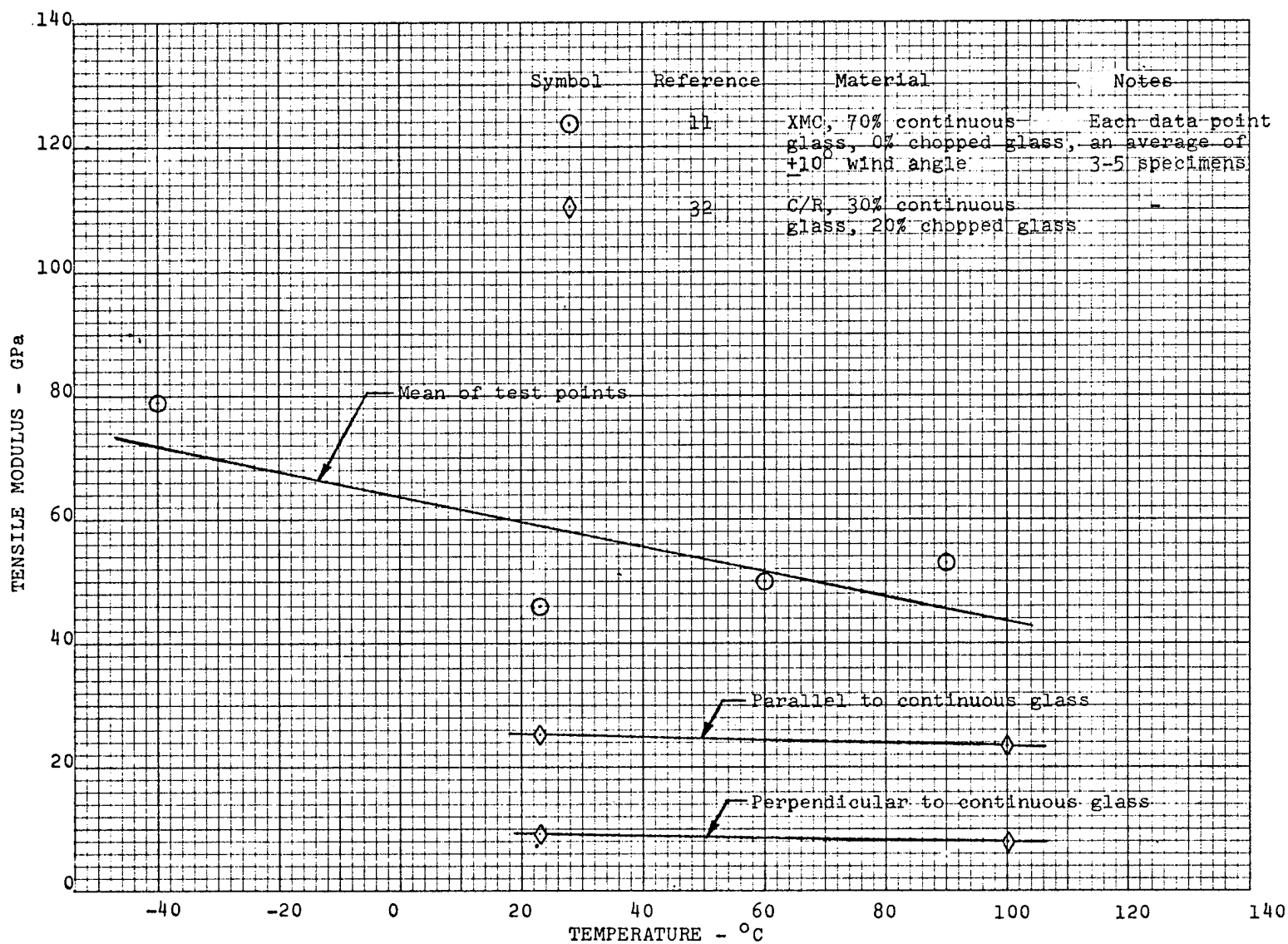


FIGURE 2-31 TENSILE MODULUS VERSUS TEMPERATURE FOR XMC AND C/R

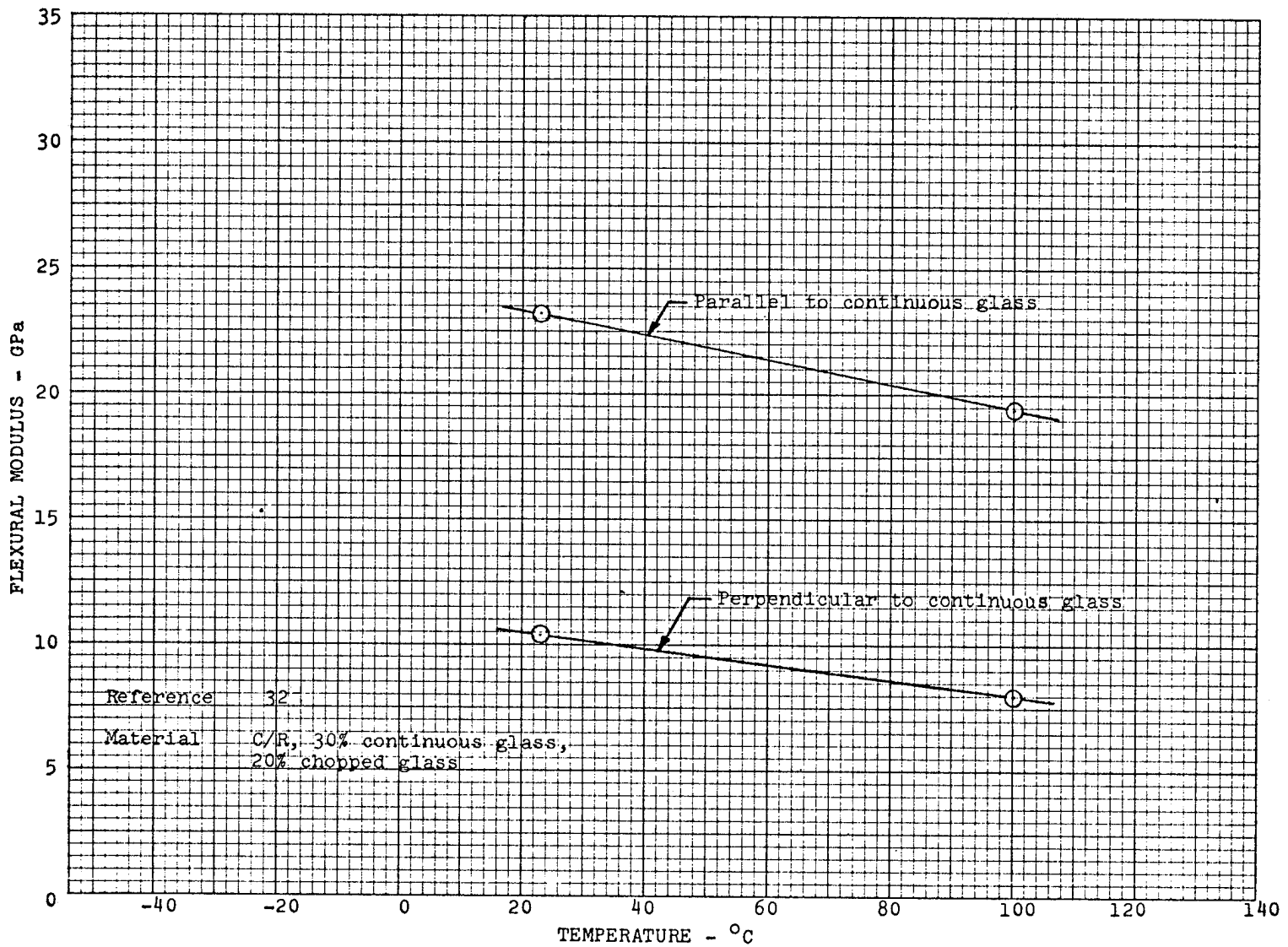


FIGURE 2-32 FLEXURAL MODULUS VERSUS TEMPERATURE FOR C/R

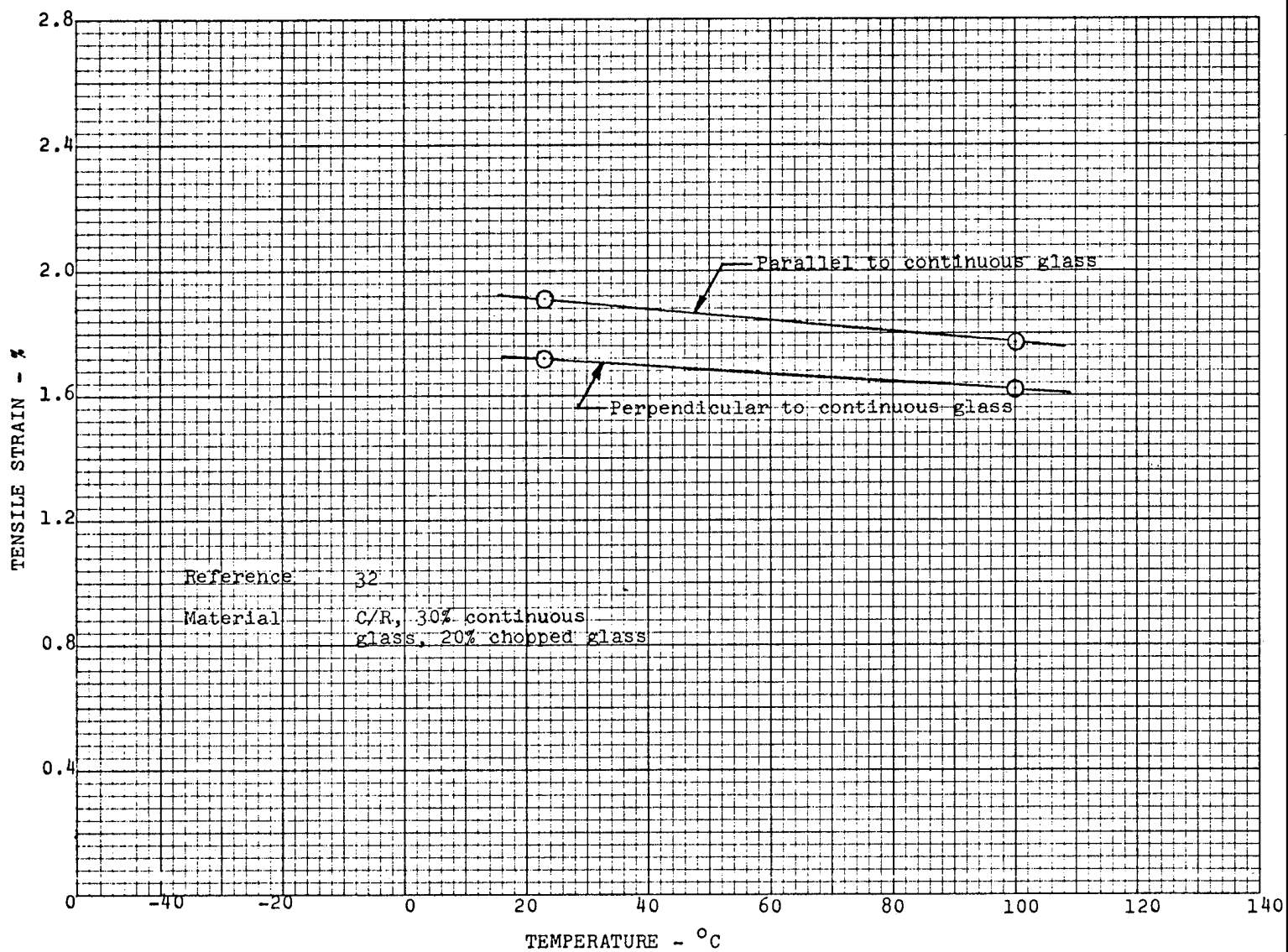


FIGURE 2-33 TENSILE STRAIN TO FRACTURE VERSUS TEMPERATURE FOR C/R

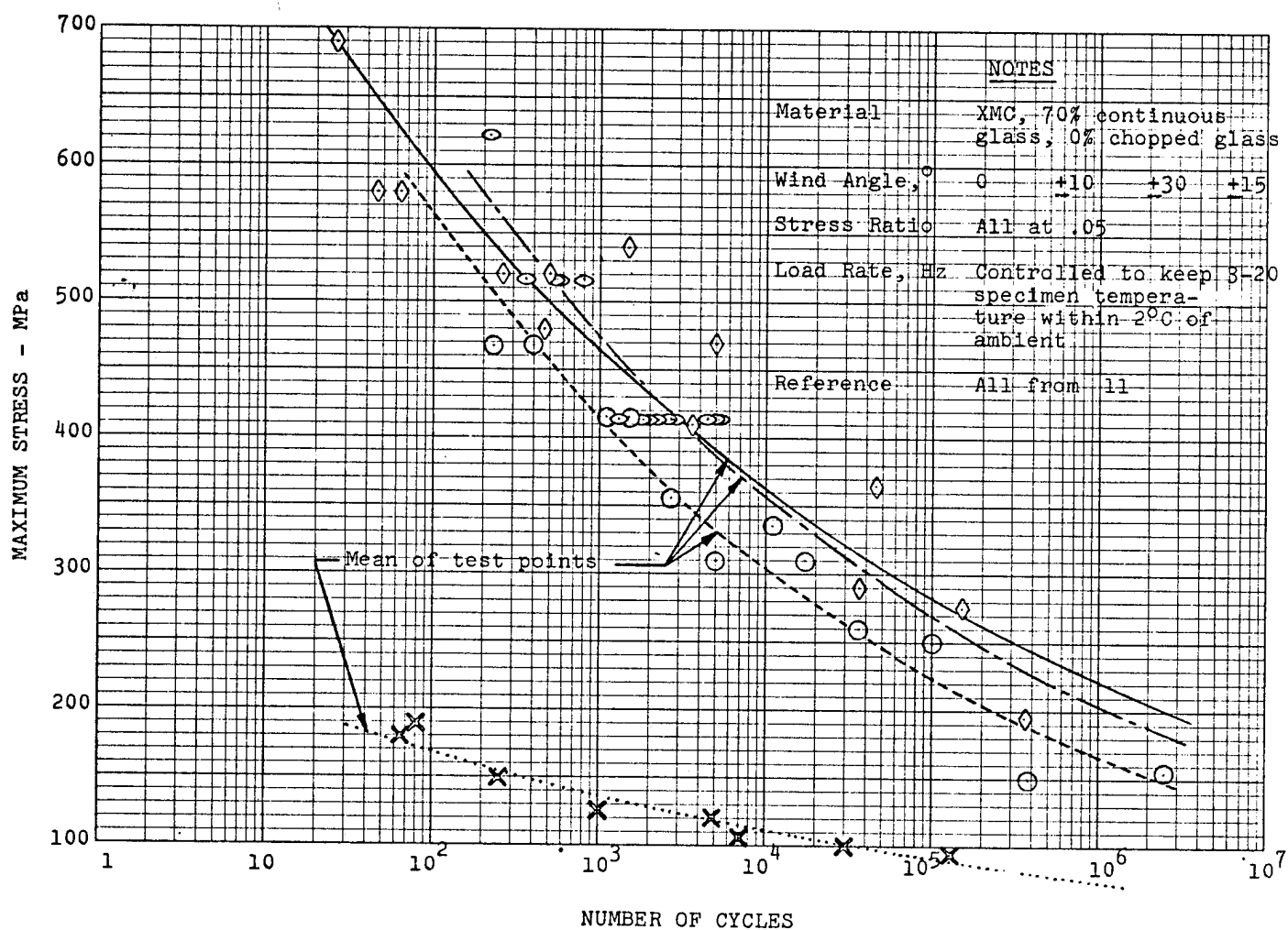


FIGURE 2-34 ROOM TEMPERATURE S-N CURVES FOR XMC LOADED IN TENSION-TENSION FATIGUE

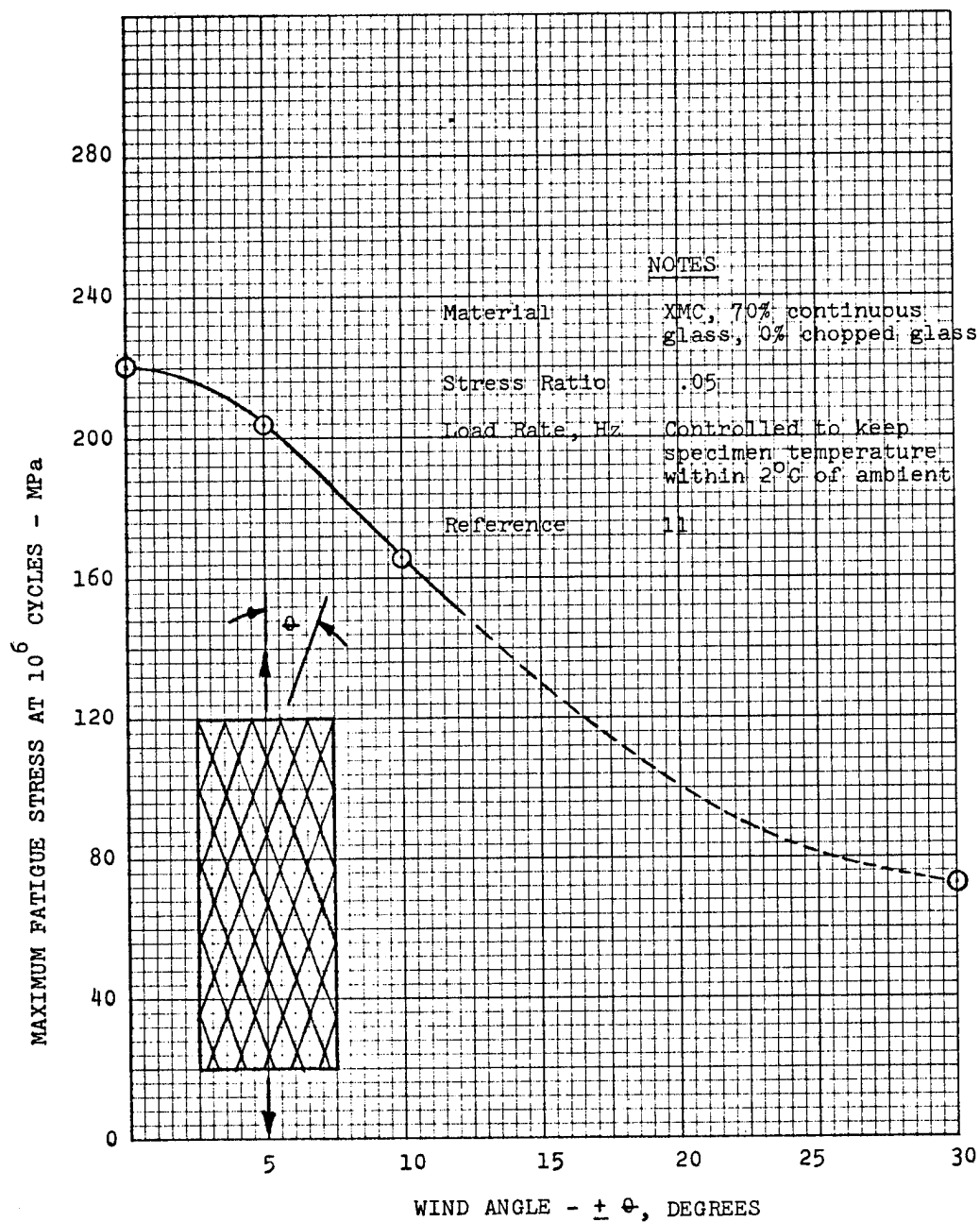


FIGURE 2-35 FATIGUE STRENGTH AT  $10^6$  VERSUS WIND ANGLE FOR XMC

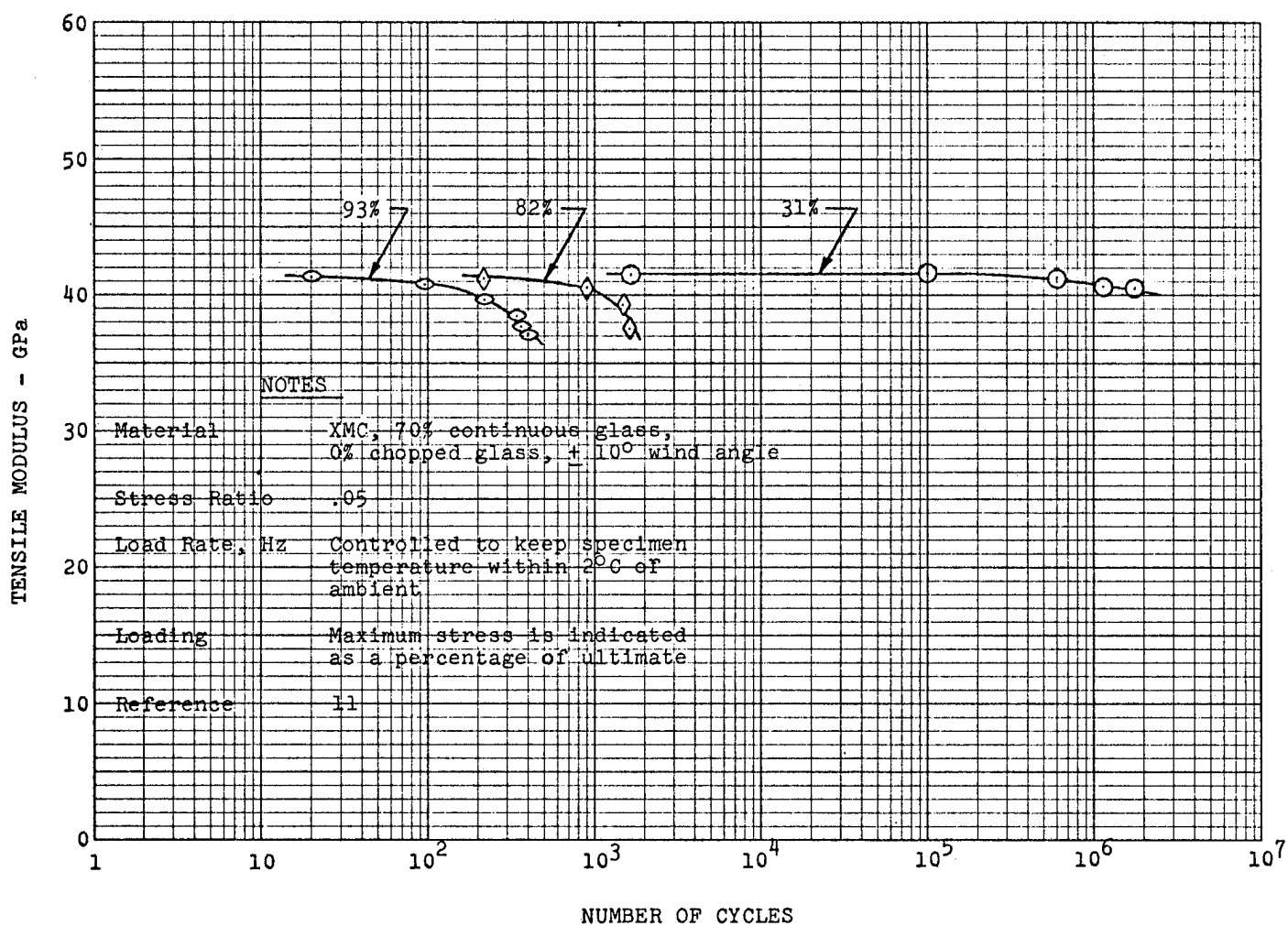


FIGURE 2-36 ROOM TEMPERATURE E-N CURVES FOR XMC  
LOADED IN TENSION-TENSION FATIGUE

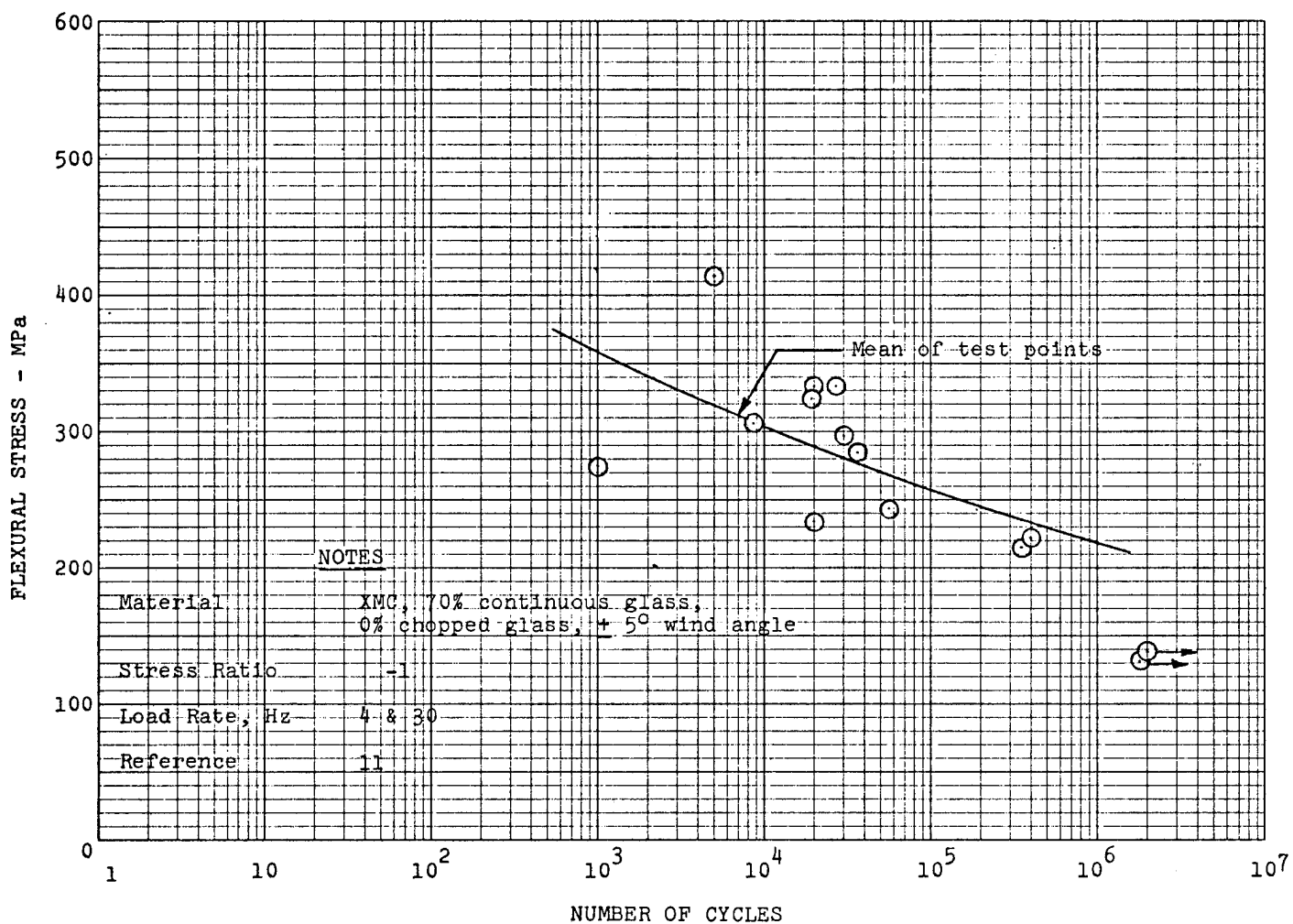


FIGURE 2-37 ROOM TEMPERATURE S-N CURVE FOR XMC  
LOADED IN FLEXURAL FATIGUE



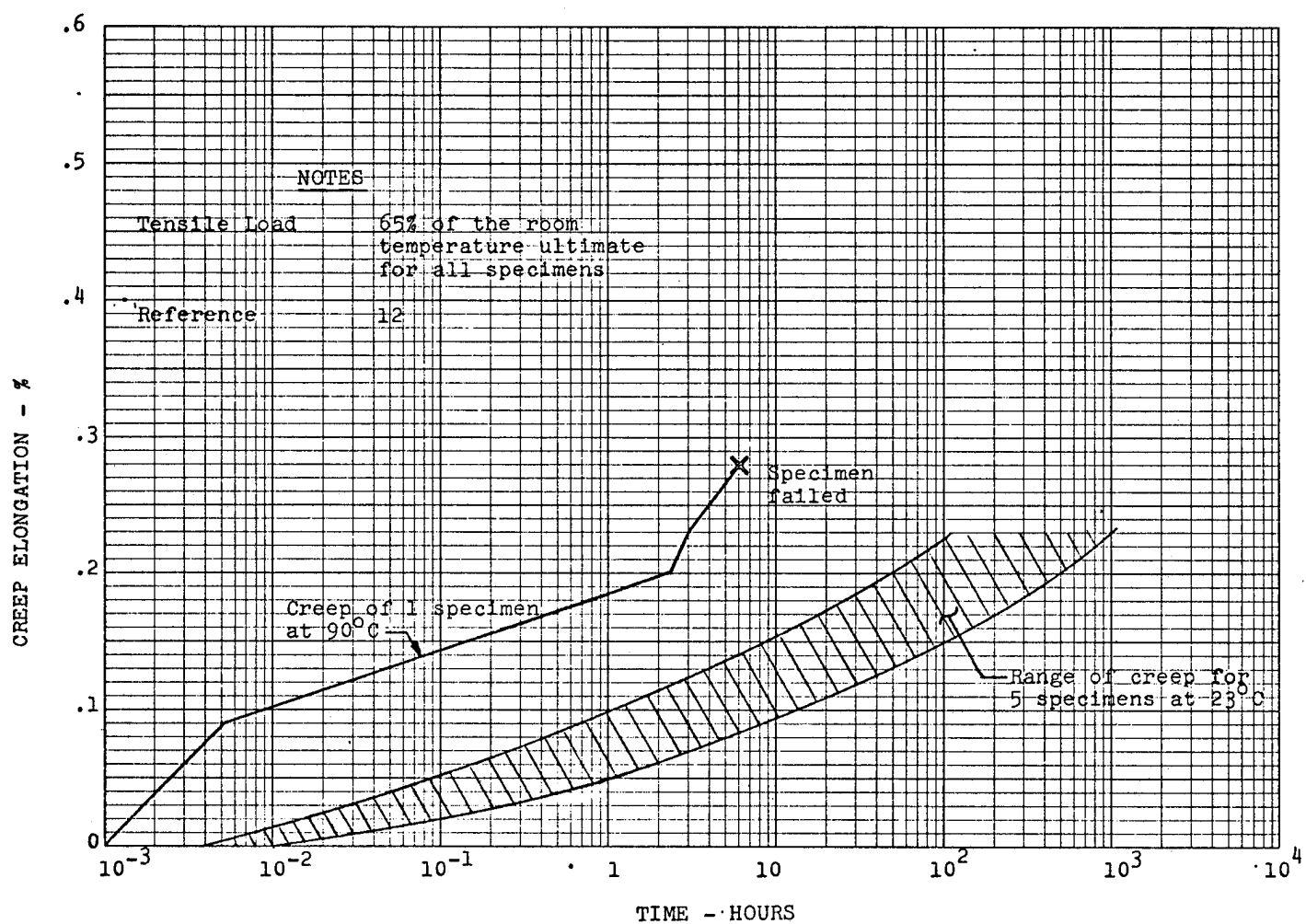


FIGURE 2-38 STATIC TENSILE CREEP VERSUS TEMPERATURE FOR SMC (R25)

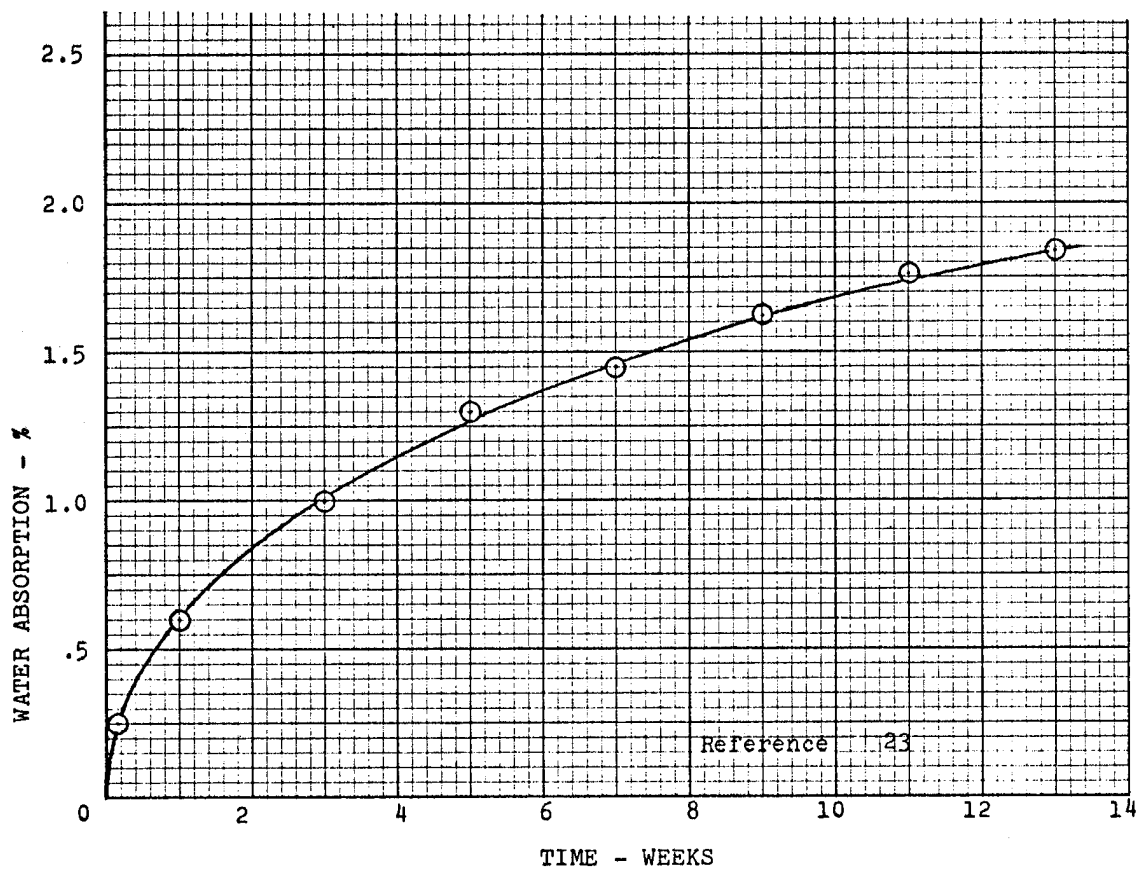


FIGURE 2-39 ROOM TEMPERATURE WATER ABSORPTION  
VERSUS TIME FOR SMC (R30)

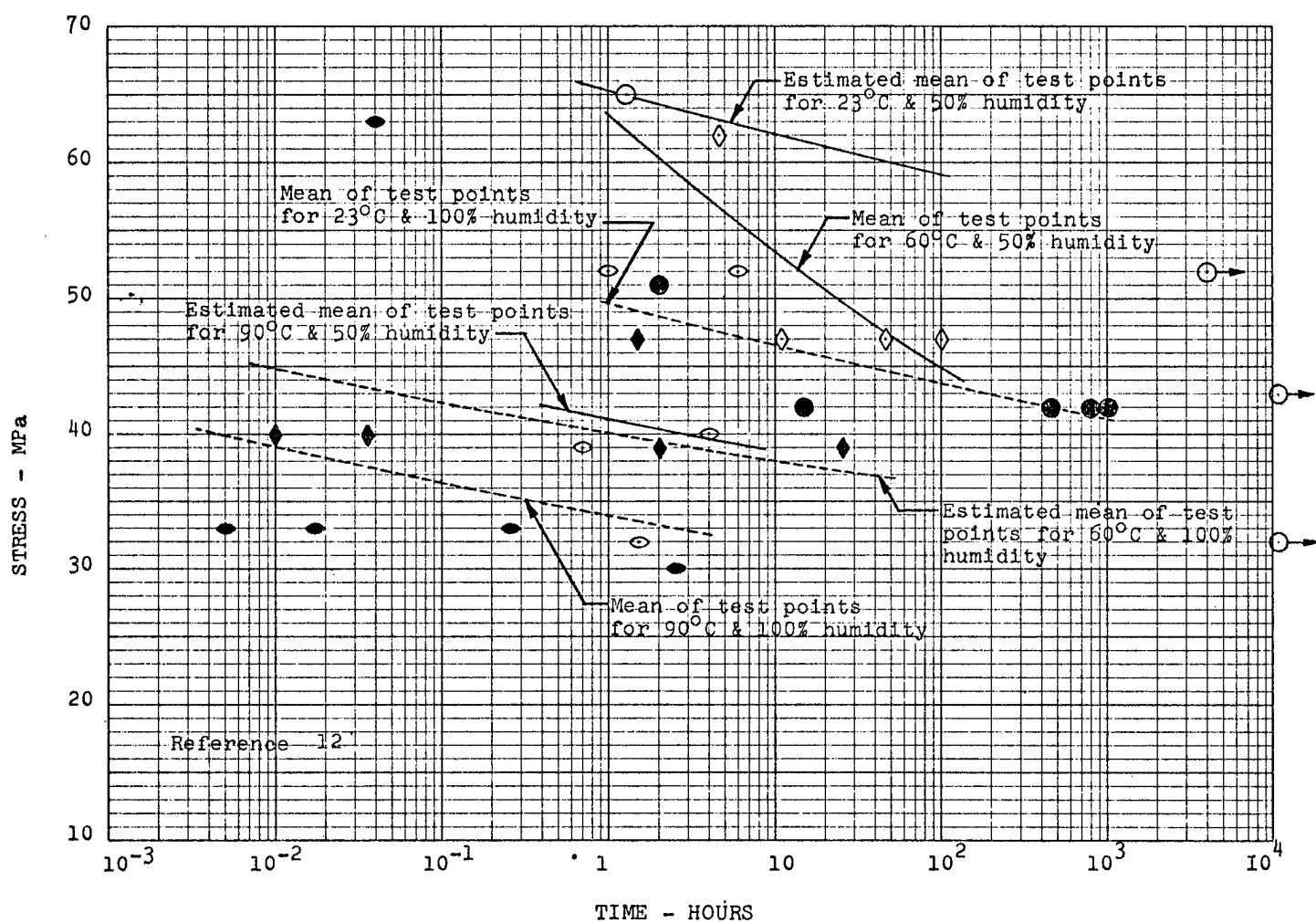


FIGURE 2-40 ENVIRONMENTAL STRESS RUPTURE DATA FOR SMC (R25)

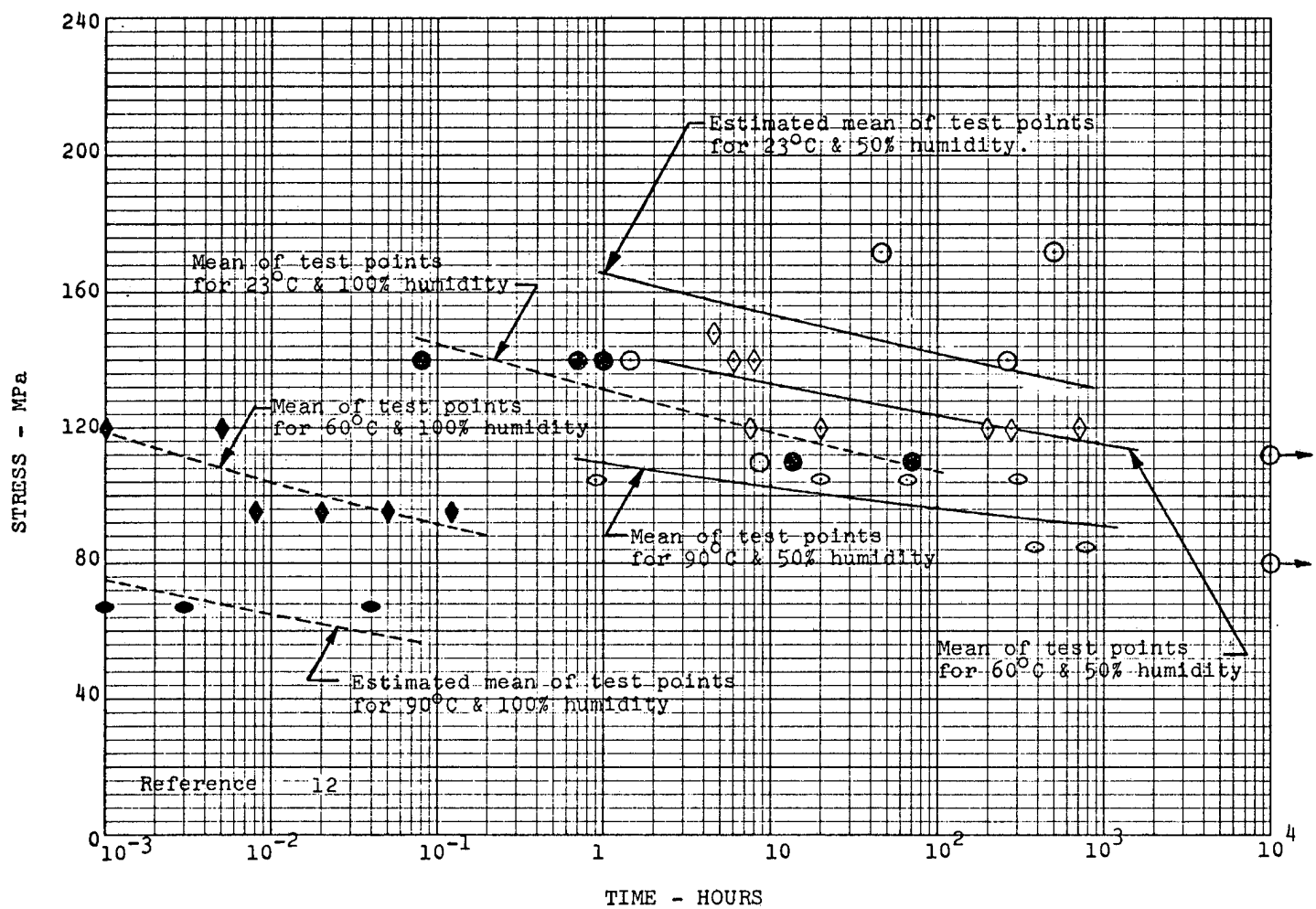


FIGURE 2-41 ENVIRONMENTAL STRESS RUPTURE DATA FOR HMC (R65)

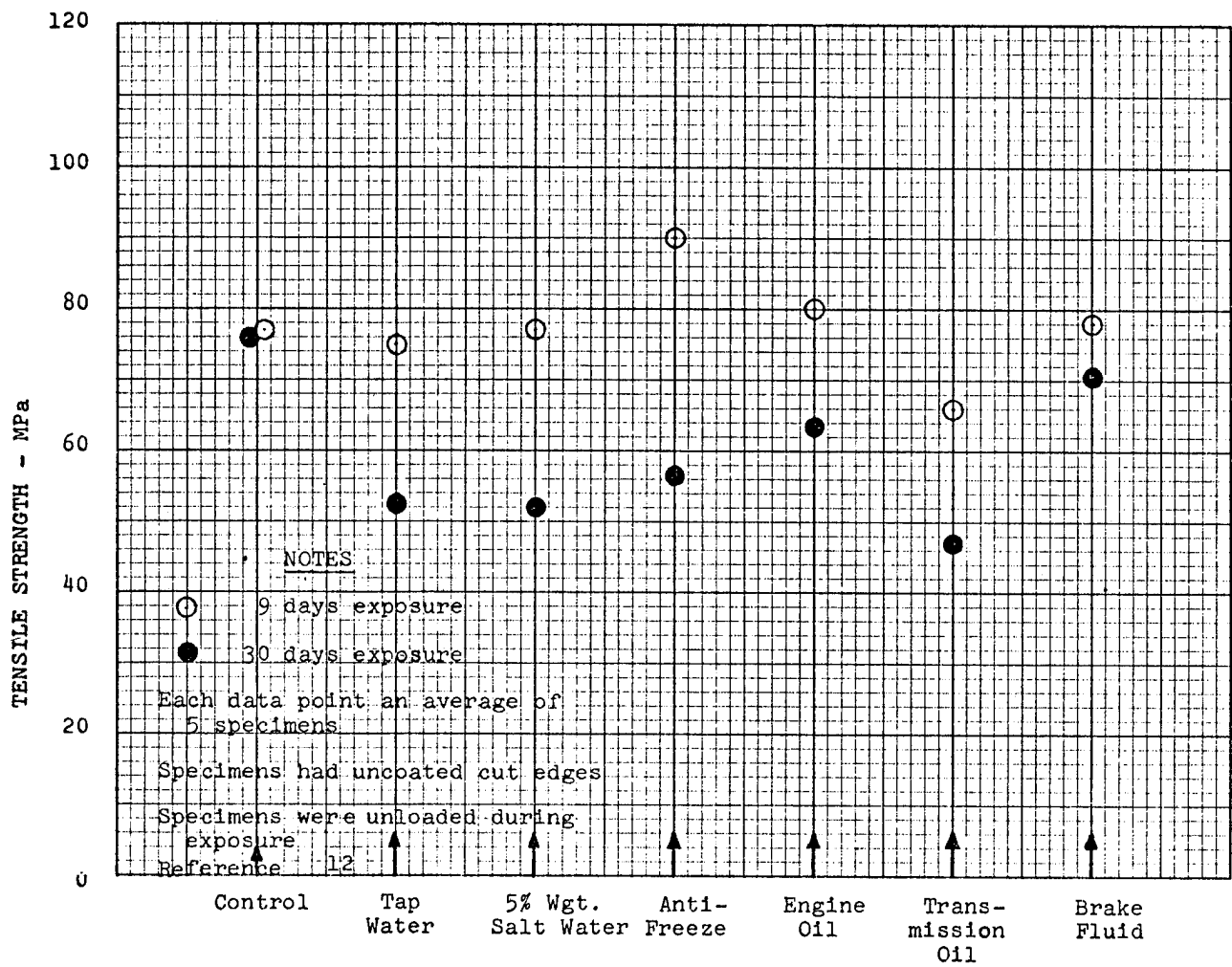


FIGURE 2-42 ROOM TEMPERATURE ENVIRONMENTAL INFLUENCE ON TENSILE STRENGTH FOR SMC (R25)

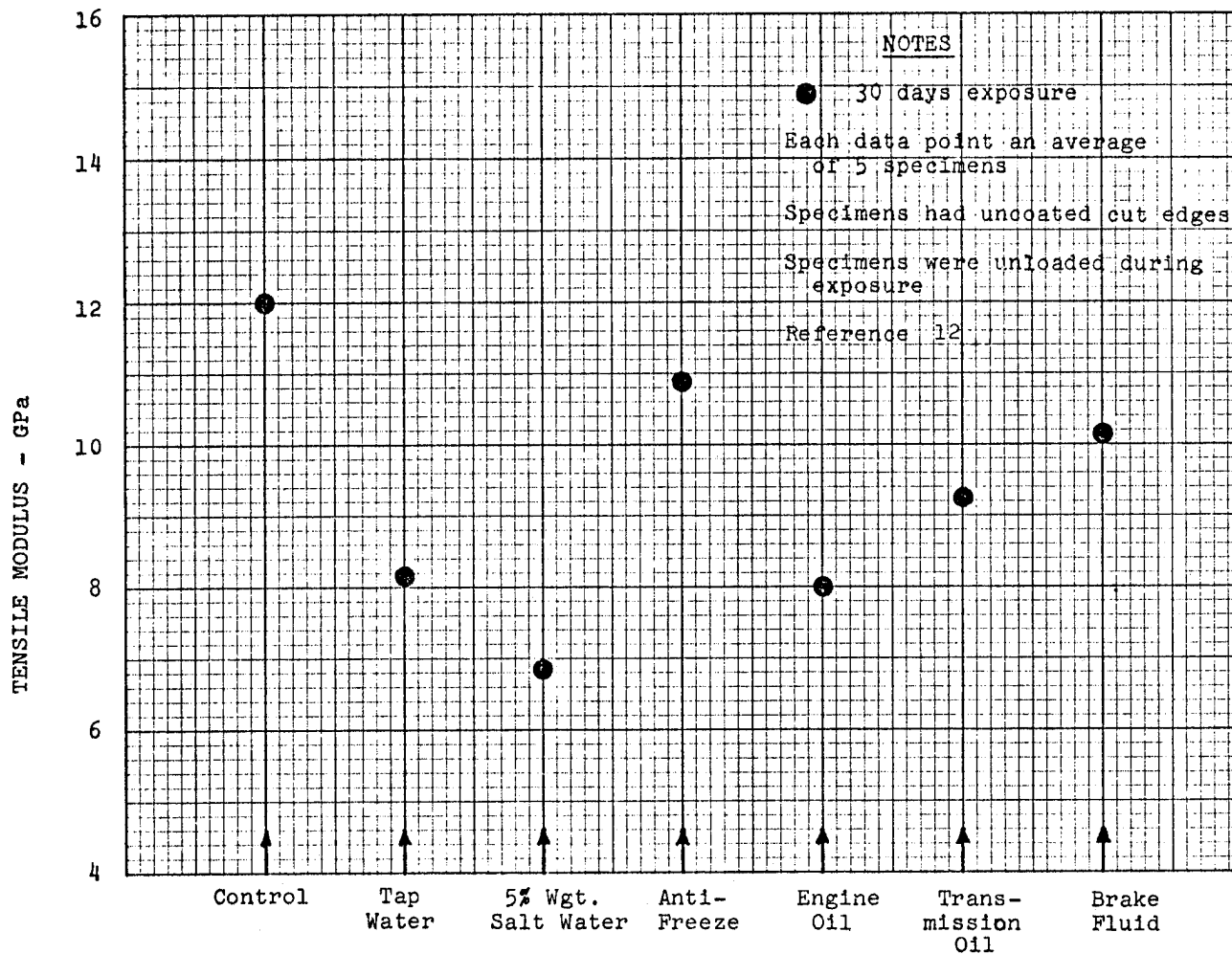


FIGURE 2-43 ROOM TEMPERATURE ENVIRONMENTAL INFLUENCE ON TENSILE MODULUS FOR SMC (R25)

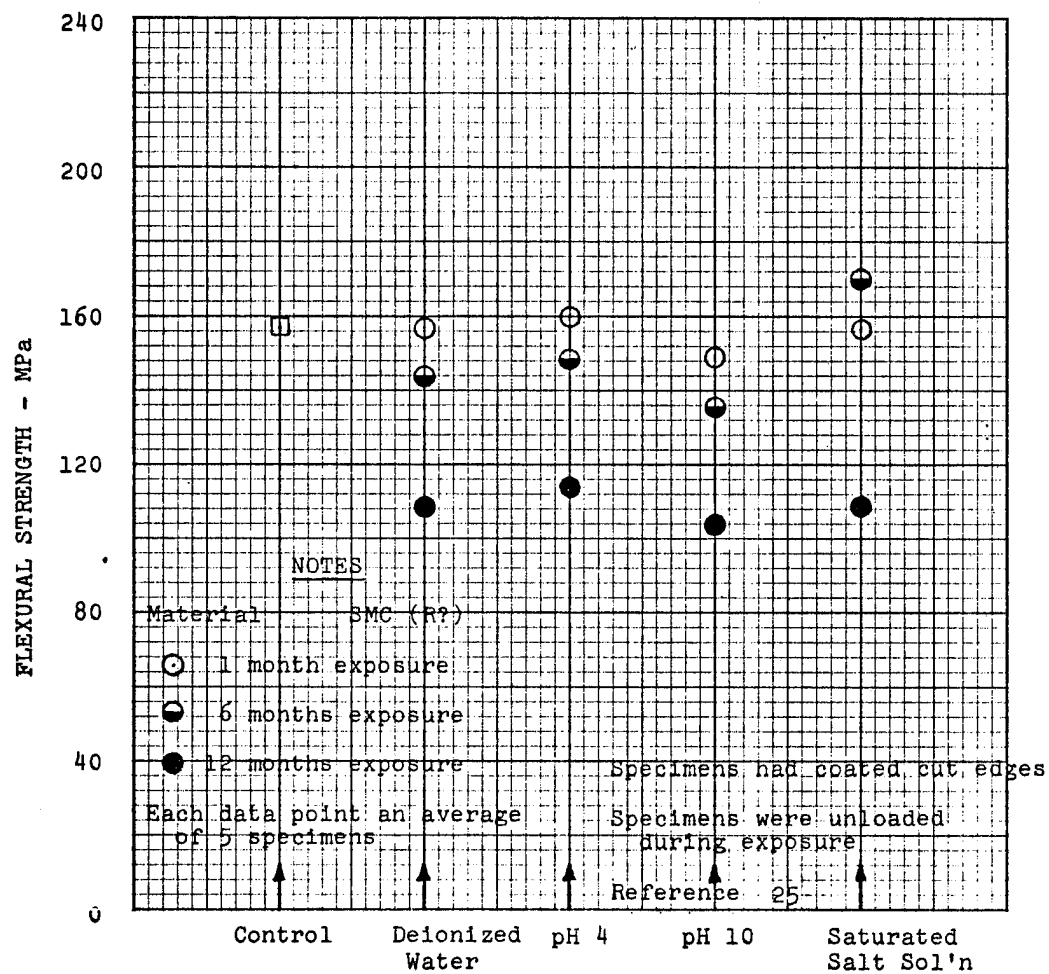


FIGURE 2-44 ROOM TEMPERATURE ENVIRONMENTAL INFLUENCE ON FLEXURAL STRENGTH FOR SMC

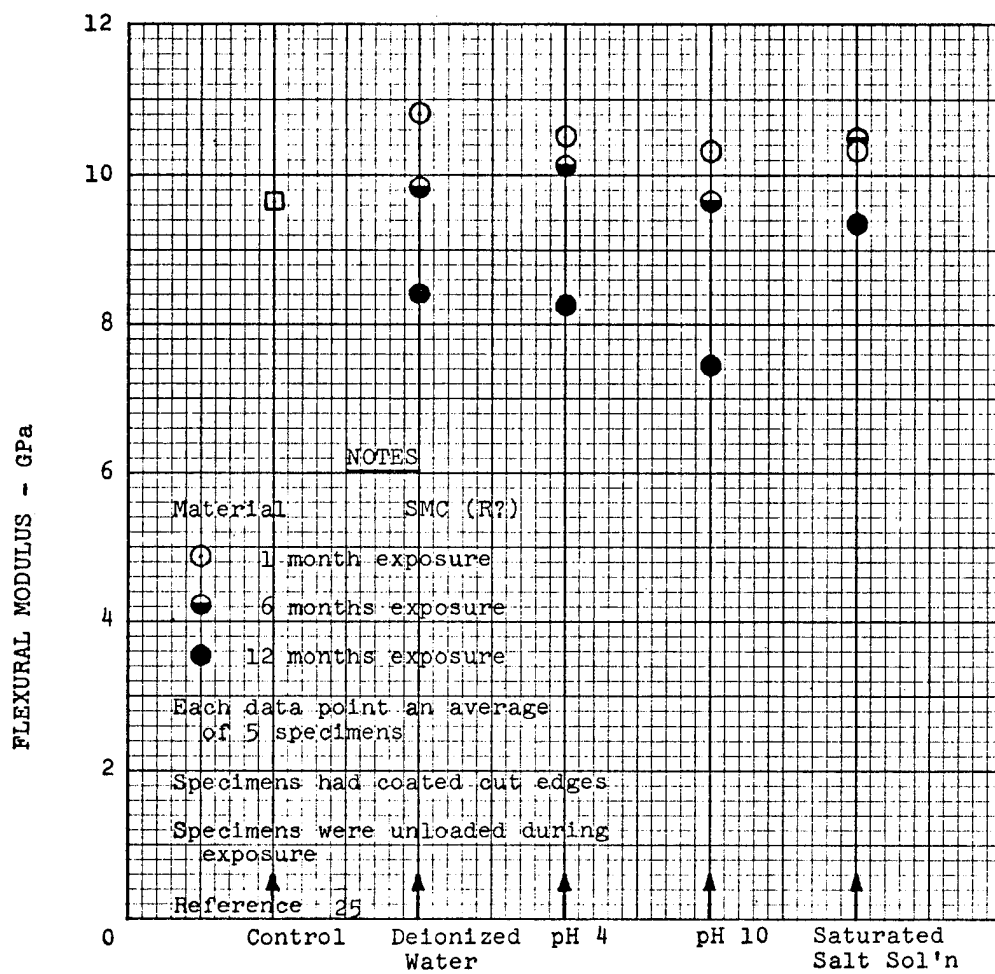


FIGURE 2-45 ROOM TEMPERATURE ENVIRONMENTAL INFLUENCE ON FLEXURAL MODULUS FOR SMC



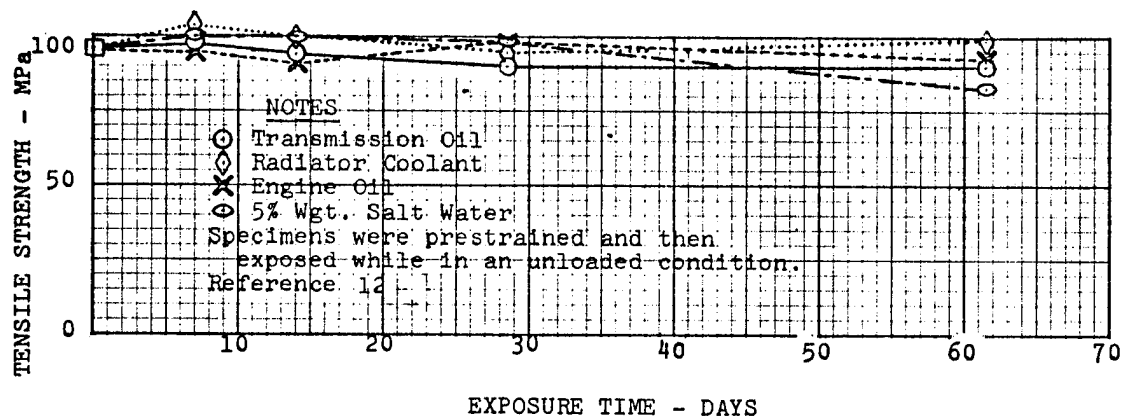


FIGURE 2-46 ROOM TEMPERATURE ENVIRONMENTAL INFLUENCE ON TENSILE STRENGTH FOR PRESTRAINED SMC (R25)

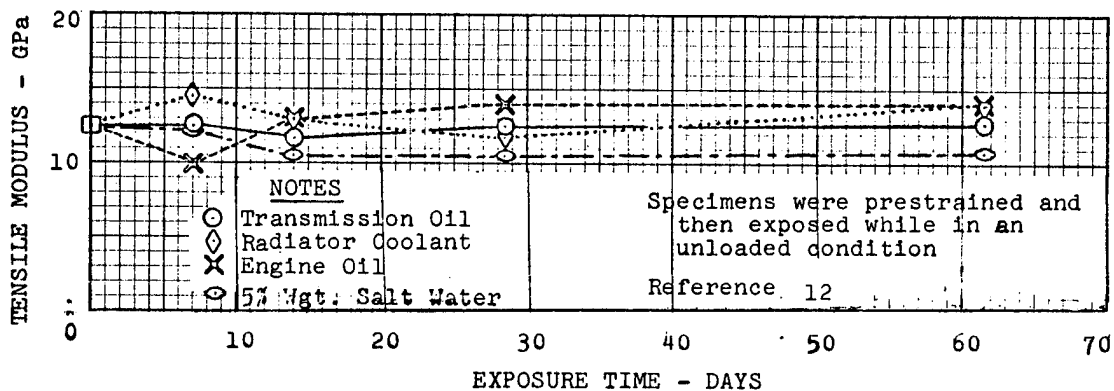


FIGURE 2-47 ROOM TEMPERATURE ENVIRONMENTAL INFLUENCE ON TENSILE MODULUS FOR PRESTRAINED SMC (R25)

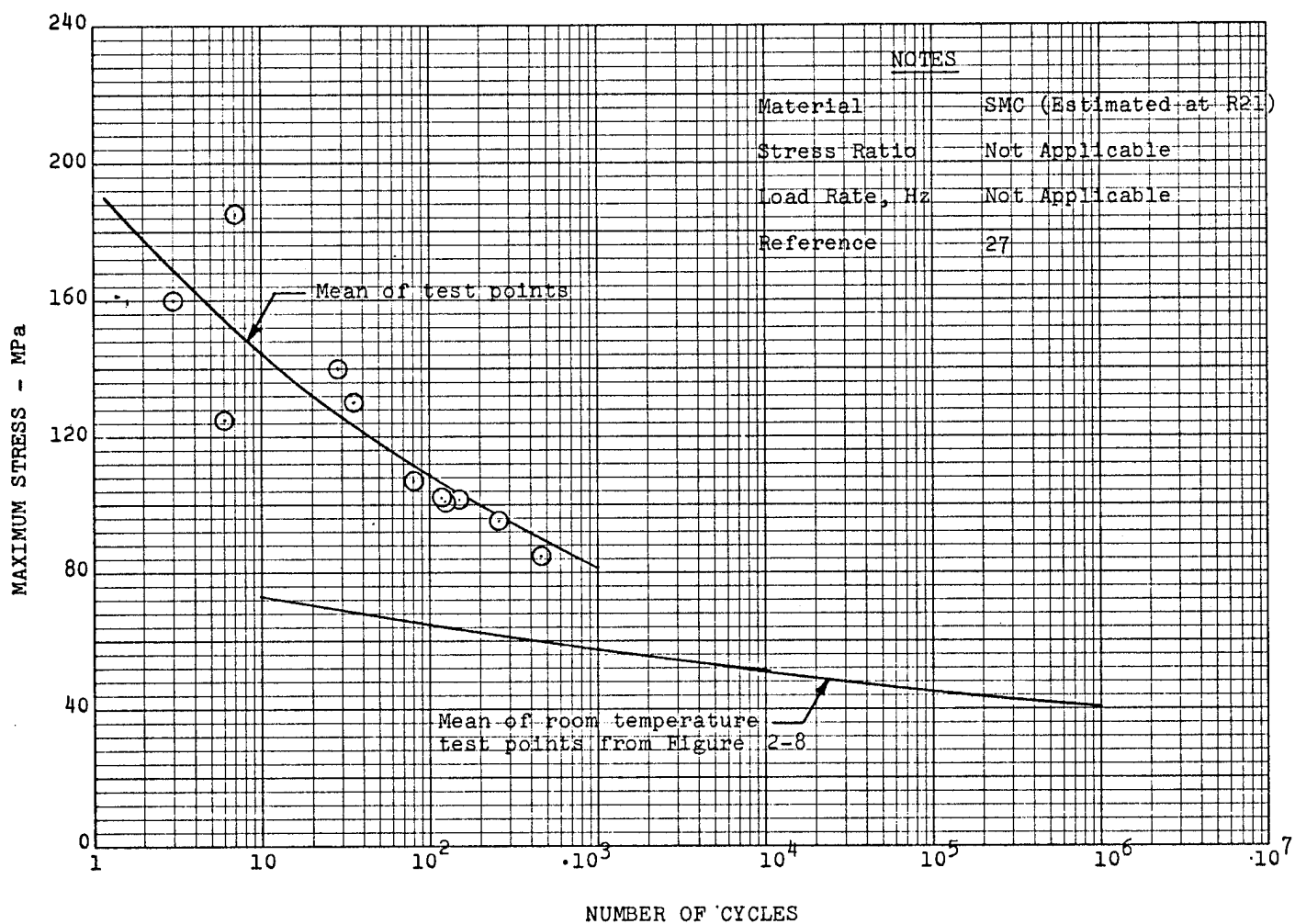


FIGURE 2-48 ROOM TEMPERATURE S-N CURVE FOR MAT (R21)  
LOADED IN TENSILE IMPACT FATIGUE

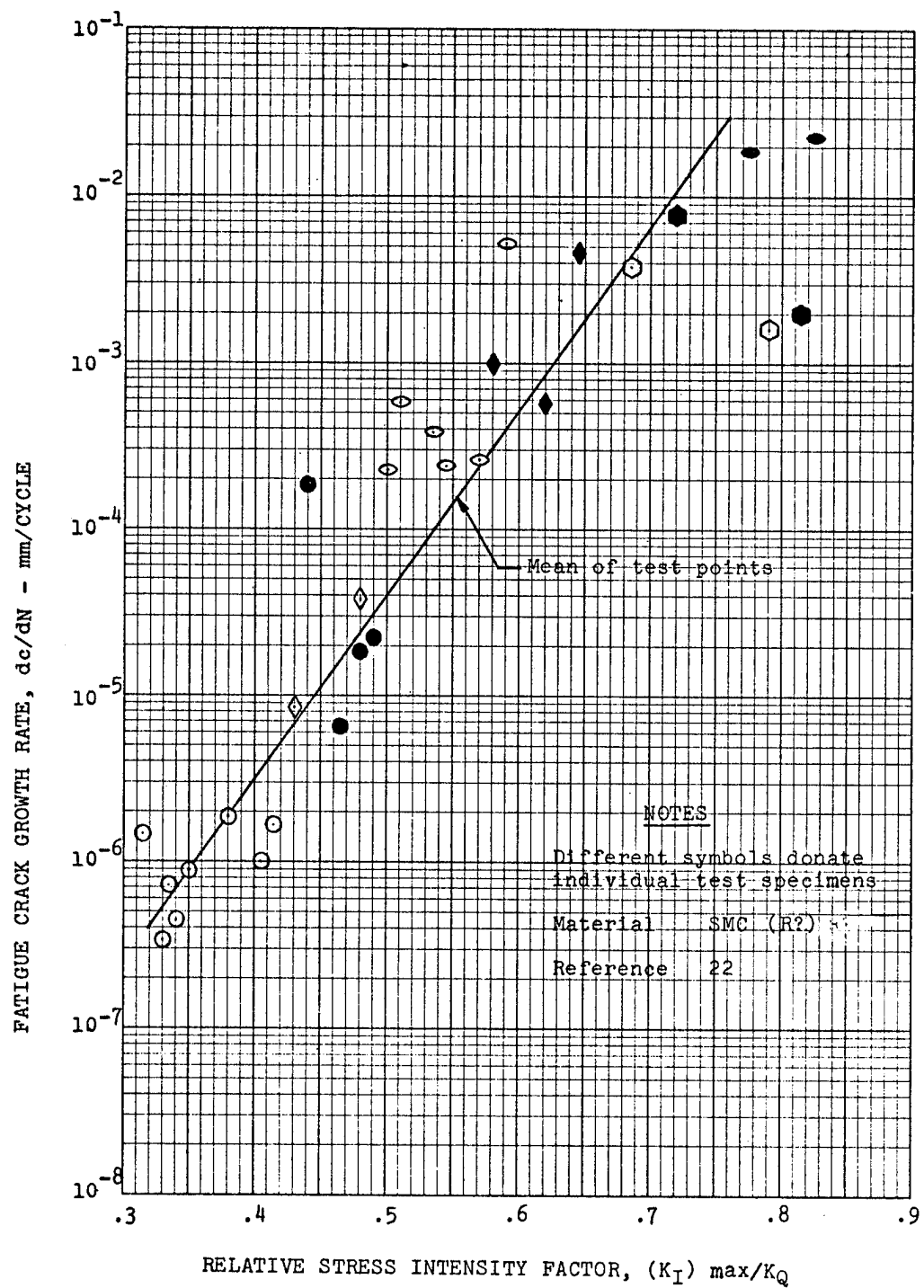


FIGURE 2-49 ROOM TEMPERATURE FATIGUE CRACK GROWTH RATE FOR SMC

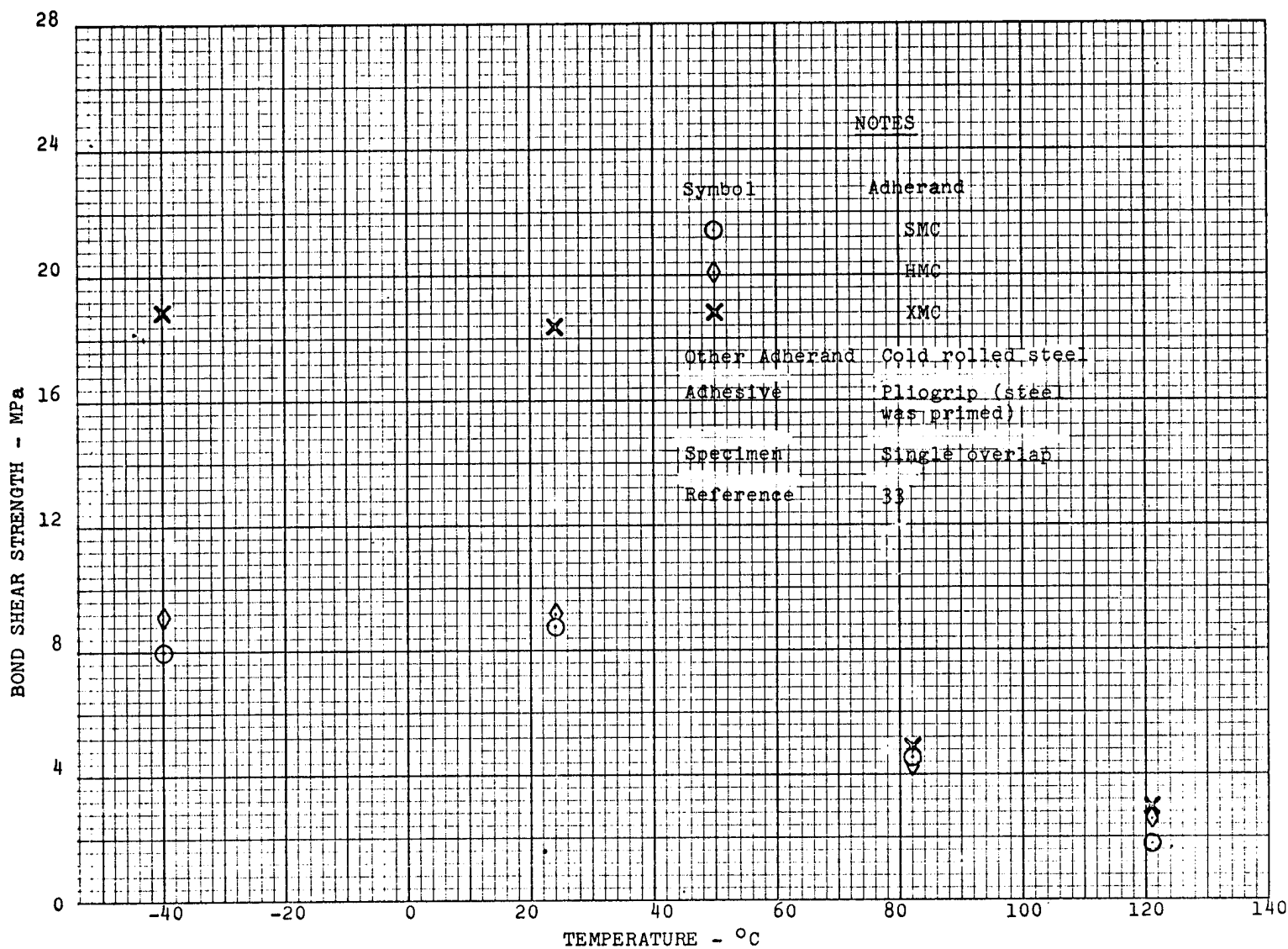


FIGURE 2-50 BOND SHEAR STRENGTH VERSUS TEMPERATURE FOR SMC, HMC, AND XMC BONDED TO COLD ROLLED STEEL

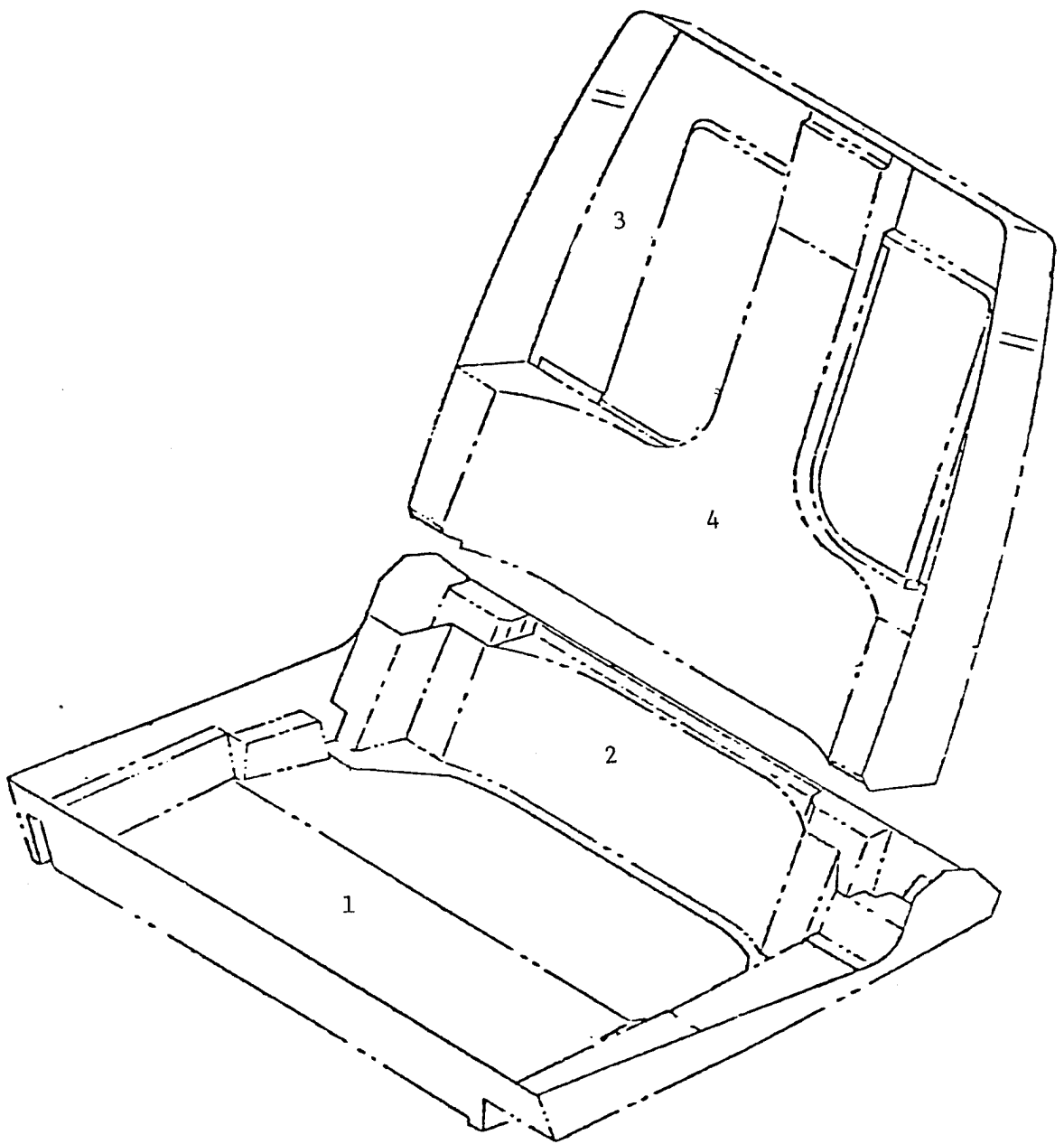


FIGURE 2-51 PROTOTYPE PLASTIC SEAT

APPENDIX B  
PROCESS SELECTION REPORT

## ABSTRACT

The compilation of the material properties presented in the Material Selection Report was based primarily on specimens fabricated by the process known as compression molding. A brief review is presented in this report of the equipment requirements including the matched metal mold and the hydraulic press. Also included are the molding requirements and their effect on the cured composite part.

In the costing effort of the program, a number of the costing scenarios involved proposed manufacturing schemes. This report also briefly describes these schemes.

## TABLE OF CONTENTS

1.0	COMPRESSION MOLDING.....	B1
2.0	EQUIPMENT REQUIREMENTS.....	B2
3.0	MOLDING REQUIREMENTS.....	B8
4.0	REFERENCES.....	B16



## LIST OF FIGURES

FIGURE	PAGE
2-1 Standard Features of a Compression Mold.....	B 3
2-2 Automatic Composite Material Loader and Automatic Part Unloader.....	B 5
2-3 Proposed Compression Mold Transfer Line.....	B 7
3-1 Mold Displacement and Hydraulic Pressure as a Function of Time.....	B 9
3-2 Determination of Curing Characteristics by Exotherm Method.....	B10
3-3 Minimum Cure Time as a Function of Plaque Thickness for an HMC Composite System.....	B11
3-4 Time for Peak Exotherm and Equalization of Temperature Across Plaque Thickness.....	B12
3-5 Variation of Flexural Strength as a Function of Cure Time.....	B14
3-6 Variation of Interlaminar Shear Strength as a Function of Cure Time.....	B15



## 1.0 COMPRESSION MOLDING

Associated with the chosen glass/polyester systems for use as the material to fabricate the door outer panel, is the required curing process. The polyester resin system, being a thermoset material, requires a combination of time-temperature-pressure to effect an acceptable cure. The large quantity of parts required in the mass production oriented automotive industry dictates that the cure cycle be as brief as possible yet provide structurally acceptable parts.

Compression molding of the glass/polyester systems was chosen for the fabrication of the door outer panel since it best meets the mass production requirements of the automotive industry for a variety of parts.

## 2.0 EQUIPMENT REQUIREMENTS

The basic equipment consists of matched metal molds which provide component shape and a hydraulic press which supplies the curing pressure. The molds are heated to the curing temperature which is approximately 150° C for polyesters. The room temperature glass/polyester is cut to the proper size charge, which generally corresponds to less than 50% mold coverage, and placed into the mold. The hydraulic press closes the mold, initially forcing the composite material throughout the mold followed by constant pressure of approximately 1000 to 2000 psi for proper cure. The cured part is removed from the mold and the next charge is loaded. The flash is removed from the cured part, and then it is assembled and finished.

The important areas of a typical compression mold are shown in Figure 2-1 (Reference 1). The material used in the construction of a production tool is a hardened steel. The molding surfaces of the appearance side of the molding should be blemish-free and chrome plated which is buffed to a high luster. The heating of the mold is provided by steam, electric, or high temperature oil, with the number and location of the heating lines designed to give uniform mold surface temperature.

The shear edge requires very close tolerance to minimize the flash and to insure that adequate pressure is developed in the composite material. The leader pins assist in achieving correct alignment of the two mold halves during closing while the heel blocks react any lateral loads caused by the molding.

The mold contains a hydraulic ejector system which uniformly raises the part away from the mold. The location of the ejector pins depend on the specific component but they usually will be placed on all bosses and ribs to insure that these sections do not lock up in the mold.

In addition to using hardened steel for the molds, the die block thickness must be sufficient so as to minimize deflection during mold closing. In addition, very accurate parallelism of the two halves of the mold must be maintained to insure accuracy in the part thickness.

In the prototype molding of the door outer panel the basic features of Figure 2-1 were incorporated in the compression mold. The only difference was that the material used for the die was a zinc alloy material. Whereas the production steel mold is machined, the zinc alloy die is cast in sand molds which were developed from plaster patterns. After casting, the zinc alloy material is generally finished and polished but no chrome finish is used. While the mold material used for the prototype molding differed from production, the molding temperature, pressure and time was

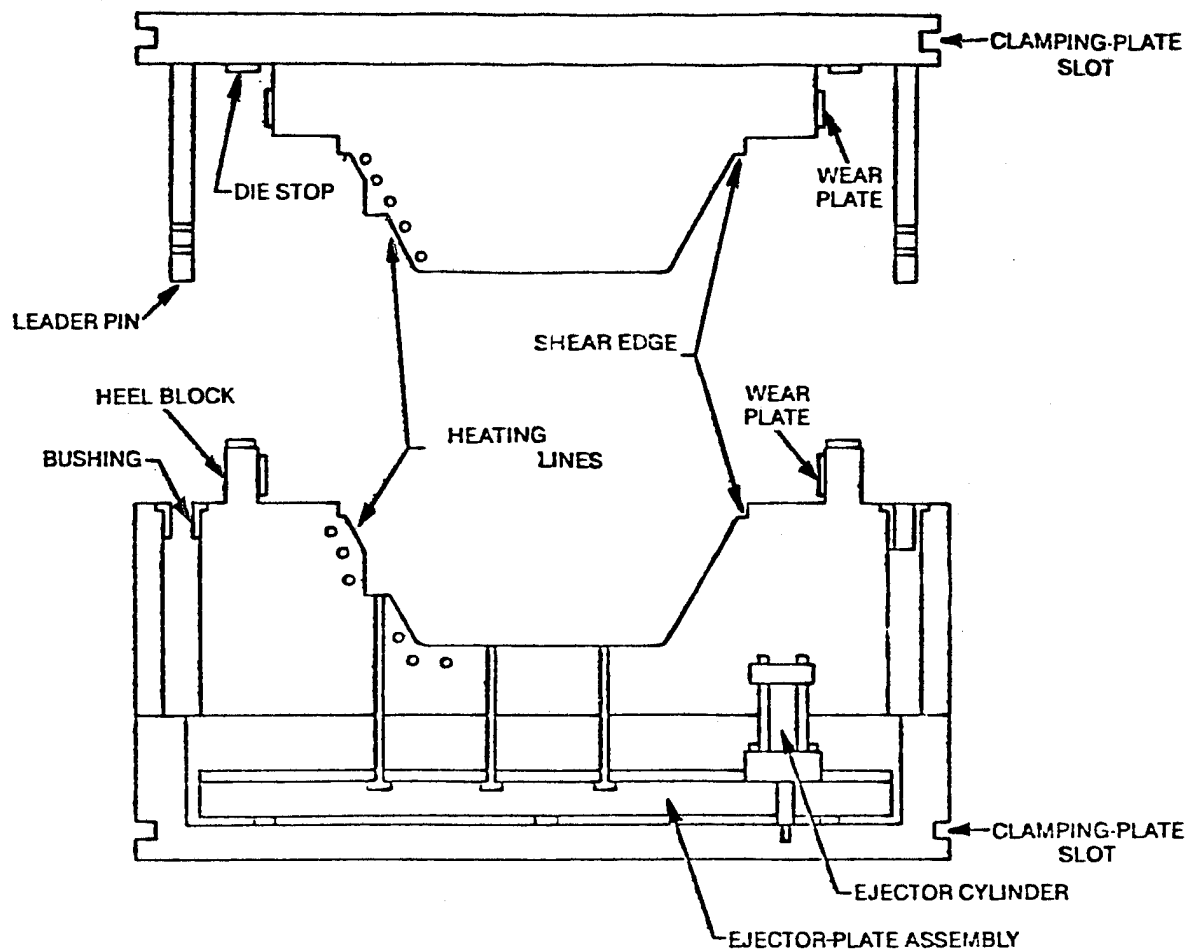


FIGURE 2-1 STANDARD FEATURES OF A COMPRESSION MOLD  
(Reference 1)

identical between prototype and production. Hence, the prototype fabrication proved to be an excellent simulation and no verification of composite material properties should be necessary between prototype and production fabricated parts.

As previously indicated, the press utilized for compression molding generally has a hydraulic ram. A significant requirement of the press involves the need for close tolerance on the platen parallelism to insure correct part thickness. In addition, the closing speed of the mold over the final 0.25 in of closing is critical to achieve proper flow of the composite material. Other important parameters which must be known in order to choose the correct press for the component are the press tonnage capability, platen size, and press daylight opening (i.e., maximum distance between platens).

The important auxiliary equipment considered in the costing exercise portion of the program involves an automatic charge loader and an automatic part unloader. Such equipment exists (Reference 2) and a schematic is shown in Figure 2-2. While the previous charge is curing, the external loader tray is charged with the precut composite pieces. Spears, attached to the loading carriage, are hydraulically lowered through the composite material and then rotated to capture it. When the press is ready for the next charge, the loading carriage moves over the bottom mold and the spears rotate back to their original position. The composite material is then forced off the spears by a stripper frame which has a mating contour to the bottom mold. The loading tray then moves away from the press and is reloaded.

When the cured part is ejected from the top mold, a catcher tray, which is contoured to fit the finished part and is mounted to the top of the unloader carriage is used. If the cured part is ejected from the bottom mold, then the unloader carriage can be equipped with vacuum cups which attach to the part and move it up and out of the press.

A number of new equipment developments regarding compression molding are in the experimental stage while others are still in the talking stage. For instance in reference 3, a system of controlling press parallelism, velocity and force has been developed. The system, known as "programmable force velocity control system", uses hydraulic cylinders on the four corners of the press platen. The system is claimed to minimize wall thickness variation, some waviness, and reduces part reject.

Another approach to improving the acceptance of compression molded composite materials involves the use of molded coatings as described in Reference 4. The component is molded as usual except near the conclusion of the cure cycle the mold is opened slightly and a thermoset coating material is injected into the opening. The mold is again closed and the coating is thus forced

UNLOADER WITH  
VACUUM CUPS

STRIPPER  
FRAME

SPEARS

COMPRESSION  
MOLDS

COMPOSITE  
CHARGE PATTERNS  
LOADED HERE

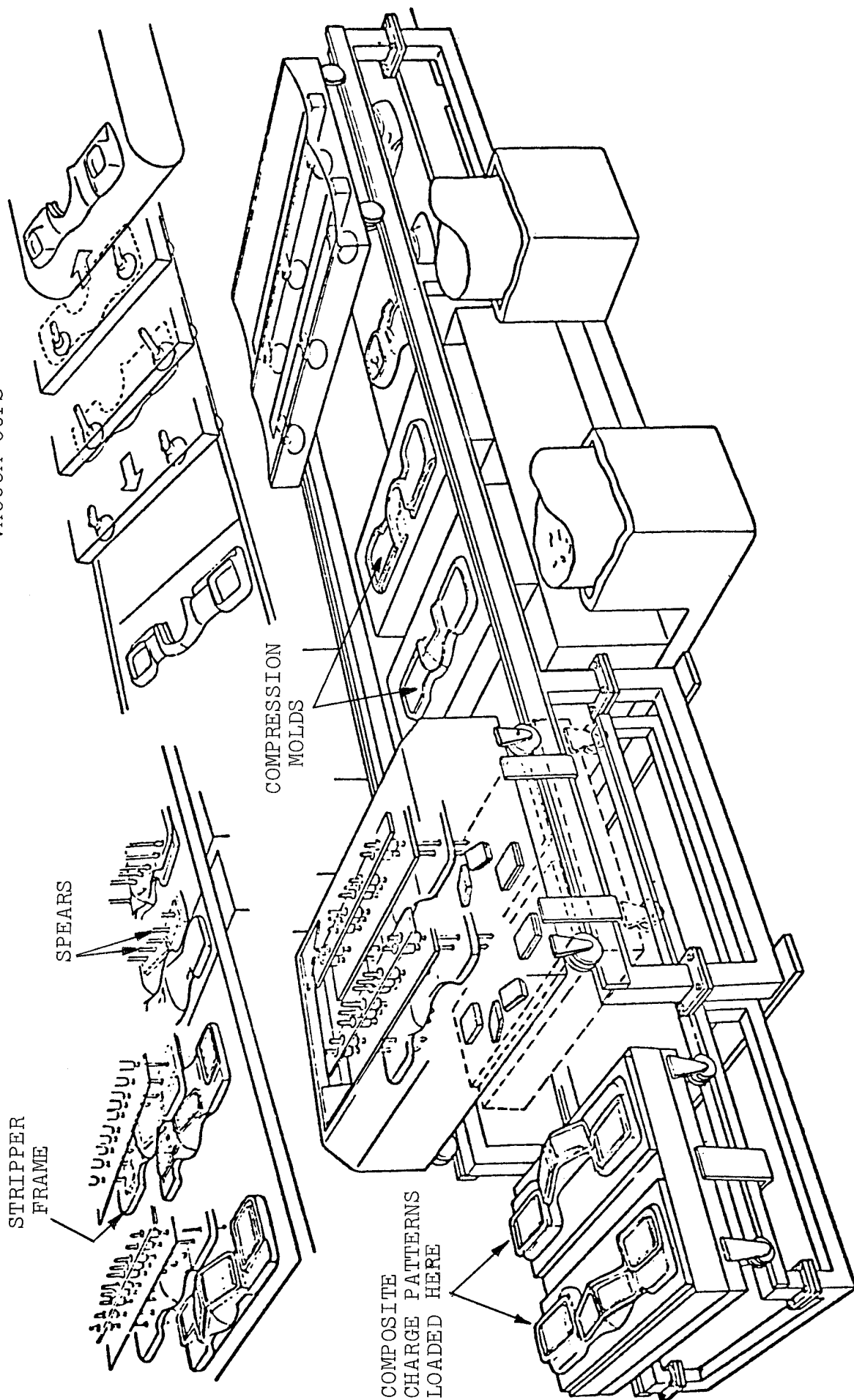


FIGURE 2-2 AUTOMATIC COMPOSITE MATERIAL LOADER  
AND AUTOMATIC PART UNLOADER (Reference 2)

to impregnate the composite substrate, thereby reducing porosity and surface pits. The result is a lowering of the finishing costs.

A number of proposals have been put forth for increasing the rate of composite component production without the need for an excessive number of conventional hydraulic presses. An actual system was developed in Reference 5 which used a carrousel approach with up to 12 molds at a time. An initial closing station forces the SMC material throughout the mold by providing a high curing pressure. Once the mold has been closed, a lower mechanical clamping force is maintained throughout the remainder of the cure.

Figure 2-3 shows the approach proposed in Reference 3 where a series of moving stations were used with stationary presses. As with the system presented in Reference 5, the composite material sees a high initial closing pressure followed by a lower one during the remainder of the cure. Tensile and flexural tests were reported to show no difference between SMC parts molded with the high/low pressure cycle compared to the conventional high pressure cure. Surface porosity was, however, increased but the mold coating is expected by the author to eliminate this problem. Such a concept is expected to produce one part every 15 seconds.



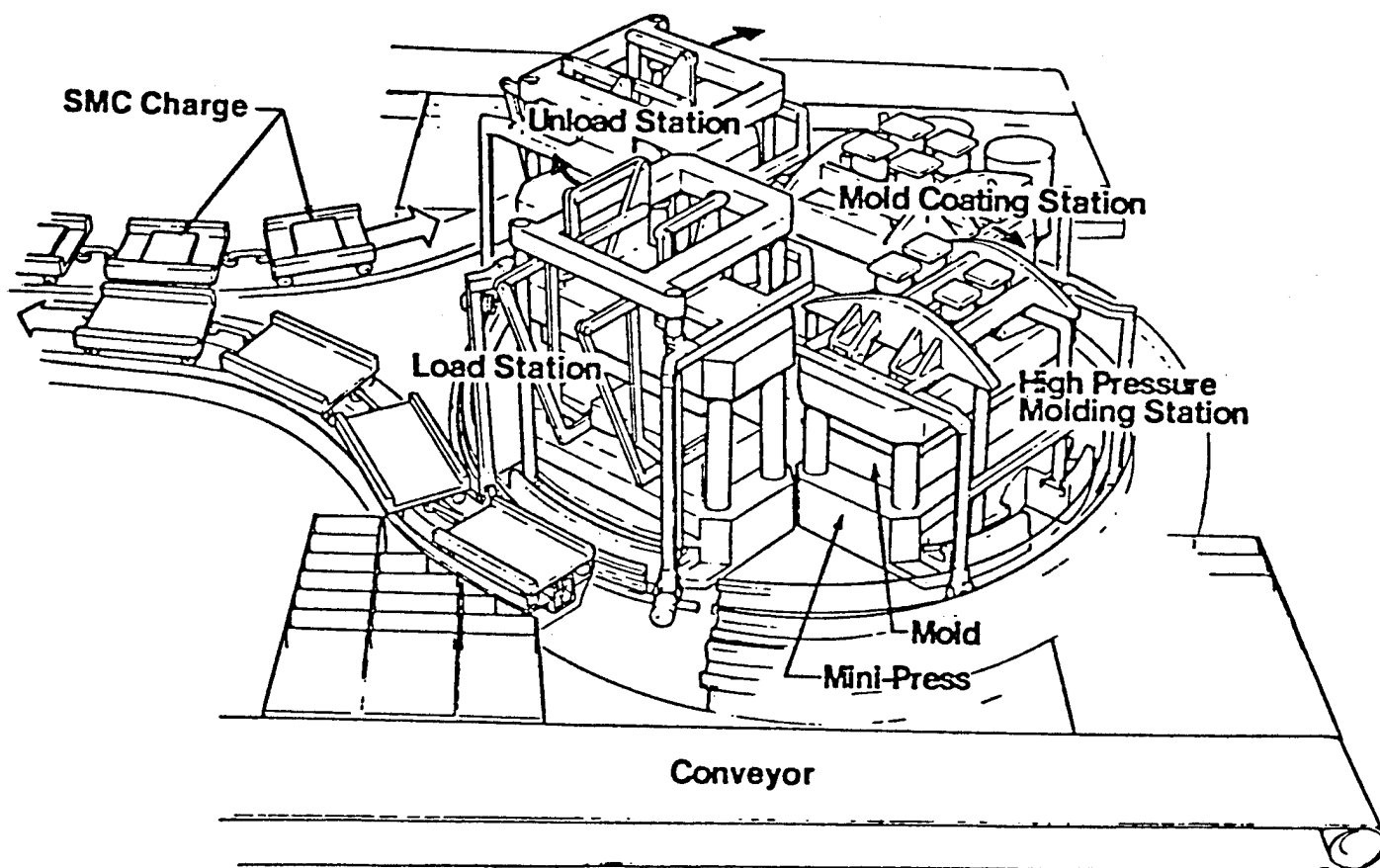


FIGURE 2-3 PROPOSED COMPRESSION MOLD TRANSFER LINE  
(Reference 3)

### 3.0 MOLDING REQUIREMENTS

Initial placement of the composite material into the mold is quickly followed by the platen closure to force the material throughout the mold. The rate at which the platens close is important in obtaining an acceptable cured part. If the closing speed is too great a condition known as resin-wash, or a separation of glass and resin, occurs (Reference 6). In addition, a too rapid mold closure would result in high local pressures which could abrade the mold surface and also trap air in the molded part (Reference 7).

If the mold closes too slowly then a pre-gel condition exists where the polyester resin starts to cure prior to filling the mold (Reference 6). The final speed thus chosen depends on the viscosity-time-temperature curve of the composite material. The chosen speed will keep the composite material in a state of continuous flow until the mold has been filled. The time could take 2-10 seconds for the last approximately 1/4 in of closing (Reference 7). Figure 3-1 shows a typical record of hydraulic pressure and mold displacement as a function of time (Reference 8).

The normal range of the mold temperature is 132 to 165°C depending on the composite system. Once the proper cure temperature has been established with the aid of an SPI Gel Time Test (Reference 6), then the curing time needs to be established. Generally, the cure time is defined (Reference 8) as that amount of time for the composite material to advance through the heat-up stage and then to just beyond the exotherm peak. Figure 3-2 shows a typical heating curve and the definition of cure time. If the mold temperature is not monitored and is allowed to go too low, then a long cure time will be necessary to completely cure the part. If the part is removed after the normal cure time the peak exotherm may not have been reached which would result in an undercured part. Structurally, this could cause poor interlaminar properties and blisters. If, on the other hand, the mold temperature is allowed to go too high, the peak exotherm will be reached sooner and its value will be higher. In extreme cases the resulting large thermal gradient which would occur across the thickness of the part could cause internal cracking if the part is removed prior to some degree of temperature equalization having occurred. (Reference 9).

The determination of the time to reach peak exotherm temperature will depend on the part thickness. Figure 3-3 (Reference 10) shows the effect of part thickness on cure time for a specific HMC material. Most parts, however, are not of a uniform thickness but have bosses and ribs attached which delay the total component's curing.

At the correct curing pressure and temperature, the effect of cure time becomes important. As Figure 3-4 (Reference 9) shows,

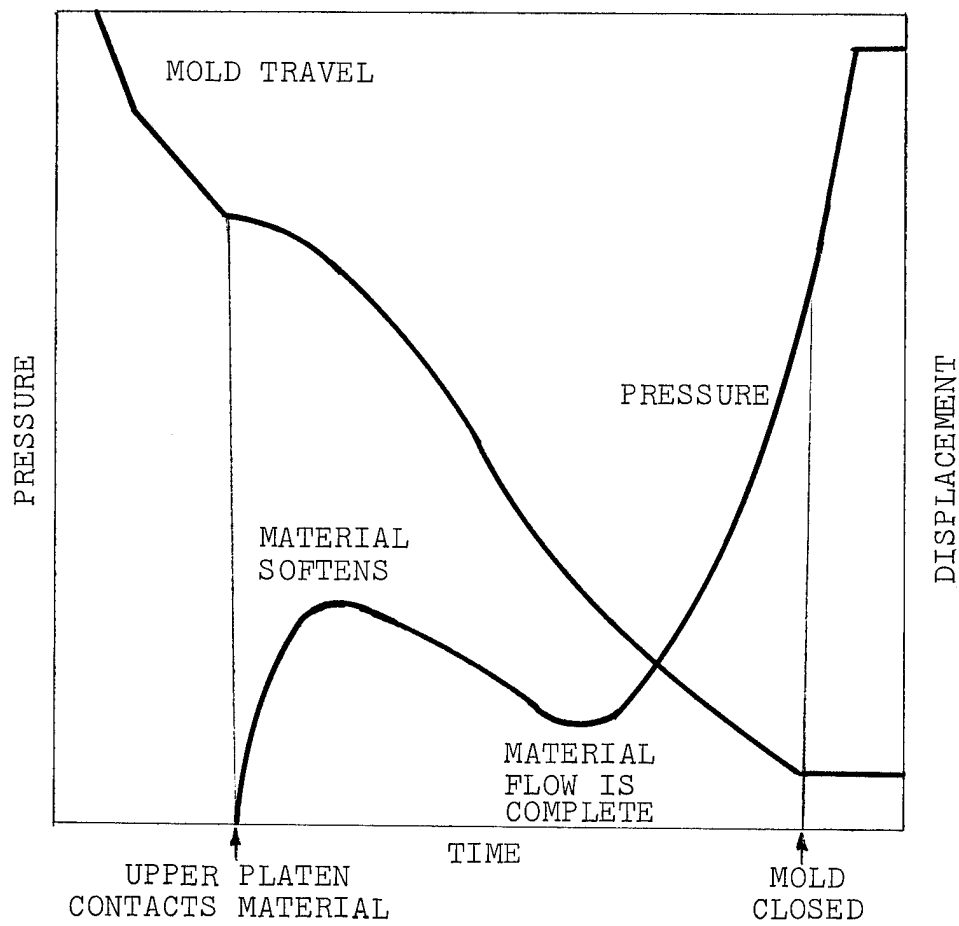


FIGURE 3-1 MOLD DISPLACEMENT AND HYDRAULIC PRESSURE AS A FUNCTION OF TIME  
(Reference 8)

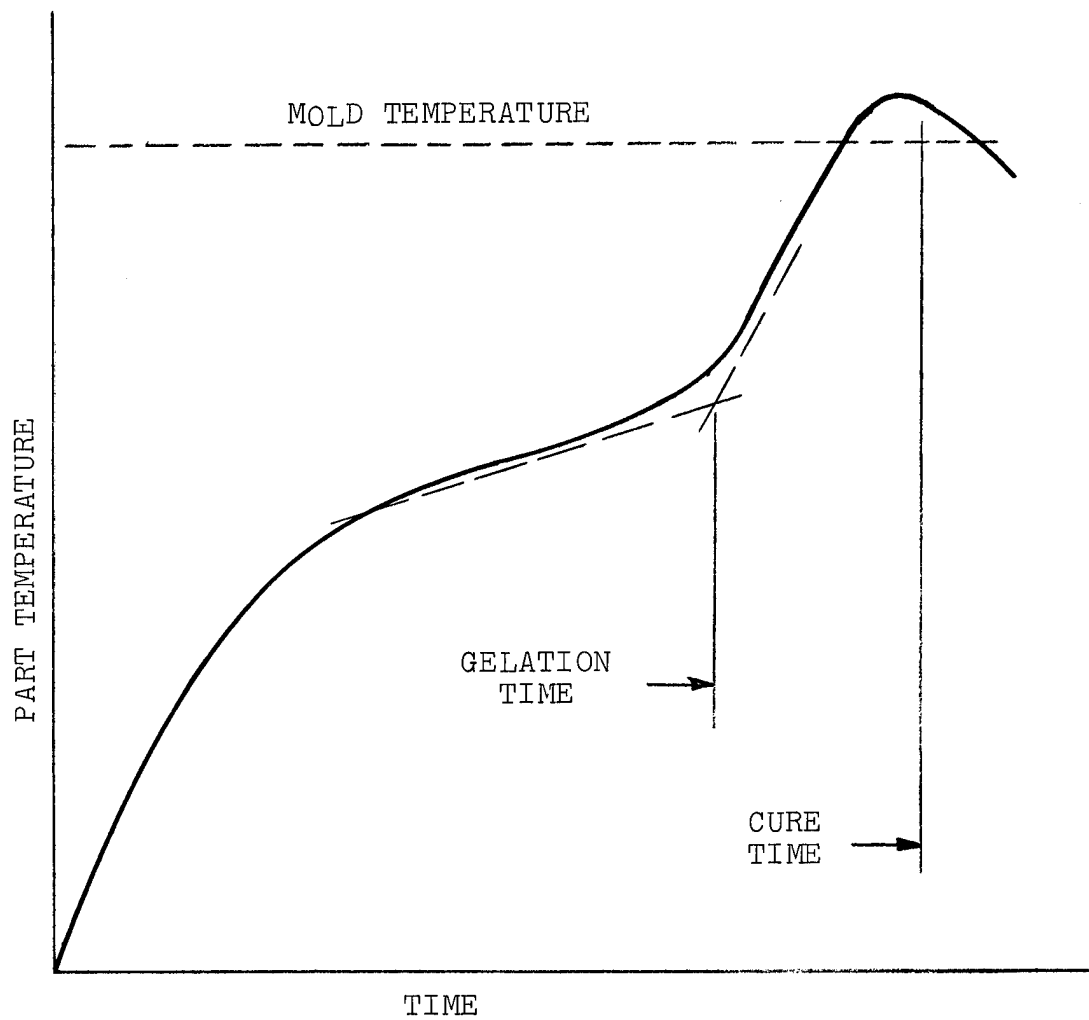


FIGURE 3-2 DETERMINATION OF CURING CHARACTERISTICS  
BY EXOTHERM METHOD  
(Reference 8)

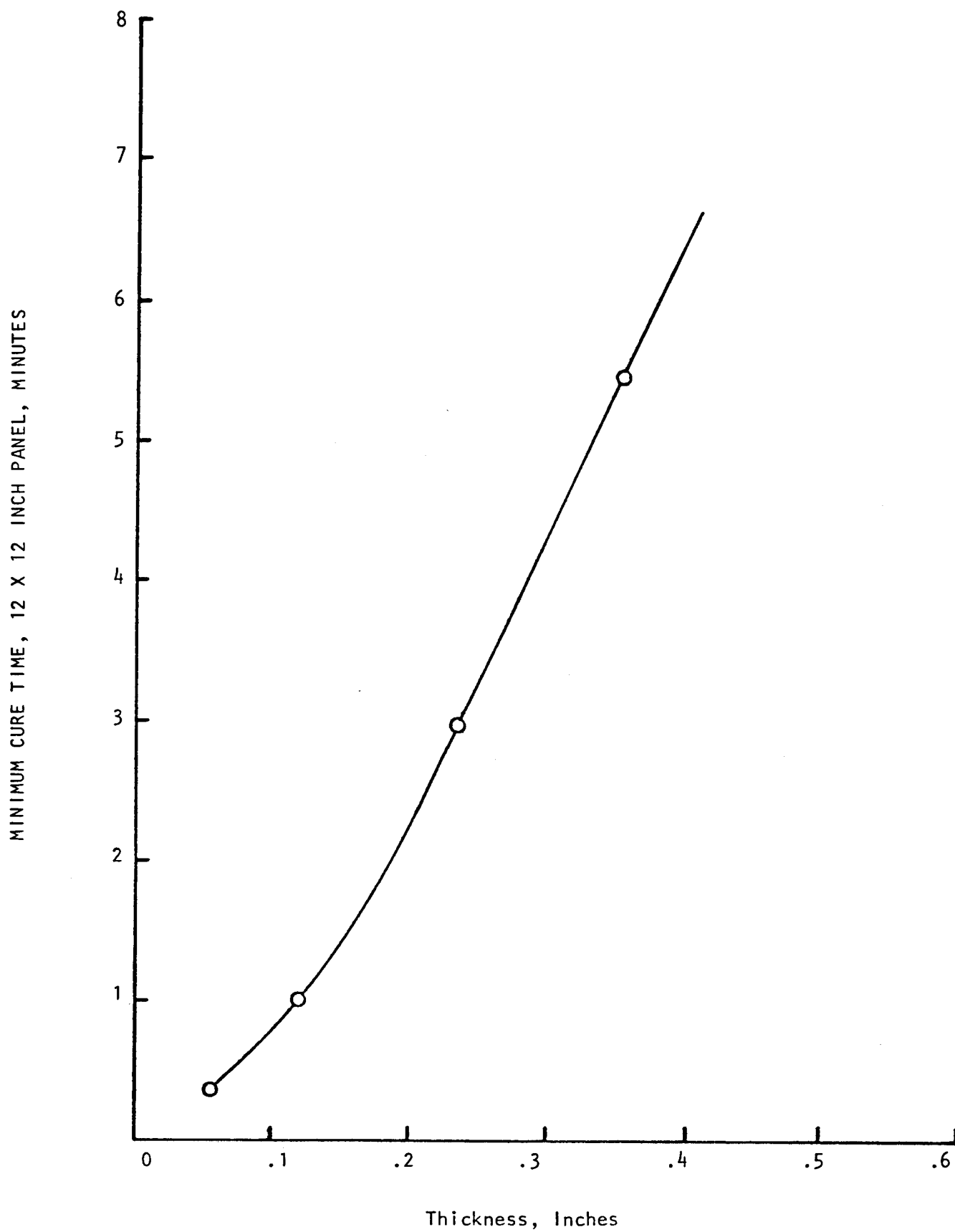


FIGURE 3-3 MINIMUM CURE TIME AS A FUNCTION OF PLAQUE THICKNESS FOR AN HMC COMPOSITE SYSTEM  
(Reference 10)

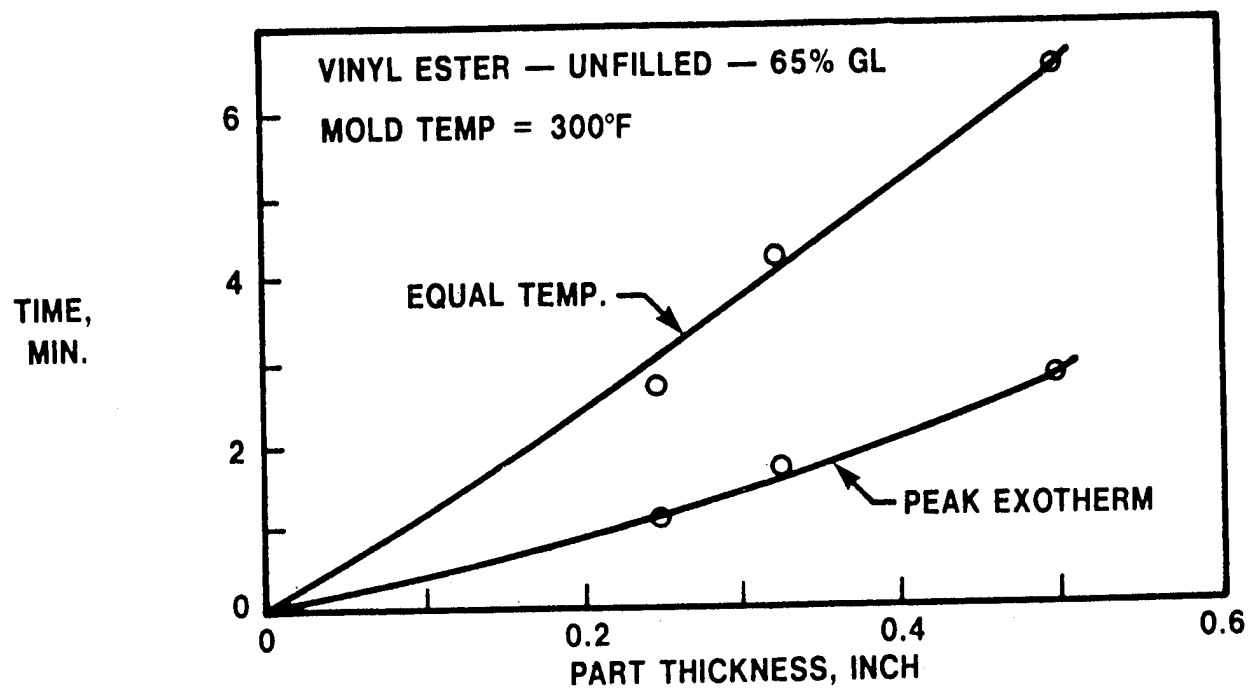


FIGURE 3-4 TIME FOR PEAK EXOTHERM AND EQUALIZATION  
OF TEMPERATURE ACROSS PLAQUE THICKNESS  
(Reference 9)

for a given part thickness, the longer the cure time the more the part reaches a uniform temperature after the peak exotherm temperature is obtained. If time permits, such an equilization of temperature through the thickness would avoid some resultant residual thermal stresses. If the part is removed too soon then the mechanical properties can suffer. From Reference 9, Figures 3-5 and 3-6 show the effect on flexural strength and interlaminar shear strength respectively for a 0.5 in. thick plaque as a function of cure time.

In some of the costing scenarios evaluated in this study the possibility of preheating the composite material prior to molding was included. The effects of preheating HMC material was investigated in Reference 9 with the results that preheating reduced the time to reach the peak exotherm. This would indicate that the cure cycle could be reduced although no mechanical testing was performed for verification. The other result was that for a chosen preheat temperature, the exotherm temperature was reduced compared to the value for a no preheat condition.

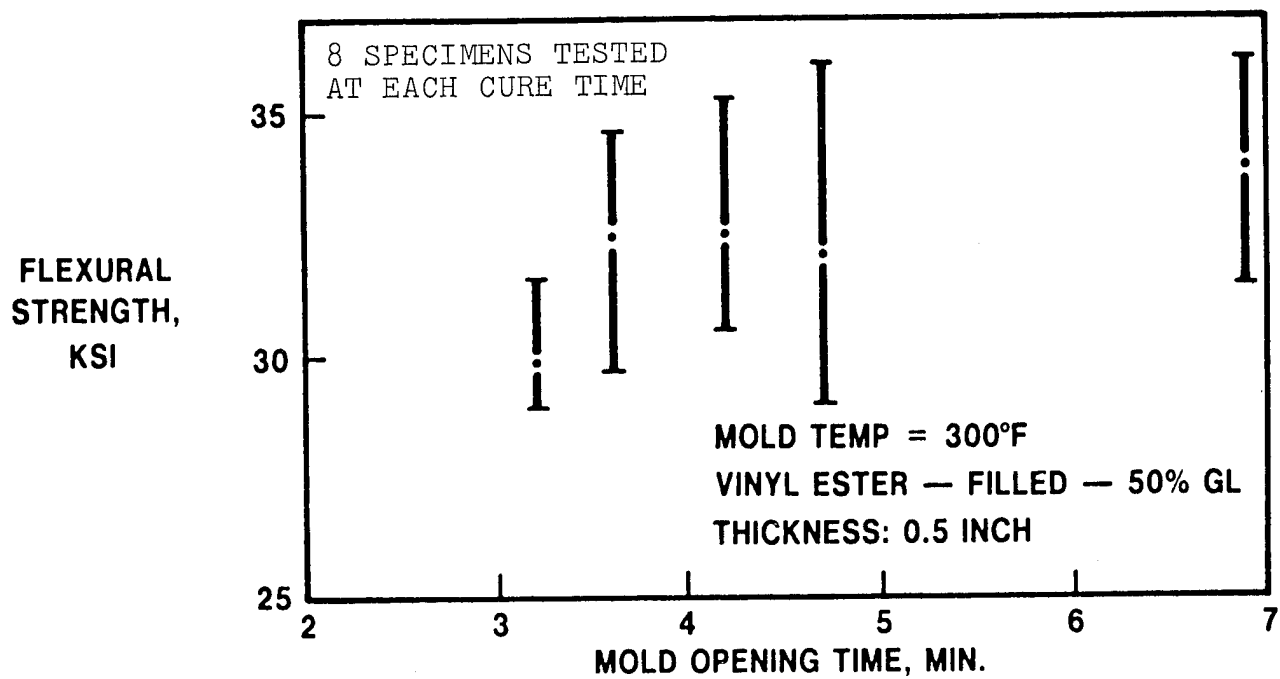


FIGURE 3-5 VARIATION OF FLEXURAL STRENGTH AS A  
FUNCTION OF CURE TIME  
(Reference 9)



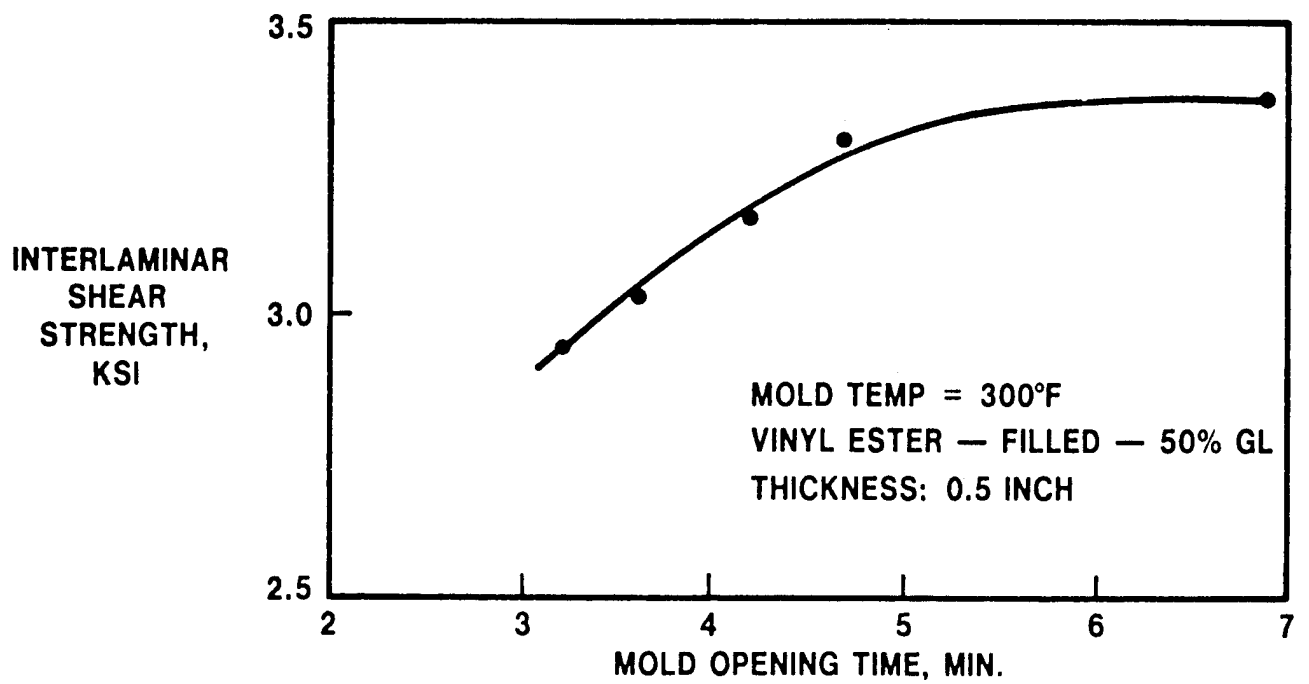


FIGURE 3-6 VARIATION OF INTERLAMINAR SHEAR STRENGTH  
AS A FUNCTION OF CURE TIME

#### 4.0 REFERENCES

1. "Specification Tips for Buyers of Molds for Reinforced Plastics", Plastics Machinery and Equipment, Vol. 8, No. 6, June 1979.
2. Brochure describing equipment sold by the Sheet Molding Compound Machinery Company, Inc. of Livonia, Michigan.
3. "Innovative Sheet Molding Compound Processes", by Yee, Geary Y., SAE paper 790170, March, 1979.
4. "The Mechanics of Molded Coating for Compression Molded Reinforced Plastics Parts", by Ongena, Robert, presented at the 33rd Annual Technical Conference, Reinforced Plastics/Composites Institute, SPI, 1979.
5. "Carrousel Machine and SMC", Plastics World, June, 1973.
6. "Sheet Molding Compound", Owens-Corning Fiberglas Publication No. 5-TM-6991-A, June, 1976.
7. "Molding of Plastics", edited by Bikales, Norbert M., Wiley-Interscience, 1971.
8. "Having Trouble Evaluating Processability of SMC? Here are Some Handy Approaches You Can Try", by Okuto, Hiroshi, Hirano, Hideyuki, and Yotsuzuka, Masaru, Plastics Technology, August, 1973.
9. "Effect of Cure Cycle on Mechanical Properties of Thick Section Fiber-Reinforced Poly/Thermoset Moldings", by Mallick, P. K. and Raghupathi, N., Polymer Engineering and Science, August, 1979.
10. "HMC, High Strength Molding Composites - New Formulations, Processing and Molding", Technical Service Bulletin TS-201A, P.P.G. Industries, June 1977.